

**Surface Modulation Towards Next Generation  
Vascular Grafts**

**By**

**Debra Siew Theng Chong**

**iBSc, MBBS, MRCS**

**Thesis submitted for the degree of**

**Doctor of Philosophy (PhD)**

**Division of Surgery and Interventional Science**

**University College London**

**2016**

I, Debra Siew Theng Chong, confirm that the work presented in this Thesis is my own. Where information has been derived from other sources, I confirmed that this has been indicated in this Thesis.

## **Abstract**

This Thesis is based on the surface modification of a platform-technology polymer, POSS-PCU. This POSS-PCU polymer has been primarily developed for use as a small diameter vascular bypass graft. The mechanical properties and compliance of this material is thought to be superior to current vascular graft materials in clinical use. However, the lack of endothelialisation of this polymer in preclinical evaluation is a cause for concern. The hydrophobic nature of the POSS-PCU polymer is thought to be the culprit and therefore the need to render the surface of the polymer suitable for endothelialisation forms the basis of this Thesis.

It is possible to engineer the surface of the polymer without affecting the beneficial bulk properties of the polymer. Recent technological advances have made this possible. A combination of plasma treatment and surface topology modification on the micro- and nanoscale has been shown to encourage the growth of endothelial cells. However, nanofeatures show a subtle improvement in endothelial cell adherence.

Two different nanopit topographies, SQ and NSQ, have formed the main focus of this Thesis to further investigate the effect of nanotopography on endothelial cells. These two topographies are different from each other only by an offset of 50nm and therefore are very similar. Despite this, they have shown to illicit different responses by the endothelial cells, especially in the up-regulation of different adhesion proteins. These topographies also have a strong effect on mesenchymal stem cells, by either directing them to maintenance or osteogenic differentiation, and unfortunately this effect can also be enhanced by the presence of endothelial cells, causing calcification. This can be detrimental in a vascular graft.

The results of this Thesis highlight the potential of using a combination of plasma treatment and surface nanoengineering to create a new generation of vascular graft, that requires further investigation.

## **Acknowledgements**

My deepest gratitude goes to my Primary Supervisor, Professor George Hamilton, who believed in me before I even believed in myself and still continues to believe in me. Without his continual support, encouragement and constant ‘pep-talks,’ this Thesis and PhD would not be possible.

My sincerest thanks goes to Dr. Umber Cheema, my Subsidiary Supervisor, who took me and my PhD on without a second thought and has since been extremely quick with the guidance and support.

I will forever be grateful to Professor Matthew Dalby, University of Glasgow, who took me under his ‘wing’ and opened up his laboratory to me, as well as agreeing to be my external supervisor. Without his help and encouragement, I would not have been able to complete a PhD.

I am also extremely thankful to Professor Nikolaj Gadegaard, University of Glasgow, who also unreservedly agreed to be my external supervisor and treated me as one of his own engineering students.

My warmest thanks goes to Professor David Abrahams (UCL) and Ms Korsa Khan who not only gave me access to their laboratories but also gave both scientific advice and unwavering support and encouragement all throughout my PhD.

My PhD would have not been possible without the continual encouragement and knowledge of Mr Arnold Darbyshire, who guided me through the ‘dark times’ and cheered me up with jokes and stories.

I am extremely grateful to the Centre of Cell Engineering (University of Glasgow) for ‘harbouring’ me for many months, feeding me cake as well as renewing my love for science. Special thanks goes to Professor Adam Curtis, Dr Mathis Riehle, Dr

Lesley-Anne Turner, Ms Carol-Anne Smith, Mr Anil Patel and Dr Louisa Lee for their advice and help throughout my time in CCE.

Without Victor Lopez-Davila and Tarig Magdeldin and their entertainment in the office, work would not have been possible and I am grateful to them for their advice and their comforting words when things got bad. I would also like to thank Miss Meryl Davis, Dr Tara Mastracci, Mr Ben Lindsey, Dr Jennifer Hague and Dr Angela Pereira for their words of advice and support especially when the going got tough!

I would like to dedicate this Thesis to my parents, Mr Nicholas Chong and Loh Yoke Lan, without whose love, support and encouragement, nothing would have been possible.

## Abbreviations

2D	2-Dimension
3D	3-Dimension
AFM	Atomic Force Microscopy
ALP	Alkaline Phosphatase
BM-MSC	Bone Marrow – Mesenchymal Stem Cell
BMP-2	Bone Morphogenic Protein - 2
BSA	Bovine Serum Albumin
CA	Contact Angle
CB	Cassie Baxter Theory
CBAS	Carmeda® Bioactive Surface
CHCl <sub>3</sub>	Chloroform
CO <sub>2</sub>	Carbon Dioxide
COOH	Carboxyl Group
DAPI	4'6 diamidino-2-phenylindole
DMAC	N N'-dimethylacetamide
DMEM	Dulbecco's modified Eagle Medium
DNA	Deoxyribonucleic Acid
EBL	Electron-Beam Lithography
EC	Endothelial Cell
ECGS	Endothelial Cell Growth Serum
ECM	Extracellular Matrix
eNOS	Endothelial Nitric Oxide Synthase

ePTFE	Expanded Polytetrafluoroethylene
FBS	Foetal Bovine Serum
FDA	United States Food and Drug Administration
FIB	Focussed Ion Beam
FITC	Fluorescein isothiocyanate
FTIR	Fourier Transform Infrared Spectroscopy
GAPDH	Glyceraldehyde-3-Phosphate Dehydrogenase
H <sub>2</sub> O	Water
HCl	Hydrochloric Acid
HEPES	4-(2-hydroxyethyl)-1-piperazineethanesulfonic acid
HITAEC	Human Internal Thoracic Artery Endothelial Cell
HP-POSS	Hybrid Plastics POSS-Chlorohydrin
HUVEC	Human Umbilical Vein Endothelial Cell
ICW	In Cell Western
IL-6	Interleukin-6
JWNC	James Watt Nanofabrication Centre
KMnO <sub>4</sub>	Potassium Permanganate
LiOH	Lithium Hydroxide
MDI	4,40-methylenebis (phenyl isocyanate)
MG	Microgrooves
MHC	Major Histocompatibility Complex
MSC	Mesenchymal Stem Cell
Na <sub>2</sub> CO <sub>3</sub>	Sodium Carbonate
NaHCO <sub>3</sub>	Sodium Bicarbonate

NaOH	Sodium Hydroxide
NIR	Near Infra-red
Ni-V	Nickel-Vanadium
NMII	Non-myosin II
NO	Nitric Oxide
NP	Nanopit
NSQ	Near Square Topography
OCN	Osteocalcin
OH	Hydroxyl Group
P	Planar
PB-MSC	Peripheral Blood – Mesenchymal Stem Cell
PBS	Phosphate Buffer Solution
PC	Polycarbonate
PCU	Polycarbonate urea urethane
PDMS	Polydimethylsiloxane
PECAM	Platelet endothelial cell adhesion molecule
PET	Polyethylene Terephthalate
POSS	Polyhedral Oligomeric Silsesquioxane
POSS-PCU	Polyhedral oligomeric silsesquioxane Polycarbonate Urea Urethane
PTFE	Polytetrafluoroethylene
REDV	Arg-Glu-Asp-Val Tetrapeptide
RGD	Arginylglycylaspartic acid Tripeptide
SEM	Scanning Electron Microscopy
SQ	Square Topography

TGF- $\beta$	Transforming Growth Factor- $\beta$
THF	Tetrahydrofuran
TLC	Thin Layer Chromatography
UCL-POSS	University College London POSS- Chlorohydrin
UV	Ultraviolet
VCAM-1	Vascular Cell Adhesion Molecule -1
VEGF2	Vascular Endothelial Growth Factor 2
VSMC	Vascular Smooth Muscle Cell
WCA	Water Contact Angle

## Contents

<b>Chapter 1</b>	<b>Introduction .....</b>	<b>27</b>
1.1	<i>Vascular Disease .....</i>	<i>27</i>
1.2	<i>'Ideal' Properties of Vascular Grafts.....</i>	<i>28</i>
1.3	<i>Current Vascular Graft Materials .....</i>	<i>29</i>
1.4	<i>Modification of Existing Materials .....</i>	<i>31</i>
1.5	<i>Decellularized Vascular Grafts.....</i>	<i>33</i>
1.6	<i>Biodegradable Polymeric Vascular Grafts.....</i>	<i>36</i>
1.7	<i>Tissue-Engineering Vascular Grafts by Self-Assembly .....</i>	<i>39</i>
1.8	<i>Why Synthetic Non-Biodegradable Vascular Grafts May Still have the Advantage?.....</i>	<i>41</i>
1.9	<i>Aims of This PhD Thesis.....</i>	<i>43</i>
1.10	<i>Hypothesis of This PhD Thesis .....</i>	<i>43</i>
1.11	<i>Chapter Description .....</i>	<i>44</i>
<b>Chapter 2</b>	<b>Materials and Methods .....</b>	<b>47</b>
2.1	<i>Cell Culture of Human Umbilical Vein Endothelial Cells.....</i>	<i>47</i>
2.2	<i>Conditioning Cell Culture of HUVECs for Co-Culture Experiments.....</i>	<i>47</i>
2.3	<i>Cell Culture of Mesenchymal Stem Cells (MSCs) .....</i>	<i>48</i>
2.4	<i>Cell Culture of Co-Culture of MSCs and HUVECs .....</i>	<i>48</i>
2.5	<i>Fabrication of POSS-PCU .....</i>	<i>48</i>
2.6	<i>Fabrication of Nanopatterned Surfaces on POSS-PCU .....</i>	<i>49</i>
2.7	<i>Preparation of Polycarbonate Surfaces for Cell Seeding .....</i>	<i>50</i>
2.8	<i>Immunofluorescence.....</i>	<i>50</i>
2.9	<i>Live/Dead Staining.....</i>	<i>51</i>
2.10	<i>Coomasie Blue Staining .....</i>	<i>51</i>
2.11	<i>Scanning Electron Microscopy (SEM) Preparation.....</i>	<i>51</i>
2.12	<i>Atomic Force Microscopy.....</i>	<i>51</i>
2.13	<i>Statistical Analysis.....</i>	<i>51</i>
2.14	<i>Conclusion.....</i>	<i>52</i>
<b>Chapter 3</b>	<b>Surface Focus: Manufacture and Optimisation of POSS Nanoparticle</b>	
	<b>54</b>	
3.1	<i>Introduction.....</i>	<i>54</i>
3.2	<i>Hypothesis.....</i>	<i>60</i>
3.3	<i>Materials and Methods .....</i>	<i>61</i>

3.3.1	Synthesis of partial-cage of (i-C <sub>4</sub> H <sub>9</sub> ) <sub>8</sub> Si <sub>8</sub> O <sub>12</sub> from Isobutyltrimethoxysilane	61
3.3.2	'Corner-Cap' Reaction.....	62
3.3.3	Formation of POSS-Chlorohydrin.....	63
3.3.4	Solid State NMR .....	63
3.3.5	Melting Point.....	63
3.3.6	Fournier Transmission Infrared (FTIR) Spectroscopy.....	63
3.3.7	Thin Layer Chromatography (TLC) .....	63
3.3.8	POSS-PCU Polymer solution manufacture.....	64
3.3.9	POSS Dispersion .....	65
3.3.10	Soft Lithography.....	65
3.3.11	Contact Angle Measurement .....	65
3.3.12	Live/ Dead Staining.....	66
3.3.13	Alamar Blue® Cell Viability.....	66
3.4	<i>Results</i> .....	67
3.4.1	Synthesis of POSS-Chlorohydrin.....	67
3.4.2	Testing the Toxicity of POSS-Chlorohydrin associated POSS-PCU polymer	72
3.4.3	Surface Modification of POSS-PCU using POSS nanoparticles.....	74
3.4.4	Costs .....	79
3.5	<i>Discussion</i> .....	79
3.6	<i>Conclusion</i> .....	84
3.7	<i>Further Work</i> .....	85

## **Chapter 4      Surface Modulation of the POSS-PCU Polymer: Plasma Treatment**

### **87**

4.1	<i>Introduction</i> .....	87
4.2	<i>Aims</i> .....	93
4.3	<i>Materials and Methods</i> .....	94
4.3.1	POSS-PCU Preparation.....	94
4.3.2	Control Polycarbonate Urea Urethane Preparation .....	94
4.3.3	Plasma Treatment of POSS-PCU.....	95
4.3.4	Live/Dead Staining.....	95
4.3.5	Immunofluorescence.....	95
4.3.6	Coomasie Blue Staining .....	96
4.3.7	Cell Number Count .....	96

4.3.8	In Cell Western.....	96
4.3.9	Statistical Analysis.....	97
4.4	<i>Results</i> .....	97
4.4.1	Plasma Treatment.....	97
4.4.2	Live/ Dead Staining.....	100
4.4.3	Coomasie Blue Staining.....	101
4.4.4	Cell Number.....	101
4.4.5	Immunofluorescence.....	103
4.4.6	In Cell Western.....	104
4.5	<i>Discussion</i> .....	105
4.6	<i>Conclusion</i> .....	111
4.7	<i>Further Work</i> .....	112
<b>Chapter 5</b>	<b>Surface modulation of POSS-PCU: Surface topography.....</b>	<b>114</b>
5.1	<i>Introduction</i> .....	114
5.1.1	Fabrication Techniques.....	115
5.1.2	'Disordered' and 'Ordered' Surface Topography.....	117
5.1.3	Cell Engineering.....	118
5.2	<i>Aims and Hypothesis</i> .....	122
5.3	<i>Materials and Methods</i> .....	122
5.3.1	Photolithography and Electron Beam Lithography.....	122
5.3.2	Soft Lithography.....	123
5.3.3	Plasma Treatment and Contact-Angle Measurement.....	123
5.3.4	Scanning Electron Microscope (SEM) and Atomic Force Microscopy (AFM) 123	
5.3.5	4',6-diamidino-2-phenylindole (DAPI) Cell Count.....	124
5.3.6	Coomasie Blue Staining.....	124
5.3.7	Immunofluorescence of the HUVECs on the POSS-PCU Films.....	125
5.3.8	In-Cell Western for eNOS and P-myosin of HUVECs on the POSS-PCU Films 125	
5.3.9	Statistical Analysis.....	126
5.4	<i>Results</i> .....	126
5.4.1	Replication Fidelity.....	127
5.4.2	DAPI Cell Count and Coomassie Blue.....	128
5.4.3	Immunofluorescence of HUVECs of POSS-PCU.....	130
5.4.4	In Cell Western Quantification of Endothelial Cell Function.....	132

5.4.5	In Cell Western Quantification of P-Myosin Expression.....	133
5.5	<i>Discussion</i> .....	134
5.6	<i>Conclusion</i> .....	141
5.7	<i>Further Work</i> .....	142
<b>Chapter 6</b>	<b>Endothelial Cell Adhesion to Nanotopography.....</b>	<b>145</b>
6.1	<i>Introduction</i> .....	145
6.1.1	Endothelial Cell Adhesion.....	145
6.1.2	Nanopit Topography (NSQ and SQ).....	146
6.1.3	Injection Moulding.....	148
6.1.4	Nanotopography and Vascular Grafts .....	149
6.2	<i>Aims and Hypothesis</i> .....	150
6.3	<i>Materials and Methods</i> .....	151
6.3.1	Injection Moulding of Polycarbonate (PC) Substrates.....	151
6.3.2	Plasma Treatment of the PC Substrates .....	151
6.3.3	Sterilisation and Seeding of the PC substrates.....	152
6.3.4	Contact Angles Measurements .....	152
6.3.5	In Cell Western.....	152
6.3.6	Cell Count using DAPI.....	153
6.3.7	Scanning Electron Microscopy (SEM) of the HUVECs on the PC Substrates 153	
6.3.8	Statistical Analysis.....	153
6.4	<i>Results</i> .....	153
6.5	<i>Discussion</i> .....	161
6.6	<i>Conclusion</i> .....	166
6.7	<i>Further Work</i> .....	166
<b>Chapter 7</b>	<b>The Influence of Mesenchymal Stem Cells on Endothelial Cells in the Presence of Nanotopography .....</b>	<b>169</b>
7.1	<i>Introduction</i> .....	169
7.1.1	Mesenchymal Stem Cells (MSCs).....	169
7.1.2	Mesenchymal Stem Cells, Nanotopography and Tissue Engineering.....	170
7.1.3	Calcification of Vascular Grafts.....	171
7.1.4	Mesenchymal Stem Cells and Endothelial Cells Cross-Talk and the Link with Surface Topography .....	172
7.2	<i>Aims</i> .....	173
7.3	<i>Materials and Methods</i> .....	174

7.3.1	Fabrication of Polycarbonate (PC) substrates .....	174
7.3.2	Mesenchymal Cell Culture .....	174
7.3.3	MSC/ HUVEC Co-culture .....	174
7.3.4	Sterilising of the PC Substrates and Seeding of the Co-Culture .....	175
7.3.5	Immunofluorescence .....	175
7.3.6	Coomasie Blue Staining .....	175
7.3.7	Von Kossa Staining .....	176
7.3.8	In-Cell Western .....	176
7.3.9	Statistical Analysis .....	177
7.4	<i>Results</i> .....	177
7.5	<i>Discussion</i> .....	185
7.6	<i>Conclusion</i> .....	191
7.7	<i>Further Work</i> .....	191
<b>Chapter 8</b>	<b>Conclusion and Future Work</b> .....	<b>194</b>
8.1	<i>POSS-Nanoparticle for Chemically Altering the Surface</i> .....	195
8.2	<i>Plasma-Treatment for Increasing the Hydrophilicity and Biological Activity of the POSS-PCU surface</i> .....	196
8.3	<i>Combining Plasma Treatment with Surface Topographical Modifications on POSS-PCU</i> .....	197
8.4	<i>Investigating the Effect of Nanopits on Endothelial Cells Adhesion</i> .....	197
8.5	<i>Will Nanopit Topography have an effect on Calcification leading to Premature Vascular Graft Failure?</i> .....	198
8.6	<i>Future Work</i> .....	199
<b>Chapter 9</b>	<b>References</b> .....	<b>202</b>
<b>Chapter 10</b>	<b>Awards, Prizes, Presentations and Papers</b> .....	<b>215</b>
<b>Chapter 11</b>	<b>Appendix</b> .....	<b>217</b>



## Figures

- Figure 1-1 A simplified diagram to show the decellularization process using porcine arteries to create a functional vascular graft. This diagram has been taken from (23)..... 35
- Figure 2-1 This is a step-wise diagram which shows how photolithography and electron beam lithography (a) are used to produce micro- and nano-sized features, respectively. B) shows how soft lithography can be used to produce the surface features onto the POSS-PCU polymer and c) shows the SEM of a silicon master, and in this case, this is the NSQ nanopattern..... 49
- Figure 3-1 Figure to show A) the chemical structure of the full cage POSS nanoparticle and B) the 3D structure of the POSS cage ..... 56
- Figure 3-2 Diagram to show the proposed step-wise methodology of producing POSS-functionalised with a chlorohydrin group which can then be chemically attached to a polymeric chain..... 58
- Figure 3-3 This figure shows the chemical structure of the UCL patented POSS-PCU vascular graft material. Note the POSS nanocage is at the end of the polymeric chain. .... 59
- Figure 3-4 Diagram to show the preparation of the partial cage POSS  $(i-C_4H_9)_8Si_8O_{12}$  from Isobutyltrimethoxysilane ..... 62
- Figure 3-5 Diagram to show the measurement of contact angles using the sessile drop method. The wettability of the surfaces is evaluated regarding the static and dynamic behavior of the droplet itself and therefore in the static stage, this is evaluated over three different interphases in contact with the contact angle. Under dynamic conditions, this is related to the sliding angle ( $\alpha$ ) which is the inclination angle of the surface which causes the water droplet to roll off..... 66

Figure 3-6 Comparative FTIR diagrams of the products produced at each stage of the chemical synthesis where a) is POSS Trisilanol, b) is POSS Epoxy and c) is POSS Chlorohydrin..... 69

Figure 3-7 NMR spectra showing the comparison of POSS-PCU produced commercial (HP-POSS) and that produced in-house (UCL-POSS) where a) UCL-POSS proton NMR, b) HP-POSS Proton NMR, c) UCL-POSS 13C NMR spectra and d) HP-POSS 13C NMR spectra ..... 71

Figure 3-8 This figure shows the exposure of a thin layer chromatography (TLC) plate highlight the different POSS products, where A is mixture of Hybrid Plastics POSS- Chlorohydrin and UCL POSS- Chlorohydrin, B is Hybrid Plastics POSS-Chlorohydrin only and C is UCL POSS-Chlorohydrin only. A mixture of the two POSS samples is used to further confirm that the two products are the same. The green arrow indicates the presence of the POSS cage which is seen across all three products. .... 72

Figure 3-9 Toxicity studies conducted to show HUVECs survival in the presence of POSS-PCU and when compared with normal conditions (control). The top diagram shows Live/Dead assay of the live cells (green) and dead cells (red) using fluorescence microscopy after 48 hours. The bottom graph shows comparison intensity when using Alamar Blue ® to measure the metabolic activity of the HUVECs in the presence of POSS-PCU and without. There is no statistical difference between the two conditions on any of the days (n = 12) .. 74

Figure 3-10 Shows the chemical structures of a) Fluoro-POSS and b) POSS Chlorohydrin. C) shows the 3D rendition of the surface topography of POSS-PCU with the POSS-nanoparticle aggregating on the surface using and d) phase image of the same area with AFM. .... 75

Figure 3-11 a) and b) shows a snapshot of the angle measurements taken for the contact angle measurements of the sessile water droplet on the POSS-PCU polymer and PCU polymer. The table below shows the contact angles for these two polymers as well as the clinical control, PTFE (n = 3). .... 76

- Figure 3-12 The two graphs illustrate the similarities between the original polymer, POSS-PCU and PCU, and the modification of excess POSS nanoparticle. The contact angles of each polymer is recorded in the table below (n = 3)..... 77
- Figure 3-13 FTIR spectrums taken of both the top and bottom of cast polymers where the spectrums are a) POSS-PCU, b) POSS-PCU with 2% POSS-Chlorohydrin, c) POSS-PCU with 2% Fluoro-POSS, d) PCU, e) PCU with 2% POSS-Chlorohydrin and f) PCU with 2% Fluoro-POSS. The arrows indicate the extra peaks of the POSS nanoparticle at 1100 cm<sup>-1</sup> wavelength ..... 78
- Figure 4-1 Figure to show the step-wise effect of O<sub>2</sub> plasma treatment on POSS-PCU polymer, a) and when O<sub>2</sub> plasma is initially applied b), and when chemical groups start to form on the surface c). D) shows the chemical structure of the POSS-PCU polymer itself..... 93
- Figure 4-2 Where a) is a simplified diagram to illustrate the concept of the plasma chamber and b) shows the step-wise drop in water contact angle (°) when increasing the power (watts) of the plasma treatment (inset: sessile water contact angle measurement)..... 98
- Figure 4-3 This figure shows the consistent contact angles obtained d) over a seven-day period after plasma treatment and the different images of at Day 1 a), Day 5 b) and Day 7 c) showing that there are no changes of the contact angle and therefore no degradation in the initial 7 days post plasma treatment (n = 3)..... 99
- Figure 4-4 Live/ Dead staining for the different plasma-treatment levels, where a) 40W at 60s, b) 60W at 60s and c) 80W at 60s. (Scale bar: 20 μm) This shows that the plasma treatment is not toxic to the endothelial cells and illustrates that despite the plasma treatment, biocompatibility of the POSS-PCU polymer is retained..... 100
- Figure 4-5 This figure shows the morphology of the HUVECs using Coomassie Blue staining on the POSS-PCU polymer post-plasma treatment of a) 40W for 60s, b)

60W for 60s and c) 80W for 60s and the increased spreading of the HUVEC cells with the increasing plasma treatments (Scale Bar: 20 $\mu$ m) ..... 101

Figure 4-6 Box plot showing cell numbers on plasma modified POSS-PCU films and unmodified POSS-PCU (0) and PCU films. Significant differences calculated using One-Way Anova are highlighted on the graph as follows: \*\*\*\* (p<.0001), \*\*\* (p<.001), \*\* (p<.01)..... 102

Figure 4-7 Immunofluorescence of the HUVECs again highlight the normal morphology of the cells on the different plasma-treated polymer where a) 40W for 60s, b) 60W for 60s and c) 80W for 60s, where actin is red, vinculin is green and the nuclei is blue. (Scale bar: 10 $\mu$ m)..... 103

Figure 4-8 This figure shows the use of In Cell Western (ICW) to quantify the amount of eNOS expression and the image on the left shows the near-infrared fluorophores tagged to eNOS (green channel) and the cell stain (red channel) and when it is merged. The intensity of this is then measured giving a quantifiable measurement on the different channels. ICW looks at quantifying the intensity of these fluorophores and therefore giving the graph on the right, where the eNOS expression is quantified on the different plasma-treated POSS-PCU polymer: \* (p<0.05) (n = 4)..... 104

Figure 4-9 This graph shows the P-myosin expression by the HUVECs on the different plasma treatments compared with planar untreated POSS-PCU surface. \* p<0.05 (n = 4)..... 105

Figure 5-1 Table to show a selection of publications in which grooves have been used to identify in both static and shear flow conditions and a brief description of the findings. [Adapted from Table 2 in (37)] ..... 121

Figure 5-2 A) This figure shows scanning electron microscopy images of planar, microgroove and nanopit POSS-PCU surfaces before plasma treatment, insets show higher magnification images of the topographies; nanopit inset was imaged after plasma treatment for 60s at 80W. B) AFM scans of planar (upper

two images) and nanopit (lower two images) POSS-PCU films before (left hand side images) and after (right hand side images) plasma treatment. C) Box-plot showing roughness values of planar and nanopit POSS-PCU films..... 127

Figure 5-3 This figure recaps from the previous chapter about the cell number (a) and from this original graph, it can be seen that plasma treatment levels of 80W for 60S has the highest cell count and extrapolating this treatment level as the optimal treatment, cells were cultured on the different topographies using this plasma treatment (b) with no significance differences found ( $p > 0.05$ ). C) Upper image shows a scan of Coomassie Blue staining on the different topographies and the lower is a fluorescent image is Live/Dead staining (green = Live, red = Dead) of cells on a nanopit substrate with plasma treatment (80W for 60s). (n = 4) ..... 129

Figure 5-4 Cell morphology and function on topographically patterned POSS-PCU films. Fluorescent micrographs show nuclei (blue) and actin (red). Specific proteins, namely vinculin (highlights focal adhesions at cell periphery) and nitric oxide synthase (marker of endothelial cell function) are highlighted in a) and b) respectively. Grey arrows in a) in the lower right image highlight focal adhesions. Images were enhanced using contrast/ brightness controls with the exception of the insets in b) which show the unmodified images of eNOS expression using identical microscope settings. .... 131

Figure 5-5 Graph showing eNOS expression at 5 days after cell culture on microgroove and plasma-treated POSS-PCU surfaces using In Cell Western. There is a statistical significance in eNOS expression at 80W and 100W at 60s plasma treatment levels on the micron grooved POSS-PCU substrates (\*  $p < 0.05$ ) (n = 4) ..... 133

Figure 5-6 This graph showing P-myosin expression after 5 days on incrementally increasing plasma treatment on POSS-PCU substrates with microgrooves. There is no statistical significance at any of the plasma-treatment levels on the micro-grooved surfaces. (n=6)..... 134

Figure 5-7 This figure shows three SEM images to illustrate how to create a topography similar to that found in native basement membranes and using the current technology that we have. A) is an SEM image adapted from (70) which shows the carotid basement membrane of a rhesus macaque (Scale bar: 600nm). B) is an SEM (conducted using a field electron source (Hitachi S4700)) the silicon shim that has been produced from electron beam lithography in an attempt to reproduce the nanopores seen in A) in a slight disordered fashion. C) is an SEM image of the POSS-PCU polymer with after soft lithography has imprinted the nanofeatures of the shim onto the polymer. Although this is not an exact replica of the basement seen in the SEM due to the limitations of the current technology, the nanopores can be replicated to a certain extent and then molded into the POSS-PCU polymer with good fidelity..... 136

Figure 5-9 The middle diagram is adapted from (94) and illustrates POSS-PCU film with a micro-gradient of grooves (pitch of grooves from 8 $\mu$ m to 100 $\mu$ m with shallow groove depth of 10nm increasing to 1 $\mu$ m along the 10mm grooves) transferred on it using soft lithography and a polycarbonate master. The films are then plasma-treated at 80W for 60s. The top two images are SEMs of the POSS-PCU substrate at different points to illustrate the smaller grooves (left) and the bigger grooves (right). The bottom images show Human Umbilical Vein Endothelial Cells (HUVECs) stained with Coomassie Blue stain of the same areas as the SEM images. The yellow arrows on the left image show the HUVECs which have aligned along the smaller grooves and this is in contrast with the HUVECs on the flat surface which have more spread and rounded morphology. The image on the bottom right show that on the larger pitch sizes the HUVECs are small and rounded in morphology which may indicate that they are unhealthy on this surface..... 143

Figure 6-1 This figure shows a) the injection moulder [image adapted from the JWNC website] used to create the PC substrates and then the b) plasma cleaner used to render the PC surfaces hydrophilic (with the red plasma glow in the chamber to indicate the plasma treatment is taking place) and c) graph to shows the difference in contact angles pre- and post-treatment using University of

Glasgow standard protocols. There is a statistical significance pre- and post-plasma treatment ( $p < 0.05$ ). (n = 3) ..... 154

Figure 6-2 This figure shows normal microscopy of Day 1 post-seeding of the HUVECs on the PC substrates where a) planar, b) NSQ and c) SQ surfaces where the treatment has been 10 minutes of exposure to air plasma. The cells are noted to have adhered successfully to the surfaces. The graph on the right shows the significant differences (\* in SQ and \*\* in NSQ). The control bar is used for comparison purposes. It should also be noted that there is a statistical significant difference with all the planar treatments and both SQ and NSQ topographies but there is no significance between the three planar treatments. [Scale bar is 10  $\mu\text{m}$ ] (n = 4) ..... 155

Figure 6-3 This figure highlights the contact angles which seem to promote endothelial cell adhesion on the polycarbonate substrates. On the left is a table which shows the mean of all the contact angles and highlighted in 'orange' colour are the contact angles which have consistently and successfully been able to grow HUVECs on. .... 156

Figure 6-4 SEM images of the endothelial cells on the surface of the three topographies, planar, NSQ and SQ in both low and high magnifications. Red arrows indicate the filopodia of the HUVECs and these tend to be found in the leading edge of the cell. Yellow arrows indicate the retraction fibers of the cell found at the tail-end of the migrating cell. .... 157

Figure 6-5 This figure shows the cell stain on the substrates when using ICW as a detection method for conducting cell counts, where a) shows the intensity of the cell stain as visualised by the ICW plate reader and b) the quantifiable data comparisons. C) uses DAPI count to count the number of nuclei on the substrates. (\*  $p < 0.05$ , \*\*\*  $p < 0.0005$ )..... 158

Figure 6-6 Graphs to show P-myosin expression by the HUVECs on the different topographies (Planar, NSQ and SQ on polycarbonate substrates) at different time points of Day 1 (top graph), 3 (middle graph) and Day 5 (bottom graph)

using In Cell Western analysis. As can be seen on Day 5, there starts to be seen a statistical significance in the expression of P-myosin on the NSQ surface (\* p<0.05) (n = 4) ..... 160

Figure 6-7 Graph to show VE-Cadherin expression by HUVECs on the different topographies (planar, NSQ and SQ on polycarbonate substrates) after 5 days of cell culture (\* p<0.05) (n=3)..... 161

Figure 7-1 These are phase-contrast microscopy images of a) HUVECs and b) mesenchymal stem cells (bone-marrow derived) cultured on the polycarbonate substrates (planar) [Scale Bar: 10µm]..... 177

Figure 7-2 This is a phase-contrast microscopy image of the co-culture of MSCs/ HUVECs on a planar substrate 2 days after seeing of the MSCs. The MSC (red arrows) is sitting surrounded by HUVECs and shows the effectiveness of the co-culture and hence successful ‘seeding’. [Scale Bar: 10µm] ..... 178

Figure 7-3 Coomassie Blue-stained images after 5 days of co-culture of the MSCs and HUVECs at a ratio of 1:50. Yellow arrows point out the presence of the MSCs, on the different topographies planar (left), NSQ (middle) and SQ (right). As can be seen, they are adhered quite sparsely on the staining and can be quite difficult to see. [Scale bar: 20µm]..... 179

Figure 7-4 This figure shows a fluorescence microscopy image of the immunostaining of MSCs on topographical surfaces A) NSQ and B) SQ, where red is actin (rhodamine-phalloidin) and blue is the cell nucleus (DAPI). It is interesting to find that MSCs stain with rhodamine-phalloidin more intensely and the actin fibres are more defined than endothelial cells. Note that on A) it is possible to compare with the endothelial cells on the left which are not as well stained. [Scale bar: 10µm] ..... 180

Figure 7-5 These are fluorescent microscopy images of the MSCs also noted to be adhering on the top of the endothelial cell sheets on all three topographies, a) planar, b) NSQ and c) SQ, where red is actin (rhodamine-phalloidin) and blue is

the cell nucleus (DAPI). The yellow arrows point to the MSCs on top of the endothelial cells.....	181
Figure 7-6 Fluorescence microscopy images highlighting the difference between the MSCs and HUVECs. CD31+ staining (green) is a surface marker for endothelial cells and therefore it is possible to differentiate between the two types of cells. Red highlights actin (rhodamine-phalloidin) and blue is the cell nucleus (DAPI). [Scale bar: 10µm].....	182
Figure 7-7 This is phase-contrast microscopy to look at the results from Von Kossa staining on the different PC substrates and their topographies by the co-culture of MSCs/ HUVECs. A) is a positive reference sample and adapted from (127). A positive Von Kossa will show dark deposits which are not seen on our test samples on the three topographies, as highlighted. [Scale bar: 10µm].....	183
Figure 7-8 Graph to show osteocalcin expression on the different topographies by the co-cultures of MSC/ HUVEC, using In Cell Western, after 3 weeks of cell culture. [Where * <0.05 and *** <0.0001] (n=3).....	184
Figure 7-9 Graph to show a cell count comparison using cell stain of the ICW methodology. This shows that there are more cells on the planar surfaces with statistical significance over NSQ and SQ surfaces. [Where **<0.05] (n=3)...	185
Figure 7-10 Simplified diagram to show the three stages of MSC differentiation down towards osteogenic lineage and the timeline of the expression of different protein markers and deposition of calcium and phosphate. ....	187
Figure 11-1 Table to show ‘trial and error’ of all the different conditions which were attempted to make the POSS-Trisilanol. This table illustrates that unfortunately despite altering of these conditions, T-Gel predominantly featured as the end product. (n=2).....	218

Figure 11-2 This graph shows the effect on water contact angle of POSS-PCU when the duration of plasma treatment (at 40W) is increased rather than power. ( \* p<0.05, n=6)..... 219

# **Chapter 1: Introduction**

## **Chapter 1 Introduction**

### **1.1 Vascular Disease**

Atherosclerotic peripheral arterial disease (PAD) has been quoted to be ‘one of the most prevalent, morbid and mortal diseases’(1, 2). A recent published systematic review looked at the prevalence of PAD from 2000-2010 and revealed a global estimate of 202 million people in 2010, which is a 23.5% increase over the 10 years. It was also noted that more than two-thirds (69.7%) of PAD was concentrated in the lower-middle income class(3). If left untreated, this can lead to loss of limbs or even mortality. However, despite these high numbers, there appears to be not much in the place of preventative measures being undertaken and recent studies have advocated a more preventative stance needs to be taken.

The advent of endovascular interventions has led to first line recommendations for the treatment of peripheral vascular disease, usually, being angioplasty and endovascular stenting. This is done on the basis that the least invasive procedures should be tackled first line and this should be continued until they are no longer suitable, prior to more invasive techniques being utilized. However, in a proportion of patients this will not be suitable. This can be due to repeated unsuccessful endovascular interventions, lesions which are unsuitable for endovascular intervention or multi-level lesions. These patients will have to undergo surgical intervention in the form of a peripheral bypass. This is a very invasive procedure, leaving the patient with unsightly scars on their limbs and with success rates which are dependent on the vascular graft material. The most common peripheral bypasses are usually femoro-popliteal bypass and femoro-crural bypasses.

The use of autologous vessels for these surgeries have always been thought to be the ‘gold standard’ as their patency rates have been found to be far superior to any other synthetic material. The autologous vessel is harvested from the patient’s own vein and is usually sourced from the superficial venous system of their leg. These veins are also the same venous source for patients who require operation for their coronary artery bypass. A large portion of patients who go on requiring vascular surgery would also have a previous surgical history of having undergone coronary artery

bypass surgery. This means that these veins would have previously been harvested and therefore will not be available for their peripheral bypass surgery. In addition, varicose veins, small and unsuitable veins (usually in diabetic patients) and other previous surgical procedures on them would render these veins unsuitable or unavailable for autologous vein bypass. Although there are other potential sources of autologous vein, such as from the upper limb or internal mammary artery, these are less used due to the poor quality of vein for a peripheral vascular bypass and the greater morbidity and invasiveness in accessing some of these vein sources. Autologous vein bypass grafting has the benefit of being less likely to be prone to infection, good integration within the host's environment and obviously biocompatible, especially when compared with synthetic grafts. In some cases, due to the unavailability of the autologous vessel, patients are then limited to synthetic or alternative graft materials.

## **1.2 'Ideal' Properties of Vascular Grafts**

Vascular grafts are used when there is a discontinuation of blood supply leading to critical limb ischaemia and a threatened limb. In this Thesis, vascular grafts for the peripheral arterial side will be mainly considered. These vascular grafts are usually known as small-diameter vascular grafts (<6 mm diameter) to distinguish them from the aortic grafts which are of larger diameter. This is important as the haemodynamic flow and pressure properties will be different and accounting for these factors play an important part in the success of the graft.

The ideal vascular graft would be a native human vessel replacement. However, a direct arterial replacement is mostly impossible, but instead, autologous vein replacements have tended to be an excellent substitute. Unfortunately, a variety of conditions can mean that patients do not have adequate supply of autologous veins and will require synthetic vascular graft replacements as mentioned. Traditionally, these synthetic vascular grafts do not have patency rates which match autologous vein replacements. The patency rates of autologous vein grafts have been found to have patency rates of 77% and 50% at 5 and 10 years respectively(4, 5).

Therefore, the 'ideal' properties of a vascular graft would need to be anti-thrombogenic, have mechanical and compliant properties like a native vessel as well as be able to allow tissue integration as well as the formation of an endothelial layer within the luminal surface of the vascular graft. The grafts also need to be durable and non-toxic and, in paediatric cases, be able to grow with the child. There should also be properties incorporated within the graft to make it less prone to infection.

### 1.3 Current Vascular Graft Materials

Vascular bypass grafts for peripheral arterial disease are usually known as small diameter bypass grafts with a luminal diameter of <6mm. Traditional materials have mainly been made of polytetrafluorethylene (PTFE) and polyethylene terephthalate (PET or Dacron®). These materials have been utilized by many vascular surgeons for the last 30 years. However, patency rates have mainly been variable and are not as high as those of autologous vessel.

PTFE is made of the monomer tetrafluoroethylene which is then reacted together by free radical vinyl polymerization. It was discovered by Roy Plunkett in 1938 and patented in 1941(6). Since 1946, it has been sold commercially as Teflon®. There are many beneficial properties of PTFE making it a very popular polymer for a large range of applications. Unlike other carbon-based polymer chains, PTFE differs in having its hydrogens in reactive C-H bonds replaced by fluorines. These then become strong C-F bonds that are extremely resistant to attack by any other agents. This gives PTFE a strong chemical stability and makes it resistant to attack by other reagents and as well as allowing it to be inert. In 1969, Gore patented expanded PTFE (ePTFE) calling it Gore-tex®. ePTFE is manufactured by means of heating, stretching and extruding processes that produces a microporous material which is more supportive of tissue adhesion. This has been found to be a very durable material and does not degrade within the body as well as having biocompatible properties making it suitable for medical implantation(6).

Patency rates of ePTFE vascular grafts for femoro-popliteal bypasses have been found to have patency rates at 3 and 5 years, respectively, of 61% and 45%(4, 7). Compared with those of autologous vein, these can be seen to have a much poorer

outcome. Despite these poorer outcomes, ePTFE has been a stable synthetic material in vascular bypass surgery for the last 30 years, for patients who do not have the option of an autologous vein bypass.

Commercially known as Dacron®, the polymer is also known as polyethylene terephthalate or PET, and is another material which is clinically available for vascular bypass grafting. Dacron® vascular grafts were first implanted by Julian in 1957 and DeBakey in 1958(6). Commercially Dacron® grafts can be woven or knitted as they can be made into thin fibrils. Multifilament Dacron® threads in woven grafts are fabricated in ‘over-and-under’ patterns which results in a very limited porosity and minimal creep of the final material and finished graft. In contrast, knitted grafts are made with a textile technique in which the Dacron® threads are looped to create greater porosity and radial distensibility. Nowadays, due to this, Dacron® grafts tend to be knitted over woven. Other techniques such as the velour technique extends the loops of yarn on the surfaces of the fabrics and this has been done in an attempt to increase tissue incorporation. A crimping technique has also been employed to increase the flexibility, distensibility and kink-resistance of textile grafts.

In above knee applications, there is no differences in the patency rates between Dacron® and ePTFE vascular(8). However in below knee applications, there is a trend towards increased patency rates in ePTFE vascular grafts which reaches statistical significance at 24 months(7). Due to this, there is a trend towards preference by clinicians to use ePTFE vascular grafts for peripheral vascular bypass procedures.

Recently, there is introduction of another polymer which has shown some initial promise, polyurethane. This is a biocompatible, non-toxic, elastic and compliant polymer. The polyurethane elastomers comprise of a family of block co-polymers with alternating soft and hard segments. Their advantageous physical properties are a result of their 2-phase morphology caused by the incompatibility of the hard and soft segments(9). Unfortunately, the first few polyurethane-based polymers available commercially were found to have poor long-term biostability but this was soon found

to be due to the chemical 'make-up' of the polyurethane. Poly(ester) polyurethanes have been found to hydrolyse and poly(ether) polyurethanes have been found to oxidize in a biological environment (10). It is thought that the soft-segment of the polyurethane chemistry is of significance and would need altering to improve the final biostability of the final polymer.

A few groups have worked to modifying the polyurethane polymer to improve the mechanical properties by modifying the soft segments. Pursil® is a commercially available material which has an altered soft segment to try and combat the oxidation propensity of the polyurethane. Silicon-based elastomers (poly(dimethyl siloxanes [PDMS])) were used due to their good blood compatibility, low toxicity and good oxidation and thermal stability. PDMS was incorporated as the soft segment of the polyurethane so as to improve polymer stability(11). Unfortunately, the resulting polymer was not compliant and elastic enough to be a vascular graft. Therefore, Soldani(9) *et al* altered this formulation to produce a more versatile elastomeric polymer in the form of a semi-interpenetrating polymeric network. Initial large animal studies have shown that this formulation is comparable with ePTFE grafts.

Salacinski(12) *et al* also tried to formulate a polymer that was more resistant to breakdown whilst retaining its compliance and replaced the soft segment to make a final polymer, a polycarbonate urea urethane, which was commercially known as Myolink®. To further enhance the mechanical properties, a nanoparticle has been added to the formulation, polyhedral oligomeric silsesquioxane (POSS), and to date this has been found to have improved mechanical properties(13). This vascular graft material is currently undergoing a clinical 'first in man' evaluation and forms part of this Thesis.

#### **1.4 Modification of Existing Materials**

Prosthetic rings and coils have been applied to the external surfaces of the vascular grafts. This external support was deemed necessary to resist kinking and possible mechanical compression. It is thought to be invaluable in bypasses which go past a limb joint, especially one that is a hinge joint such as the knee, where kinking and

compression of the graft can alter haemodynamic flow leading to graft failure. Externally reinforced vascular grafts are currently available commercially.

More recently, there has been the addition of heparin sulfate bonded to the luminal surface of ePTFE vascular grafts and this is meant to prevent thrombogenic occlusion of the graft especially immediately post-implantation.

The heparin-bonded graft is manufactured and produced as the Gore Propaten™ vascular graft (W.L. Gore and Associates, Inc. Flagstaff, Arizona) and uses the Carmeda® Bioactive Surface (CBAS) which uses covalent end-point linkage to retain heparin on the device surface, in this case, ePTFE graft. There have been many attempts to bind heparin to the surface of either PET or ePTFE grafts. The aim is to control the formation of initial fibrin and platelet layers. The mechanism of action is that the immobilized heparin binds to anti-thrombin and therefore retains its anticoagulant properties on the graft surface. The heparin-binding process occurs at the nanometer level and therefore does not affect the overall structure of ePTFE grafts. They retain their 30µm intermodal distance and porosity structure and therefore elasticity, mechanical and handling properties are retained. This graft is also noted in *in vivo* studies to have a decrease in thrombin and platelet deposition. The heparin activity of the Propaten™ grafts is noted to be maintained for up to 12 weeks *in vivo* (14).

One of the first large clinical evaluations of the graft by Bosiers(15) *et al*, looked at the patency rates of these grafts when implanted as femoro-popliteal and femoro-crural bypass grafts. They found that the primary patency rate at 1 year was 82% and 97% for secondary patency rates. The limb salvage rate for patients with critical limb ischaemia (CLI) was 87%. These were very encouraging initial results and were thought to be better than those obtained for non-heparin bonded ePTFE bypass grafts. For comparison, a 2003 meta-analysis showed non-heparin ePTFE bypass grafts had a 1-year patency rate of 59% for primary patency and 66% for secondary patency(16).

In a larger multi-center study (The Scandinavian Propaten™ Trial), Lindholt(17) *et al* analyzed the patencies of 454 grafts. The primary patency rate after 1-year was

86.4% for Propaten™ grafts and 79.9% for PTFE grafts with significance ( $p=0.043$ ). And again, at 1-year, the secondary patency was 88% for Propaten™ grafts and 81% in PTFE grafts. On comparison with autologous vein, primary patency rates at 48 months were significantly higher in the autologous vein group (63.5%) compared with the Propaten™ group (46.3%)( $p<0.03$ ). However interestingly when it comes to secondary patency rates there were no statistical significance between the two groups where autologous vein was 69.6% and Propaten™ was 57.5%(14). This observation with the secondary patencies was considered interesting in that it was possible to salvage the Propaten™ graft once occlusion has occurred. However, on a practical note, surgeons have noted that once occlusion has occurred in vein grafts, it is much more difficult technically to salvage these grafts.

These clinical results show that surface modification using heparin can have a positive result clinically on patients and illustrates a good example of the current research in modifications of existing materials.

## 1.5 Decellularized Vascular Grafts

The concept of decellularised vascular grafts has been around for a while and has evolved over the years. The use of decellularized natural matrices allows the advantage of retaining the natural structure, especially the 3D microarchitecture of natural tissue and mechanical performance of natural tissue and extracellular matrix (ECM) whilst avoiding any immunological adverse reactions. This is the aim of the decellularization process which removes all the antigenic cellular material from the tissue and allows repopulation with the host's cellular material. Another added advantage of the decellularization technique is that there is the potential for repair, growth and remodeling *in vivo*. This makes the decellularization technique a technique which, if it works, has lots of advantages and uses, including suitability for paediatric use as the graft can be incorporated within the host tissues and 'grow' with the child.

The decellularization technique has evolved over the years and involves the use of chemical agents, hypo- and hypertonic solutions, detergents, solvents, biological agents (enzymes and chelating agents) and also physical methods such as abrasion

and agitation. All these techniques have been used to remove all the cellular material without destroying the integrity of the scaffold itself(18).

The technique was first developed in the 1960s using animal tissue and since then a range of vascular grafts have been developed with some even making it to commercial availability. The source of these vascular grafts can be from allogenic or xenogenic sources with the more popular ones mainly being bovine blood vessels and bovine ureter. There have since been prospective randomized trials using these grafts which have concluded that there is no clear advantage of the grafts compared with synthetic grafts(19-21). In addition to these grafts there is concern that cellular components of the allogenic or xenogenic tissues will trigger immune responses in the host. Therefore, techniques have to be employed in which the immunogenic components need to be masked or eliminated, again, without destroying the mechanical integrity of the scaffold itself.

Small intestinal submucosa (SIS) was a scaffold which was explored as a possibility for decellularized vascular grafts. It is essentially a cell-free collagen matrix derived from small intestine. It was implanted as small diameter vascular grafts into carotid and femoral interposition of 18 dogs for 8 weeks. Although there was graft patency rate of 75% and the grafts showed no evidence of infection, thrombus or intimal hyperplasia; the SIS grafts tended towards developing aneurysmal dilation in 11% of the arterial grafts(22). Histologically the grafts tended to develop a dense organized collagenous connective tissue with very little trace of endothelial layer on the luminal surface. The lack of efficient cellular infiltration and poor remodeling of SIS vascular grafts suggested that in the long term this methodology may not be appropriate for vascular graft production.

The main technical problem which was noticed by vascular surgeons was that these vascular grafts tend to lose mechanical strength and post-implantation will result in false aneurysm formation. Another problem with decellularized scaffolds were that they require 're-seeding' with the recipient's cells prior to implantation. This tends to be difficult in normal hospitals without associated specialist tissue culture facilities and means that these grafts do not have 'off-the-shelf' potential. Due to these

complications and issues, clinical favour towards decellularized grafts were quickly withdrawn.

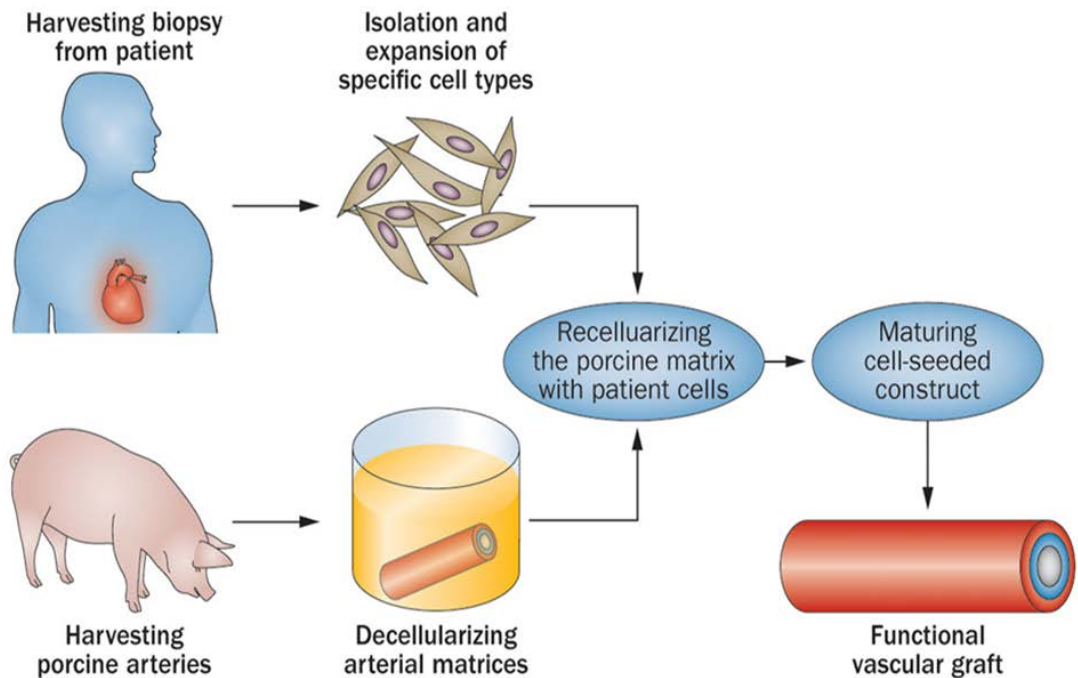


**Figure 1-1 A simplified diagram to show the decellularization process using porcine arteries to create a functional vascular graft. This diagram has been taken from (23).**

Although in recent years, the decellularizing techniques have become more refined and there have been highly optimized techniques coming through which also focus on preserving the mechanical integrity of the scaffolds(24). A combination of either allogenic or xenogenic scaffolds have been used such as ovine arteries(24) and human umbilical arteries(25) and there has been some initial success. However, due to previous failed attempts, there is still concern within the clinical community about the mechanical integrity of these grafts. In the clinical scenario of infection, these grafts would be invaluable and therefore there is still hope that there will be a successful decellularized vascular graft which would be commercially available for these scenarios.

## 1.6 Biodegradable Polymeric Vascular Grafts

There are essentially two types of synthetic polymeric vascular grafts, biodegradable and non-biodegradable. Currently PTFE and Dacron® vascular graft materials are considered non-biodegradable synthetic materials. Popular known biodegradable polymers are usually polyglycolic acid (PGA) and polylactic acid-based constituents and these polymers have been mainly used in biodegradable vascular graft research.

As the polymer is biodegradable, it is thought that the polymer would act initially as an important scaffold for the pre-seeded cells to integrate and gain mechanical strength post-implantation whilst the scaffold slowly degrades over time and in the end, leaving a vessel which is made of only the recipients' cells and tissues. It is important that the original polymer is biocompatible, as well as the breakdown end-products being the non-toxic and excreted by the recipient's body without any systemic or local effect. One of the main struggles for these biodegradable vascular grafts is achieving the balance of scaffold degradation rate with tissue deposition and maintaining mechanical strength. This is highly affected by the type of polymer used, their degradation rate in vivo and various other additional factors such as interpatient variability to take into account.

Initially these biodegradable scaffolds were implanted without prior seeding. However, it was difficult to control the degradation of the scaffolds and usually there was not enough time for the host's cells to repopulate the graft in its entirety. Despite these problems, there has been quite few high-profile attempts in human implantation of these grafts. As one of the main concerns of these graft materials is mechanical strength, arterial substitutes using these materials were not initially advocated. In 2001, Shin'oka(26) *et al* reported the first use of a biodegradable scaffold for use in a 4 year old girl with occlusion of a right intermediate pulmonary artery (a low flow vessel). They isolated a 2 cm peripheral vein for sourcing autologous cells and cultured them for 8 weeks prior to implantation. A tube made of polycaprolactone-polylactic (PLA) acid co-polymer reinforced with woven polyglycolic acid (PGA) was fabricated as the biodegradable scaffold and this was seeded with the autologous cells prior to implantation. This scaffold was designed to degrade in 8 weeks. This operation was a success and led to further attempts at human implantation, whilst

over the years refining their technique. In 2010, Hibino(27) *et al* reported late term results for these further implantations using this technique. Instead of vein harvest and prolonged cell cultures, bone marrow aspirates were now taken and the mononuclear cell component were separated and used to seed the scaffolds. 25 patients underwent implantation of these grafts and although there was no graft related mortality of an average follow-up period of 5.8 years, they did find a 24% incidence of graft stenosis, which was higher than those found in synthetic non-biodegradable vascular grafts. Of note, there were no cases of graft-related mortality, aneurysmal dilatation, graft infection, graft rupture or calcification. 96% of patients were also able to discontinue anticoagulation therapy after 6 months which is a huge advantage when compared with patients with synthetic grafts who have to have long-term anticoagulation.

Shin'oka and Chris Breuer have led their multidisciplinary team at Yale, and now at Ohio, over the years, in their quest for a biodegradable vascular graft. Their research and clinical team went back and forth from 'bench to clinic' multiple times to elucidate the exact mechanisms they observed *in vivo*. Because of their seminal work, they were able to demonstrate the natural history post-implantation of their vascular graft. They found that there was rapid initial infiltration by macrophages, late endothelialization, initial dilation of the grafts with PLA followed by fiber degradation and late contraction of the grafts. There was also increased collagen deposition over time and increasingly organized tissue resembling native vessel over the course of the following year post implantation(28). They also found the cause of the stenosis which they had observed in their human trials. This was thought to be due to due to initial macrophage infiltration and was inversely related to bone marrow (BM) – mononuclear cell seeding (MNC) on the scaffolds. There was early stenosis seen in 80% on unseeded scaffolds and only 20% in seeded. The seeding of the BM-MNC recruited the appropriate cells which induced the correct inflammatory response. A lot of work was conducted over the last few years to understand the mechanisms underlying their therapeutic approach(29). In 2011, the team received the United States Food and Drug Administration (FDA) approval to conduct a clinical trial in the US. Results from their clinical trial is still awaited.

Although Shin'oka and Breuer are not the only research group to initiate research into biodegradable vascular grafts, they are one of the leading research groups in the world and the timeline of their research gives a very good illustration of the evaluation of their vascular grafts both *in vitro* and *in vivo*.

From another angle, Wu(30) *et al* used a fast-degrading polymer composed of a composite polymers containing poly(glycerol sebacate) and polycaprolactone. There was no prior cell-seeding prior to implantation as interposition grafts within the rats' abdominal aorta for 3 months. At the end of the time point, the grafts were found to have fully integrated and remodeled within the host's environment and showed high patency rates of 80.9%. The explanted arteries were found to be compliant and had high burst pressures of up to  $2360\pm 673$ mmHg, which is approaching that of native aorta  $3415\pm 529$ mmHg. In comparison with human saphenous vein which has a burst pressure of  $1680\pm 307$ mmHg, and this is a well-known conduit in peripheral bypass surgery. They found that despite the lack of pre-seeding, the grafts were very well-integrated within the host environment despite the results found by Shin'oka. These grafts would have a large 'off the shelf' potential. Unfortunately, one of the downfalls of this type of approach is the question of 'what would happen' in the event that the graft material degrades before host integration has taken place.

The Niklason Group(31) has taken a combination of techniques to try and produce vascular grafts with a reduced fabrication time. They sourced smooth muscle cells from cadaveric donors and seeded them onto polyglycolic acid (PGA) polymer scaffolds and incubated them in a pulsatile bioreactor. During this period the cells would secrete extracellular matrix proteins, mainly collagen, building its own biological scaffold over the polymer scaffold. At the end of the incubation period, which is when the polyglycolic acid scaffold has degraded away, the resultant tissue is then decellularized to remove all the antigenic components within the tissue. These grafts can then be stored in phosphate buffer solution (PBS) until use or if required they can be seeded, prior to implantation, with endothelial cells.

These are examples of the different approaches which have been taken by different research teams looking into the use of biodegradable polymers as vascular grafts.

The interest in biodegradable vascular grafts comes from paediatric surgeons who require a vascular graft which will eventually be remodeled into a native vessel, with eventual biodegradation of the synthetic components. The biodegradable vascular graft means that in paediatric cases, these grafts can grow with the child. In the case of the traditional synthetic grafts, PTFE and Dacron®, the grafts are not 'living grafts' and will not grow with the child. Therefore, operations, sometimes, have to be delayed till the child reaches a certain size so that much of normal growth has already taken place, before the implantation of the graft.

### 1.7 Tissue-Engineering Vascular Grafts by Self-Assembly

Tissue-engineered vascular grafts were first produced by Weinberg and Bell in the 1980's(32). They used bovine endothelial cells, fibroblasts and smooth muscle cells and these were co-cultured in a collagen matrix and then shaped into tubes. Although tissue architectures analogous to natural blood vessels were achieved, the constructs required the support of a Dacron® mesh for extra strength and despite this, the mechanical properties were still poor.

Despite this, Weinberg and Bell had set a trend in attempting to construct a completely biological, 'living' laboratory-grown vascular graft in a 'self-assembly' approach. Although there have been a few attempts in manufacturing these vascular grafts, L'Heureux(33) *et al* were able to develop one of the first implantable biological-based tissue engineered vascular graft that was free from any synthetic material for extra support. The fabrication process is complex and long for one of these grafts but recently has shown some initial success in being used as a vascular access graft.

The methodology for making these grafts required time and patience. The resulting blood vessel was to be composed of three layers which was a functional endothelium seeded onto an 'internal membrane' layer made of smooth muscle cells and fibroblasts. The internal membrane layer is constructed by rolling a sheet of fibroblasts around a cylindrical support and culturing it until the individual layers are

fused together forming a homogenous tissue. This tissue is then devitalized by dehydration and thus is itself a scaffold for the vascular graft itself. After this tissue has been devitalized a further sheet of smooth muscle cells is then rolled around it forming the medial layer. A further sheet of fibroblasts is then rolled around this layer and the layers are then allowed to fused for a further 8 weeks. At the end of this maturation period, the mandrel is removed and the resulting lumen is then further seeded with endothelial cells(34).

Over time the methodology for production of these vascular grafts have improved in particular to fit a commercial setting. Recently the graft has been commercialized as Lifeline® (Cytograft Tissue Engineering Inc., Novato, California) and is undergoing clinical evaluation. They have undergone clinical evaluation as haemodialysis access grafts. Initially, these grafts were constructed from autologous cells from patients with end-stage renal failure and were delivered as ‘living’ grafts with a production time of 6-9 months(35). Post implantation of the graft there was a safety phase of 3 months prior to grafts being used for dialysis access. They initially enrolled 10 patients for the study but one had to be withdrawn prior to implantation due to poor health. Of the 9 implanted, 3 grafts failed prior to the end of the safety period with 1 patient dying shortly after implantation of unrelated causes and 1 patient withdrawn due to successful kidney transplantation. Of the remaining patients only 4 of the grafts were still function at the end of 21 months. Failures were due to dilatation, thrombosis and aneurysm formation.

Further evolution of the Lifeline® graft meant that although produced in the same way, these grafts were then dehydrated and then stored in -80°C and stored for 9 months. Pre-implantation testing showed that this treatment did not destroy the mechanical properties of these grafts and these grafts were not endothelialized prior to implantation. This was a trial at making the Lifeline® graft ‘off the shelf.’ Wystrychowski(36) *et al* reported 3 cases which used the ‘non-living’ version of the Lifeline® graft. These grafts were inserted in the brachio-axillary position and were first used for dialysis at 8-12 weeks. Immunological and inflammatory blood markers were within normal limits. However, there were 2 thrombogenic failures at 3 and 5 months respectively. The third failure was due to pre-existing sepsis which the

patient succumbed to. There were some questions as to the graft performance due to the lack of 'pre-seeding' as it was noted that at the puncture site there was delayed extravasation and slight bleeding which was not seen with the 'living' Lifeline® grafts which are 'pre-seeded'. They thought that this might be due to slower repair processes due to the absent cells. Furthermore, the thrombogenic failures were thought to be due to stenosis occurring within the graft rather than the lack of endothelium.

Although there is some initial success in these clinical evaluations of these grafts, there are still concerns about the mechanical properties especially seen with failures due to dilatation and aneurysm formation. The 'living' version of the Lifeline® grafts have a long fabrication time and therefore this makes these graft unsuitable for 'off the shelf' uses. There is potential that the 'non-living' version may make this use a possibility but at present, further optimization and development is still required. However, these grafts do possess many advantages such as lack of immunological activation, low infection risk as native tissue, lack of synthetic graft material and the ability of the host system to integrate and remodeled with the graft, thereby being integrated like a native vessel. Unfortunately the long fabrication time of 6 to 9 months and the high associated cost >US\$15,000 means that these grafts are unlikely to be regularly adopted by clinicians in the future(31).

### **1.8 Why Synthetic Non-Biodegradable Vascular Grafts May Still have the Advantage?**

Although at present there are still many avenues of research being undertaken to produce the 'ideal' vascular grafts, none of the methods have managed to produce the 'perfect' vascular graft. Some of the common techniques which have been employed to produce vascular grafts have been discussed in this introduction.

However, at present, although there have been some very interesting grafts which are currently undergoing clinical evaluation, they all suffer from a variety of faults. The most common cause of graft failure of the newer grafts tends to be mechanical

integrity and the unavailability of these grafts for 'off the shelf' use. Synthetic non-biodegradable vascular grafts may have the present advantage. These materials do not degrade *in vivo* and are also available as 'off the shelf' entities and thereby allowing usage in emergency situations.

With the current and emergent vascular graft materials, there is still a lot of scope for improvement as these grafts still do not promote endothelialization. A layer within the luminal surface of the graft ensures the patency of the vascular graft. The endothelial layer is able to release protective factors that lead to anti-thrombogenicity thereby protecting the graft from premature failure(37). They also have anti-inflammatory and angiogenesis properties and lead to reduce intimal hyperplasia, thereby increasing graft patency. Professor Zilla and his team conducted a clinical trial in which endothelial cells were seeded onto ePTFE grafts prior to implantation(38) and their results showed significantly improved long term patency of PTFE groups pre-seeded with endothelial cells compared with standard. Primary patency was 69% at 5 years for endothelialised ePTFE grafts compared with 45% at 5 years with unendothelialised grafts(7).

Thereby the rational lies that currently, due to limited technology, we are still limited in our efforts to come up with the 'ideal' vascular graft. Thereby, modification of current biomaterials remains the best course of action to ensure that these vascular grafts do not fail mechanically post implantation and also are available as 'off the shelf' options.

The current idea is to modify the luminal surface of these grafts so that they are able to incorporate a layer of endothelial cells. To ensure that this is possible, as well as eliminate the 'pre-seeding' step, which would not allow these grafts to be 'off the shelf', there are efforts to produce 'self-endothelialising' vascular grafts. These grafts would ideally be able to recruit endothelial cells through a variety of methods; inward migration of endothelial cells, or transmural migration or endothelial cell capture, so as to endothelialise the graft post-implantation.

## **1.9 Aims of This PhD Thesis**

The aims of this PhD is to produce a ‘self-endothelialising’ synthetic non-biodegradable vascular graft, using a material previously already developed in the laboratory, POSS-PCU. This is a polycarbonate urea urethane (PCU) which is attached to a nanoparticle, polyhedral oligomeric silsesquioxane (POSS) and has shown promise as compliant vascular graft material. However, in large animal studies, this POSS-PCU polymer has shown that there is a lack of endothelialisation despite out-performing standard ePTFE grafts when implanted as a carotid interposition graft in a sheep model(39).

Thus the aim of this Thesis is to explore different methodologies in how to physically and chemically alter the luminal surface of the material so as to encourage endothelial cells to adhere on the surface. This is in addition to studying and looking in depth the endothelial cell interaction with the surface and also with other cell types, when present.

## **1.10 Hypothesis of This PhD Thesis**

The hypothesis of this Thesis is based on the manufacture of a polymer, POSS-PCU, which can be used as a small diameter vascular graft material and its subsequent modification to achieve this.

Firstly, it was thought that it is possible to produce all the components of POSS-PCU in-house from raw materials and thereby reducing the productions costs of the polymer. Furthermore, as this is a graft material which will be eventually used for implantation in humans, toxicity testing will be required to prove that this is a possibility. It has also been noted that despite improvements of this material over those in current clinical use, there were still properties of the material which could be improved. One of these properties was the patency rates of these vascular grafts which can be achieved by fine-tuning the luminal surface of these grafts. This Thesis aims to use different techniques to either promote a ‘non-stick’ surface or to achieve endothelialisation so that patency rates can be improved.

From previous work(40-42) by other authors, it has been shown that it is possible to modify surface topography and chemistry to improve endothelial cells adhesion. The hypothesis of this Thesis is that this is possible on POSS-PCU polymer and thereby this will enhance the process of endothelialisation as it will make it an environment on which endothelial cells are able to adhere. This can be achieved by fine-tuning both the surface chemistry and topography of the polymer surface. Endothelial cells are known to also interact with surface topography and it is thought that cell adhesion especially will be improved with the introduction of surface topography in both the microscale and nanoscale. However, in addition to this, surface chemistry also plays a crucial role and this will be measured in terms of water contact angle. The importance of these surface properties will be explained in the upcoming Chapters of this Thesis.

## **1.11 Chapter Description**

Chapter 1 – This Chapter looks at the in-house production of the nanoparticle, POSS, and the use of this nanoparticle to modify the surface chemistry of the polymer itself

Chapter 2 – This Chapter uses plasma treatment to alter the surface of the POSS-PCU polymer and looks at its effect on endothelial cell biology

Chapter 3 – This Chapter combines nanopatterning with the plasma treatment on the POSS-PCU polymer and again looks at the effect on endothelial cell biology

Chapter 4 – This Chapter focuses on the effect that nanotopography has specifically on endothelial cell adhesion

Chapter 5 – This Chapter looks at the effect of co-culture endothelial cells with mesenchymal stem cells on topography and whether this would have a potential effect on calcification



## **Chapter 2: Materials and Methods**

## **Chapter 2 Materials and Methods**

This chapter contains the materials and methods of the experiments which were commonly conducted throughout the different chapters of this thesis. The majority of the experiments were conducted between two laboratories, Division of Surgery and Interventional Science (Royal Free Campus), University College London and Centre for Cell Engineering, University of Glasgow. The methodology of these experiments were taken in combination from both these laboratories' protocols.

### **2.1 Cell Culture of Human Umbilical Vein Endothelial Cells**

Human Umbilical Vein Endothelial Cells (HUVECs) were sourced from both Life Technologies (Paisley, United Kingdom) and Promocell (Heidelberg, Germany). For the initial experiments, they were sourced from Life Technologies and for these experiments, the media used was M200 and Low Serum Growth Serum (LSGS) (both from Life Technologies).

The decision to source them from Promocell was undertaken as the experiments went on due to the ability to have utter traceability for the cell source and also to have a common cell source for all the cells.

The passage for all experiments undertaken with HUVECs were between P3 – P7.

The cells were all incubated in an incubator with 5% Co<sub>2</sub>/ 20% O<sub>2</sub>.

### **2.2 Conditioning Cell Culture of HUVECs for Co-Culture Experiments**

HUVECs from Promocell were placed in conditioning media for at least 24 to 48 hours and check using normal microscopy, prior to co-culture experiments. The HUVEC conditioning media were made as M199 medium (Gibco), 10% inactivated Fetal Bovine Serum (Gibco), 2% Penicillin-Streptomycin (Gibco), 0.03mg/ml Endothelial Cell Growth Supplement (Sigma Aldrich) and 0.1mg/mL of Heparin (Sigma Aldrich). The cells were then incubated. This protocol is modified for our laboratories from Bidarra *et al*(43).

### **2.3 Cell Culture of Mesenchymal Stem Cells (MSCs)**

Mesenchymal stem cells were sourced commercially from Promocell. Basal media was made up in Dulbecco's Modified Eagle's Medium (DMEM) medium (Gibco), 10% inactivated Fetal Bovine Serum (Gibco), 2% Antibiotic Mix (Penicillin-Streptomycin, Fungizone and L-Glutamine) (Life Technologies), 1% Essential Amino Acids (Life Technologies) and 1% Sodium Pyruvate (Life Technologies). MSCs were used at as low passage as possible (ideally below P3) as there is a high risk of differentiation of the MSCs at a higher passage.

### **2.4 Cell Culture of Co-Culture of MSCs and HUVECs**

The media for made of a ratio of 50:50 of the HUVEC conditioning media and MSC basal media. This has been taken from the optimized protocol from Bidarra *et al*(43).

### **2.5 Fabrication of POSS-PCU**

Preparation of the POSS-PCU polymer has been reported extensively. In brief, polycarbonate diol and transcyclohexanechlorohydrinisobutyl-POSS were added to a reaction vessel then heated to 130°C while being stirred under nitrogen gas. The reactants were then cooled before 4, 4'-methylenebis (phenyl isocyanate) (MDI) was added and all components reacted for 30 minutes under nitrogen gas.

This reaction then forms a prepolymer before dimethylacetamide (DMAC) was added to convert this prepolymer into a solution. This solution was then cooled before the chain extender, ethylenediamine, was added dropwise until the reaction was completed. The chain stopper, 1-butanol, was then used to prevent further unwanted polymerisation. All of the reagents were supplied by Sigma Aldrich (Dorset, UK) and used as provided with the exception of POSS, which was supplied by Hybrid Plastics Inc (Mississippi, USA).

## 2.6 Fabrication of Nanopatterned Surfaces on POSS-PCU

The fabrication of the both the micropatterned and nanopatterned surfaces were undertaken at the James Watt Nanofabrication Centre (JWNC) Cleanroom, University of Glasgow.

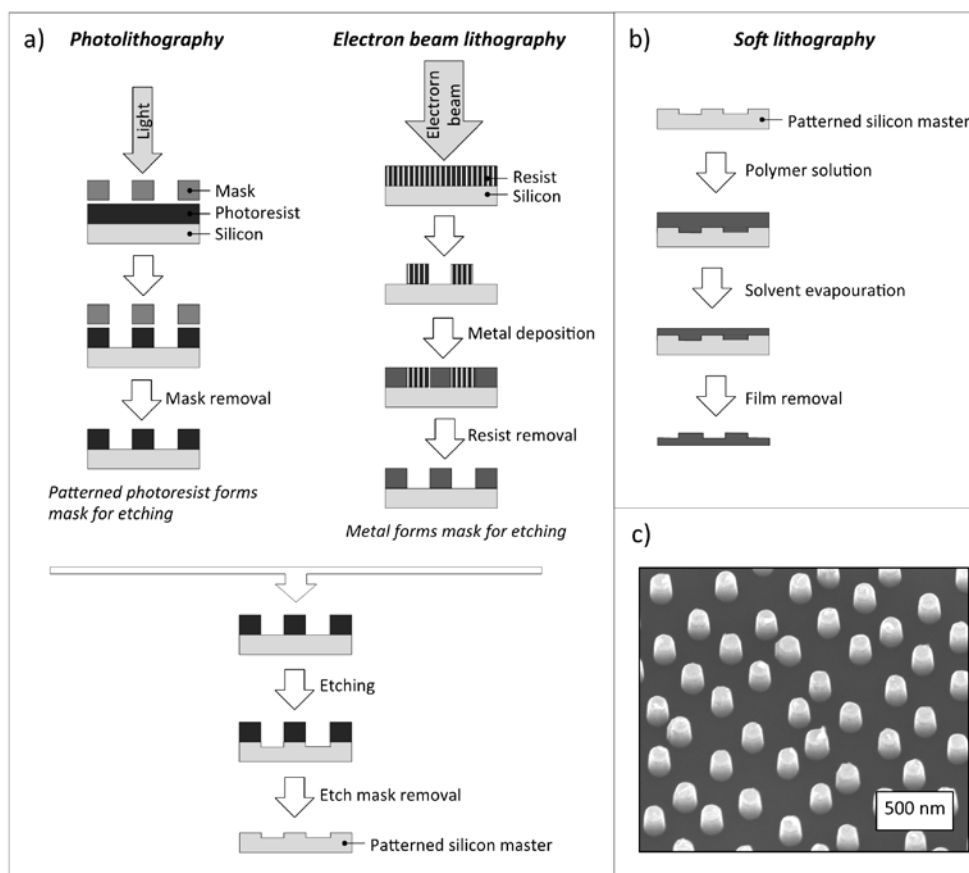


**Figure 2-1** This is a step-wise diagram which shows how photolithography and electron beam lithography (a) are used to produce micro- and nano-sized features, respectively. B) shows how soft lithography can be used to produce the surface features onto the POSS-PCU polymer and c) shows the SEM of a silicon master, and in this case, this is the NSQ nanopattern

Photolithography was used to micro-sized features and electron-beam lithography is used to create nano-sized features. The diagram above shows a step-wise process in which these substrates are fabricated. Once a silicon master is fabricated, soft lithography is used to produce the features on the POSS-PCU polymer. This is conducted by pouring the polymeric solution onto the silicon master and then placed

in an oven at 65°C for a minimum of two hours until all the solvent DMAC (Dimethylacetamide) has evaporated. The resulting polymeric film is then removed.

## **2.7 Preparation of Polycarbonate Surfaces for Cell Seeding**

The polycarbonate substrates are plasma-treated prior to sterilizing with 70% Ethanol for 20 minutes. The substrates are then washed with HEPES-Saline generously. Cell seeders (under patent at University of Glasgow) are also sterilized in the same fashion. The cell seeders are carefully placed on top of the substrates and placed in 6-well plates (Corning). 400µL of media and cells for seeding is pipetted carefully on the cell seeder. The cells are allowed to adhere (2 hours for MSCs and 4 hours for HUVECs) in an incubator. Adherence of the cells are checked using microscopy prior to removing cell seeders carefully and flooding with excess media. Confirmation of cell adherence was by visualizing cell morphology as having a 'flat and spread-out' appearance on the surfaces compared with a 'rounded' appearance as non-adherence.

## **2.8 Immunofluorescence**

Samples were fixed in 4% formaldehyde for 15 minutes at 37°C then washed before placing in permeabilising buffer and blocking in 1% (w/v) bovine serum albumin/PBS. Samples were then stained with anti-vinculin antibody (1:150) (Sigma) in 1% (w/v) BSA/PBS or anti endothelial nitric oxide synthase (eNOS) antibody (1:50), in conjunction with rhodamine/phalloidin (1:500), and incubated at 37°C for 1 hour. Samples were subsequently washed 3 times for 5 minutes (0.5% Tween-20 in PBS) and then the secondary antibody, which was biotinylated, was added (Vector Laboratories) at 1:50 in 1%(w/v) BSA/PBS. Samples were then incubated for 1 hour at 37°C. After further washing, FITC-conjugated streptavidin (1:50, Vector Laboratories) was added and incubated for a further 30 minutes at 4 °C. Samples were given a final wash before mounting using Vectashield with DAPI nuclear stain (Vector Laboratories).

## **2.9 Live/Dead Staining**

Live/Dead staining was undertaken using the Live/Dead Viability/ Cytotoxicity kit for mammalian cell (L-3224, Invitrogen) from Life Technologies. In short, calcein AM and ethidium homodimer-1 were made up to concentrations of 2 mM and 4 mM, respectively, using phosphate buffered saline (PBS). These solutions were incubated with the samples for 30 minutes at 37°C, before washing samples with PBS and then analysing with a fluorescence microscope (Zeiss Axiovert M200).

## **2.10 Coomassie Blue Staining**

Coomassie Blue staining was undertaken to look at cell morphology. The Coomassie Blue solution is composed of 0.2% Coomassie Blue, 46.5% Methanol, 7% Acetic Acid and 46.8% Water. The Coomassie Blue solution is filtered post-preparation (using 0.2µm filters) prior to applying the solution to the samples for 2 minutes. The solution is then removed and the samples are washed thoroughly with deionized water. The samples are then dried prior to visualizing under a microscope.

## **2.11 Scanning Electron Microscopy (SEM) Preparation**

For visualising substrates, sample preparation was undertaken by drying and sputtering coating with gold at a thickness of 20nm. The samples are then visualized under vacuum by a scanning electron microscope.

## **2.12 Atomic Force Microscopy**

Substrate samples were dried and then super-glued onto glass slides to make sure that the samples do not move and interfere with the sensitivity of the instrument (JPK Nanowizard 3, JPK). Analysis of the results was completed using Nanoscope®.

## **2.13 Statistical Analysis**

When there are three or more samples with normally distributed data one-way analysis of variance (ANOVA) is used to compare the means of the samples to see if they come from the same population. To test that the samples contain normally

distributed data, normality tests have been applied such as D'Agostino's K-squared Test.

Non-parametric data have been analysed with both Kruskal Wallis and Mann-Whitney tests. Mann-Whitney has been used with there has been only two samples of data and Kruskal-Wallis when there are three or more samples.

Calculation using these statistical tests have been facilitated with the statistical program, Prism® (GraphPad Software Inc., California).

## **2.14 Conclusion**

More specific methodology for the specific chapters will be found in the 'Materials and Methods' of the Chapters themselves.

## **Chapter 3: Surface Focus: Manufacture and Optimisation of POSS Nanoparticle**

## Chapter 3 Surface Focus: Manufacture and Optimisation of POSS Nanoparticle

### 3.1 Introduction

Commercially available vascular grafts are made of polytetrafluoroethylene (PTFE) and polyethylene terephthalate (PET, Dacron®). Dacron® was first developed by two chemists in Manchester in 1941, JR Whinfield and JT Dickinson. In vascular surgery, this material was made famous by Dr DeBakey in 1952 who made the first Dacron® tube graft for aortic reconstruction on his wife's sewing machine. To this day, Dacron® is the most used material for aortic replacement and large diameter lower extremity bypass surgery. PTFE, on the other hand, was developed by DuPont in 1938 and marketed under the trademark Teflon (DuPont) in 1945. WL Gore and Associates further developed a more compliant and porous version for biomedical applications naming it expanded PTFE (ePTFE)(6). These two materials have therefore been the mainstay of vascular bypass surgery. In a recent Cochrane Review(8), there were 4 studies comparing PTFE with Dacron® for above knee bypass applications and there were no significant differences in primary patency seen in 24 months. For below knee bypasses, there is very limited evidence and one of the main studies by Post *et al*, showed there is a trend towards improved primary patency rates for PTFE compared to Dacron® and significance was reached at 24 months(7).

Radial compliance is thought to be an important feature of vascular grafts, more so than material strength. This meant that an ideal material would have to be able to incorporate this feature and therefore, polyurethane polymers were investigated as they had a highly elastic nature and other beneficial properties of being biocompatible, compliant and non-toxic. These properties provide an interesting alternative to Dacron® and PTFE.

Polyurethanes (PU) are essentially copolymers of flexible macrodiols (soft segments) combined with sequences of diisocyanates and short diols (hard segments). Unfortunately, depending on the soft-segment of the polyurethane that is being used, there can be potential caveats of danger due to long term stability of the material in

vivo. This is due to biodegradation and therefore pose a hazardous risk in vascular implants, (i.e. pseudoaneurysm formation). The choice of soft-segment in the polymer usually governs this property of the polymer meaning that choice of poly(ester) polyurethane will hydrolyse and poly(ether) polyurethane will oxidise(10). More recently, for the use of vascular grafts, polycarbonate urea urethane has been investigated and been marketed as Cardiotech® but these grafts have shown an abnormally high rate of thrombosis (unpublished data) and have been withdrawn from the market. Therefore, there is a need for improvements to be made to polyurethane-based polymers to overcome these short-comings. Compared with other materials such as metals and ceramics, polymers generally have lower moduli and strength. It was discovered that the mechanical properties of polymers can be reinforced by incorporating nano-size inorganic particles (defined as having at least one dimension in the range 1-100nm) within the polymeric chain(44). This allows the polymer to be efficiently improved whilst maintaining its inherently low density and high ductility. The idea is to build the nanoparticle into part of the polymeric chain, and this can either be as a pendant group or a terminal group, forming a polymer nanocomposite. One such nanoparticle which has played an important role in the development of polymer nanocomposites is the POSS nanoparticle, in recent years.

Polysilsesquioxanes are represented by the formula  $(\text{RSiO}_{1.5})_n$ , and can be regarded as organic-inorganic hybrid materials at a molecular level. A subtype of these are known as polyhedral oligomeric silsesquioxane (POSS) and these possess a cubic rigid (T8) structure represented by the formula  $\text{R}_8\text{Si}_8\text{O}_{12}$  where the central inorganic core ( $\text{Si}_8\text{O}_{12}$ ) is functionalized with organic moieties (R) at each of the 8 corners. The R-group may be a hydrogen-atom or an inorganic functional group (e.g. alkyl, alkylene, hydroxyl, epoxide or acrylate). These are usually formed from hydrolysis and condensation reactions of chloro- or alkoxy silanes. Historically, they can include long reaction times, months in some cases, with very low yields. Intense research by Edwards Air Force research facilities have meant that these particles could be produced in many different forms and at yields conducive for commercial use(45). However recent improvements in their manufacture means that there have since been shorter reaction times allowing commercial manufacture of some of these particles to

include high yield. In recent years, a commercial company Hybrid Plastics® have become the main suppliers for these nanoparticles in many different forms on a commercial basis.

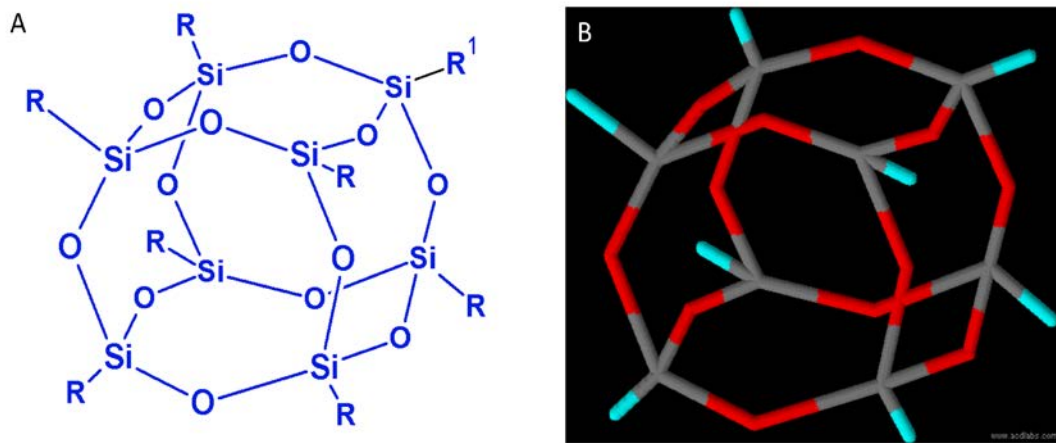


**Figure 3-1** Figure to show A) the chemical structure of the full cage POSS nanoparticle and B) the 3D structure of the POSS cage

There are some important general features of POSS which allow for their use as a nanoparticle of choice(46):

1. Their nanoscale dimensions
2. Unreactive R groups, usually organic for stability, solubility and compatibility
3. One or more reactive X-groups (may be the same as R for further modification, grafting or polymerisation)
4. Well-defined, three dimensional structure with different R and R1 groups for introduction into polymers and composite materials
5. Thermally and chemically robust structure

The incorporation of POSS nanoparticle into the formulation of the polymer can be achieved and produces a hybrid nanocomposite polymer. This can be conducted by

blending the POSS into a polymer matrix, by covalently bonding POSS into a polymer or by using POSS as a pendant group of a polymer. These three methods have been extensively studied by many different research groups. The incorporation of POSS with the polymer chain has been shown to improve the mechanical properties and enhance the stability of the polymer(47). Other beneficial effects include fire retardant, oxidation resistant and surface hardening which would be important in more industrial applications(48).

Covalent bonding allows for the POSS nanocage to be incorporated as a terminal group within the polymeric chain. To be able to achieve this, a reactive pendant group needs to be available in the POSS-nanocage to allow this to happen. Different structures of the POSS-nanocage are available and demonstrate the versatility of the molecule. The POSS-trisilanol is available as partially condensed cage version of the complete POSS-nanocage. This allows for the required reactive group to be 'corner-capped' onto the POSS nanocage and therefore allow further reactions to take place.

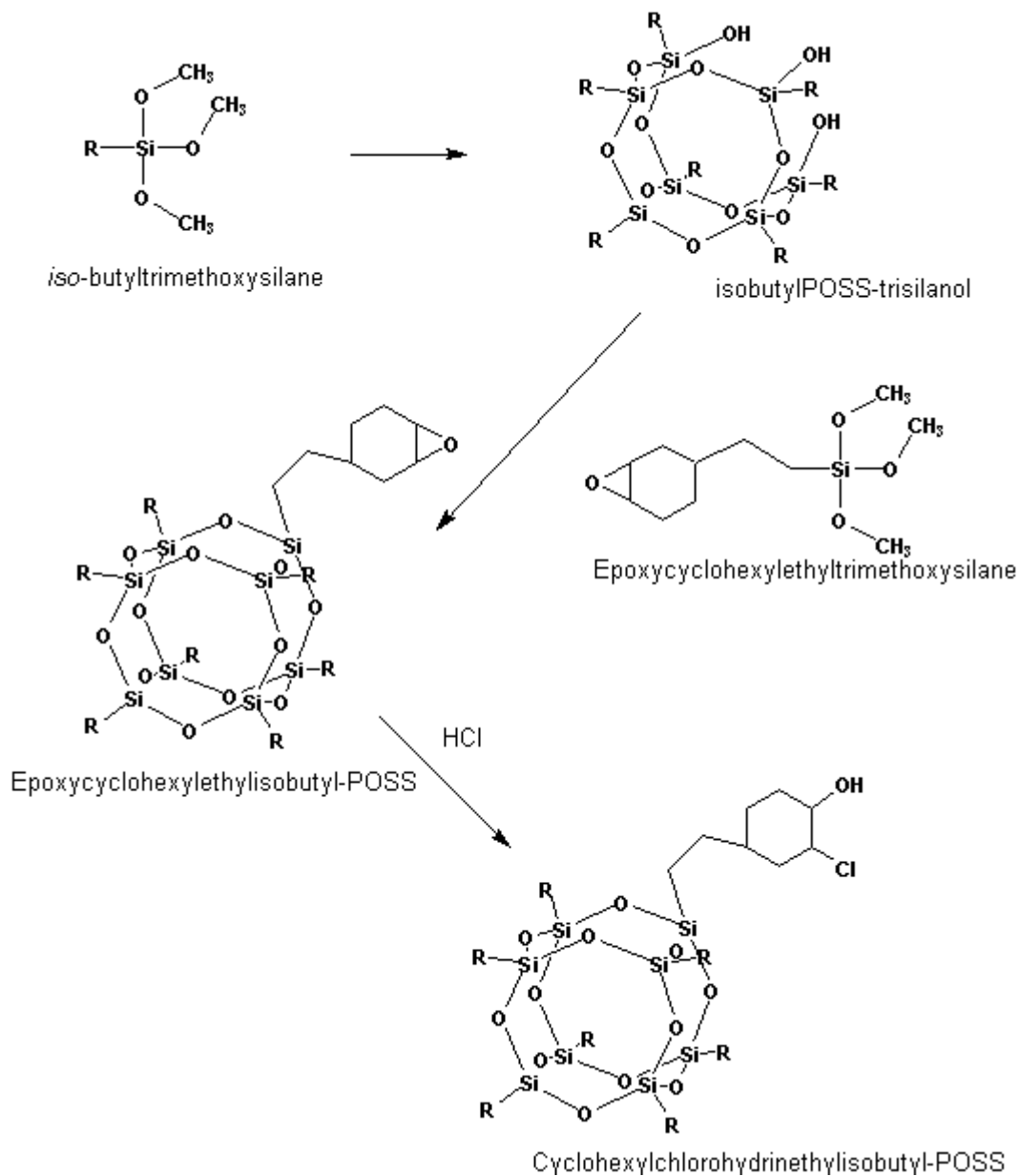


**Figure 3-2** Diagram to show the proposed step-wise methodology of producing POSS-functionalised with a chlorohydrin group which can then be chemically attached to a polymeric chain

A proposed methodology for the generation of a POSS which allows incorporation into a polymeric chain was designed.

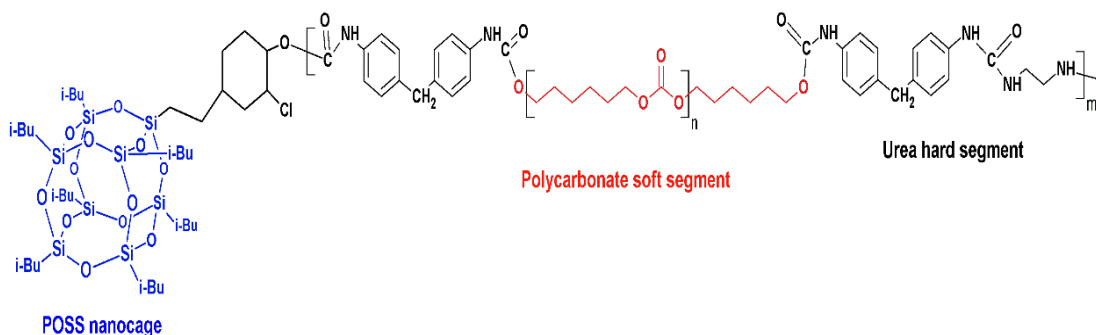


**Figure 3-3** This figure shows the chemical structure of the UCL patented POSS-PCU vascular graft material. Note the POSS nanocage is at the end of the polymeric chain.

The ideology for the fabrication of the POSS nanoparticle is to tailor-make one which is compatible for incorporation into the polycarbonate urea urethane backbone of the polymer. This POSS nanoparticle will play an important role in improving the mechanical properties of the polymer itself. This is an important feature in the development of vascular grafts, especially with the further development of polyurethane-based vascular grafts.

In addition, the POSS nanoparticle itself can enhance the bulk properties of the material itself and can also play an important role in the surface properties of the material. The ability to fabricate the POSS nanoparticle itself allows for a more tailored approach to the development of a vascular graft. This means that desirable properties can be elucidated by the covalent positioning of the nanoparticle to the polymeric chain.

The tailored approach of fabrication of a vascular graft is important as the properties of the material can be tailored to suit the purpose of the application. The use of dispersion of different POSS nanoparticles with different chemical moieties so as to change the bulk properties of the polymer itself is a patented technique of Hybrid Plastics Inc, but holds an important use for changing certain properties of the polymer. Certain POSS chemical moieties such as one incorporating a fluoro-group can render the polymer hydrophobic as well as chemically inert.

A medical device has important implications in the commercial market as well as the clinical arena. However, new start-ups and spin-offs with innovative ideas are rarely

given opportunities from large corporations. This is due to a heavy saturation in the medical devices of products which clinicians feel adequately provide and meet current clinical needs. On top of this, health committees such as National Institute for Health and Care Excellence (NICE) and individual primary care trusts in the UK demand proof of superiority of the product over current established treatments with clinical evidence and also evaluations of health economics. Figures from the US FDA (Food and Drug Association) show that there are more applications for extension of the roles of current devices or improvements, rather than completely new products or devices. Large manufacturers of medical devices have confessed that they do not spend on R&D services anymore and money is spent on 'buying' up the new generation of products. This has important implications for small companies and spin-offs as access to venture capital is now lower. Research councils do have funding available for bringing new medical devices to market, however, although there is money for research and development, a sense of trepidation is still felt for clinical trials of medical devices. This is due to the high risk of failure of the device and subsequent 'fall-out' such as insurance pay-outs if the damage caused to the subject is high, as well as other heavy financial implications if there was device failure.

Therefore, this shift in mentality has meant that there is a significant decline in large vascular graft manufacturers such as WL Gore Cook Medical taking on novel innovations such as the POSS-PCU vascular grafts without at least a good clinical outcome. Despite a recent Wellcome Trust grant to fund the clinical trials for this novel material as a vascular access graft, material sourcing is still a problem and high costs, especially with agreements from Hybrid Plastics for the source of their nanoparticle. The ability to manufacture the nanoparticle in-house would help with the production costs of the POSS-PCU vascular graft.

### **3.2 Hypothesis**

The hypothesis for this chapter is:

1. The POSS nanoparticle can be synthesised in our local laboratories

- a. Partially condensed POSS- trisilanol can be synthesised via a hydrolytic reaction
  - b. POSS trisilanol is functionalised by the introduction of an epoxy-group
  - c. POSS-isobutyl-chlorohydrin nanoparticle is then produced in which it has a reactive group with which to incorporate into our polycarbonate urea urethane polymer for fabrication into a vascular graft
2. This POSS nanoparticle can be incorporated into our polycarbonate urea urethane polymer<sup>4</sup>. Reduction in costs overall for an in-house system compared with purchasing the POSS nanoparticle
  5. This POSS nanoparticle has also the ability to initiate subtle chemical changes onto the surface of the polymer and therefore alter the surface to make the surface more cytophilic

### **3.3 Materials and Methods**

#### **3.3.1 Synthesis of partial-cage of $(i-C_4H_9)_8Si_8O_{12}$ from Isobutyltrimethoxysilane**

Isobutyltrimethoxysilane (523.3 mmol) was added to  $LiOH \cdot H_2O$  (238.3 mmol) which has been dissolved in deionised  $H_2O$  (444 mmol), acetone and methanol mixture (88/12 ratio). This is then left to stir and refluxed at  $50^\circ C$  for at least 18 hours (a). At the end of the reaction time, the mixture is then quenched with 1N HCl and then stirred vigorously for 2 hours at room temperature (b). A white precipitate will appear and precipitate out of solution, during this time the solution will also turn yellow in colour. At the end of the 2 hours continuous stirring, the white precipitate is separated from the solution using filter paper (c).

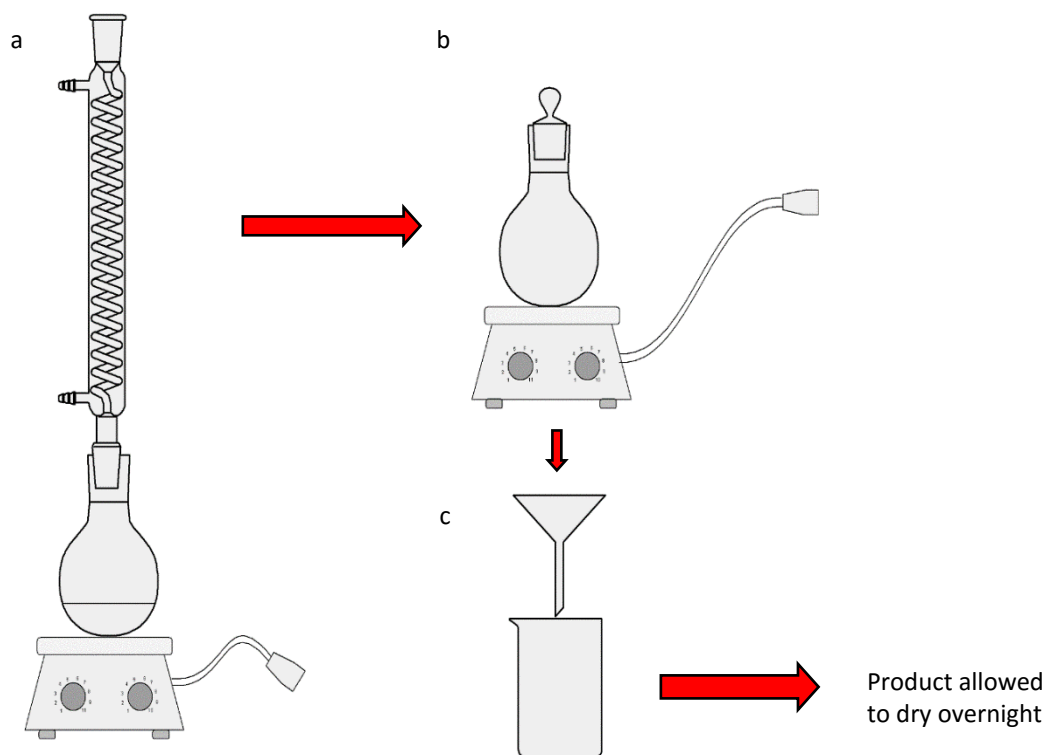


**Figure 3-4** Diagram to show the preparation of the partial cage POSS  $(i\text{-C}_4\text{H}_9)_8\text{Si}_8\text{O}_{12}$  from Isobutyltrimethoxysilane

The resulting solid is then washed liberally with acetonitrile and then the product is left to air dry overnight. The product yield was found to be 88%.

### 3.3.2 ‘Corner-Cap’ Reaction

POSS-Trisilanol (2.52 mmol) was combined with trimethoxy-2,7-oxabicyclohept-3-ethylsilane (2.6mmol), deionised  $\text{H}_2\text{O}$  (3.6mmol), tetraethylammonium hydroxide (0.24mmol) in a solution of THF in a flat-bottom flask. This is left to stir at room temperature overnight to allow the reaction to occur.

Following this, half the THF was left to evaporate in a fume cupboard for 8 hours and excess methanol is added to precipitate out the product. A white product will appear and this is then filtered out of solution. This is then washed in Ethanol and the product left to dry overnight in an evaporating dish.

### **3.3.3 Formation of POSS-Chlorohydrin**

Epoxy-POSS is taken added to  $\text{CHCl}_3$  to dissolve it. Concentrated hydrochloric acid (37%) was then added and vigorous stirring for 30 minutes. Two miscible layers are seen with the top layer being HCl and  $\text{CHCl}_3$ . Using a separating column, the  $\text{CHCl}_3$  is filtered off and kept. Sodium Bicarbonate is placed in excess to neutralise any remnants of HCl acid. The resulting mixture is then centrifuged with  $\text{Na}_2\text{CO}_3$  at 3000rpm for 1 minute. The liquid is then poured off leaving the salt at the bottom. The liquid is then allowed to evaporate, leaving a crystalline solid to form, this being POSS-Chlorohydrin.

### **3.3.4 Solid State NMR**

The POSS to be analysed was dissolved in deuterated chloroform ( $\text{CDCl}_3$ ) into a 5mm NMR tube (Norell®). This was then processed in a Bruker NMR detector.

### **3.3.5 Melting Point**

The solid sample to be tested was placed with a thermometer in a small test tube surrounded externally with glycerol. The glycerol is slowly heated and the moment the solid sample melts, this is taken to be the melting temperature.

### **3.3.6 Fournier Transmission Infrared (FTIR) Spectroscopy**

The crystal is cleaned with Propanol and allowed to air dry before using. The crystallised product is placed on the detector and secured before the scan. A 'fingerprint' of the spectrum is then generated.

### **3.3.7 Thin Layer Chromatography (TLC)**

A potassium permanganate ( $\text{KMnO}_4$ ) solution was made up, consisting of 1.5g  $\text{KMnO}_4$ , 1.25ml of 10% NaOH, 10g  $\text{NaHCO}_3$  in 200ml deionised  $\text{H}_2\text{O}$ . This solution was well mixed and ready to use. Vertical linear development was used to carry out the TLC. A solvent solution is made up for the solvent tank. From experience, it was found that a mixture of 20% ethyl acetate and 80% cyclohexane was the optimal solution. Silica gel plates (glass or aluminium) were used and a horizontal line drawn

at the base of the plate to indicate the starting point of the applied samples. A microcapillary tube (5 $\mu$ l) are used to place discrete spots on the starting line, after each application the spot is allowed to dry before application of another. The plate is then placed in the solvent tank and the capillary forces allow the mobile phase of the solvent to run up through the front of the plate. Once the mobile phase of the solvent passes the sample line, the chromatographic process is initiation. The elution comes to an end the moment the mobile phase of the solvent is close to the upper side of the chromatography plate. At this point, the TLC plate is removed from the solvent tank and a line is used to make the border of the mobile phase of the solvent. The TLC plate is then allowed to air-dry before drops of KMnO<sub>4</sub> solution is placed over the plate, covering the surface. This is allowed to dry before heating gently to expose the sample constituent's spots.

In TLC, the movement of a compound is known as the  $R_f$  value or retardation factor. The  $R_f$  of a compound is described as the distance the compound is eluted ( $L_{\text{compound}}$ ), divided by the distance from the application line to the mobile phase front ( $L_{\text{mobile phase}}$ ). Although the  $R_f$  value can be calculated, it was thought that in this Thesis, this was not necessary as the focus is more on the comparison of two products rather than the synthesis of a new product which needs further analysis.

### **3.3.8 POSS-PCU Polymer solution manufacture**

Preparation of the POSS-PCU polymer has been reported extensively. In brief, polycarbonate diol and trans-cyclohexanechlorohydrin-isobutyl-POSS were added to a reaction vessel then heated to 130°C while being stirred under nitrogen gas. The reactants were then cooled before 4,4'-methylenebis(phenyl isocyanate) (MDI) was added and all components reacted for 30 minutes under nitrogen gas.

This reaction then forms a prepolymer before dimethylacetamide (DMAC) was added to convert this prepolymer into a solution. This solution was then cooled before the chain extender, ethylenediamine, was added dropwise until the reaction was completed. The chain stopper, 1-butanol, was then used to prevent further unwanted polymerisation. All of the reagents were supplied by Sigma Aldrich

(Dorset, UK) and used as provided with the exception of POSS, which was supplied by Hybrid Plastics Inc (Mississippi, USA).

### **3.3.9 POSS Dispersion**

2% (of the polymer weight) of POSS nanoparticle is first dissolved in DMAC before adding to the polymeric solution of POSS-PCU and making the final solution to 15% solids content. The hard segment of the polymer remains at 28%.

### **3.3.10 Soft Lithography**

Once the POSS nanoparticle has been incorporated into the polymer as part of a polymer solution (18-22% solids content). A cast version of this polymer can be fabricated using soft lithography. This is done by pouring the polymer solution onto a substrate (such as a glass slide) and then this is placed into a vented oven at 65°C for a minimum of 2 hours, until the solvent (dimethylacetamide (DMAC)) has evaporated. The cast polymer is then removed from the substrate.

### **3.3.11 Contact Angle Measurement**

Contact angle measurements were taken using the Kruss Drop Shape Analysis DSA100. Contact angles are usually evaluated under static or dynamic conditions. In this case, this is conducted by measuring the static contact angle (CA,  $\theta$ ) of the water droplet over three interphases, gLV, gSV and gSL, where it is liquid/ vapour (LV), solid/ vapour (SV) and solid/ liquid SL).

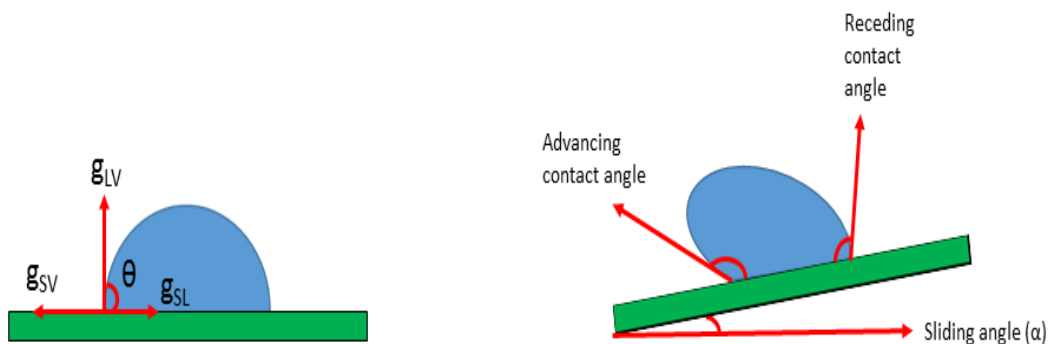


**Figure 3-5** Diagram to show the measurement of contact angles using the sessile drop method. The wettability of the surfaces is evaluated regarding the static and dynamic behavior of the droplet itself and therefore in the static stage, this is evaluated over three different interphases in contact with the contact angle. Under dynamic conditions, this is related to the sliding angle ( $\alpha$ ) which is the inclination angle of the surface which causes the water droplet to roll off.

### 3.3.12 Live/ Dead Staining

This has been described in the Material and Methods Chapter. In brief, Live/Dead staining was undertaken using the Live/Dead Viability/ Cytotoxicity kit for mammalian cell (L-3224, Invitrogen) from Life Technologies. In short, calcein AM and ethidium homodimer-1 were made up to concentrations of 2 mM and 4 mM, respectively, using phosphate buffered saline (PBS). These solutions were incubated with the samples for 30 minutes at 37°C, before washing samples with phosphate buffer solution (PBS) and then analysing with a fluorescence microscope (Zeiss Axiovert M200).

### 3.3.13 Alamar Blue® Cell Viability

Alamar Blue® reagent was purchased from Thermo Fisher Scientific and used as supplied. HUVECs are cultured in 6-well plates, with some containing POSS-PCU polymer and some acting as control (no POSS-PCU) and cultured for 24 hours initially. Cell media was removed from the cell samples and then gently washed with copious amounts of sterile PBS. Then a known amount of fresh cell media was then placed in the well. 10% of the cell media volume of Alamar Blue® was then placed each of the sample wells. There should be a cell-free well with only cell media and Alamar Blue. This will act as a baseline for standardising. The cells are then wrapped in foil and then placed back into the incubator at 37°C for 4 hours. At the end of the

incubation period, the cells are removed from the incubator and 3 x 100µl media samples are removed from each well and each 100µl sample is then allocated a well in a 96-well plate. These samples are then analysed using a microplate reader. The media and Alamar Blue® solutions are then removed from each of the wells. The cells are, once again, washed with copious amounts of PBS before replacing with fresh media. The cells are then replaced back into the incubator. This process is repeated every 24 hours for 4 days.

### **3.4 Results**

Each of the stages of the reaction was compared with commercially available products from Hybrid Plastics®, such as POSS-Trisilanol and POSS-Epoxy.

#### **3.4.1 Synthesis of POSS-Chlorohydrin**

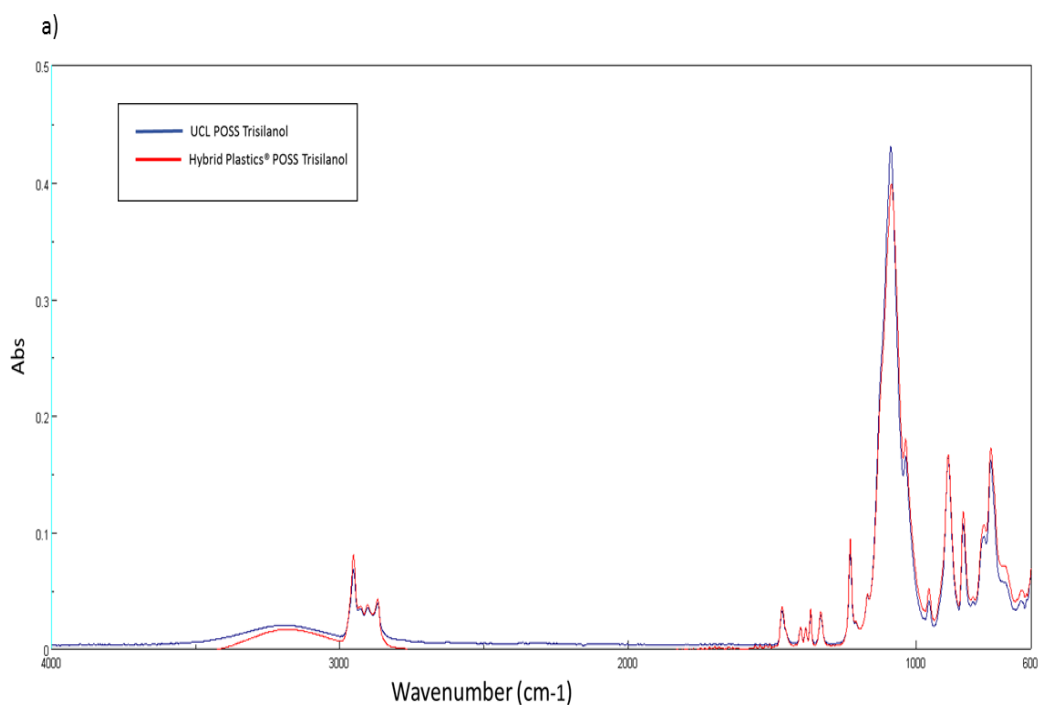
The synthesis of POSS-Trisilanol is known to be a base-catalysed hydrolytic condensation reaction in which the presence of a base, which in this case is Lithium Hydroxide (LiOH), of  $i\text{-BuSi}(\text{OMe})_3$ . Interestingly, the availability of  $i\text{-BuSi}(\text{OMe})_3$  is widespread as it is a bulk chemical used in the construction industry, as a crosslinking agent for silicones and for use as a waterproofing agent in the manufacture of concrete.

The direct synthesis of trisilanol from  $i\text{-C}_4\text{H}_9\text{Si}(\text{OMe})_3$  through a selective base-catalysed hydrolysis of  $i\text{-C}_4\text{H}_9\text{Si}(\text{OMe})_3$ . If the conditions are not exact for the formation of the trisilanol, T-gel is formed. T-gels are gelled silsesquioxanes and in this case, it is a white waxy material and of sticky consistency. The formation of T-gel is usually noted on quenching of the reaction with 1N HCl. The formation of T-gel is noted to be present if the conditions of the reaction are not correct.

The conditions at which to form the POSS-Trisilanol was found to be very dependent on temperature, conditions of the solvent, quenching, reaction time and product formation was very dependent on these conditions. If product was produced this was

in the form of a white, fluffy material which did not gel on extended stirring and did not dissolve on washing with acetonitrile.

The 'corner cap' reaction follows on from the first reaction to 'functionalise' the partial POSS cage so that there is an epoxy group attached. And after this, the epoxy group needs to be 'ring-opened' which leads to the POSS-chlorohydrin. In the three steps as detailed above this can be achieved and the following results are presented as such.



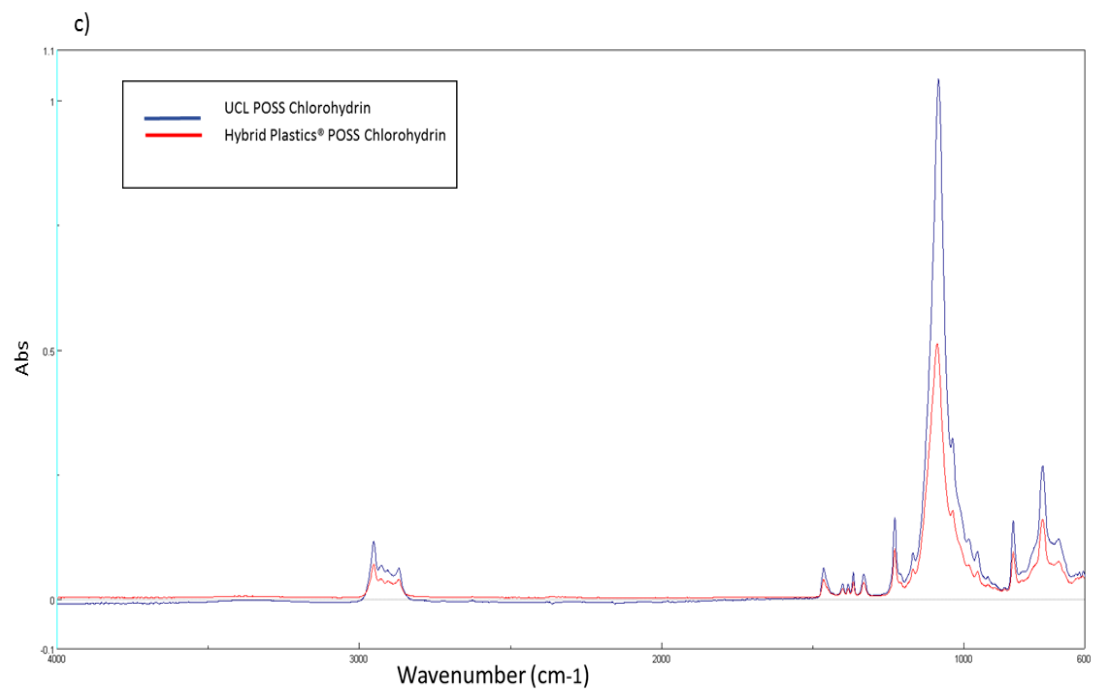
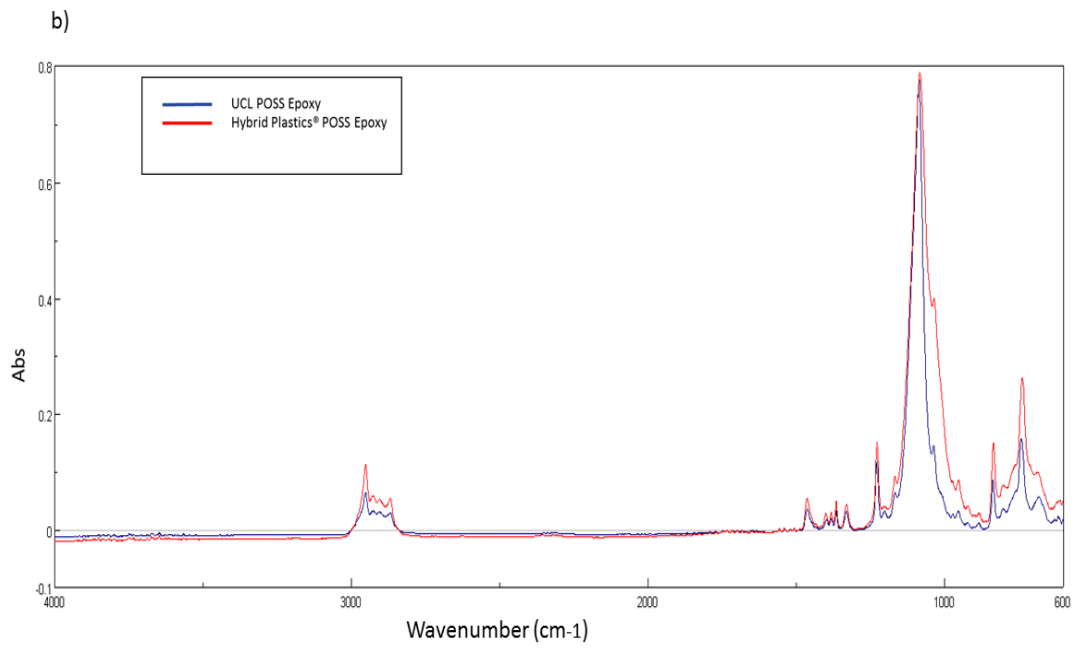


**Figure 3-6 Comparative FTIR diagrams of the products produced at each stage of the chemical synthesis where a) is POSS Trisilanol, b) is POSS Epoxy and c) is POSS Chlorohydrin.**

The FTIR spectrum of the UCL POSS-Trisilanol (UCL1) is comparable to Hybrid Plastics® POSS Trisilanol (HP1). It can be seen the intensity of the UCL1 product is higher than HP1. This is due to the crystalline nature of the material and the more crystalline the final product is the higher the intensity. This shows that UCL1 is more crystalline than the commercially available HP1. This pattern is also seen in the both the POSS-Epoxy and POSS-Chlorohydrin steps. The intensity of the FTIR is higher the more crystalline the product is. Therefore, the POSS-Epoxy from Hybrid Plastics appear to be more crystalline than the UCL POSS-Epoxy. But this is reversed again for the final POSS product, which is the POSS-Chlorohydrin.

The FTIR spectrum shows the characteristic peaks at 1120cm<sup>-1</sup> which are known for the Si-O-Si bond and also another peak at 1030cm<sup>-1</sup> indicating the Si-O-Si framework(49). This is a very strong indication for the presence of the POSS nanocage.

In all the FTIR spectrums, the UCL-POSS that is produced is comparable to the commercially available HP-POSS at each step of the process as seen by the FTIR ‘fingerprints.’

<sup>1</sup>H NMR and <sup>13</sup>C NMR shows how matching the spectrums of UCL POSS-Chlorohydrin to HP POSS-Chlorohydrin indicating the same material has been produced. Again, this is an identical ‘finger-print’ of the two products which have been produced.

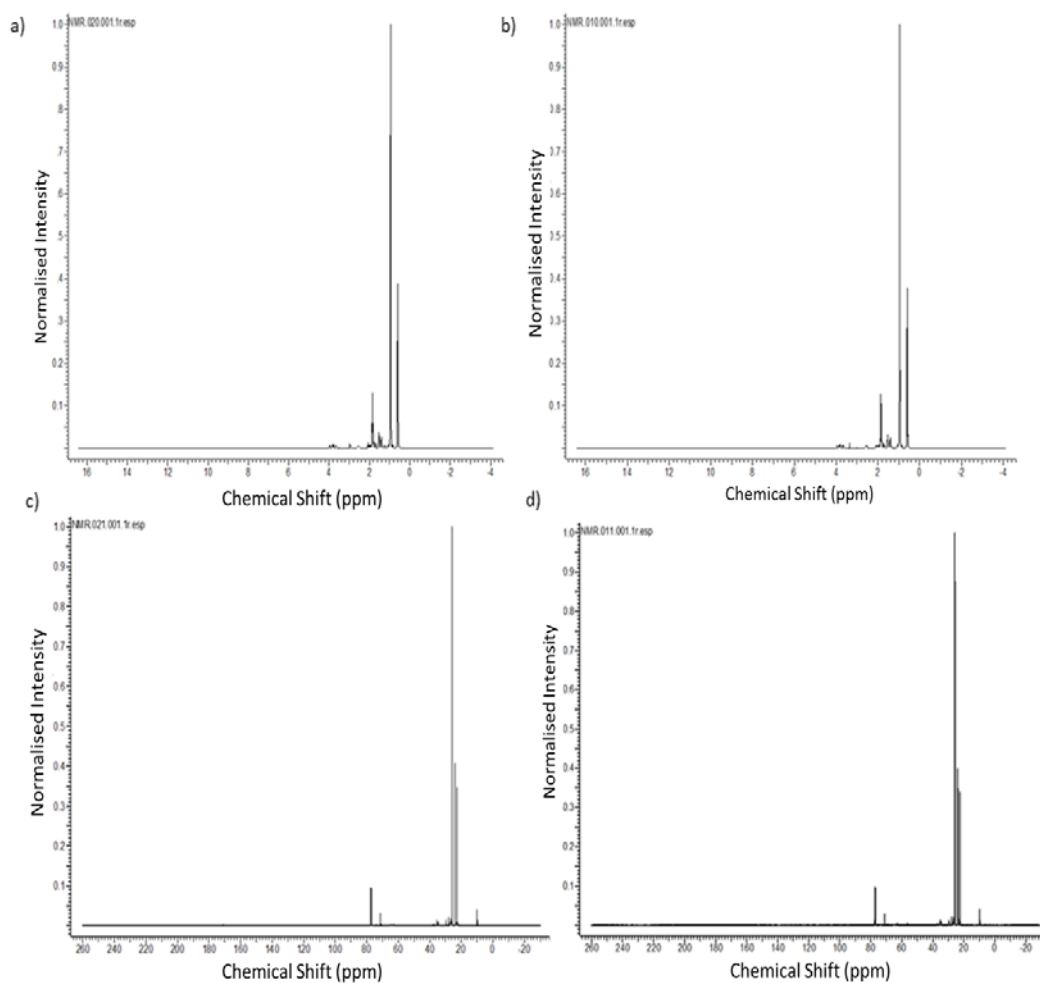


**Figure 3-7 NMR spectra showing the comparison of POSS-PCU produced commercial (HP-POSS) and that produced in-house (UCL-POSS) where a) UCL-POSS proton NMR, b) HP-POSS Proton NMR, c) UCL-POSS 13C NMR spectra and d) HP-POSS 13C NMR spectra**

Melting points for both the UCL-POSS and HP-POSS were found to be both at 123°C. This indicates that the products produced at the end of the synthesis is comparable. If any significant impurities are present, this will usually lower the melting point.

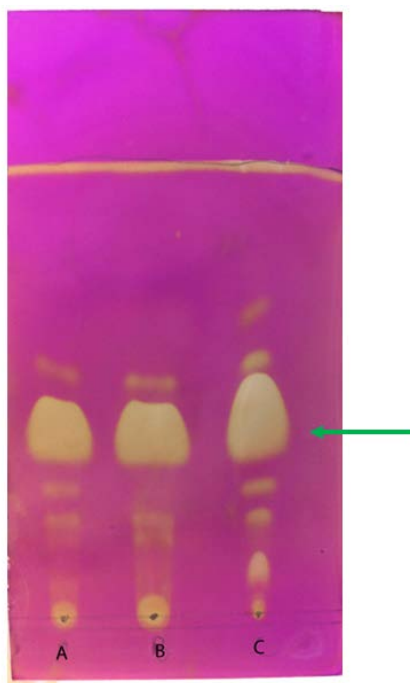


**Figure 3-8** This figure shows the exposure of a thin layer chromatography (TLC) plate highlight the different POSS products, where A is mixture of Hybrid Plastics POSS- Chlorohydrin and UCL POSS- Chlorohydrin, B is Hybrid Plastics POSS-Chlorohydrin only and C is UCL POSS-Chlorohydrin only. A mixture of the two POSS samples is used to further confirm that the two products are the same. The green arrow indicates the presence of the POSS cage which is seen across all three products.

Thin layer chromatography (TLC) also shows further confirmation of the product which has been produced, UCL-POSS. On the TLC plates it was seen that the fingerprints of the products are nearly the same. The main product which is the POSS cage is the most dominant product which is produced and can be seen to be the same product moving the same distance across the TLC plate. There are also smaller amounts of mostly, similar side-products which have been produced. However as can be seen the ‘fingerprints’ of HP-POSS and UCL-POSS seen on the TLC plate is not exactly the same and this is thought to be due to different impurities and will require further purification processes which will ensure a purer product is produced.

### **3.4.2 Testing the Toxicity of POSS-Chlorohydrin associated POSS-PCU polymer**

Toxicity testing was undertaken to ensure that the incorporation of the POSS nanoparticle does not affect the normal growth of the endothelial cells. This was conducted using Live/ Dead staining which will stain ‘live’ cells green and ‘dead’ cells red. In conjunction with the Live/ Dead staining Alamar Blue® staining was

also undertaken to illustrate that endothelial cell metabolism has not changed in the presence of the polymer.

This testing was undertaken in an environment in which human umbilical vein endothelial cells (HUVECs) are known to proliferate and this is on tissue culture plastic. This experiment was conducted on tissue culture plastic (TCP) in which HUVECs are known to grow. A piece of cast 1cm x 1cm POSS-PCU polymer, polymer in which the solvent has been evaporated, was placed also in the TCP well with the HUVECs. For the Live/ Dead staining, the results were analysed after 48 hours whereas for the Alamar Blue® the time-point was after 4 days so as to give a better growth chart.

The results show that after 48 hours, in both the wells with POSS-PCU or without POSS-PCU (control), the majority of the cells were still alive and there were really few dead cells. It is also possible to note that the natural morphology of endothelial cells was retained in both conditions, with and without POSS-PCU being present.

The Alamar Blue® results show that there is a similar growth rate or proliferation of the HUVECs with or without the presence of POSS-PCU in the wells. This was conducted over 4 days and intensity readings were taken every day to establish a pattern. It was possible to see that there is a positive growth pattern over the four days and there was no statistical significance between with or without POSS-PCU at each of the days. This indicates that the presence of POSS-PCU does not impede HUVEC proliferation and that POSS-PCU is non-toxic and biocompatible.

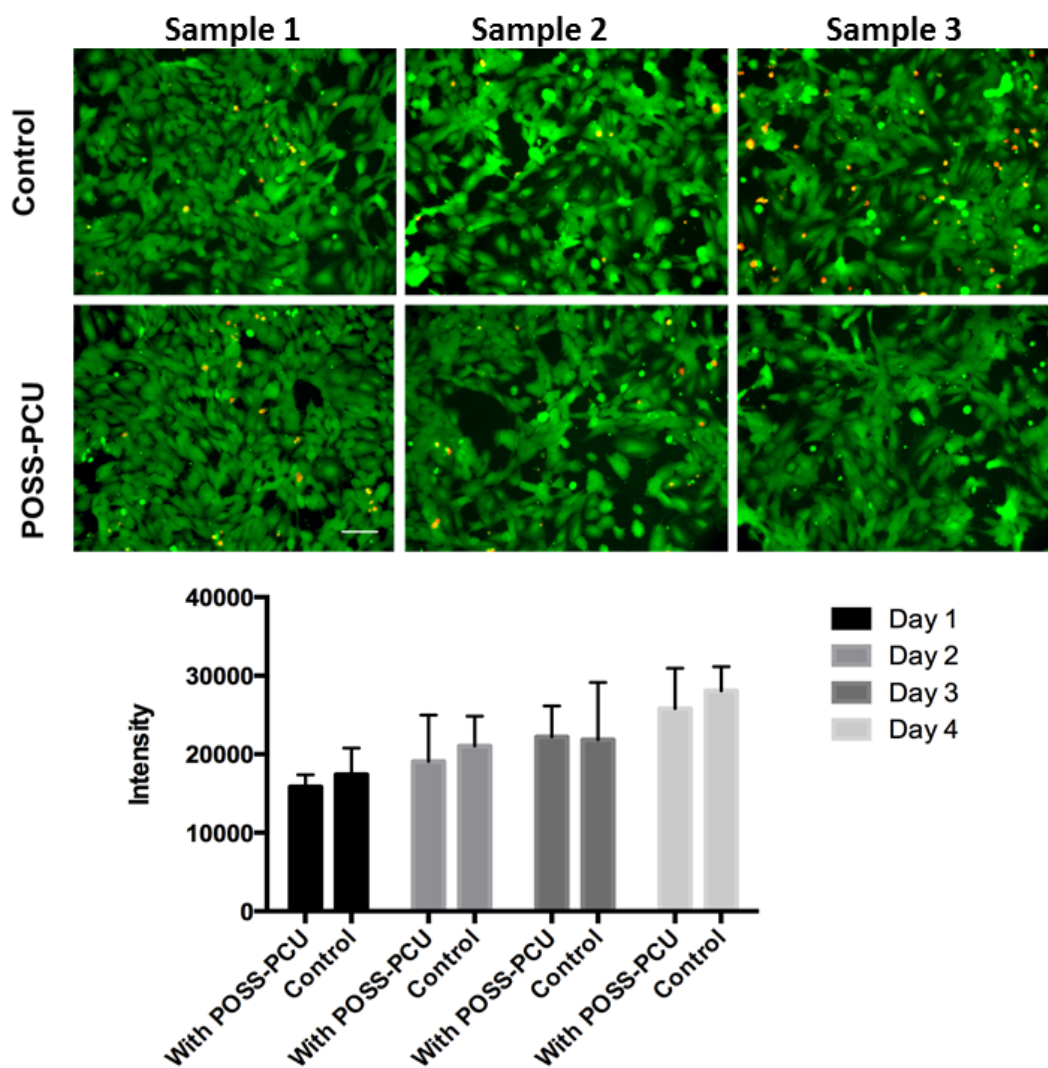


**Figure 3-9 Toxicity studies conducted to show HUVECs survival in the presence of POSS-PCU and when compared with normal conditions (control). The top diagram shows Live/Dead assay of the live cells (green) and dead cells (red) using fluorescence microscopy after 48 hours. The bottom graph shows comparison intensity when using Alamar Blue ® to measure the metabolic activity of the HUVECs in the presence of POSS-PCU and without. There is no statistical difference between the two conditions on any of the days (n = 12)**

### 3.4.3 Surface Modification of POSS-PCU using POSS nanoparticles

Once the POSS nanoparticle has been reacted within the polymer, this leaves the POSS-PCU polymer to be relatively unreactive. Therefore, the addition of further nanoparticles was mixed in with the polymer in an attempt to allow subtle modification of the polymeric surface. This is based on previous observations that the POSS nanoparticle tends to migrate to the surface in aggregates.

AFM and SEM images confirmed the migration of the nanoparticles to the surface and these nanoparticles tend to promote a hydrophobic property to the surface.

Therefore, it was thought that in excess further nanoparticles can induce more of a definitive change to the surface properties of the polymer. Two different types of POSS nanoparticles were dispersed within the polymeric solution and casted till the evaporation of the DMAC. These were Fluoro-POSS and POSS-Chlorohydrin and these were dispersed at a concentration of 2% excess of the solids percentage of the polymeric solution. This was compared with POSS-PCU and also polyurethane without the POSS nanoparticle, polycarbonate urea urethane (PCU).

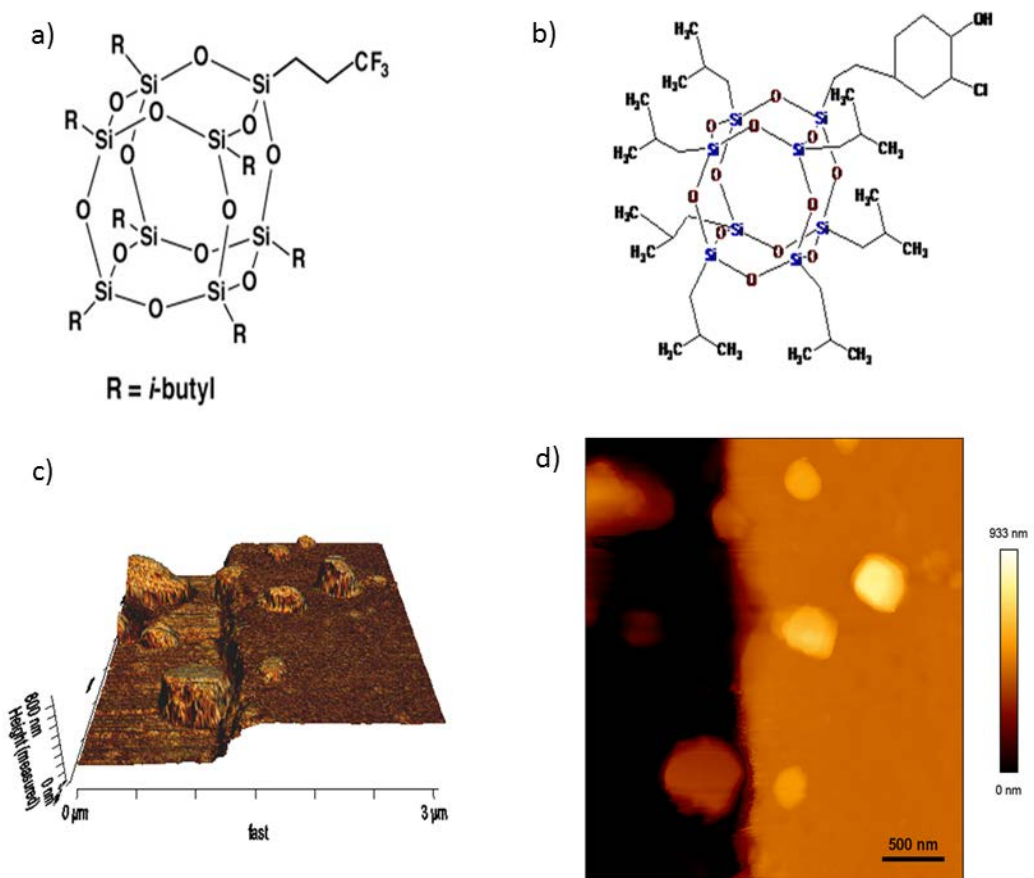
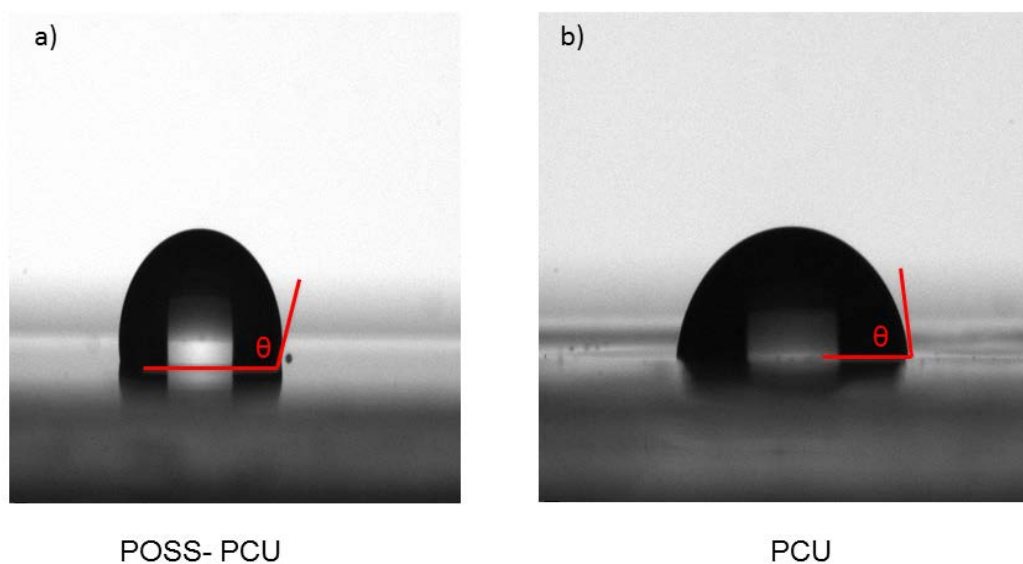


Figure 3-10 Shows the chemical structures of a) Fluoro-POSS and b) POSS Chlorohydrin. C) shows the 3D rendition of the surface topography of POSS-PCU with the POSS-nanoparticle aggregating on the surface using and d) phase image of the same area with AFM.

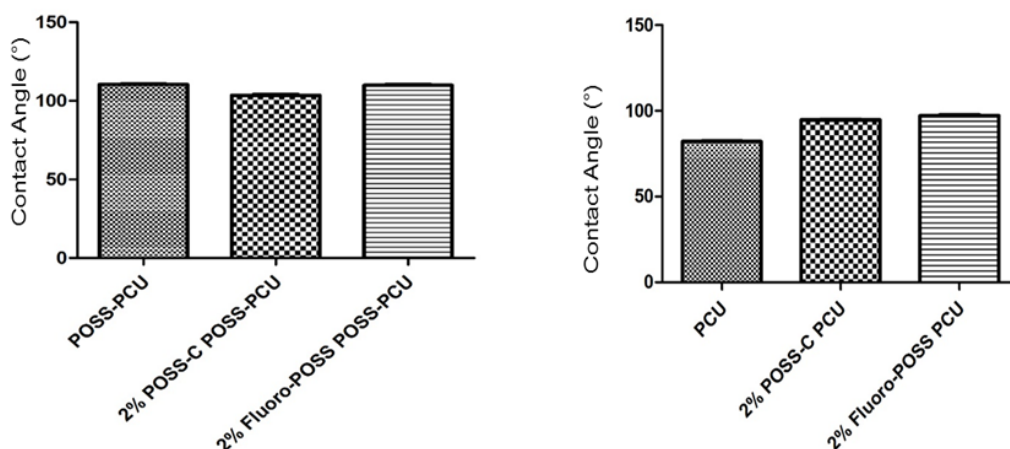
The contact angle for these modified polymers were measured and compared with the current polymer in use, polytetrafluoroethylene (PTFE).



Sample	Contact Angle (°)
POSS-PCU	110.43 ± 1.00
PCU	83.04 ± 0.96
PTFE	103.19 ± 2.29

**Figure 3-11 a) and b) shows a snapshot of the angle measurements taken for the contact angle measurements of the sessile water droplet on the POSS-PCU polymer and PCU polymer. The table below shows the contact angles for these two polymers as well as the clinical control, PTFE (n = 3).**

The baseline contact angles show that POSS-PCU is actually more hydrophobic than PTFE. However, PCU has the lowest contact angle out of the three polymers and therefore is more hydrophilic. In comparison with POSS-PCU, this could be due to the POSS nanoparticle and therefore implies that the incorporation of the nanoparticle confers an increase of contact angle of around 30°.



Sample	Contact Angle (°)
POSS-PCU	110.43 ± 1.00
PCU	83.04 ± 0.96
2% POSS Chlorohydrin POSS-PCU	103.59 ± 1.71
2% POSS Chlorohydrin PCU	94.69 ± 1.21
2% Fluoro-POSS POSS-PCU	109.98 ± 1.78
2% Fluoro-POSS PCU	97.23 ± 1.47

**Figure 3-12** The two graphs illustrate the similarities between the original polymer, POSS-PCU and PCU, and the modification of excess POSS nanoparticle. The contact angles of each polymer is recorded in the table below (n = 3).

There is no statistical significant difference between all the contact angles, even on the additional dispersion of POSS nanoparticles and the known ones which are meant to be hydrophobic. This indicates that on the addition of excess POSS nanoparticles the chemistry of these nanoparticles is very important as well as the polymer chemistry to predict what is going to happen. In this case, it appears that despite the POSS nanoparticles which have been chosen for their perceived hydrophobic properties, on addition of these nanoparticles to the polymers, there is no appreciable difference in the contact angles.

FTIR analysis of both the top and the bottom of the cast polymer sheet were analysed to see if there were any predictable migration to the surface of the POSS nanoparticle.

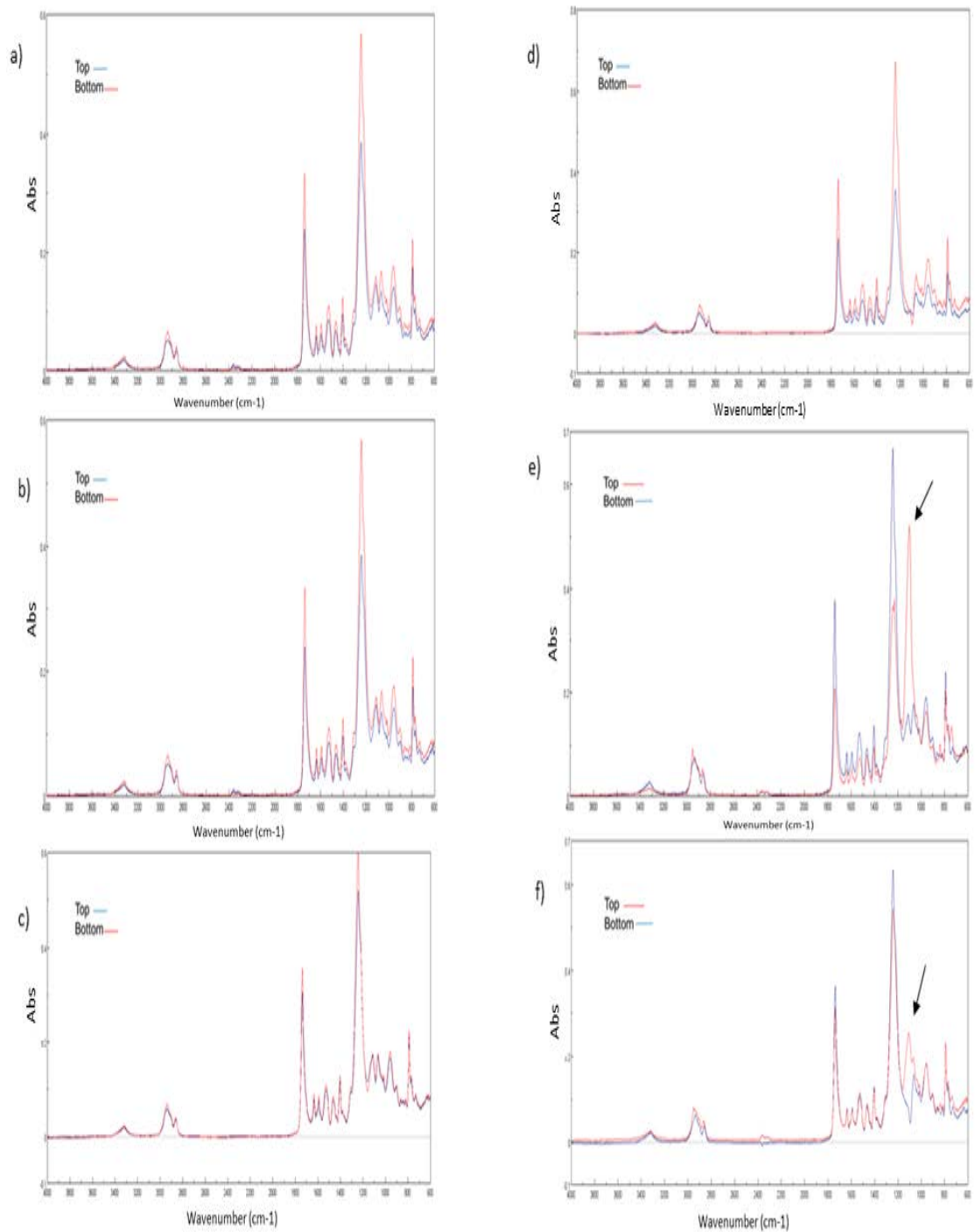


**Figure 3-13 FTIR spectra taken of both the top and bottom of cast polymers where the spectra are a) POSS-PCU, b) POSS-PCU with 2% POSS-Chlorohydrin, c) POSS-PCU with 2% Fluoro-POSS, d) PCU, e) PCU with 2% POSS-Chlorohydrin and f) PCU with 2% Fluoro-POSS. The arrows indicate the extra peaks of the POSS nanoparticle at 1100 cm-1 wavelength**

The FTIR spectra taken of the cast polymers with the different dispersions show that in POSS-PCU there is no difference to the chemical fingerprint whether there is excess POSS-Chlorohydrin or Fluoro-POSS dispersed within the polymeric solution

before being casted. However, with the PCU, there are extra peaks seen at 1100cm<sup>-1</sup>, mostly seen on the topside of the cast polymer and not on the bottom-side of the polymer. This shows that the POSS nanoparticle might be migrating to the surface of the polymer during its fabrication using soft lithography.

#### **3.4.4 Costs**

The commercial costs to source POSS-Chlorohydrin from Hybrid Plastics Inc. has been quoted to us as £3157 / kg. The costs calculated to produce POSS at UCL was £885/kg. This is assuming that the raw materials were sourced from Fluroochem Ltd where the advertised prices for Isobutyltrimethoxysilane is £20/100g and for Epoxycyclohexylethyltrimethoxysilane is £18/25g. These costings are accurate as of 2013.

However due to licensing agreements between Hybrid Plastics and UCLB, the negotiated costs of 1kg of POSS-Chlorohydrin is much higher than this. Therefore, the reduction in costs, if POSS can be produced in-house, will be phenomenal and make the final product more commercially viable.

#### **3.5 Discussion**

These results have shown that it is, indeed, possible to produce the POSS nanoparticle required to produce POSS-PCU polymer in-house. This is an important step in the production and commercialisation process of the POSS-PCU polymer as it allows a degree of independence in the supply of the nanoparticle. However, this is obviously very dependent on the status of patents and will require consultation with patent lawyers, especially if the manufacture is to be taken into a commercial setting. Further optimisation will be required to get the product into a setting which is appropriate to production which attains regulatory standards such as ISO especially if it is to be part of a medically implanted device.

The use of a base-catalyzed hydrolytic condensation reaction for POSS synthesis is well-known but it should be known that if the conditions are incorrect, it can often lead to intractable resins (T-gel) rather than discrete molecular clusters. Under these favourable conditions the formation of a POSS framework is typically observed with

thermodynamic control. This is due to the cleavage of the Si-O-Si linkages which are facile(50).

The formation of the trisilanol is thought to occur via the stabilisation of a lithium salt, lithium silanolate or trisilanolate for stability during the base-catalysed reaction. Upon quenching with acid (1N HCl), the trisilanol is freed and production of the partial cage is possible.

The 'corner-capping' of trisilanols have been investigated and is a very useful reaction as it involves functionalising the silsesquioxane cage structure. These functional groups are important as they can be carefully selected to allow a desired chemical group to be 'corner-capped' onto the silsesquioxane cage structure. Common reactions have involved the use of chloride salts but this requires high amounts of solvent and the waste products were large precipitates of chloride salts with a potential environmental impact. Good yields were difficult without these consequences and long reaction times.

When compared to the commercially available products, it is obvious that the possibility to produce the POSS-chlorohydrin in-house is possible. However, the purity levels of this POSS-chlorohydrin is difficult to assess due to the lack of professional chemical synthesis equipment in our own laboratories. Furthermore, to enhance the purification of the final product of the POSS nanoparticle is still an ongoing project. Melting point indicates that the POSS-chlorohydrin produced in this project has similar purity levels to those available commercially as both the melting points were the same. As mentioned before, melting points can decrease the melting point of a product and although the UCL-POSS which has been produced has similar melting point to the reference product, HP-POSS, TLC reveals that there are impurities in the both the products. It might be that the purity level in both products are the same or similar but due to manufacture techniques differing this would mean that there are different impurities present. Unfortunately, the ability to quantify this to that required at a commercial level is not possible currently as is the ability to further purify the product to a satisfactory level.

An advantage of being able to produce POSS-chlorohydrin in-house would be the huge reduction in manufacturing costs. This Chapter has shown that this is a potential but the system still requires optimization and purification of the final product. In addition to this, the process would need further consultation with patent lawyers to make sure that producing POSS-chlorohydrin on a commercial basis would not interfere with any existing patents currently held by Hybrid Plastics.

The incorporation of the POSS nanoparticle has been shown to be especially beneficial in improving the mechanical properties of the polycarbonate urea urethane polymer over polycarbonate urea urethane polymer by itself. It has been suggested that POSS incorporation in the polymers reduce chain mobility and this is the reason for the improvement in the results of both mechanical and thermal properties(50). In the case of POSS-PCU, the POSS nanoparticle is at the end of the polymeric chain. Polyurethanes are partial crystalline structures due to the amorphous soft segment and crystalline hard segment, and this is also the case of POSS-PCU. The resulting polymer produced is relatively inactive.

One of the downfalls of the POSS-PCU polymer is its inability to harbor an endothelial layer in the luminal surface(39), which has been confirmed in large animal studies. The endothelial layer in a luminal surface of a vascular graft has been shown to have important implications as discussed previously, however a surface which is shown to be completely repellent against any cells or protein material is also desirable. This means that no biological material is allowed to settle on the surface of the polymer. By achieving a superhydrophobic state ( $CA >150^\circ$ ), this allows for a surface that is not conducive to any protein adsorption, and hence platelet adhesion. Focused surface modification of the polymeric surface without affecting the polymer bulk is desirable as bulk mechanical properties can be retained. Previous attempts to do this with expanded PTFE (ePTFE) have been reported as a failure(51).

Although cells have not been able to directly adhere to POSS-PCU, we do know that the polymer is non-toxic to them. As shown, experiments have shown that the polymer is able to be in the same vicinity as the endothelial cells and this does not affect the growth of the endothelial cells. This suggests that the POSS-PCU polymer

does not emit any toxic substances which would otherwise affect cell death and this is especially important in the presence of endothelial cells in which the primary aim is to grow cells eventually on the polymer itself.

Alamar Blue® is a very useful reagent as it allows evaluation of the metabolism of live cells and does not require the cells to be fixed or destroyed for analysis. It uses resazurin which is a non-toxic and cell permeable compound. In its native state it is a blue colour and does not fluoresce. However, upon entering the cell, it is converted to resorufin, by reduction. Resorufin is a compound which is red in colour and highly fluorescent and thereby detectable using a plate-reader and allows for intensity readings. Although it is possible to conduct a quantitative evaluation of the amount of resazurin reduced, it was decided that in this case it was not necessary. This experiment is intended to be used as comparison data and therefore the comparison in fluorescence intensity was considered adequate.

Both Alamar Blue® and Live/ Dead staining have shown that POSS-PCU polymer is, indeed, a biocompatible polymer and does not require any further modifications from that point-of-view. However, it does need to have a surface which is conducive for direct cell adherence and proliferation, leading to the aim of this Thesis.

Initially, there were two ‘trains of thought’ in modifying the POSS-PCU polymeric surface. The first one, as mentioned, was to enhance the surface so that cells are able to adhere and proliferate on the surface, especially endothelial cells. Currently, this would require lowering of the surface contact angle to make the surface more hydrophilic so that cells are able to grow. The second train of thought was to ‘tune’ the luminal surface of the vascular graft to the other end of the spectrum. This involves making the surface super-hydrophobic (contact angles  $> 150^\circ$ ) instead of hydrophilic, meaning that water droplets would just roll off it and would not be able to ‘wet’ the surface at all. This would also mean that cells, platelets and proteins would not be able to adhere on the surface and the vascular graft would function as a tube, but one that would have a non-adherent luminal surface. Initial attempts were made towards making the surface hydrophobic using the intrinsic nanoparticle, POSS. This focused in finding different functional and chemical groups which were

known to promote hydrophobicity. After noticing that the nanoparticles aggregate on the surface of the POSS-PCU polymer, it was hypothesised that excess of nanoparticles can be used to induce subtle changes in the chemistry of the polymer especially the surface without affecting the bulk properties. The Fluoro-POSS was selected due to the known hydrophobic nature of fluorine groups within the chemical structure. POSS-chlorohydrin was also selected as it was a known hydrophobic molecule as well as being a nanoparticle that we have already in abundance in our laboratory to test out this hypothesis.

Despite the known hydrophobic properties of these nanoparticles, it would seem that there is a lack of change in the overall surface contact angle of the surface of the cast polymer. It is thought that the reason for this is due to the individual chemical structure of the POSS nanoparticle involved and is likely due to the caged structure which does not allow water molecules to penetrate. For unmodified POSS-PCU polymer, the aggregation of the POSS nanoparticle on the surface is due to the fabrication technique employed. For fabrication of the cast polymer, this is usually placed on a glass substrate and the surface of the glass is hydrophilic in nature. This hydrophilicity means that the hydrophobic nanoparticles will orientate themselves as far away from the hydrophilic glass substrate as possible and therefore this means that they will aggregate on the surface furthest away from the glass surface.

In POSS-PCU, the presence of excess POSS nanoparticle (either in the form of Fluoro-POSS or POSS-Chlorohydrin) did not make any difference to the CA of the cast polymer as previously thought. It is thought that as the POSS nanoparticle is incorporated as part of the POSS-PCU polymer, their presence allowed excess POSS to penetrate the bulk of the polymer, as it was already anchored within the polymer, allowing an interplay between 'free' POSS and 'anchored' POSS. In reverse, PCU polymer is more hydrophilic than POSS-PCU as there is no POSS nanoparticle as part of the polymer. This hydrophilicity means that it will force the 'free' POSS to migrate to the surface, away from the hydrophilic nature of the PCU. This effect is reminiscent of phase separation. This is why the FTIR shows large peaks of POSS nanoparticles on the top of the polymer surface. However, despite these aggregations of POSS nanoparticles on the surface there is still no discernable change in the CA.

The use of CA to measure the subtle surface changes is an important technique as this will give us quite a sensitive indication of the hydrophobic or hydrophilic nature of the surface. This allows a sensitive methodology of fine-tuning the surface till a desirable CA is reached to which further testing can be initiated and functions as a sensitive indicator.

A vascular graft was released by Vascutek Ltd (Renfrewshire, UK), Fluoropassiv™, which was essentially a knitted polyester skeleton with the surface having been treated with a proprietary fluoropolymer solution before gelatin impregnation(52). In animal models, the addition of this fluoropolymer exhibited reduced thrombogenicity and suture hole bleeding(53). However, when this graft was moved to clinical evaluation, Robinson(54) *et al* found that when compared with ePTFE vascular grafts, Fluoropassiv™ functioned less effectively as a vascular graft. The primary patencies at 6 months were found to be 50% for Fluoropassiv™ compared with 71% for ePTFE. In addition, it was found that 36% of the enrolled patients with Fluoropassiv™ vascular grafts developed graft thrombosis compared with 8.8% of those with ePTFE grafts. Fluoropassiv™ uses a similar reasoning to what was attempted in this Chapter. The idea is to increase the surface to a hydrophobic level in which cells and platelets are not able to adhere. The use of POSS nanoparticles to disperse within the polymeric solution did not seem to have as strong an effect as was intended and combined with the clinical efforts of the Fluoropassiv™ vascular graft, it may appear that this line of investigation may be futile.

### **3.6 Conclusion**

This chapter shows that it is possible to produce the POSS-Chlorohydrin nanoparticle in the laboratory and incorporate it within a polyurethane-based polymer, polycarbonate urea urethane (PCU). However once the polymer that is produced, POSS-PCU, is quite hydrophobic in nature. Endothelialisation of its unmodified form, has already shown it to impossible in preclinical studies. Therefore, further modification of the polymer will be required at this point, either to increase the hydrophilicity or the hydrophobicity of the polymer. Surface modification to increase the hydrophobicity of the polymer using nanoparticles dispersed within it, did not change the surface contact angle an appreciable amount.

When compared with the recent clinical attempts to increase hydrophobicity of the luminal surface, it was concluded that increasing the hydrophilicity of the surface may be a better strategy.

### **3.7 Further Work**

As mentioned already, although it is possible to prove that the POSS-chlorohydrin molecule is a particle that can be synthesized in-house, there is still much work to be conducted in which POSS-chlorohydrin can also be produced on a commercial scale. This will involve optimisation, formal assessment of the purity levels of the product and also scale-up of the production line. Unfortunately, the current laboratory in which this initial work is conducted in, is not suitable for this further work and would require further dedicated chemistry laboratories with associated specialist chemistry help. Ideally, if funding was available, a specialist chemical synthesis company would be consulted in bringing this work to such a place.

Production of this nanoparticle will then need to be formally tested for biocompatibility and its ability to be made into the POSS-PCU polymer with the same results as those obtained using the POSS-Chlorohydrin produced commercially from Hybrid Plastics. Although we have tested the biocompatibility of POSS-PCU in this Chapter, the POSS-PCU was made using POSS from Hybrid Plastics and not the POSS made in-house. Therefore, this does need to be investigated further and, again, in a more formal environment which will take into account ISO standards.

Further work needs following this Chapter needs to also focus on endothelialisation. This will require a method which involves surface modification technique which does not destroy the bulk properties of the POSS-PCU polymer. Physical and chemical techniques are usually preferable over biological techniques. This is mainly due to the fact that biological techniques tend to have further problems regarding storage, cell culture, cell/ protein sourcing, for example, and tend to require specialist facilities to be made available on-site. Therefore, further Chapters in this Thesis will concentrate on further surface modification techniques to encourage endothelialisation.

## **Chapter 4: Surface Modulation of the POSS-PCU Polymer: Plasma Treatment**

## **Chapter 4 Surface Modulation of the POSS-PCU Polymer: Plasma Treatment**

### **4.1 Introduction**

Surface modulation of the vascular graft surface allows for a more focused approach when designing a vascular graft more conducive to endothelialisation. It has long been acknowledged that the main factors allowing an endothelial cell layer to line the luminal surface of a vascular graft, are surface chemistry and topography. Despite several new materials undergoing extensive investigation for use as an implantable medical device such as a vascular graft, it has been difficult to achieve both an endothelialised surface as well as a durable polymer with mechanical properties suited for a vascular graft. Therefore, a methodology which allows for modulation of both factors as well as allowing independent adjustment from each other is a desirable effect.

In the fabrication of vascular grafts, it is essential to understand that the luminal surface of the graft has a very close interaction with the blood and haemodynamic flow. Therefore, the design of this surface has to be non-thrombogenic, non-inflammatory and endothelial-cell ‘friendly’, to name a few things. The ‘holy grail’ of vascular surgery is known to be the ability to produce of an endothelial cell layer on the luminal surface of the graft. This endothelial layer ensures the patency of the grafts as there is an important haemostatic balance to be achieved here by the endothelial cells themselves. In addition to this, this endothelial layer must also be able to withstand the high pressures and haemodynamic flow encountered within arterial vessels without delaminating. Clinical research conducted by Zilla *et al*(38) has added weight to the need for endothelialisation. They found that when endothelial cells were seeded onto PTFE grafts, long-term patency rates were superior when compared to non-endothelialised PTFE grafts. Despite the viability of this process already proven by these clinical trials, unfortunately this methodology is limited to specialized cell culture facilities, university hospitals or tertiary hospitals and where the cell culture facilities are close to the operating theatres. Pre-seeding of these endothelial cells also limits the usage of this technique for emergency and urgent operations.

'Off the shelf' vascular grafts which are self-endothelialising are therefore considered to be the ideal solution to the problem. This means that the proposed vascular graft would be accessible to all different types of scenarios, emergency and elective cases. Once the graft is implanted, it would be able to recruit endothelial cells from neighbouring vessels to endothelialise itself. This would preclude the need for prior endothelial cell seeding and allows this graft to be used even in emergent situations. A reliable and reproducible fabrication methodology is required to achieve this. However, although this is not a new idea, previous observations have shown that inward endothelial cell growth is limited to 2-3 cm at best and therefore continued efforts to make this work have waned in recent years.

One of the more popular strategies used to induce endothelialisation has been to incorporate protein and peptide molecules into the luminal surface of the vascular graft. Many methods have been used such as grafting, coating and anchoring but none have really progressed to a clinical setting beyond preclinical trials. For proteins, sourcing would be very difficult as there are problems with testing of transmittable diseases, high costs, ethical approval and also difficult FDA approval. Peptides would potentially also run into the same problems, although short-chain peptides such as REDV and RGD(55) have been produced in the laboratory without too much problem, but their production in bulk, amounts to huge costs, which is yet another problem. There are still discussions as to whether there are potential complications resulting in downstream effects of the 'attached' proteins and peptides and whether a systemic reaction may be a problem.

Within the body, endothelial cells reside in an extracellular matrix within the luminal surface of the vessel, which provides physical, chemical and biological cues to allow it to function and reaction to different stimuli. To attempt a full reconstruction of the extracellular matrix is beyond the capability of our current technology at this point(37). However, it has been identified that altering some of the more gross aspects such as surface chemistry and topography can help benefit cell adhesion and function onto some synthetic biocompatible materials. These materials can be designed to have bulk properties which have similar mechanical and compliance features to that of a native arterial vessel. Polyurethane has been a biocompatible

synthetic polymer of choice in the recent years and as mentioned in the previous chapters, problems in long-term degradation through oxidation and hydrolysis have mainly been fixed by the addition of the POSS nanoparticle. The addition of this POSS nanoparticle has also improved the mechanical and compliance properties of the polymer(44). However, endothelialisation is still a problem as demonstrated in large animal studies(39). Therefore, other strategies to allow endothelialisation to happen without compromising on the bulk properties of the material is further investigated. One of the strategies of this type of modification was to alter the luminal surface chemistry of the POSS-PCU polymer, using plasma treatment.

Plasma treatment offers a reproducible methodology to alter the surface chemistry of the surface of a material without affecting the bulk properties of the material itself. Plasma is referred to as the 4<sup>th</sup> state of matter and was coined by Langmuir in 1928(56). Plasma is composed of partially ionized gas and can be defined as particle system in which a mix of free electrons, ions and radicals, composed of neutral particles (atoms and molecules). Some of these may be in the excited state and return to ground state by photon emission. This accounts for the light emission visualized. Electrons can also be free meaning that positive and negative charges move independently of each other. This plasma state is usually activated by radio-frequency or electrons from a hot discharge.

Plasma is divided into two distinct categories, equilibrium (thermal) and non-equilibrium (non-thermal). In our usage, non-equilibrium is used most commonly, as high temperatures can have a detrimental effect on polymers. Plasma is highly reactive and therefore there are three main categories of plasma reactions:

- Plasma polymerization
- Plasma treatment
- Plasma etching

These are not mutually exclusive and can happen in unison and therefore this, overall, ends in a lack of control over the final product, which can present as a

disadvantage of the technique. However, at low enough power (wattages) and careful monitoring and planning, it is possible to control certain aspects of the plasma.

Although wet chemical treatment of a surface can also induce a chemical modification within the surface, the undesirable effects of a wet chemical treatment include causing partial degradation and scissions of the polymers at the surface. This can lead to loss of mechanical strength of the overall bulk polymer and lead to faster degradation. Whereas plasma treatment has the ability to modify the surface of the polymer regardless of the geometrical configuration as well as being a solvent-free method and no toxic solvents are required to induce a chemical change. This chemical change allows the hydrophilicity to be induced onto the surface of a polymer and therefore encourage cytophilicity.

There are many different ways to induce a state of plasma and one of the most common ways is to use a radio-frequency discharge. The plasma is excited and sustained by high-frequency electromagnetic waves. When the frequency of the electromagnetic wave is increased, the ions and the electrons can no longer reach the electrode surface during the acceleration phase of the exciting external field. This means that at these radiofrequencies, the interaction between power supply and the plasma generated are really displacement currents rather than actual currents. This adds the extra advantage that any impurities at the electrodes can be avoided.

Theories have been produced to take into account the surface energy and the surface roughness when measuring the contact angle. The three main models are Young's model, Wenzel's model and Cassie-Baxter's (CB) model(57).

Young's model is based on the contact of the sessile drop on a flat, homogenous, rigid and inert surface. Unfortunately, in reality, surfaces are not completely flat, rigid, homogenous and inert as assumed in this theory and therefore this may be a more simplistic way to look at contact angles.

$$\cos \theta_0 = \frac{\gamma_{SV} - \gamma_{SL}}{\gamma_{LV}}$$

Where  $\cos\theta_0$  is the contact angle and  $\gamma_{SV}$ ,  $\gamma_{SL}$  and  $\gamma_{LV}$  represent surface-vapour, solid-liquid and liquid-vapour interphase.

Wenzel's theory is described by the equation below:

$$\cos\theta_w = r\cos\theta_0$$

Where  $\theta_w$  is the apparent contact angle which corresponds to the stable equilibrium state (Wenzel's theory),  $r$  is the surface roughness ratio and  $\theta_0$  is Young's contact angle. This equation takes into account of the surface morphology and roughness on the contact angle. This assumes that the water penetrates into the grooves and irregularities of the surface structures.

CB theory is based on the equation:

$$\cos\theta_{CB} = r_f\cos\theta_0 + f - 1$$

Where  $\theta_{CB}$  is the contact angle calculated by CB theory,  $r_f$  is the roughness ratio of the wet surface area,  $f$  is the fraction of solid surface area wet by the liquid and  $\theta_0$  is Young's contact angle. This equation takes into account the surface morphology and roughness much like Wenzel's theory but it assumes that water is unable to penetrate right into the grooves or irregularities of the surface structures and there are 'air bubbles' stuck inside these grooves.

In theory, there is probably an intermediate state that exists between the Wenzel's and CB theory.

However, these theories help to understand the actual current state when the sessile drop lands on the surface of the material and the measurements are taken for the WCA.

Polymers that do not possess polar groups or chemically reactive groups, have a low surface energy (and are therefore hydrophobic) with minimal polar contribution.

These polymers have been shown to have a higher affinity for platelets(58). Plasma-assisted oxidations produced in low-pressure glow discharges ensures that all inert polymer surfaces can be oxidized easily (except for fluorinated polymers like PTFE), with well-controlled oxidation and no thermal exposure of polymers.

Oxygen introduction by low-pressure plasma treatment is associated with the formation of O-polar groups, which is reflected in increasing of surface energy and its polar contribution. Using plasma oxidation treatment, chemical surface modification can be used to incorporate additional '-OH' and '-COOH' groups which has been seen to lower the WCA of the surface. This has been shown by previous groups to enhance hydrophilicity of the surface and therefore encouraging cytophilicity. The successful incorporation of these chemical groups can be easily checked by the measurement of contact angle. It is the polarity of these chemical groups that will increase the wettability of the surface and therefore allow cells to adhere to the surface of the polymer without damaging the bulk properties of the polymer.

POSS-PCU has been developed as a polymeric scaffold for the main purpose of a vascular graft. Previous data has shown that POSS-PCU is a polymer which has been found to be biocompatible(39), anti-thrombogenic(59) and compliant(60), but with a surface which does not endothelialise(39). This indicates that further surface optimization needs to be conducted so that it will also incorporate endothelialisation. Therefore, the idea is to modify the surface of the polymer without affecting the bulk properties using plasma treatment and rendering the surface of the polymer to become bioactive. It is hoped that the bioactive surface would be able to produce a surface which will encourage endothelialisation, in particular 'self-endothelialisation' potential.

The inherent chemical properties of POSS-PCU means that it is an inert polymer which has no polar groups on its surface when it is in its cast form. This means that there is low surface energy present and therefore the WCA measured indicate high hydrophobic measurements. Therefore, the introduction of oxygen using plasma treatment allows the introduction of O-polar groups and thereby lowering of the

WCA. It has been shown that cells are more adhesive on surfaces which are moderately hydrophilic rather than super-hydrophilic, and therefore the subsequent lowering of WCA will render the surface hydrophilic.

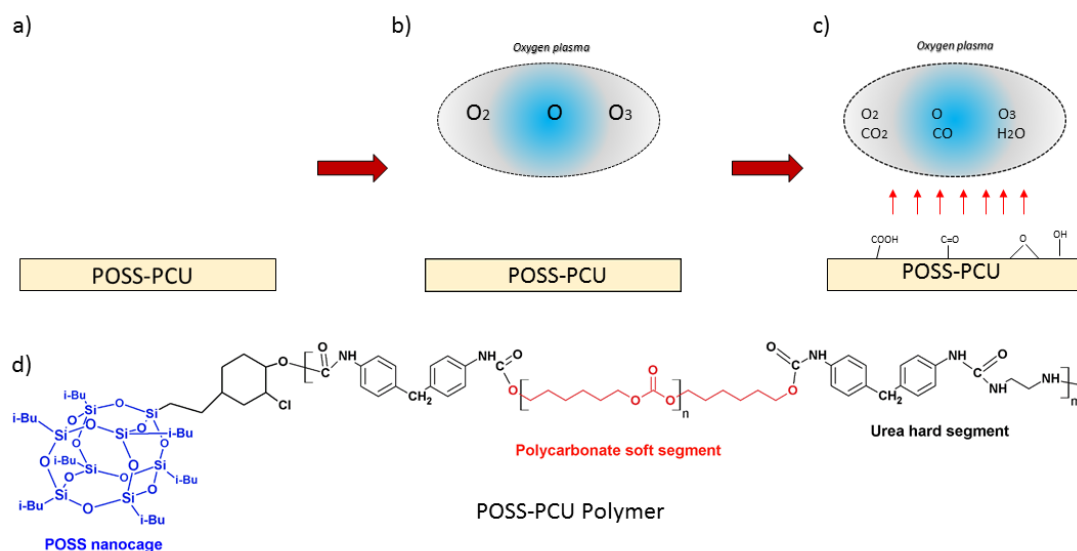


**Figure 4-1** Figure to show the step-wise effect of O<sub>2</sub> plasma treatment on POSS-PCU polymer, a) and when O<sub>2</sub> plasma is initially applied b), and when chemical groups start to form on the surface c). D) shows the chemical structure of the POSS-PCU polymer itself.

This Chapter therefore has focused on testing whether the use of plasma-treatment would be an option of producing surfaces which can encourage this endothelialisation.

## 4.2 Aims

The aim of this Chapter is to:

- Establish that the water contact angles of POSS-PCU can be lowered successfully using oxygen plasma treatment
- Demonstrate that on altering the surface, the surface of POSS-PCU is now able to allow endothelial cells to adhere

### **4.3 Materials and Methods**

#### **4.3.1 POSS-PCU Preparation**

Polycarbonate diol and trans-cyclohexanechlorohydrinisobutyl-POSS were added to a reaction vessel then heated to 130°C while being stirred under nitrogen gas. The reactants were then cooled before 4,4'-methylenebis(phenyl isocyanate) (MDI) was added and all components reacted for 30 minutes under nitrogen gas.

This reaction then forms a pre-polymer before dimethylacetamide (DMAC) was added to convert this pre-polymer into a solution. This solution was then cooled before the chain extender, ethylenediamine, was added dropwise until the reaction was completed. The chain stopper, 1-butanol, was then used to prevent further unwanted polymerisation. All of the reagents were supplied by Sigma Aldrich (Dorset, UK) and used as provided with the exception of POSS, which was supplied by Hybrid Plastics Inc (Mississippi, USA).

#### **4.3.2 Control Polycarbonate Urea Urethane Preparation**

Dry polycarbonate polyol of 2000 molecular weight was placed in a 250ml reaction flask, equipped with a mechanical stirrer and nitrogen inlet. The polyol was heated to 60°C and then flake MDI was added and reacted with the polyol, under nitrogen gas, at 70-80°C for 90 minutes in order to form a pre-polymer. Anhydrous Dimethylacetamide (DMAC) was then added slowly to the pre-polymer to form a solution; the solution is then cooled to 40°C. Chain extension of the pre-polymer was carried in a dropwise fashion with the addition of chain extenders, ethylenediamine and diethylamine in dry DMAC. After completion of the chain extension, 1-butanol in DMAC was added to the polymer solution. Again, all reagents were purchased from Sigma Aldrich (Dorset, UK) and used as supplied.

### **4.3.3 Plasma Treatment of POSS-PCU**

The polymer solution of POSS-PCU is aliquoted into eppendorfs and centrifuged at 3000 rotations per minute (rpm) for 60 seconds. The top layer of the solution is then poured onto the different surfaces and placed in an oven at 65°C for a minimum of 2 hours so that the DMAC is able to evaporate leaving behind a thin film. These films are peeled off from the master surface. These films are plasma treated in a Cleanroom (James Watt Nanofabrication Centre, University of Glasgow) using a plasma cleaner (Gala Prep 5 Instrumente) using different power and times.

The rest of the films are then sterilized in 70% Ethanol for 10 minutes and then washing with PBS for three times. These films are then cut into 1cm x 1cm squares and place in low adhesion 24 well plates (Corning).

HUVECs are seeded at a seeding density of  $1 \times 10^5 / \text{cm}^2$  and these are then incubated for 5 days. The samples are then analysed using a variety of methods.

### **4.3.4 Live/Dead Staining**

This method is to look at cell survival on the different treatments of the polymer. Live/Dead staining was undertaken using the Live/Dead Viability/ Cytotoxicity kit for mammalian cell (L-3224, Invitrogen) from Life Technologies. In short, calcein AM and ethidium homodimer-1 were made up to concentrations of 2 mM and 4 mM, respectively, using phosphate buffered saline (PBS). These solutions were incubated with the day 5 samples for 30 minutes at 37°C, before washing samples with PBS then analysing with a fluorescence microscope (Zeiss Axiovert M200).

### **4.3.5 Immunofluorescence**

Samples were fixed in 4% formaldehyde for 15 minutes at 37°C then washed before placing in permeabilising buffer and blocking in 1% (w/v) bovine serum albumin/PBS. Samples were then stained with anti-vinculin antibody (1:150) (Sigma) in 1% (w/v) BSA/PBS or anti endothelial nitric oxide synthase (eNOS) antibody (1:50), in conjunction with rhodamine/phalloidin (1:500), and incubated at 37°C for 1 hour. Samples were subsequently washed 3 times for 5 minutes (0.5%

Tween-20 in PBS) and then the secondary antibody, which was biotinylated, was added (Vector Laboratories) at 1:50 in 1%(w/v) BSA/PBS. Samples were then incubated for 1 hour at 37°C. After further washing, FITC-conjugated streptavidin (1:50, Vector Laboratories) was added and incubated for a further 30 minutes at 4 °C. Samples were given a final wash before mounting using Vectashield with DAPI nuclear stain (Vector Laboratories).

#### **4.3.6 Coomassie Blue Staining**

Day 5 samples were fixed using 4% formaldehyde then stained with Coomassie blue (0.2% Coomassie blue w/v in 46.5% methanol, 7% acetic acid, 46.5% water) for 2 minutes. Samples were subsequently washed with de-ionised water before being visualised using optical microscopy.

#### **4.3.7 Cell Number Count**

Cell numbers were measured after 5 days of culture by taking fluorescence microscope images, at a magnification of x20, of cells stained with DAPI. Cell nuclei were counted as an indicator of cell number. Images were taken at random locations on the substrates; ten locations were imaged on each film, and a minimum of six films were assessed for each treatment type.

#### **4.3.8 In Cell Western**

In- Cell Western has been increasingly used in recent times over the more traditional Western Blot technique. ICW uses the near-infrared (NIR) fluorophore-conjugated antibodies and employ a similar technique to immunofluorescent methodology. NIR fluorophores extended the linear range of detection and potentially can improve sensitivity of detection(55).

Cells are fixed using 4% formaldehyde and then placed in permeabilising buffer before blocked in 1% milk power/ PBS solution. Samples were then incubated with primary antibody (anti-eNOS or anti-P-myosin) at a concentration of 1:50 for 2 hours at 37°C. The samples are then washed and then a fluorescent-labelled secondary antibody at a concentration of 1:1000 is then added with Cell Stain (CellTag 700

Stain, Li-cor, Cambridge, UK) for normalisation. This is left at room temperature for 1 hour on a shaker. The secondary antibody is then washed off. The samples are then analysed using Odyssey Sa (Li-Cor, Cambridge, UK) plate reader and the results were analysed.

#### **4.3.9 Statistical Analysis**

The statistical testing of the results from these experiments were conducted using the statistical program, Prism®.

Statistical analyses were carried out on the data as follows; WCA data sets and cell number on the different substrates were compared using a Kruskal-Wallis one-way analysis of variance (non-parametric) test. In-Cell Western data used the Mann-Whitney test to compare each topography individually with the other topographies.

### **4.4 Results**

#### **4.4.1 Plasma Treatment**

Plasma treatment was conducted in a cleanroom (James Watt Nanofabrication Centre, University of Glasgow, UK). This was to ensure that the plasma treatment was conducted in an atmosphere which would discourage any impurities or unwanted deposition. It is important to point out here that the plasma cleaner used, required 2 vacuum ‘pump-downs’ to ensure that there are no impurities and also to make sure that the vacuum atmosphere activates the plasma. The first pump-down ensures that any atmospheric impurities are removed from the plasma treatment chamber and the second pump-down is to get the appropriate vacuum level to activate the plasma. This is an important consideration as previous experience has found that there was impure deposition on the polymer when the plasma was conducted under just one ‘pump-down’ and when the infiltration was of atmospheric air rather than pure oxygen.

The results show that increasing power for a fixed period of time, led to the reduction of WCA in a step-wise predictable manner. However, this was not seen when treatment times were increased and this was thought to be related to the plasma

treatment power reaching a natural equilibrium with the surface chemistry and polymer chains.

Therefore, it was decided that increasing power for a fixed period of time (60s) was adequate to allow for the step-wise decrease in WCA.

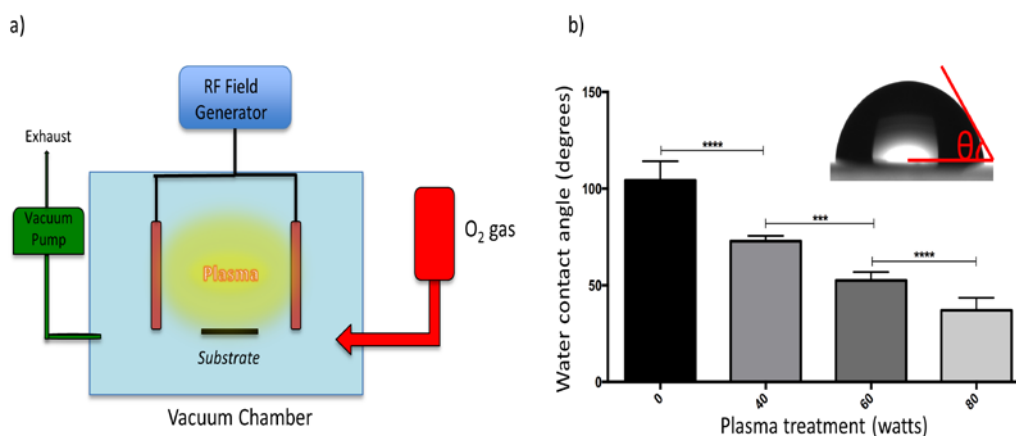


**Figure 4-2** Where a) is a simplified diagram to illustrate the concept of the plasma chamber and b) shows the step-wise drop in water contact angle (°) when increasing the power (watts) of the plasma treatment (inset: sessile water contact angle measurement)

It was important at this point to check the degradability of the plasma treatment as the plasma treatment is not a permanent effect as the surface tends to revert back to its untreated state, an effect known as ‘aging.’ Establishing a rough baseline for this was important as this research project takes place over two institutions (University College London and University of Glasgow) and therefore substrates need to be transferred from one institution to the other and it should not have ‘aged’ during the transfer process.

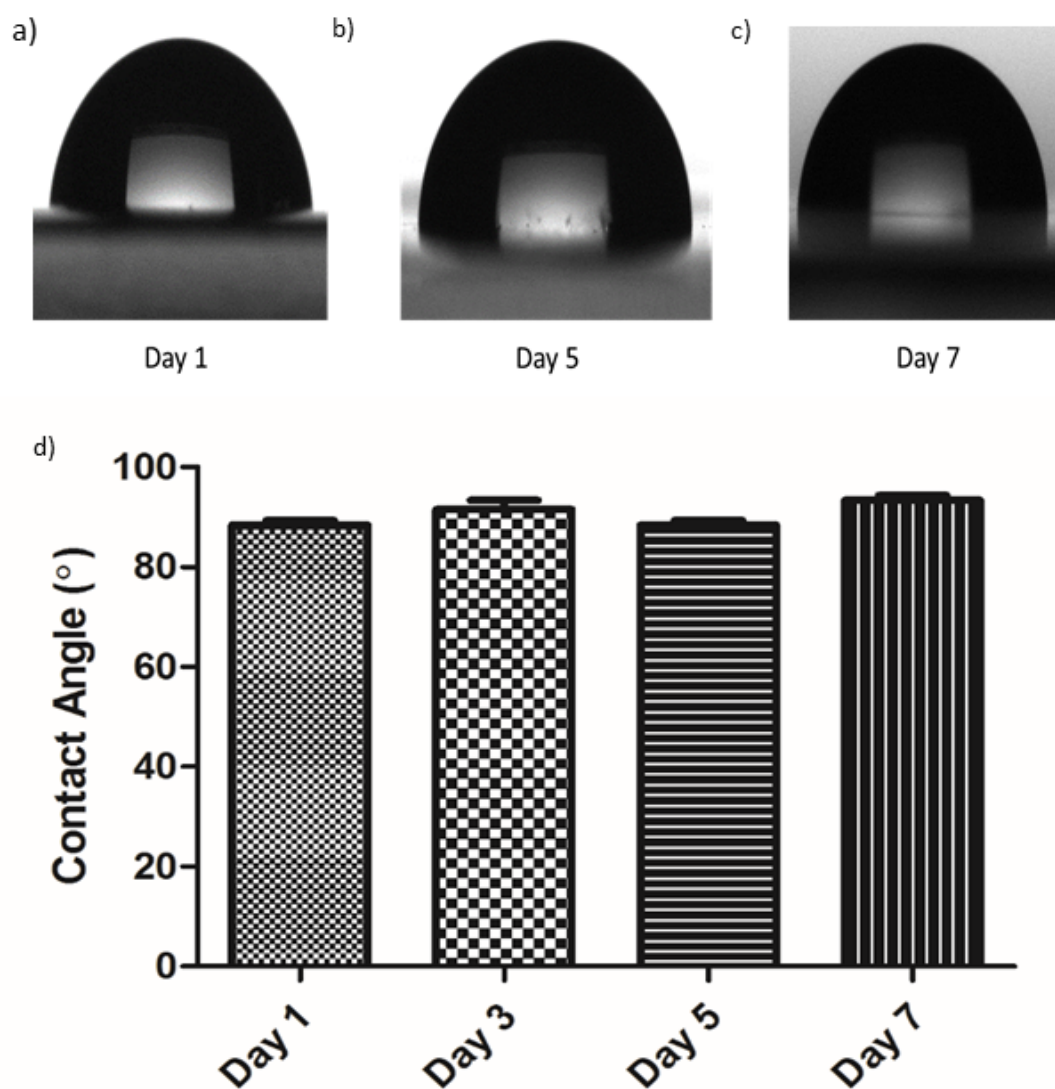


**Figure 4-3** This figure shows the consistent contact angles obtained d) over a seven-day period after plasma treatment and the different images of at Day 1 a), Day 5 b) and Day 7 c) showing that there are no changes of the contact angle and therefore no degradation in the initial 7 days post plasma treatment (n = 3)

Over the period of 1 week since the plasma treatment there is no significant changes seen in the contact angles. This indicates that over the period of one week there is not much change to contact angles of the plasma treated surfaces and therefore these samples can keep for a minimum of one-week post-treatment without any significant changes in contact angle.

#### 4.4.2 Live/ Dead Staining

Live/Dead staining is a technique that allows visualization of cell survival on the POSS-PCU polymer. This experiment is used to confirm that the chemical surface modification of the bulk polymer has not caused the surface to be toxic to cells and detrimental to cell growth. This staining technique takes into account that characteristics for a live cell requires there to be a ubiquitous intracellular esterase activity and an intact cell membrane. The green-fluorescent calcein AM indicates intracellular esterase activity and the red-fluorescent ethidium homodimer-1 indicates the lack of plasma membrane integrity. Therefore, these work in conjunction to produce a fluorescent image which shows the live (green) and dead (red) cells.

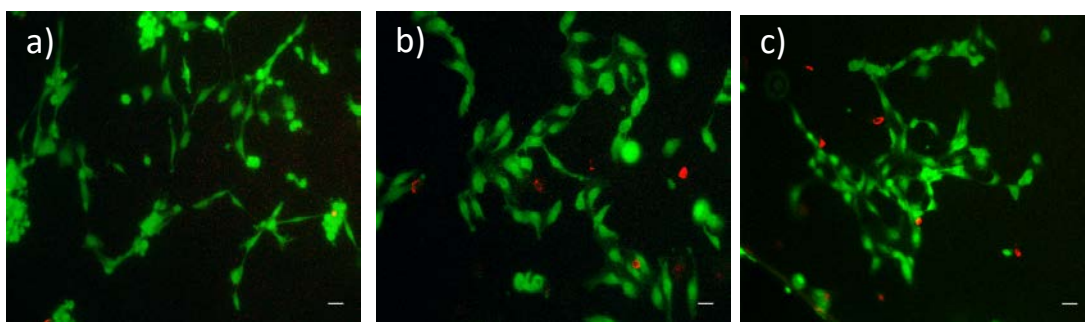


**Figure 4-4 Live/ Dead staining for the different plasma-treatment levels, where a) 40W at 60s, b) 60W at 60s and c) 80W at 60s. (Scale bar: 20  $\mu$ m) This shows that the plasma treatment is not toxic to the endothelial cells and illustrates that despite the plasma treatment, biocompatibility of the POSS-PCU polymer is retained**

It was seen that at all the plasma treatment levels there were minimal amounts of dead cells (red) and the majority of the cells appear to be highlighted green meaning that they are still alive. This indicates that overall plasma treatment, whichever the level of treatment, is not detrimental or toxic to endothelial cells. It should be noted that the cells show a similar morphology as that known for endothelial cells whereas the dead cells are rounded and lack any of the known endothelial morphology, however, it was also noticed that although the cells were highlighted in green (and therefore alive) there were a few more rounded cells seen in the lower treatment levels (40w at 60s). This was an indication that the cells were not as healthy as those that appeared more spread.

However, it can be seen that on some of the surfaces there were more cells seen growing than on some of the other surfaces although it was not possible to quantify this and this is more of a qualitative result. This technique highlights that the chemical modifications of POSS-PCU do not affect the cytocompatibility of the POSS-PCU polymer.

#### 4.4.3 Coomassie Blue Staining

Using Coomassie Blue as a cell-stain, the morphology of the HUVECs on the different plasma-treated POSS-PCU (40W at 60s, 60W at 60s and 80W at 60s) were examined under normal microscopy. At the lower treatment levels (40W at 60s), the HUVECs look rounded, less well spread on the polymer and less in abundance, which was also noticed on the Live/Dead staining. This indicates that at these plasma-treatment levels, the surface chemistry is still not optimized for HUVEC adhesion. However, with the increasing plasma-treatment, it is possible to see that the HUVEC morphology starts to change by becoming more spread on the surface of the POSS-PCU and there are more of them in abundance. The higher plasma-treatment allows more HUVEC adhesion and therefore coincides with a lower contact angle. Again, as this is not a quantitative measure but gives another qualitative result which also correlates with the Live/Dead staining.

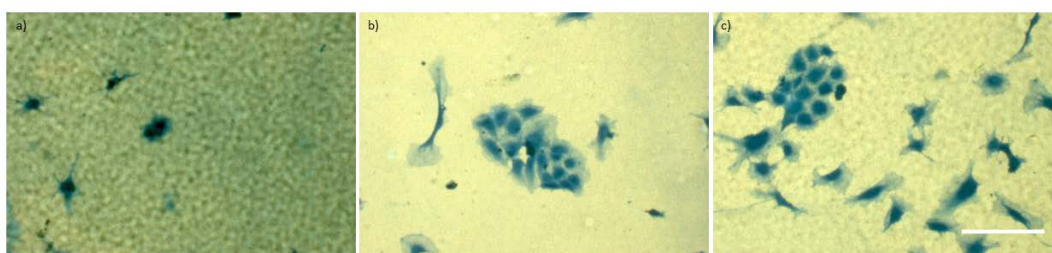


**Figure 4-5** This figure shows the morphology of the HUVECs using Coomassie Blue staining on the POSS-PCU polymer post-plasma treatment of a) 40W for 60s, b) 60W for 60s and c) 80W for 60s and the increased spreading of the HUVEC cells with the increasing plasma treatments (Scale Bar: 20 $\mu$ m)

#### 4.4.4 Cell Number

To estimate the number of cells proliferating on the surface of the plasma-modified POSS-PCU surface, a simple technique of highlighting the nucleus of the cell using

DAPI (4',6-diamidino-2-phenylindole) was used. DAPI is a well-known fluorescent stain that binds to the A-T rich region of DNA and therefore highlights the nuclei when viewed under fluorescent or confocal microscopy. As DAPI can pass through the nuclear membrane intact, it can be used as a 'live' or fixed cell stain, although the concentrations required for 'live' staining tend to be higher.

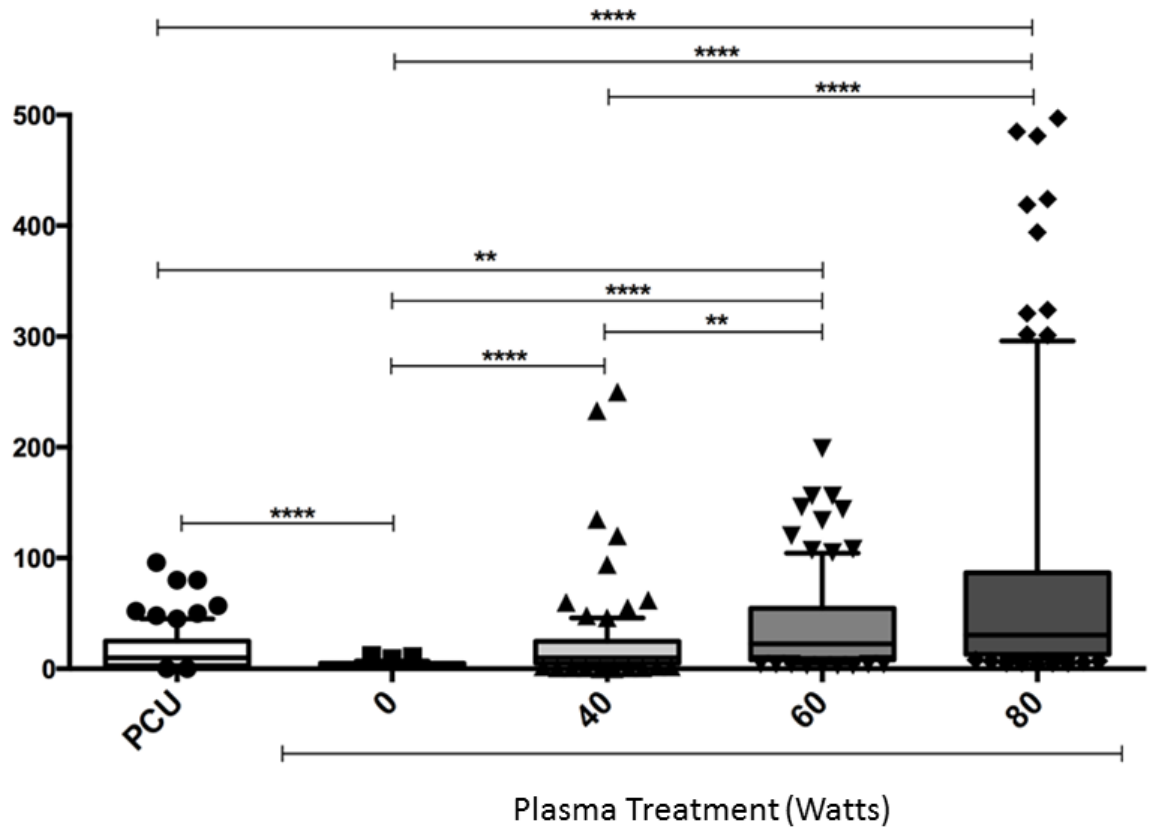


**Figure 4-6** Box plot showing cell numbers on plasma modified POSS-PCU films and unmodified POSS-PCU (0) and PCU films. Significant differences calculated using One-Way Anova are highlighted on the graph as follows: \*\*\*\* (p<.0001), \*\*\* (p<.001), \*\* (p<.01)

The controls that were used act as a comparative marker were polycarbonate urethane (PCU) which is without essentially polycarbonate urea urethane without the

POSS nanoparticle. The plasma samples were also compared with untreated POSS-PCU polymer to demonstrate the difference in cell number.

As it was seen, progressive higher plasma treatments showed a corresponding increase in cell number on the polymer. This is of particular importance as it proves that plasma-treatment has a definite improvement in cell number compared over untreated POSS-PCU and also PCU. Interestingly, there is statistical difference between all the plasma treatments except for 60W and 80W (for 60 seconds), indicating this may be the optimal treatment range.

#### 4.4.5 Immunofluorescence

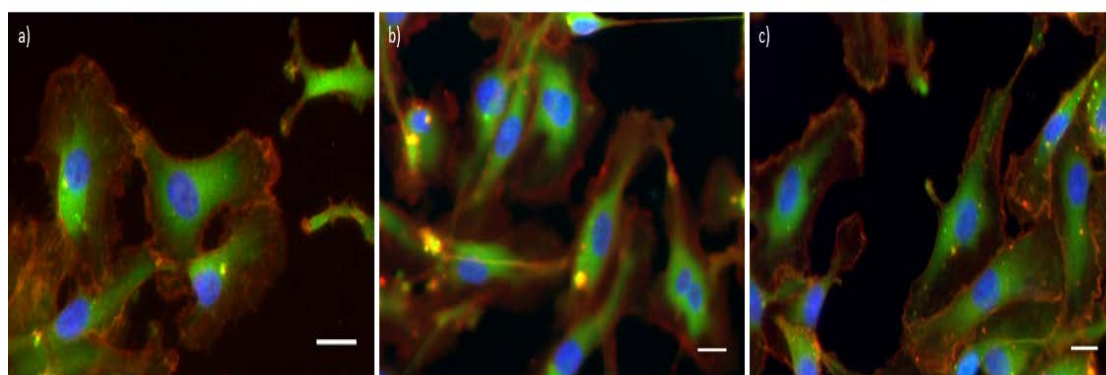


**Figure 4-7** Immunofluorescence of the HUVECs again highlight the normal morphology of the cells on the different plasma-treated polymer where a) 40W for 60s, b) 60W for 60s and c) 80W for 60s, where actin is red, vinculin is green and the nuclei is blue. (Scale bar: 10 $\mu$ m)

Immunofluorescence was conducted after 5 days of culture of HUVECs on the different plasma-treated POSS-PCU substrates. Immunofluorescence tagged one of the focal adhesion proteins, vinculin to look for signs of cell adhesion, as well as actin filaments and nuclei-staining.

The results of this immunostaining show that although it is possible to see the intracellular vinculin being present, it is less apparent to see the actual formation of the focal adhesions at the periphery of the cell. Again, the HUVECs are seen to spread out more in the POSS-PCU substrates with the higher plasma-treatment levels, whereas at the lower treatment levels these are much more rounded in morphology.

#### 4.4.6 In Cell Western

The use of the newer technique named In-Cell Western (ICW) over the more traditional Western Blot analysis means that there is the ability of a high throughput analysis and an easily quantifiable methodology.

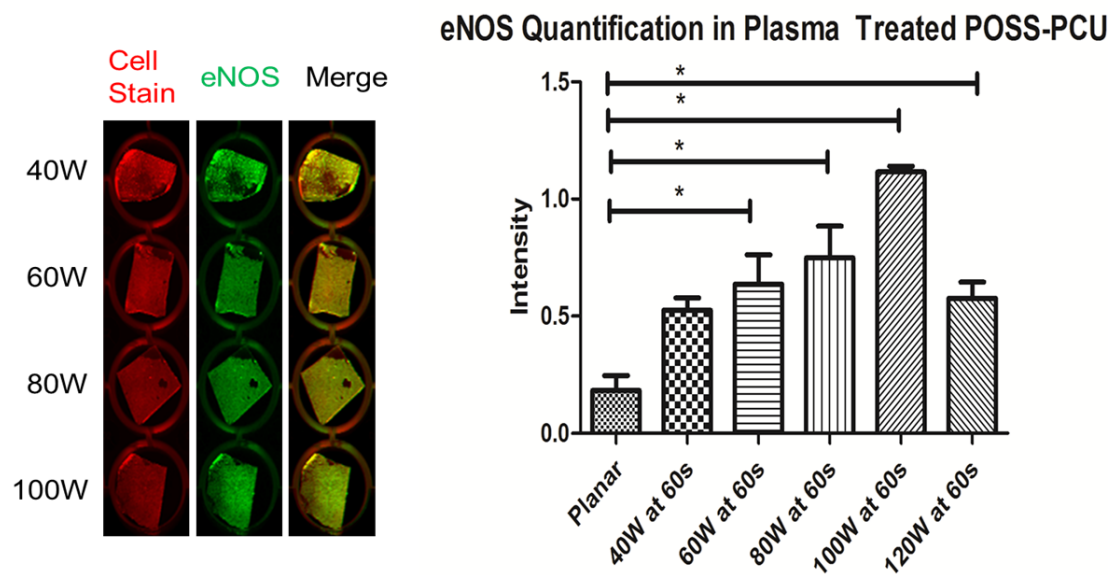


**Figure 4-8** This figure shows the use of In Cell Western (ICW) to quantify the amount of eNOS expression and the image on the left shows the near-infrared fluorophores tagged to eNOS (green channel) and the cell stain (red channel) and when it is merged. The intensity of this is then measured giving a quantifiable measurement on the different channels. ICW looks at quantifying the intensity of these fluorophores and therefore giving the graph on the right, where the eNOS expression is quantified on the different plasma-treated POSS-PCU polymer: \* ( $p < 0.05$ ) ( $n = 4$ )

These results looked at the expression of eNOS (endothelial nitric oxide synthase) which would indicate the function of the endothelial cells on the plasma treated POSS-PCU at the end of 5 days. These results show that on untreated planar POSS-PCU there is really very little expression of eNOS but with increasing plasma treatments there is increased eNOS expression until it experiences a drop at the treatment level of 120W at 60s. This indicates that this might be the limit of the beneficial effects of the plasma treatment in terms of the expression of eNOS and therefore endothelial cells function.

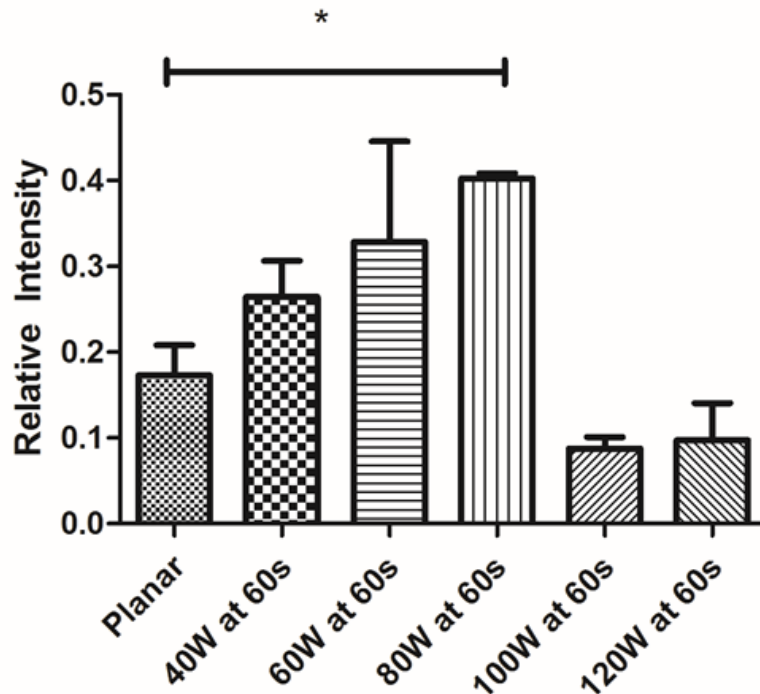


**Figure 4-9** This graph shows the P-myosin expression by the HUVECs on the different plasma treatments compared with planar untreated POSS-PCU surface. \*  $p < 0.05$  (n = 4)

P-myosin expression by the endothelial cells was measured on the different plasma-treated POSS-PCU surfaces after 5 days of cell culture. It was seen that there was only a significant difference in p-myosin expression when plasma-treatment levels reached 80W for 60s. However increased power in the plasma treatment levels only served to have a decreased in P-myosin expression levels, thereby indicating that the optimal plasma treatment level would be 80W for 60s.

#### 4.5 Discussion

Plasma treatment is an established physical surface modification technique which has been used in changing the surface chemistry of materials. This technique allows the modification of the surface of the substrates without jeopardizing the bulk properties of the material. The addition of hydroxyl (-OH) and carboxyl (-COOH) using pure oxygen plasma is known to decrease the surface water contact angle. This is an added advantage as this renders the surface of the substrate more conducive to cell growth (increased cytophilicity). It has been shown that different cells on different substrates will require different optimal contact angles and although it is possible to

predict the range of contact angles which are required, it will require further testing to confirm this prediction as not all cells behave uniformly.

A technical aspect of the plasma treatment is that the treatment itself needs to be conducted under vacuum and not under atmospheric pressure. This is due to the plasma discharge being more stable with the consequent plasma reactions being easier to control. This was even more evident during these experiments, as it was found that when a proper vacuum was not applied, the contact angles that were produced were not consistent. Plasma treatment of the substrates under atmospheric pressure would be a more desirable option as this means that there will be less technical equipment required, however practically, it was found that deposition of impurities was also problem when not conducted under a vacuum.

Another technical aspect of the plasma treatment is that moisture of the substrate does increase the resistivity of the substrate to plasma treatment(61). This can be a problem to ensuring that the plasma treatment is effective. It has been described by Nissan(62, 63) the three potential ways in which moisture can affect plasma treatment:

1. Low moisture content – means that the hydrogen bonds (H-bonds) can potentially dissociate individually into water molecules and then become absorbed into the structure of the polymer
2. Intermediate moisture content – a number of H-bonds can break in a group at the same time as diffusion of additional water molecules. A H-bond breakage, due to the presence of other water molecules, has a knock-on effect on other neighbouring bonds to break simultaneously.
3. High moisture content – the water molecules interact with one another and resulting in a high number of broken H-bonds.

The molecular structure of the polymeric substrate can be altered, including the physical properties and therefore the plasma treatment can alter the substrate completely. Bearing this in mind and thinking about the fabrication of the coagulated

form of POSS-PCU (extrusion into water), it was thought that this form of POSS-PCU would not be suitable for plasma treatment, especially plasma treatment in the most controllable form.

Therefore, the cast polymeric version of POSS-PCU was chosen as the moisture can be evaporated away and dried in the oven, as compared with the coagulated form of POSS-PCU which is hygroscopic. This was an important consideration when choosing a version of POSS-PCU to undergo plasma treatment to test the different surface modification techniques. A consideration for fabrication of a future vascular graft would be that the luminal surface of the vascular would be laminated with the cast version of the POSS-PCU whereas the bulk of the graft would be made of the coagulated version of POSS-PCU. Although this may impact slightly on the compliance of the POSS-PCU.

In this chapter, it can be seen that a step-wise lowering of contact angles can be seen with increasing levels of plasma treatment. This is a very important observation as it means that by using plasma treatment it is possible to lower the contact angle to a level in which a suitable biological response was seen. Furthermore, this shows that the use of plasma treatment conditions can elicit this controllable chemical modification in POSS-PCU polymer but without also changing the chemically toxic.

HUVEC adhesion is noted on the plasma treated samples and it can be seen that with the increasing treatments there are more cells seen adhering to the polymer at the end of 5 days of incubation, especially compared to non-treated POSS-PCU surfaces and even just polycarbonate urea urethane (PCU) surfaces. This is encouraging as it means that there is a predictable effect when trying to improve HUVEC adhesion onto the POSS-PCU substrates especially in lowering the surface WCA. There is no statistical significance seen of the cell count at the plasma treatment levels of 60W and 80W at 60s and this is an indication that at these treatment levels, this lowers the WCA to a level in which cells are optimally adhered and proliferating.

Increasing plasma-treatment has also shown a change in the cell morphology of the cells adhered to the surface of the POSS-PCU polymer. The HUVECs are seen to be spread out and become less rounded with increasing plasma-treatments indicating a

healthier cell morphology with these treatments. By the Live/Dead staining, this also indicates that the cells are healthy and that by altering the surface chemistry of the POSS-PCU polymer, there are no toxic effects rendered to the cells after 5 days of cell culture. This observation is crucial as changes to surface chemistry can also confer detrimental effects to the cells and therefore lead to cell death. This is also an important test of the biocompatibility nature of the chemical changes and indicates a safe environment for cells. These results are also correlated by those seen in the Coomassie Blue staining.

Cell count using DAPI staining provided some interesting results. As mentioned previously, DAPI binds to the AT region of double-stranded DNA. When it is bound, DAPI has an absorption maximum at a wavelength of 358nm and its emission maximum is at 461nm which is blue. This means that when using fluorescence microscopy, it is possible to excite it using ultraviolet (UV) light. The cell count demonstrated that plasma treated POSS-PCU had beneficial effects over untreated POSS-PCU and even the control polymer of PCU. It also indicates that the optimal range of plasma treatment would be in the region of 60W at 60s and 80W at 60s.

Disappointingly, the immunofluorescence does not indicate more focal adhesion formation and it is thought that although the cells are adhering to the surface, this may not be wholly adequate and requires another physical change in the surface environment to allow better adhesion. This is a crucial observation as it implies that when under haemodynamic flow, the cells would not be able to survive and any cell sheets would ultimately delaminate especially under the pressures in normal arterial flow. Delamination of an endothelial cell sheet, when normal haemodynamic pressures are applied, is a crucial problem discovered by many researchers in the 1980's and early 1990's, leading to more crucial examination of cellular adhesion properties under static conditions prior to application of haemodynamic pressures as a test of the original theories. Untreated PTFE and Dacron® vascular grafts after 24 hours under flow conditions have been found to have only 4%(64) and 3.4%(65) respectively, of seeded cells remaining on the original graft. This is obviously an important consideration and under static conditions, it is thought that cell adhesion should be optimized prior to testing under normal haemodynamic flow.

In Cell Western (ICW) results looking at the function of the HUVECs on the treated POSS-PCU surfaces compared with the untreated POSS-PCU surfaces have shown that function is maintained. Expression of eNOS is an important indicator of HUVEC function. Functional eNOS is found to be primarily associated with the plasma membrane and is highly regulated by multiple extracellular stimuli and the nitric oxide (NO) that is produced is a labile, cytotoxic messenger molecule with primarily paracrine function. However, the detection of the presence of eNOS is a sensitive indicator of function of the HUVECs on the POSS-PCU polymer. This is important as there is the potential for the HUVECs to enter into a senescent phase. NO is produced from the conversion of L-arginine to L-citrulline by eNOS. In endothelial cells, the isoform that exists is responsible for endothelium-derived NO production. Under certain conditions, human endothelial cells enter senescent, with eNOS activity being reduced in the process(66). The results show that this is not an issue and function of the HUVECs are maintained despite the chemical changes of the surface.

The ICW results have also shown an interesting pattern of results and even at higher plasma treatments, beyond the original boundary of 80W for 60s, it was seen that for endothelial function, 100W for 60s, might be the optimal plasma treatment level for the expression of eNOS, especially since a sharp drop is seen at 120W for 60s. This is in slight conflict with the cell count results which suggest that the optimal plasma treatment level might actually be in the range of 60-80W for 60s. It is thought that a fine balance has to be reached for further evaluation of this plasma treatment level and whether it is the treatment effect at this level or whether it is the consistent CA level reached. This is because the power levels on different plasma cleaners can also be another variable in the experiment (ie. plasma treatment levels can vary between different plasma machines).

Overall the process of ICW, it was found to give quantitative results which is a benefit over the more traditional Western Blot technique which is considered to only produce semi-quantitative assay results(67). The use of ICW gives high throughput quantitative results and does not require the labour-intensive and technically demanding steps of the more traditional Western Blot.

Therefore, this technique was also employed to investigate the presence of P-myosin expression by the HUVECs on the different plasma treatments of POSS-PCU. Non-muscle myosin II (NMII) is essentially comprised of 3 pairs of peptides(68). These are two heavy chains of 230kDa, two 20kDa regulatory light chains (RLCs) that regulate NMII activity and two further 17kDa essentially known as light chains (ELCs) that work to stabilize the light chain structures. NMII is important as it is known to be fundamental in processes such as cell adhesion, cell migration and cell division. NMII uses actin-cross linkage and contractile functions for these purposes. The active form of NMII is usually expressed as the phosphorylated form, and the phosphorylated version of this abbreviated P-myosin. The phosphorylation of NMII is a complex subject and involves a number of different kinases which initiate this process, which is beyond the scope of this PhD.

As NMII regulates cell adhesion and also polarity in cell migration by dynamic remodeling of the actin cytoskeleton and the environmental interaction. In particular, NMII is essential for the assembly and disassembly of nascent adhesions inside the lamellipodium. There is an important integrin-actin linkage which translates the effect of NMII to adhesions and will mediate adhesion formation and maturation. This means that in the activated form NMII plays an essential role in mediating cell adhesion and therefore the investigation of P-myosin (the activated form of NMII) would give a useful direct indication of cell adhesion on the substrate. Interestingly again the results support that that at treatment levels of 80W for 60s, the presence of P-myosin is at the maximal and any further plasma treatment seems to have a negative effect on this. This is interesting as it supports that cell count is the highest at this treatment level as well.

Consistently over the experiments conducted in this Chapter, it has been shown that the unmodified POSS-PCU has performed significantly worse than the plasma-modified POSS-PCU. Interestingly, the results have also shown that the optimal range for treatment appears to be around 80W for 60s on the POSS-PCU polymer. This treatment level appears to maintain endothelial cell proliferation, cell adhesion and function under all the investigated parameters. This important finding indicates

that this would be an acceptable plasma treatment level for the POSS-PCU polymer to create a surface which is conducive to endothelial cell adhesion.

These results are a vast improvement over that of untreated POSS-PCU in an *in vitro* setting and potentially also in an *in vivo* setting as seen in the sheep model(39) where no endothelialisation was seen at the end of the 9-month implantation period. This is an important consideration as it shows, in this chapter, that the use of plasma treatment is already part of the way to producing a biologically active surface although further work is required for further optimization of this. This is an important step into producing a POSS-nanocomposite polymer with a bioactive surface and proving that this physical method of surface modification, plasma treatment, is an essential methodology for this. However, although the results do show that plasma treatment is an essential first step in producing a surface in which endothelial cells are able to adhere and grow on and maintain their function, these results also show that perhaps further surface modification is required to further optimize HUVEC adhesion on the plasma treated POSS-PCU surfaces.

#### **4.6 Conclusion**

This Chapter has shown that it is possible to change the surface chemistry of the POSS-PCU polymer in a controlled manner to a contact angle which is conducive to cell, especially HUVEC growth. There is no toxicity of the POSS-PCU chemical changes to the cells, indicating that the chemical changes don't affect the biocompatible nature of the polymer. The function of the HUVECs are maintained through expression of eNOS. Optimal treatment levels have been indicated to be 60-80W for 60s although slightly higher treatment levels (100W at 60s) have also been seen to not impair the function of the HUVECs. Plasma treatment is indeed a viable option into surface modification of POSS-PCU without changing the bulk properties of the polymer. The ability to confirm this biologically active surface is an important finding towards creating POSS-PCU surfaces with bioactive surfaces especially in which self-endothelialisation is possible

However, although there is P-myosin expression, with an optimal plasma treatment level at 80W for 60s, it would appear that expression of vinculin is not detected as strongly on the immunofluorescence and begs the question of whether the cells are not as strongly adhered to the surfaces as we would have liked.

#### **4.7 Further Work**

Despite the first step in this work as being a positive finding in that POSS-PCU surfaces can be made bioactive, further optimization is still required. As cell adhesion has not been seen to be as evident due to the lack of focal adhesion formation found in the immunofluorescence, it has been suggested that a further physical factor might come into play which may also allow the formation of focal adhesion machinery. This other physical factor that is also known to have an effect is surface topography, and comes into a synergistic relationship with surface chemistry(42, 69). In vitro, many studies have shown that endogenous proteins are the first to be rapidly adsorbed onto the surface of a material, and it is these proteins which provide the structural framework on which further cell adhesion can begin. This effect has been extensively studied since the 1960s by Vroman(70) (and hence this is dubbed 'Vroman's effect'). The Vroman's effect is also dependent on surface chemistry as well as topography(71). This shows that surface topography probably will need to work synergistically with surface chemistry to enhance cell adhesion and growth.

Recent studies have shown that cells are responsive to micro and nanoscale topography. Harrison(72) in 1911 noted that cells were able to align themselves according to surface topography. However, until recent technological advances, the ability to study cell behavior on surface topography has not been possible. However, as we have seen in this chapter that surface chemical modification is possible but there may be extra factors which may contribute to cellular adhesion and this may be surface topography. Further work will concentrate on adding controlled surface topography to the plasma treated surface of POSS-PCU. In combination, it is hoped that this will provide both further cell adhesion and proliferative surfaces.

# **Chapter 5: Surface modulation of POSS-PCU: Surface topography**

## Chapter 5 Surface modulation of POSS-PCU: Surface topography

### 5.1 Introduction

The development and research of vascular grafts have driven many researchers to either improve on current materials in clinical use (such as PTFE and Dacron®) or to develop new materials. The investigation of POSS-PCU as a potential novel vascular graft material has shown some very promising results. The mechanical and compliance properties of the material is shown to be similar to native vessel when compared with PTFE(60). Unfortunately, this material does not endothelialise and this has both been confirmed in both *in vitro*(73) and *in vivo*(39) experiments. Therefore, the ability to retain the beneficial bulk properties of POSS-PCU but still allowing the fine-tuning of the luminal surface of the vascular graft, produces a desirable aspect of research.

In the last Chapter, the experiments have shown that plasma treatment does have a positive effect on endothelial cell adhesion and function on the surface-modified POSS-PCU. However, it is not certain that this is the complete solution as ‘strong’ endothelial cell adhesion is still questionable, due to the lack of vinculin seen forming as ‘localised’ focal adhesions on the immunofluorescence images. This raises the question of the adequacy of the endothelial cell adhesion. Therefore, it is concluded that other physical factors must come into play and that altering surface hydrophilicity (through chemistry) alone was not enough. Another physical factor that would play a synergistic role with surface chemistry would be surface topography.

Harrison first noticed in 1919 that cells were adaptive to surface topographical features(72). This was an interesting observation but unfortunately research on it has since come to a standstill from then to only recently due to the lack of technological advance allowing the creation of surface topographical features in which to study the cells on the topography. From the moment, Richard Feynman(74) mentioned that ‘there was plenty of room at the bottom’ in his infamous speech to Drexler coining the term of ‘nanotechnology’, this has meant that the scientific research has allowed fine-precision tuning to the nanoscale.

Cells have been seen to react with surface topography both in the micro- and nanoscale and both will have an impact on cell behaviour. It is thought that the cell as a whole is more likely to react to topography in the microscale but nano-sized topographies will have further impact on entities which are in the same size, namely cell receptors. Topography provides a biomimetic physical-cue to cells which is similarly found on the topography-rich surfaces of basement membranes found *in vivo*(75). Cells *in vivo* are known to reside on surfaces with physical cues (and not just flat surfaces) and this has been observed. These cues come in the form of pillars, pits, fibres, channels, pores, etc. and can be uniformly or randomly textured.

However technological advances in the semiconductor industry has meant that surface features can be created in the micro- and nanoscale and used to study the biological responses to it. Although, it is not possible to create all the complex intricacies of what is *in vivo*, it is possible to create surfaces with simple repetitive features and therefore study cellular behaviour on these features. This has led to a flurry of research activity to investigate the extent in which surface topography can be used to control and modify cell behaviour.

### **5.1.1 Fabrication Techniques**

There have been many different fabrication techniques which have been adopted to develop features in the micro- and nanoscale. Lithographic techniques have been mainly used due to the reproducibility and the high-precision of the features which are created. This Chapter will focus on the fabrication techniques which are relevant to this PhD. In this PhD, the most used fabrication technique has been lithographic techniques to create micro- and nanostructures for our experiments.

Lithography is essentially a technique which is used in the transfer of a pattern onto a substrate by means of an etching process(76). Resist lithography makes use of an irradiation source on which a photosensitive polymer material (photoresist) is utilised to perform the pattern transfer. The process starts with coating a substrate (usually a silicon wafer) with the photoresist in liquid form. This is 'soft-baked' at a low enough temperature to evaporate the solvent off which is in the photoresist but not high enough to cause other chemical reactions, and in addition this helps improve

resist-substrate adhesion. This photoresist can then be exposed to a variety of light sources (i.e. Ultraviolet (UV) light, X-rays, electron-beam) depending on the lithographic method. Exposure to this light source initiates a photochemical process in which the resist will alter the physical and chemical properties of the exposed areas for differentiation into a subsequent image development process. The solubility of the subsequent film can be modified such as increasing the solubility of the exposed areas (yielding a positive image post-development) or decreasing the solubility to yield a negative tone image. Post-development, surfaces with negative tone images can be 'hard baked' to further strengthen the cross-linking process and improve mechanical stability of the patterns.

Standard photolithography uses a mask for its patterning potential but there are limitations to the resolution of the feature sizes that can be produced. Although it is possible to make submicron features and there have been many published techniques which have illustrated this, these techniques are pushing the boundaries of the technique and may not be reproducible from laboratory to laboratory. For example, it is possible to use extreme UV light (wavelengths from 124nm to 10nm) and X-rays (wavelengths from 10nm to 0.01nm) as the light source as the feature size possible is correlated by the wavelength of the source. However, conventional lenses are not transparent to extreme UV and are unable to focus X-rays and the energies of these radiations will damage most materials used in masks and lenses(77).

Therefore, for sub-micron features, it was more desirable to use lithography techniques based on focused beams such as e-beam lithography (EBL) and focused ion beam (FIB). EBL uses a focused beam of electrons directly onto the photoresist to produce patterns. It is possible to produce feature sizes down to 10nm and even lower, using both EBL and FIB. However, the throughput of EBL can be limited and the costs to produce small areas of patterns can be very high. A further drawback of EBL is the proximity effect caused by the scattering of the electrons in the resist. This backscattering impacts on the final resolution and contrast of the features produced(78). Although FIB is also a possibility for producing patterns and they have the potential of producing thin films (such as epitaxial films) and metal organic chemical-vapour deposition and sputter deposition, there are unfortunately

disadvantages to the technique. The process of milling and imaging can cause direct damage to the material and there is concern that doping with Gallium ions can also add to this damage. Unfortunately, this damage makes this technique unsuitable to development of biomedical devices which require more local biological effects, such as endothelialisation, to take place and such entities would be sensitive to surface damage. There is concern that with FIB being a maskless technique, direct-write using the high-energy beam onto the surface can potentially damage the surface releasing toxic elements which can also affect cell growth.

This forms the basis of many lithographic techniques on which subsequent improvements have been made to produce the smallest feature sizes possible. Photoresists themselves play an important part of the lithographic process and in the manufacture of biomedical devices, this is an important consideration as the photoresists themselves have to be non-toxic. There are a number of photoresists available for this purpose, for use under conditions which require a biocompatible and non-toxic photoresist. Photoresists such as SU-8 have been deemed to fulfil these requirements and therefore have been used for this purpose.

### **5.1.2 'Disordered' and 'Ordered' Surface Topography**

Since the fabrication techniques can be utilised to produce a wide range of topographies, two types of topographical design differences must be established. This is mainly 'ordered' and 'disordered' surface topography.

Disordered topography can be easily fabricated with techniques such as electrospinning(37) or polymer de-mixing(41). With advancements in electrospinning, this has meant that fibres can be produced in both the micro- and nanoscale. The use of electrospinning in the fabrication of vascular grafts have proven to be a very popular fabrication technique in the recent years. Electrospinning allows a facile fabrication in which surface topography can be produced on the luminal surface of the vascular graft. The capability of the technique has meant that a variety of polymers can be used for the task, ranging from synthetic to non-synthetic. The fibres that are produced can be used to create a variety of nano/ micron-sized pores to allow tissue integration and also mechanical and biological properties of the

vascular graft can be fine-tuned by varying the composition of the mixture or the size of the fibres being produced(79). This technique also benefits from being a high-throughput manufacturing process and therefore these benefits have made it a process which a lot of research focus has been. However, one of the main disadvantages of such a technique is the non-consistent reproducibility of the technique, namely no two grafts will be identical meaning that exact mechanical and biological properties will vary. The cell seeding that is required, post scaffold production, also means that this will limit the use of such scaffolds in an ‘off the shelf’ or emergency setting. Despite the ability to control the porosity of the scaffolds to allow for cell integration, many studies have shown that in electrospinning this is still a difficulty.

Ordered topography can be created with precision by techniques, as mentioned above, such as photolithography and electron beam lithography. These techniques allow a more controlled fabrication methodology to creating the surface topography. If these vascular grafts were to be manufactured commercially, this would make things easier for quality control as the predictability of each graft can be ensured.

In theory, due to the ability of such topography being able to elicit a cellular response, it is therefore possible to produce a surface topography in which the vascular graft could have ‘self-endothelialisation’ potential post-implantation. This would allow these vascular grafts to be used in an ‘off the shelf’ setting.

### **5.1.3 Cell Engineering**

With the advances of the lithographic techniques, this has allowed the study of cell behaviour on various topographies. Surface topography has mainly been fabricated in two-dimension (2D) but with newer techniques of fabrication such as two-photon polymerisation(80), fabrication techniques have also developed into 3D culture.

For biological applications, the requirements of the topographies(81) are that they should be the following:

- Occur over a large surface area so that the results are repeatable and also ‘patterning’ of medical devices will require high throughput production than currently conducted in some techniques
- Easily accessible and low-cost so that the production of the patterns is not limited to specialised equipment
- Reproducible patterns so that there is a consistency in the results that are produced time and time again

Endothelial cells, like many other cell types, react to biophysical cues from the tissue microenvironment and these modulate cell function on a different level from biochemical cues. With a particular focus on vascular endothelial cells, these cells reside in the basement membrane, which is a specialised extracellular matrix (ECM) providing complex 3D biophysical cues to the endothelial cells. These cues can be in the submicron (100-1000nm) and nanoscale (1-100nm) range and therefore being able to provide these cues can provide an interesting dimension to the research.

One topography of interest, and on which this Chapter will be focused on, is known as the NSQ (Near Square). This is an interesting topography which is essentially nanopits with diameter of 120nm, 100nm deep with an average of 300nm centre-to-centre spacing but slightly displaced with an offset of  $\pm 50$ nm. The reason for the interest is that NSQ has been found to push mesenchymal stem cells (MSCs) to differentiate into an osteogenic lineage when cultured on this topography(42). Interestingly when compared with a more ordered topography this is not seen, suggesting that the role that topography plays is essential in determining the lineage of stem cells.

There is further suggestion that cell adhesion may be promoted on this NSQ topography creating large focal adhesions, which forms a part of the differentiation process(82, 83). However, although the importance of the role of the NSQ topography has been investigated for MSCs, this has not been fully explored for HUVECs. The NSQ topography will therefore form an important part of this Chapter. It is postulated that the large focal adhesions which NSQ can cause the cells

to form, can help endothelial cells to adopt a similar morphology and encourage better adhesion to the substrate, allowing the endothelial cells to withstand pressures and stresses that are seen in the vascular vessels.

In addition to this, micro-topography has also been a focus of study and it is not sure which scale of topography would have a good effect on endothelial cell adhesion. Previous work has suggested that endothelial cells response to micro-topography especially grooves and are able to align themselves onto the grooves.

Cell Type	Substrate	Pattern	Dimensions and Pitch	Static/ Shear Flow Culture?	Description	Year/ Ref
<b>Human microvascular endothelial cells (HMECs)</b>	Type I Collagen films	Microgrooves	Parallel channels with groove and ridge widths of 650nm with 300nm depth, 500nm with 250nm depth and 332.5nm with 200nm depth	Shear flow	Cell culture studies show that nanopattern did not affect endothelial cell proliferation and had minimal effect on cell alignment but significantly enhances cell retention under flow-shear conditions.	<b>2009(40)</b>
<b>Bovine aortic endothelial cells (BAECs)</b>	PDMS	Microgrooves	Symmetric patterns: 5x5, 3x3, 2x2 Asymmetric patterns: 5x2. Widths of ridges and channels 5 and 2µm. Separation 500µm	Shear flow	Width dimension of 3D microgroove guides direction of endothelial cell migration in absence of flow. Critical groove width for cell migration is 2µm. Microgrooves guide orientation of actin stress	<b>2008(84)</b>

					fibres parallel to grooves after exposure to flow (moderate and high shear) for at least 4 hours.	
<b>BAECs</b>	Micro-patterned ECM by injection of collagen 1 into PDMS mold	Microchannels	Width 15, 30 and 60µm	Static	ECs on 15µm collagen strips had 30% less adhesion area and lower shape index, had fewer but polarised focal adhesions and migrated faster.	<b>2001(85)</b>

**Figure 5-1 Table to show a selection of publications in which grooves have been used to identify in both static and shear flow conditions and a brief description of the findings. [Adapted from Table 2 in (37)]**

Endothelial cells in the presence of either microgrooves or channels tend to induce cell alignment along the grooves, however recent published results on this have shown conflicting results in the exact dimensions of microgrooves which induce a consistent cell alignment. This is likely due to a non-consistent use of cell type, or substrate and therefore consistent results cannot be extrapolated. However, because of this discrepancy in the results, individual results using a consistent cell type and substrate would probably elucidate a more consistent conclusion.

In addition to this, microgrooves have also been seen to promote endothelial cell migration by giving the cells ‘contact guidance’. This would have an additional beneficial effect when designing the luminal surface of vascular grafts as this would potentially encourage the inward migration of endothelial cells from neighbouring native vessel. Prior to the use of topography, there has been other interest in using different methodologies of in situ endothelialisation, however, as Professor Zilla pointed out, there has only ever been 1-2cm inward growth of endothelium and therefore this technique was largely abandoned(86). However, the possibility of using ‘contact guidance’ by designing the surface with topographical cues on the

luminal surface of the vascular grafts offers an alternative methodology and merits further investigation.

Thus with this in mind, in this Chapter, endothelial cell behaviour on topographical cues will be observed and analysed.

## **5.2 Aims and Hypothesis**

The aims of this Chapter is to investigate the addition of surface topography in both the micro- and nanoscale onto the POSS-PCU polymer. The aims of this Chapter:

- Show that both micro- and nanoscale patterns can be replicated in POSS-PCU polymer with high fidelity
- The patterns do not cause any detrimental effect on biological cells
- These patterns in synergy with plasma treatment can provide a more biologically active surface than just with plasma treatment alone

## **5.3 Materials and Methods**

### **5.3.1 Photolithography and Electron Beam Lithography**

These processes were conducted in a Cleanroom at the James Watt Nanofabrication Centre (JWNC) at the University of Glasgow, United Kingdom.

Photolithography was conducted according to previous published methods. The technique was used to produce microscale grooves of 12.5 $\mu$ m wide grooves with 25 $\mu$ m pitch and 700nm groove depths.

Electron-beam lithography was conducted, again, as per previously published methods(87). The master substrate was fabricated using EBL (Vistec VB6 UHR EWF Electron Beam Lithography Tool) to form arrays of 120nm diameter pits of 100nm depth and 300nm pitch in a square arrangement with an offset with a random displacement of  $\pm$ 50nm.

Both substrates produced from the two techniques were then treated by reactive ion-etching to produce the intended features. These techniques have been briefly described in Chapter 2 (Materials and Methods).

These substrates were kindly produced by the post-doctoral research associates and technicians under the guidance of Professor Nikolaj Gadegaard at the JWNC.

### **5.3.2 Soft Lithography**

The shims that were generated by both EBL and photolithography were used as the substrates for soft lithography for pattern transfer. This involves placing the POSS-PCU polymeric solution on to the substrates and then placing in an oven set at 60°C for a minimum of 2 hours, until all the DMAC solvent has been evaporated off. The polymer films are then allowed to cool before peeling off from the substrate.

### **5.3.3 Plasma Treatment and Contact-Angle Measurement**

The POSS-PCU films were then plasma-treated in a barrel-type plasma asher (Plasma Prep 5 GaLa Instrumente) with pure O<sub>2</sub> at different powers for different time points. This was conducted under Cleanroom conditions at the JWNC to lower the risk of deposition of any other impurities on the substrate as previously found. Post-treatment with plasma, contact angles were measured to check the effectiveness of the treatment. This was conducted with an in-house built apparatus.

### **5.3.4 Scanning Electron Microscope (SEM) and Atomic Force Microscopy (AFM)**

The POSS-PCU films were sputter-coated with gold at a thickness of 2nm before being visualised with a SEM, a Carl Zeiss Sigma Variable Pressure Analytical SEM with Oxford Microanalysis (Germany). This was conducted to check the fidelity of the replication of the patterns on the POSS-PCU films.

The POSS-PCU samples were stuck onto glass-slides with super-glue for analysis with AFM (JPK Nanowizard 3). This was again conducted to check the replication fidelity of the replication of the patterns on the substrate and to check the roughness

of the surface. Surface analysis was conducted using Data Processing Software from JPK. This includes the calculation of roughness values (RMS). RMS is defined as the standard deviation of the elevation,  $z$  values, within the given area is calculated from the following equation:

$$Rq = \sqrt{\sum (z_1 - z_{ave})^2 / N}$$

Where  $z_{ave}$  is the average of the  $z$  values within the given area,  $z$ , is the  $z$  value for a given point, and  $N$  is the number of points within the given area(88). This equation can be converted using AFM-associated software so that RMS values can be generated.

### **5.3.5 4',6-diamidino-2-phenylindole (DAPI) Cell Count**

Cell numbers were measured after 5 days of culture. The cells were then fixed in 4% formaldehyde for 15 minutes at 37°C and then washed in PBS. DAPI (Vectoshield DAPI, Vector Laboratories) were placed, as per instructions on the substrates. Using fluorescence microscopy (Zeiss Axiovert M200), ten randomly selected images were taken at 10 different locations of each of the films at a magnification of x20, of cells stained with DAPI. Cell nuclei was counted as an indication of cell number. A minimum of 4 films were assessed for each treatment and topography.

### **5.3.6 Coomassie Blue Staining**

The samples were after 5 days of culture and then fixed using 4% formaldehyde before Coomassie Blue (0.2% Coomassie Blue w/v in 46.8% methanol, 7% acetic acid, 46.5% water) was added for 2 minutes. This is then removed and the samples are then washed with de-ionised water and dried before visualising with an optical microscope.

### **5.3.7 Immunofluorescence of the HUVECs on the POSS-PCU Films**

Day 5 samples were fixed in 4% formaldehyde for 15 minutes at 37°C and then washed before placing in a permeabilising buffer and then blocking with 1% (w/v) bovine serum albumin/ PBS mixture. Samples were then stained with anti-vinculin antibody (1:150) (Sigma) in 1% (w/v) BSA/PBS or anti-endothelial nitric oxide synthase (eNOS) antibody (1:50), in conjunction with rhodamine/ phalloidin (1:500), and incubated at 37°C for 1 hour. Samples were subsequently washed for 3 times at 5 minutes each (0.5% Tween-20 in PBS) and then the secondary antibody, which is biotinylated, is added (Vector Laboratories) at 1:50 in 1% (w/v) BSA/PBS. Samples were then incubated for 1 hour at 37°C. After further washing, FITC-conjugated streptavidin (1:50, Vector Laboratories) was added and incubated for a further 30 minutes at 4°C. Samples were given a final wash before mounting using Vectashield with DAPI nuclear stain (Vector Laboratories). Samples were then imaged using a fluorescence microscope (Zeiss Axiovert M200).

### **5.3.8 In-Cell Western for eNOS and P-myosin of HUVECs on the POSS-PCU Films**

Once again at the appropriate time-point of cell culture, the cells on the POSS-PCU films are firstly fixed in 4% formaldehyde at 37°C for 5 minutes. The cells are then placed in a permeabilisation buffer at 4°C for 5 minutes, before being blocked (milk powder/ PBS) for 1 hour at room temperature. The primary antibody is then added at a concentration of 1:50 (anti-eNOS and anti-P-myosin) and incubated at 37°C for 2 hours. These are then washed with 0.1% Tween/ PBS and then fluorescent-labelled secondary antibody (Licor, Cambridge, UK) at a concentration of 1:1000 with also CellStain (CellTag 700 Stain, Licor, Cambridge, UK) at a concentration of 1:500, and then left at room temperature for 1 hour. The secondary antibody is then removed and the films washed using 0.1% Tween/PBS. The results are then analysed using an automatable infrared imager with a 2-channel imaging system (Odyssey Sa, Licor, Cambridge, UK).

### **5.3.9 Statistical Analysis**

Statistical Analysis of the results were conducted using Prism (GraphPad Software, La Jolla, USA).

The statistical tests that were conducted were as follows: roughness values between sample types were compared using Mann-Whitney (non-parametric) tests, differences in cell number between samples (both plasma treated planar substrates and topographically altered substrates) were compared using Kruskal-Wallis (non-parametric) tests.

## **5.4 Results**

The results in the previous Chapter has shown that plasma treatment is able to lower the contact angle of the POSS-PCU in a step-wise fashion. This Chapter looks at whether surface topography and chemistry can synergistically encourage endothelial cell growth.

## 5.4.1 Replication Fidelity

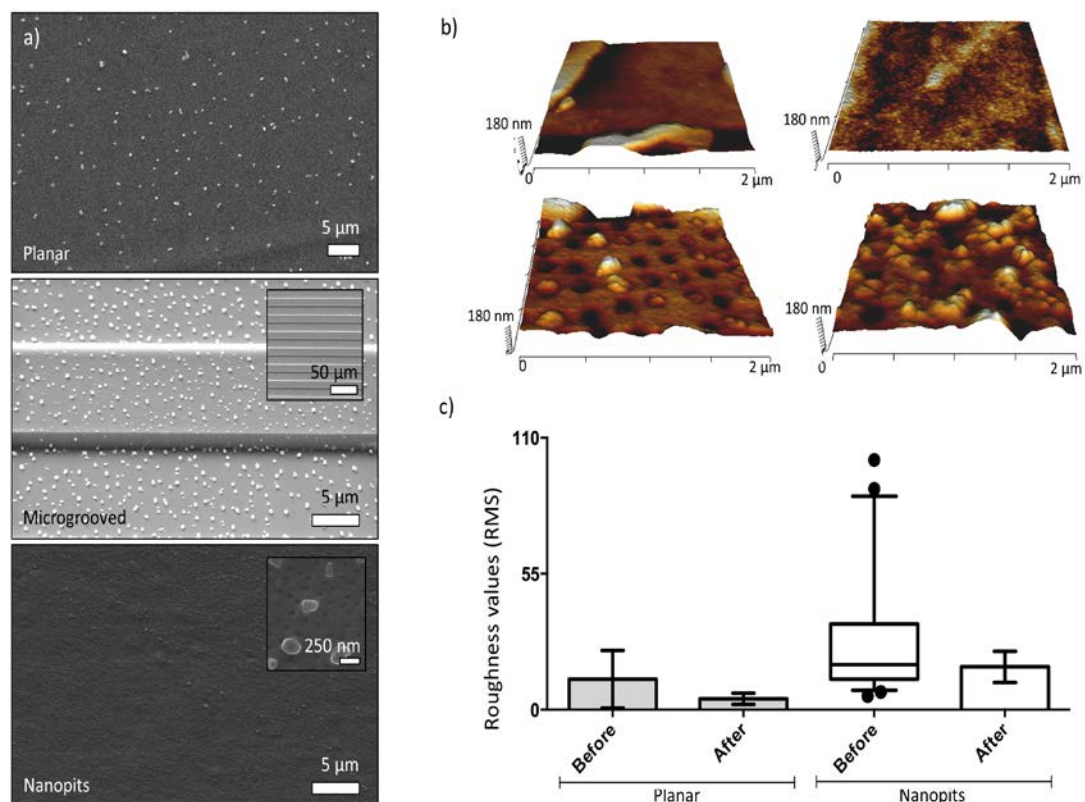


**Figure 5-2 A)** This figure shows scanning electron microscopy images of planar, microgroove and nanopit POSS-PCU surfaces before plasma treatment, insets show higher magnification images of the topographies; nanopit inset was imaged after plasma treatment for 60s at 80W. **B)** AFM scans of planar (upper two images) and nanopit (lower two images) POSS-PCU films before (left hand side images) and after (right hand side images) plasma treatment. **C)** Box-plot showing roughness values of planar and nanopit POSS-PCU films.

It is possible to see that using soft lithography, the replication fidelity of the patterns is intact and this can be confirmed on both AFM and SEM. Visually it is possible to see that on SEM that the microgrooves and nanopits features have been retained. As there is a great concern that at high plasma treatments, there is a possibility that nanopatterns would be destroyed due to the high energy bombardment of the molecules on the surface of the polymer, AFM was used to measure roughness values (RMS). There is no statistical significant difference between pre- and post-treatment with plasma. This means that the current highest level treatment of plasma at 80W for 60s is safe even in the presence of nanopatterns, or in our case, the nanopits. In addition, again, it is possible to see again the POSS aggregations on the surface of the films. It is decided as this is an inherent part of the POSS-PCU

polymer itself, it was not anything that can be changed but as both the micro- and nanofeatures are easily discernible between the aggregates, it was deemed that these aggregations would not disrupt the effect on the cell by the surface topography. As this is an inherent property of the POSS-PCU polymer, it is assumed that the distribution of POSS aggregates will be the same throughout the polymer and will not be affected by the treatment.

#### **5.4.2 DAPI Cell Count and Coomassie Blue**

The DAPI cell count has shown that the optimal plasma treatment level (80W for 60s) has no significant effect on the number of cells after 5 days of cell culture on the different topographies, namely planar, nanopit (NP) and microgroove (MG). This experiment was repeat three times.

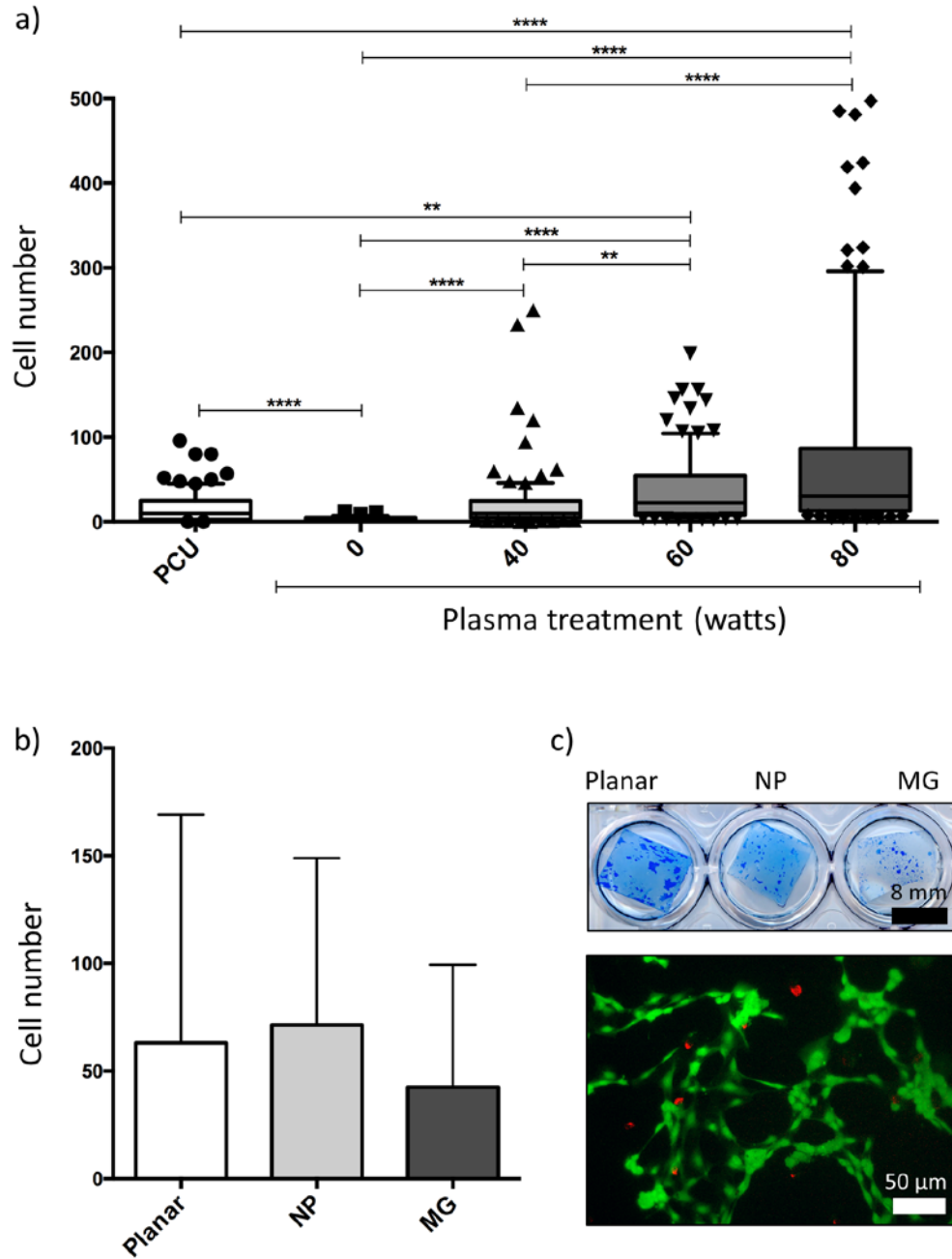


**Figure 5-3** This figure recaps from the previous chapter about the cell number (a) and from this original graph, it can be seen that plasma treatment levels of 80W for 60s has the highest cell count and extrapolating this treatment level as the optimal treatment, cells were cultured on the different topographies using this plasma treatment (b) with no significance differences found ( $p > 0.05$ ). C) Upper image shows a scan of Coomassie Blue staining on the different topographies and the lower is a fluorescent image is Live/Dead staining (green = Live, red = Dead) of cells on a nanopit substrate with plasma treatment (80W for 60s). (n = 4)

Coomassie Blue results show that after 5-day culture patchy endothelial cell growth can be seen. Live/Dead staining also indicates that the cells are still alive on the topographies. These results suggest that these surface topographies do not have any

detrimental effect on the on cell growth and proliferation and there is evidence of 'patchy' endothelialisation after 5 days of cell culture.

#### **5.4.3 Immunofluorescence of HUVECs of POSS-PCU**

These immunofluorescent images show that endothelial cell morphology is maintained on the different topographies and it is possible to form endothelial cell sheets on these plasma-treated surfaces. The HUVECs look elongated at the lower magnification (x20) and spread out which is typical of normal endothelial cell morphology on a surface which is suitable for them to adhere and proliferate on.

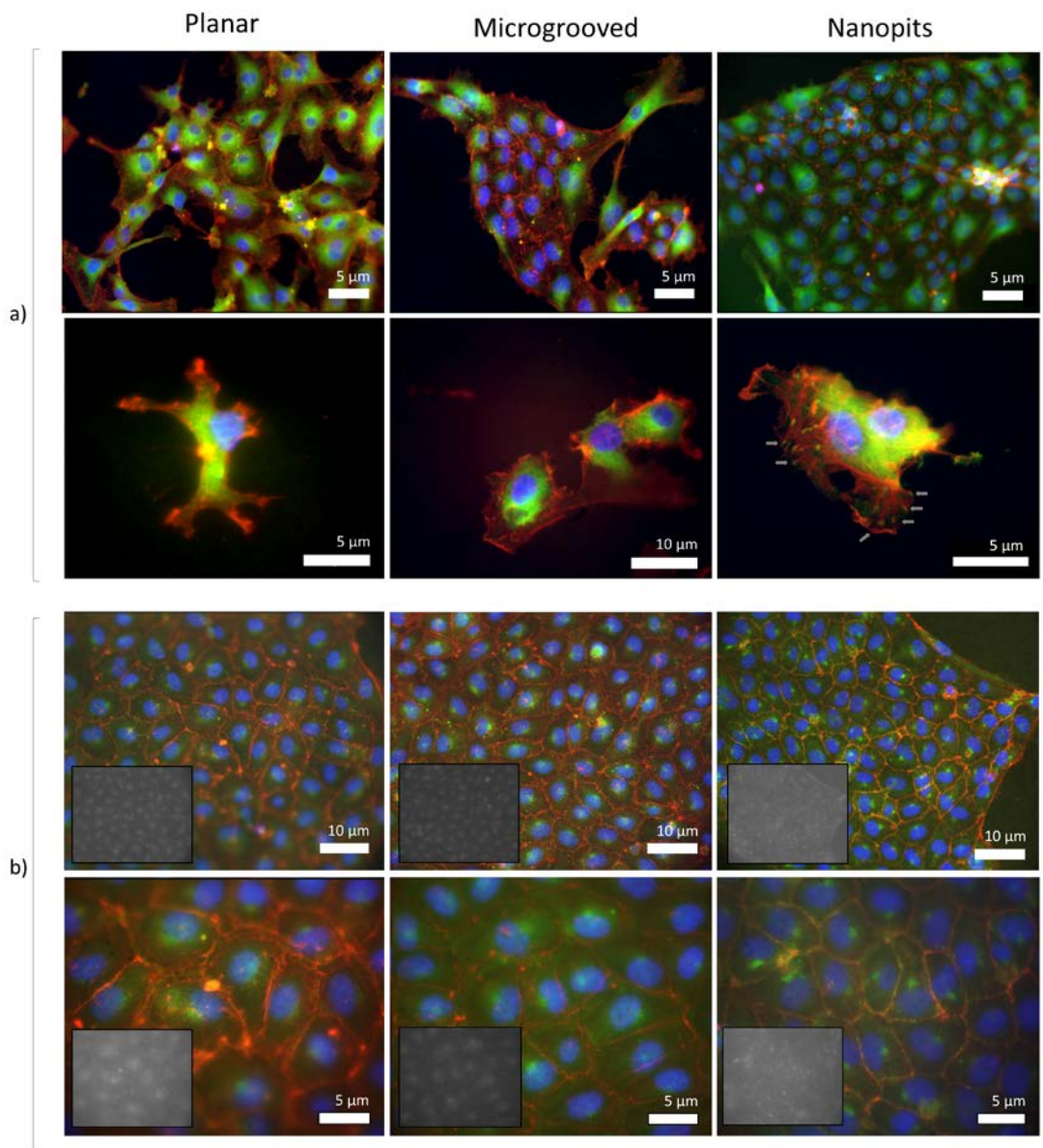


**Figure 5-4 Cell morphology and function on topographically patterned POSS-PCU films. Fluorescent micrographs show nuclei (blue) and actin (red). Specific proteins, namely vinculin (highlights focal adhesions at cell periphery) and nitric oxide synthase (marker of endothelial cell function) are highlighted in a) and b) respectively. Grey arrows in a) in the lower right image highlight focal adhesions. Images were enhanced using contrast/ brightness controls with the exception of the insets in b) which show the unmodified images of eNOS expression using identical microscope settings.**

These fluorescent images highlight the healthy morphology of the endothelial cells. However interestingly, focal adhesion formation was only seen on endothelial cells growing on NP topography compared with the microgroove and planar topography. This seems to suggest that there is a subtlety in the nanoscale topography which enhances the focal adhesion formation.

In addition, the fluorescent images also confirm that despite the topographical changes to the surface of the polymer, this does not impair the function of endothelial cells on the surface. It is possible to see eNOS expression on the three different surfaces at the highest plasma treatment level of 80W for 60s. This is a very important indication of function of the HUVECs on the different topographically and plasma-modified surfaces.

#### **5.4.4 In Cell Western Quantification of Endothelial Cell Function**

The measurement of endothelial nitric oxide synthase (eNOS) is a useful indicator of endothelial cell function and due to this, it is useful to get a quantitative indication as to the function of the endothelial cells, which was conducted using In-Cell Western. This comparison was done using MG (microgrooves) as samples of this topography can be fabricated in bulk quantity easier than with the nanoscale topography. This would give an indication as to whether topography in the microscale makes any difference to endothelial function.

It was seen that there was a statistical significance only at treatment levels of 80W at 60s and 100W at 60s compared with untreated planar, therefore suggesting that at these treatment levels in the presence of micro-topography are optimal for endothelial function. Interestingly, at the treatment level of 120W at 60s, this eNOS expression falls indicating that at this point, endothelial function is disrupted. However, although the other treatment levels (40W and 60W at 60s) did not receive a level of statistical significance, there is a step-wise pattern to the increase of eNOS production on the MG surfaces.

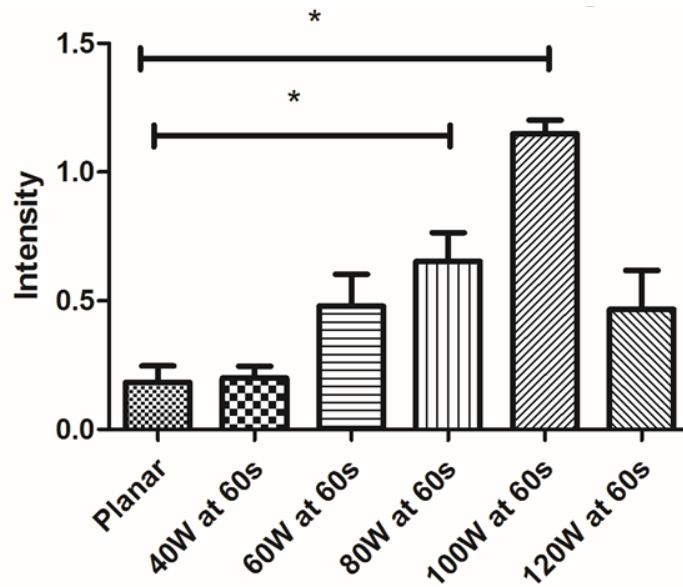


**Figure 5-5** Graph showing eNOS expression at 5 days after cell culture on microgroove and plasma-treated POSS-PCU surfaces using In Cell Western. There is a statistical significance in eNOS expression at 80W and 100W at 60s plasma treatment levels on the micron grooved POSS-PCU substrates (\*  $p < 0.05$ ) (n = 4)

#### 5.4.5 In Cell Western Quantification of P-Myosin Expression

A further measurement of HUVEC adhesion to substrate was to look at P-myosin expression. Again, due to fabrication enablement, microscale topography was used at different plasma treatment levels.

There was no clear indication that on any of the plasma treatment levels had any effect on P-myosin expression and no obvious pattern was discernible from the results. There was also no statistical significance between any of the treatment levels.

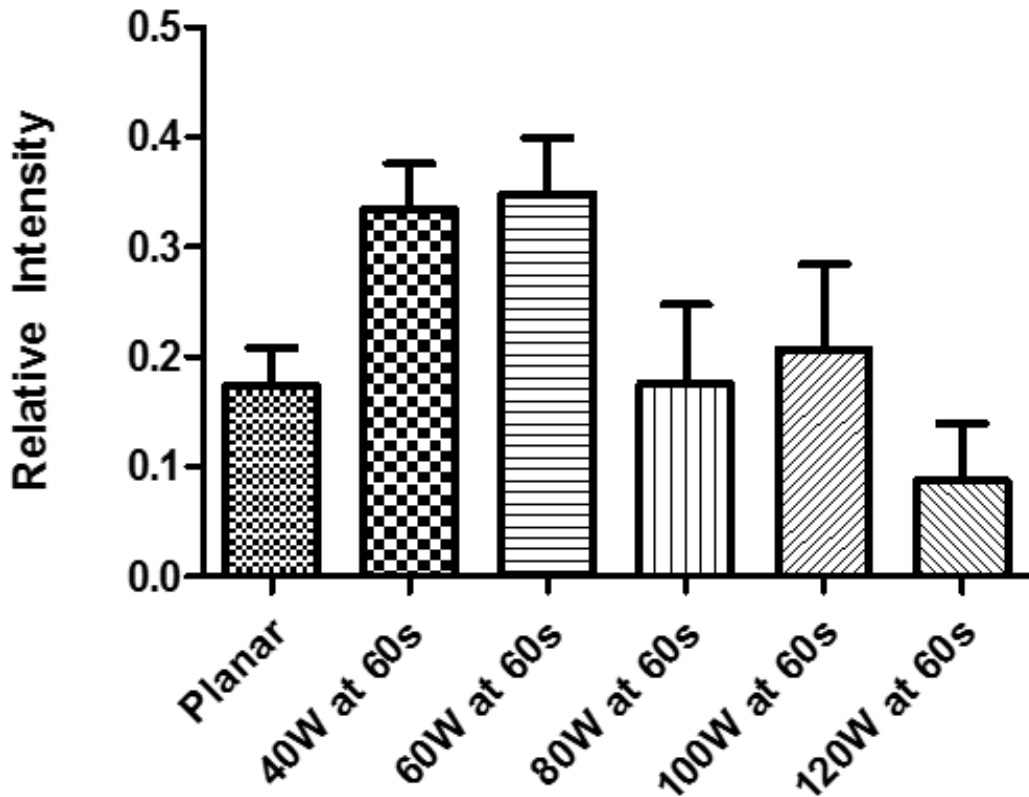


Figure 5-6 This graph showing P-myosin expression after 5 days on incrementally increasing plasma treatment on POSS-PCU substrates with microgrooves. There is no statistical significance at any of the plasma-treatment levels on the micro-grooved surfaces. (n=6)

## 5.5 Discussion

The use of a combined methodology, in the form of surface chemistry and topography to help with endothelial cell adhesion is explored in this Chapter. Previously, it has been shown that it is possible to use plasma treatment to lower the water contact angle (WCA) of the POSS-PCU films so that endothelial cells are able to grow and adhere on the surfaces of POSS-PCU films. However, it was not certain that the endothelial cells were greatly adhered to the surfaces as there did not seem to be any focal adhesion formation seen in the immunofluorescence images. Endothelial cells need to be able to withstand the high pressures and haemodynamic flow especially in arterial flow and thus the importance of good cell adhesion to the surface needs to be proved. Therefore, it was essential to be able to prove the adherence of the endothelial cells on the POSS-PCU films in a static environment prior to application of haemodynamic flow conditions.

In addition to surface chemistry, the use of surface topography is essential to providing cues for cells to differentiate, adhere, proliferate etc. The vascular basement membrane provides biochemical as well as these physical cues. The biochemical components of the basement membrane have been characterised previously and include a mixture of elastin, collagen IV, heparin-sulfate proteoglycans, laminin and nidogen/ enactin. Recently Liliensiek *et al*(75) also characterised the endothelial basement membrane nanotopography in rhesus macaque monkeys. This experiment was conducted so that it would give a guide to tissue engineers as to the topography required for vascular tissue engineering. Their decision to perform this study on nonhuman primates rather than on humans was to eliminate confounding variables introduced by human variability such as donor age and state of health. In addition to this, the time from harvest from human cadaveric tissues to fixation can vary and therefore dictate the state of the tissues. Interestingly, they found that the basement membrane in a carotid artery was made up of a combination of nanopores and nanofibres. These features would provide a combination tactile physical cues for the endothelial cells to respond to. Currently limitations of technology limit use to produce substrates with exact topographical features of that of the basement membrane seen. In addition, these features were seen to be in the nanoscale and illustrates the importance of feature sizes in the nanorange.

Due to the features in the basement membrane being in the nanorange, it is important to have a fabrication technique which is able to produce feature sizes in this scale range. EBL is a technique which allows the production of these features at this size and allows a precise production of these features in the nanoscale region. The ability to produce nanopits using this technique has provided a first step in investigating endothelial cell behaviour on the NSQ substrates.

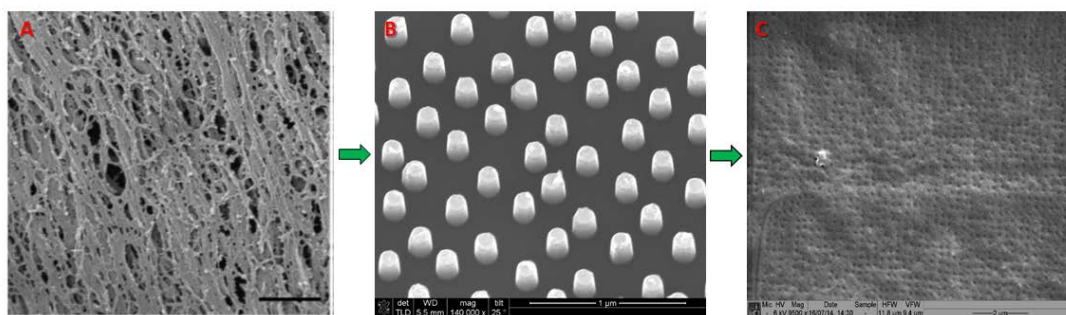


**Figure 5-7** This figure shows three SEM images to illustrate how to create a topography similar to that found in native basement membranes and using the current technology that we have. A) is an SEM image adapted from (70) which shows the carotid basement membrane of a rhesus macaque (Scale bar: 600nm). B) is an SEM (conducted using a field electron source (Hitachi S4700)) the silicon shim that has been produced from electron beam lithography in an attempt to reproduce the nanopores seen in A) in a slight disordered fashion. C) is an SEM image of the POSS-PCU polymer with after soft lithography has imprinted the nanofeatures of the shim onto the polymer. Although this is not an exact replica of the basement seen in the SEM due to the limitations of the current technology, the nanopores can be replicated to a certain extent and then molded into the POSS-PCU polymer with good fidelity.

It is therefore important to first confirm the ability to replicate the micro- and nanotopography on the POSS-PCU polymer and also the fidelity of this replication within the polymer. It was seen that the use of soft lithography, solvent-based evaporation, meant that the microgrooves and nanopits were replicated into the polymer with high fidelity when visualised under SEM and AFM. Interestingly in the SEMs, it is possible to also see white surface aggregates. This is thought to be POSS nanoparticle aggregates which migrate to the surface. However, this was taken as an inherent component of the polymer and did not seem to affect or distract from the surface topographical features.

Plasma treatment has also been known to have etching properties and this can be detrimental in the presence of surface topography especially in the nanoscale. The surface topographical changes, using plasma treatment is usually variable and non-controllable but require high energy particles to bombard the surface of the polymer to achieve this. If the energy is high enough, this will disrupt and change the surface topography and any 'intentional' surface topography such as the nanopits would render them obsolete. Therefore, AFM was used to confirm that the plasma treatment required to treat the surfaces were also not going to cause problems for the surface topography. The optimal plasma treated surfaces (80w for 60s) with the nanopits

were therefore used for this analysis. The surface roughness (RMS) of the surfaces were then used to analyse this. AFM is used as the methodology gives 3 dimensional (3D) measurements on the roughness values over other methods such as Stylus Profilers.

The roughness values showed that there is no difference pre- and post-plasma treatment and therefore this is a good indication that the current plasma treatment on the polymer surfaces does not destroy the surface topographies, allowing a combination of the surface modifications to be used.

Interestingly, the surface topographical features did not seem to have any definitive effect over planar in cell count, regardless of MG or NSQ. This suggests that there is possibly a lesser role for topography, in terms of cell proliferation. However, after 5 days of culture, there appears to be 'patchy' endothelial cell sheets on the POSS-PCU polymer (as shown by Coomassie Blue). This illustrates that at a longer time-point the polymer films would eventually be covered with endothelial cell sheets, and indicates a more positive role, but this may occur over longer time-points. These results seem to indicate that the role of topography may be lesser on endothelial cell proliferation, but more on cellular adhesion to the substrate.

There is always a danger that the wrong topography would causes apoptosis in the endothelial cells and therefore elicit cell death. Live/ Dead staining has showed that the cells are still healthy on all the topographies after 5 days of cell culture. This further shows that these surface alterations do not seem to have any detrimental effect on the endothelial cells. Endothelial cell function is also retained as shown by the presence of eNOS.

Further explanation on the role of eNOS is due at this point. Nitric oxide synthase is an enzyme found primarily in endothelial tissue and it produces the vasoprotective molecule nitric oxide (NO). eNOS is the isoform of this group of enzymes in the vasculature and is responsible for the majority of the NO produced in this tissue. NO is responsible for a plethora of vasoprotective functions and to name a few(89):

- Vasodilatory effects by activating soluble guanylyl cyclase and increasing cyclic guanosine monophosphate (cGMP) in smooth muscle cells
- Potent inhibitor of platelet aggregation when released into the vessel lumen
- It can inhibit leukocyte activation by interfering with the leukocyte adhesion molecule CD11/ CD18 by forming a bond with the endothelial cell surface or by suppressing CD11/ CD18 expression on leukocytes. Indirectly, as white cell adhesion is an early event on the onset of atherosclerosis, there is therefore a preventative role for NO in atherosclerosis formation
- NO inhibits DNA synthesis, mitogenesis and proliferation of vascular smooth muscle cells

Therefore, eNOS provides a positive indication of the function of endothelial cells and this does not seem to have been deterred by the plasma treatments or surface topographical modifications. The importance of eNOS for the survival of the small diameter vascular graft can be seen by the functions listed above. Thus its presence as well as its function is essential.

The results produced in this Chapter regarding the function of the endothelial cell is retained on the plasma treated surfaces on the MG substrates. Although the graph shows a similar pattern to that found in Chapter 4, in which increasing plasma treatment will increase the eNOS expression, there is less significance found in the lower treatment levels. There might be an indication that the presence of the MG would have a slight negative effect on the endothelial cells.

In the presence of grooves, cells have been shown to align along the grooves by contact guidance. Contact guidance is the interaction between microscale and nanoscale features and the cellular response and is usually coordinated by organized ECM proteins. However, the interest in contact guidance is due to the important role it has in the migration of individual cells or groups of cells or tissues. It forms an important component in organelle formation. The response of cell types to nanogratings by simultaneously aligning and elongating of the grating axis is not

seen by the HUVECs on the MG surfaces in this Chapter. This lack of contact guidance is due to the lack of optimisation of feature sizes. Larger responses to the surface topography is mainly seen in features with a decreased feature pitch and on increased depth. It is therefore thought that the current pitch size of 25 $\mu$ m and depth of 700nm is not optimised for the endothelial cell on the POSS-PCU surface. It is likely that the pitch size is too large and not providing enough tactile feedback to the cell to allow contact guidance. Further investigating would require investigating HUVEC reaction to other pitch sizes until HUVEC alignment due to contact guidance is seen.

Together the results so far seem to show the importance of surface plasma treatment over the use of surface topography as a main tool for enhancing endothelial cell growth. It was important to further determine if there is really a role of the modification of surface topography to enhance endothelial cell growth.

Subtle topographical cues, such as nanopits, have been known to either positively or negatively induce the recruitment of adhesion proteins enhancing endothelial cell adhesion. The ECM is linked to the cell cytoskeleton by focal adhesions, multiprotein complexes that are formed which bind to the integrin family transmembrane receptors to extracellular ligands. These are recruited and work together in a complex system within the cell so that it is able to respond to its surroundings. Famous SEM images taken by Teixeira(90) *et al* illustrate a human corneal epithelial cell reacting to its surrounding surface topography. When they are cultured on flat silicon oxide surfaces, they are of rounded morphology. The morphology changes when they are cultured on nanogratings of 70nm wide ridges with a 400nm pitch and it can be seen that they are elongated and aligned in the direction of the nanogratings (Figure 5.9). This illustrates the cells reacting to the topography by contact guidance.

The ability of the cellular machinery to explore both the micro- and nanoscale environment has therefore both complex sensory and feedback mechanisms that connect the sensory (input) and operational (output) modules, as described by Geiger(91) *et al*. These complex interactions start by the activation of integrins by

the external stimuli provided by the ECM, and which are then converted to biochemical stimuli back to the cell. Integrin-mediated adhesions are multiprotein complexes that provide this link from the ECM to the actin cytoskeleton. The biological activities of the adhesion components are diverse and include several actin regulators that affect the organization of the attached cytoskeleton. The adhesome integrin network is complex and composed of many components. There have been projects which has sought to identify all the different components of the adhesome integrin network(92).

There are complex mechanisms that underpin a cell's reaction to its surroundings. Although there are still complexities of these mechanisms that is not entirely completely understood, it is quite important to know the known aspects of it when investigating cellular behaviour.

Detecting the presence of vinculin gives a good indication as to the presence of one of the main focal adhesion proteins. Vinculin does not bind directly to integrins but plays a key role in the assembly of focal adhesions by indirectly connecting talin and  $\alpha$ -actinin to the actin. Vinculin is found ubiquitously in the cytoplasm but when it is activated to become part of the focal adhesion machinery, it is seen as contact points (1 $\mu$ m) at the periphery of the cell. These point contacts are complexes which are localised at the edges of the lamellipodia(93). The importance of vinculin is due to its ability to act as a regulator of mechanical stress as well as acting as a mechano-coupling protein. It provides a physical connection between the exterior environment and the inferior actomyosin cytoskeleton. Despite vinculin's inability to bind directly to integrins, there are linker proteins which are present such a talin and paxillin, which act to bind integrins to the focal adhesions proteins(93).

Furthermore, the detection of the presence of focal adhesions on the NSQ substrates on the immunofluorescence images indicate that the nanopits are producing a tactile stimulus in which the HUVECs are responding to and producing focal adhesions which are detectable. Unfortunately, with the planar and MG samples this is not seen

and indicates that there is not enough external stimulus to either produce such an effect or the HUVECs are not as adhered as strongly to these surfaces.

The detection of P-myosin expression on the MG surfaces using ICW has shown that the addition of the topography on the plasma-treated POSS-PCU does not have an effect. In addition, there is a suggestion that the presence of the MG surfaces may have a negative effect on the cells despite the plasma treatment effect and thereby obliterating the positive effects of the plasma treatments. This is due to the loss of the step-wise increase of P-myosin expression as seen previously on the plasma-treated only POSS-PCU surfaces. This will need further investigation as the mechanism for this is not understood at this stage.

One of the limitations of this Chapter is that the eNOS and P-myosin expression was not further investigated on the NSQ surfaces. This was due to a variety of reasons which included that the fabrication of enough thin films of NSQ made of POSS-PCU was time-intensive due to the lack of multiple masters (one master can only fabricate one film per surface and take 2-4 hours and will take at least a week of continuous fabrication to make enough for one experiment). The presence of eNOS had already been confirmed in the immunofluorescence images of the HUVECs on NSQ and would give us indirect information about the presence of eNOS and since the fabrication methodology is easier with MG, this was the pattern that was investigated.

## **5.6 Conclusion**

This Chapter has shown that plasma-treatment of the POSS-PCU films remain a very important methodology to making the surfaces cytophilic and the addition of surface topography has demonstrated mainly subtle changes. However, it is important to note that the ability to produce both micro- and nanoscale topography is possible on the POSS-PCU surfaces co-currently with plasma-treatment. The addition of the topographical features does not have a detrimental effect on the endothelial cells. However, on comparison of the different surfaces, NSQ (nanopits) seem to have a positive effect on cellular adhesion over planar and MG surfaces.

## 5.7 Further Work

As this Chapter has shown that very subtle changes in the surface topography will elicit very subtle changes in the adhering cell. There is the subtle detection of focal contact points forming in the endothelial cell periphery when cultured on the NSQ surfaces but it is not entirely clear the significance of it. It is therefore thought that, it would be crucial at this point to investigate the effect on topography on the HUVECs themselves. The nanopit topography is an important topography as mentioned due to its resemblance to that that seen in vascular vessels and since this is the topography which has elicited a response from the HUVECs.

Further work would also include investigating eNOS and P-myosin expression by the HUVECs after 5 days of cell culture on the nanopit surfaces and to observe whether there is a difference to the expression levels on the MG and planar plasma-treated surfaces. This will help to further elucidate and confirm the positive effects of NSQ topography over the other two.

As endothelial adhesion on surfaces is a very important factor when designing bioactive and cell-responsive surfaces especially for vascular grafts, further research will go into the investigation of endothelial cell behaviour on the different topographies. It is assumed that if it is possible to distinguish a particular topography that endothelial cells will respond by large focal adhesions, then this topography can play an important part in the further development of vascular grafts. This is an important study as optimal endothelial cell adhesion on the surface is crucial so as to avoid delamination especially when haemodynamic and pressure stress flows factors are applied.

In addition to this, MG surfaces of different pitch sizes require further investigation. As mentioned, it is not clear as to the reason for the lack of endothelial cell alignment and also the loss of step-wise P-myosin expression (when seen on just plasma-treated surfaces). However, this will require further investigation and further optimisation of the pitch sizes. Combinatorial and high throughput screening methodologies allow for this to be conducted in a speedy way. Preliminary work on substrates produced by Reynolds(94) *et al* of culturing HUVECs on the surfaces

have shown that at the smaller pitch sizes of the grooves, the HUVECs start to align, thereby indicating that at these sizes the grooves provide an optimal contact guidance for the HUVECs to adhere and align themselves to, and raising migration possibilities. In contrast, the HUVECs on the larger pitch sizes appear small and round and do not align themselves on the grooves, thereby also indicating a more ‘unhealthy’ HUVEC morphology. This is consistent with our earlier findings that at the higher pitch sizes (in our case, 25 $\mu$ m pitch) the HUVECs do not align. This may also account for our observation that there is no consistent P-myosin expression despite the plasma treatment. These preliminary results allow for a very interesting avenue of future work.

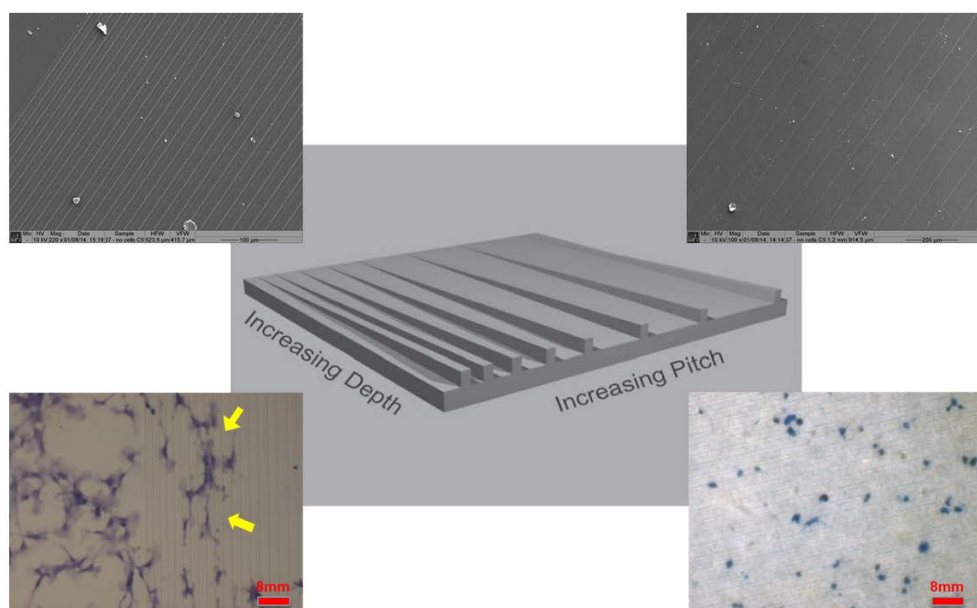


**Figure 5-8** The middle diagram is adapted from (94) and illustrates POSS-PCU film with a micro-gradient of grooves (pitch of grooves from 8 $\mu$ m to 100 $\mu$ m with shallow groove depth of 10nm increasing to 1 $\mu$ m along the 10mm grooves) transferred on it using soft lithography and a polycarbonate master. The films are then plasma-treated at 80W for 60s. The top two images are SEMs of the POSS-PCU substrate at different points to illustrate the smaller grooves (left) and the bigger grooves (right). The bottom images show Human Umbilical Vein Endothelial Cells (HUVECs) stained with Coomassie Blue stain of the same areas as the SEM images. The yellow arrows on the left image show the HUVECs which have aligned along the smaller grooves and this is in contrast with the HUVECs on the flat surface which have more spread and rounded morphology. The image on the bottom right show that on the larger pitch sizes the HUVECs are small and rounded in morphology which may indicate that they are unhealthy on this surface.

# **Chapter 6: Endothelial Cell Adhesion to Nanotopography**

## Chapter 6 Endothelial Cell Adhesion to Nanotopography

### 6.1 Introduction

Endothelial cell response to topography has been seen to play more of a subtle role than originally thought from the previous Chapters. This Chapter is more focused on finding if there is an actual response of endothelial cells to the topography, especially in terms of endothelial cell adhesion. Although there has been previous work on a number of different substrates and topographies, looking at endothelial cell response to topographical changes, there is still uncertainty of endothelial cell behaviour on the nanopits especially on polycarbonate substrates.

#### 6.1.1 Endothelial Cell Adhesion

Endothelial cell adhesion has been an intensely studied topic. Vascular endothelial cells have to be able to withstand haemodynamic stress flow and although this is an important aspect of research, it is essential to prove that the endothelial cells are able to adhere under static conditions before testing them under stress flow conditions.

Historically when endothelial cells were seeded onto vascular grafts, the endothelial cell sheets would delaminate on application of stress flow conditions, even at mild stress flow conditions. Although surface protein coatings such as fibronectin and gelatin have been applied onto the luminal surface of the vascular grafts to enhance adhesion and to help resist detachment on the application of flow, initial studies have found this not to very useful.

Publication	Author	Year	Summary
Kinetics of Endothelial Cell Seeding	JE Rosenman	1985	They looked at endothelial cell harvesting cell technique as well as seeding onto untreated ePTFE grafts and then implanted straight into canine carotid interposition. Loss of 70.2% in the first 30 mins were noted. 2nd phase was 30 mins to 24 hours and there was a slow steady loss of adherent endothelial cells.
Enhanced strength of endothelial attachment on polyester elastomer and polytetrafluoroethylene graft surfaces	KA Kesler	1986	This study compared fibronectin coated surfaces on PET and PTFE compared with uncoated and found that cell adhesion was better on fibronectin coated surfaces

with fibronectin substrate			and but only marginally better under flow conditions than uncoated surfaces.
Effect of fibronectin-coating on endothelial cell kinetics in PTFE grafts	GR Ramalanjaona	1986	This looked at pre-coating PTFE surfaces with fibronectin and then either pre-clotting with M199 or whole blood. They found that there was a significant retention of ECs after flow was applied. It was found that initial EC adherence was 46.7% and after 24 hours of flow there was 21.3% adherence. Uncoated was 19.8% to 3.4%.
Endothelial cell adhesion to vascular prosthetic surfaces	D Gourevitch	1988	These seeded ECs from human saphenous vein and also human omentum. Maximal adhesion was noted on 1% gelatin and also cold insoluble globulin coated on Dacron graft material. The maximal adhesion on gelatin was 73.4%.

**Table 6-1 Table to show some of the historical publications(64, 65, 95, 96) looking at promoting endothelial cell adhesion and correlation that the strength of adhesion prior to application of flow played an important part. These publications illustrate the problem of delamination even in the presence of proteins which promote cell adhesion onto the substrates.**

Rosenman(64) *et al* carried out one of the first comprehensive studies looking at the extent of endothelial cell delamination at the application of flow. On untreated but endothelial cell seeded PTFE surfaces, once implanted as carotid interposition grafts in a canine model, within 30 minutes there is a 70.2% delamination of endothelial cells, once the clamps were removed. This is an important finding that untreated PTFE surfaces are not enough to retain endothelial cells especially under haemodynamic stress flow. From these studies and those mentioned in the table above, it was obvious that the luminal surface of the vascular grafts plays an essential role in endothelial cell retention and therefore strategies to research the ‘optimal’ surface conditions have seen been underway.

As previously mentioned there is a complex interplay involved in cellular adhesion involving integrins and focal adhesion proteins. One of the main aims of this Chapter is to further investigate the role of nanopits in endothelial cell adhesion and whether there is a positive role of nanopits in it.

### **6.1.2 Nanopit Topography (NSQ and SQ)**

Previous publications and research conducted at the University of Glasgow have shown that MSC behaviour can be manipulated using surface topography especially

by two topographies of interest. One such topography has already been investigated in the previous Chapter and this is the NSQ topography(42). In the previous Chapter it can be seen that there might have been subtle focal adhesions formation by the endothelial cells on this topography. These subtle changes may provoke an endothelial response for recruitment of stronger adhesional factors but the exact role these changes play is still not clear. Furthermore, another interesting topography is SQ which is also a nanopit-based topography. This topography has been found to promote the maintenance of mesenchymal stem cells(97). Both topographies consist of nanopits of 120nm in diameter and 100nm in depth arranged in a square lattice. For the SQ, the centre-to-centre spacing of the pits is 300nm and for the NSQ, each pit has an offset of up to 50nm in the X and Y direction. These topographies came to attention due to their ability to have an effect on MSC maintenance and differentiation with just the slightest alteration. NSQ is a surface that promotes high intracellular tension and osteogenesis(42) and SQ is a surface that promotes self-renewal(97). However, as the majority work has been conducted on MSCs, it is not clear if a similar effect will be seen in endothelial cells.

Nanopit topography has been identified in vascular tissue and may provide an extremely important external stimulus for endothelial cells(75). Furthermore, pitted topographies have been shown to have differing effects on cellular adhesion and requires more investigation especially when there is a potential it can play a crucial role in the vascular system. Highly ordered nanopit topography has previously been shown to reduce focal adhesion formation by directly affecting filopodia formation. This study however also highlights that focal adhesions are formed in the inter-pit region and not on the pit itself. Therefore, it is modification of the inter-pit region which would affect the focal adhesion rather than the presence of the pit itself. It has also been shown that by increasing the size of the inter-pit region in a slight disordered fashion, such as an offset, could encourage the formation of more focal adhesions in the inter-pit area and therefore increase cellular adhesion. Focal adhesion formation on nanopit topology has been investigated by studying MSC behaviour on the topography.

Therefore, this forms an important avenue of investigation by looking at the response of HUVECs to both ordered and slight disordered nanopit topography and to compare it to that of the more studied, MSC response.

### **6.1.3 Injection Moulding**

Replication-based techniques such as hot embossing has been used for a long time to produce many devices such as microfluidic channels but unfortunately long heating and cooling times make these techniques undesirable.

Injection moulding has been a fabrication technique used industrially for many years with the ability to produce sub-micron features. This can be seen in the manufacture of Blu-Ray DVDs by commercial injection moulders which can produce features below 150nm in seconds. Thereby injection moulding is a desirable high throughput methodology and is largely employed in commercial manufacture. Traditionally single mould tools (the template for the injection moulder) are expensive and time-consuming to produce and can only be used for a specific purpose. However new design of mould tools allows for the surface features to be varied by introducing a 'slot' system in which a different inlay can be inserted at the mould/ melt interface. This has been used frequently in commercial settings as this means that a single mould tool can be modified with changing of the inlay and this allows for different surface features to be manufactured. The inlays are usually made of nickel which can withstand the high temperatures and pressures generated within the injection moulding system. Other materials such as silicon dioxide, which would be useful as inlays when producing micro- and nanoscale features, are not able to withstand these high pressures and would shatter, especially if they are as brittle as silicon.

The nickel inlay is manufactured by electron beam lithography (EBL) or photolithography, as mentioned in the last Chapter, to have the desired features. The injection moulder works in a cyclic way, in which the polymer is typically heated to 100°C above the glass transition temperature ( $T_g$ ) before it is rapidly injected into the mould cavity. This is kept at a much lower temperature (typically 30-50°C below the  $T_g$  of the polymer). The polymer of choice in our case, is polycarbonate. The polycarbonate used for injection moulding needs to be a thermoplastic to allow for

moulding. Polycarbonate is used as it is well-known to be a biocompatible polymer which has been used for a variety of medical devices including renal dialysis membranes. In addition, it has also been used successfully in a wide range of experiments by Professors Dalby and Gadegaard's groups and therefore proves as a 'standard.'

#### **6.1.4 Nanotopography and Vascular Grafts**

As mentioned before, it is hoped that the addition of surface topography would prove to be an important additional design for the luminal surface of vascular grafts. Surface topography provides an external physical cue for the endothelial cells to migrate and adhere on surfaces. It is therefore postulated that these observations could be harnessed to produce surfaces which are 'tailored' for endothelialisation. As these surfaces have the ability to recruit, activate and cause changes to cell behaviour, they have been promoted as 'intelligent' surfaces. In the case of vascular grafts, recruitment of neighbouring endothelial cells from native vessels by inward migration is a desirable concept and it is hoped that the use of nanotopography will improve on current observations which show this inward migration is limited by 2-3cm past the anastomosis(86).

There have been various recent attempts to utilise nanotopography within a small diameter vascular graft. One of the main attempts have been by Zorlutuna(98) *et al* in which they produced a two-sided nanopatterned vascular graft made of collagen I. The nanopatterns were parallel channels of equal grooves and ridges with width of 650nm and 300nm depth. Vascular smooth muscle cells (VSMCs) were seeded on the outside and human internal thoracic artery endothelial cells (HITAEC) were seeded in the internal lumen. The nanopatterns were seen to successfully orientate the VSMCs on the external surface of the vascular grafts, giving mechanical strength to the graft, and the HITAECs were seen to produce an endothelial layer within the luminal surface of the graft. This work highlighted the fact that it is possible to use nanopatterns in vascular graft production. Unfortunately, it is not mentioned if this vascular graft is able to withstand the stress flow and pressure conditions of the normal arterial vessel.

Several efforts have also been made to produce nanopatterned tubes using a variety of methods. Berry(99) *et al* employed a polymer de-mixing method using 20% polystyrene (PS) and poly-n-butyl methacrylate (PnBMA) to produce a luminal surface topography within a 0.5mm standard nylon tubing. Human endothelial cells were then seeded into the tubing and cell adhesion was studied. Interestingly, they show that the endothelial cells were reduced when compared with the control nylon tubes (without luminal nanotopography). The nanoislands produced by polymer de-mixing methodology gave an average feature height of 85nm. A prior study by Dalby(100) *et al* showed that cells do interact with the topography produced by polymer de-mixing but there is increased cellular adhesion when the average feature height was <20nm and when the feature sizes were >80nm (as in Berry's paper) cell adhesion is reduced. This shows cell dependency on the physical cues and the sensitivity they display towards it.

These are examples of the work so far towards producing tubes with internal surface topography with mixed results. There is a strong indication that cells will react differently to different topographies and it is essential to find out which ones will have the biggest positive on cell adhesion. Previous work by Seunarine(101) *et al* have shown that different cells will react to different topographies and that endothelial cells have adhered to nanotopography especially nanopits. Therefore, from the last Chapter, there is some positive indication that endothelial cells may preferentially be adhering to surfaces with nanopit topography. However, this merits further investigation and further elucidation and therefore this Chapter is focused on further exploring endothelial cells on nanopit topography. The use of NSQ and SQ topographies is important there has been prior extensive investigation of these topographies with regards to MSCs and therefore this serves as an important comparison.

## **6.2 Aims and Hypothesis**

The aims of this Chapter is to:

- Optimise the growth and adhesion of HUVECs on nanopit topology

- Investigating HUVECs adhesion on different nanopit topology whilst being compared with planar surfaces

### **6.3 Materials and Methods**

#### **6.3.1 Injection Moulding of Polycarbonate (PC) Substrates**

This is a process which has been optimised by the University of Glasgow Engineering Department and James Watt Nanofabrication Centre and have been previously published(102, 103).

A ‘near square’ (NSQ) and ‘square’ (SQ) arrangement of nanopits with a 120nm diameter, 100nm depth and with an average of 300nm centre-to-centre spacing with no off-set (SQ) or with a  $\pm 50$ nm offset (NSQ) are to be fabricated. These were initially fabricated with electron beam lithography (EBL) and dry etch. This is to create a nickel die or inlay in which is used in the injection moulder.

A hydraulic injection moulder (Victory 28, Engel GmbH) is used to produce the polycarbonate substrates with the nickel inlay. The inlays are inserted into the mould tool and injection moulded with the polycarbonate (PC) (Makrolon OD 2015) which has been air-dried at 110°C for 3 hours under vacuum. The use of an injection moulder ensures higher throughput for production of the substrates.

Again, the fabrication of the PC substrates was kindly produced by Professor Nikolaj Gadegaard’s Team.

#### **6.3.2 Plasma Treatment of the PC Substrates**

Plasma treatment of the polycarbonate substrates is a standardised procedure for rendering the surface of the polycarbonate substrates hydrophilic. The treatment of these substrates have been optimised by University of Glasgow for the use of mesenchymal stem cells (MSCs). The plasma treatment has mainly been in air plasma and therefore the protocol for this was maintained for this Chapter. The plasma cleaner utilised for this was the Harrick Plasma (PDC-32G, Harrick Plasma,

USA). This plasma cleaner only has limited settings for ‘tuning’ the power and therefore this uses the local standard protocol.

### **6.3.3 Sterilisation and Seeding of the PC substrates**

Once the PC substrates have been treated with plasma treatment, prior to any biological work, sterilisation of the substrates need to be performed. In a cell culture hood, the substrates are first placed in two lots of 70% Ethanol solution for 10 minutes each. They are then washed in HEPES-Saline solution generously and then placed in 6-well plates (Corning). Cell seeders (under patent application, University of Glasgow) are also sterilised in the same manner and then placed on top of the substrates ready for cell seeding. Endothelial cells are seeded onto the substrates on a cell density of  $1 \times 10^5/\text{cm}^2$  and then left in an incubator for 4 hours to allow the endothelial cells to adhere. Adherence is checked using normal light microscopy and if the cells are spread, then the cell seeders are gently removed, and the cells and substrates gently placed back into the incubator.

### **6.3.4 Contact Angles Measurements**

The contact angles measurements were conducted in the same way as the previous Chapters and this was done on an ‘in-house’ manufactured machine.

### **6.3.5 In Cell Western**

Once again at the appropriate time-point of the cell culture, the cells on the POSS-PCU films are firstly fixed in 4% formaldehyde at  $37^\circ\text{C}$  for 5 minutes before being washed in PBS. The cells are then placed in a permeabilisation buffer at  $4^\circ\text{C}$  for 5 minutes, before being blocked (milk powder/ PBS) for 1 hour at room temperature. The primary antibody is then added at a concentration of 1:50 (P-myosin and VE-Cadherin) and incubated at  $37^\circ\text{C}$  for 2 hours. These are then washed with 0.1% Tween/ PBS and then fluorescent-labelled secondary antibody (Licor, Cambridge, UK) at a concentration of 1:1000 with also CellStain (CellTag 700 Stain, Licor, Cambridge, UK) at a concentration of 1:500, and then left at room temperature for 1 hour. The secondary antibody is then removed and the films washed using 0.1%

Tween/PBS. The results are then analysed using an automatable infrared imager with a 2-channel imaging system (Odyssey Sa, Licor, Cambridge, UK).

### **6.3.6 Cell Count using DAPI**

As in the previous chapters, the endothelial cells were fixed after 5 days of culture. The cells are placed in 4% formaldehyde solution for 15 minutes in 37°C. A few drops of DAPI (Vectoshield DAPI, Vector Laboratories) are placed on the substrates and then using fluorescence microscopy (Zeiss Axiovert M200), ten random images were taken at 10 different locations of each of the polycarbonate substrates at a magnification of x20, of cells stained with DAPI. Cell nuclei was counted as an indication of cell number. A minimum of 4 substrates were assessed for each topography.

### **6.3.7 Scanning Electron Microscopy (SEM) of the HUVECs on the PC Substrates**

The cells were fixed in 4% glutaldehyde and then osmium tetroxide. They are then dehydrated through a graded alcohol series and hexamethydisilane (HDMS) and air dried prior to sputter coating with 20nm gold/ palladium. The images are then taken using a Zeiss Sigma FE-SEM. Sample processing and sample imaging were kindly conducted by Margaret Mullin (University of Glasgow).

### **6.3.8 Statistical Analysis**

The statistical analysis for this Chapter was conducted using Prism. The data was analysed using the one-way Anova statistical test.

## **6.4 Results**

The polycarbonate samples have been proven to be effective in the replication of nanopit topography and the fidelity of the replication of these patterns have been published previously(103). Once these PC substrates have been fabricated by the injection moulder, the surfaces have to be rendered hydrophilic with a short treatment in the plasma chamber before further experiments can take place. There

have been previous protocols developed at the University of Glasgow, but these have mainly been developed for mesenchymal stem cell work.

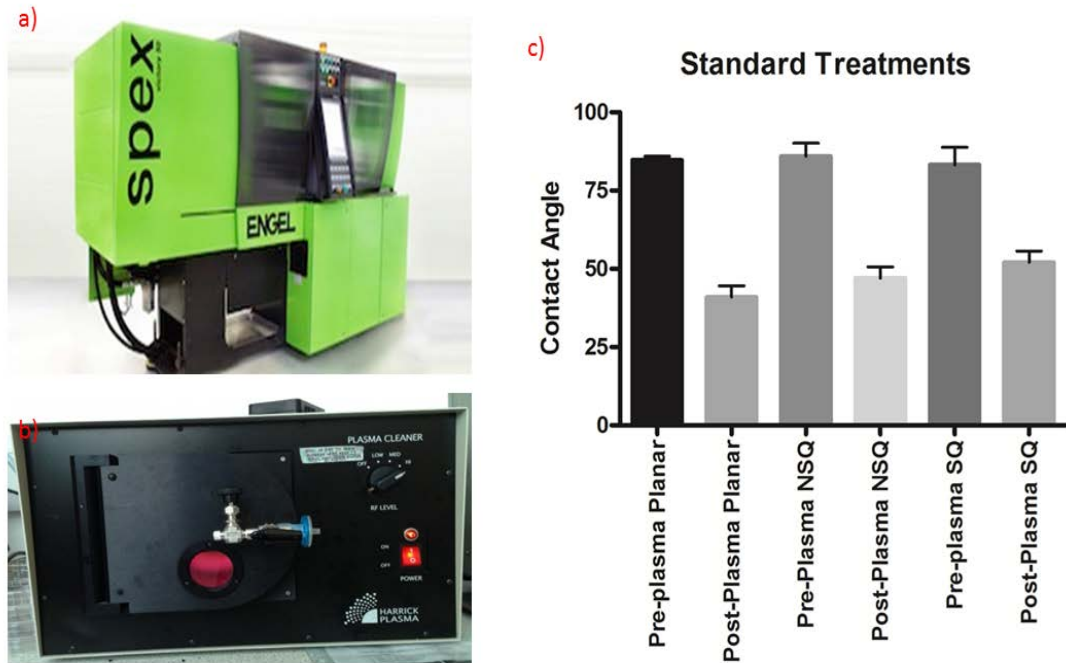


**Figure 6-1** This figure shows a) the injection moulder [image adapted from the JWNC website] used to create the PC substrates and then the b) plasma cleaner used to render the PC surfaces hydrophilic (with the red plasma glow in the chamber to indicate the plasma treatment is taking place) and c) graph to shows the difference in contact angles pre- and post-treatment using University of Glasgow standard protocols. There is a statistical significance pre- and post-plasma treatment ( $p < 0.05$ ). ( $n = 3$ )

Contact angles show that the University of Glasgow methodology pre- and post-treatment with 45 seconds of air plasma treatment, does have a significant difference on the contact angles of the polycarbonate surfaces. The Glasgow protocol has been determined locally (*unpublished data*). This has been a reliable method of treatment of the PC surfaces so that MSCs are able to adhere and proliferate on these PC substrates, across the board of NSQ, SQ and planar topographies.

However, it was noted that these treatment levels were not able to elicit the same response by the HUVECs and they were unable to adhere to the surfaces as the MSCs. Therefore, a further period of optimisation was required to re-adjust and lower the contact angles so that they are optimal for the HUVECs to grow. It was

therefore realised at this point that contact angle requirements by each cell type is different from each other and that cells which are ‘sensitive’ to their environment like HUVECs will require further optimisation protocols to be developed.

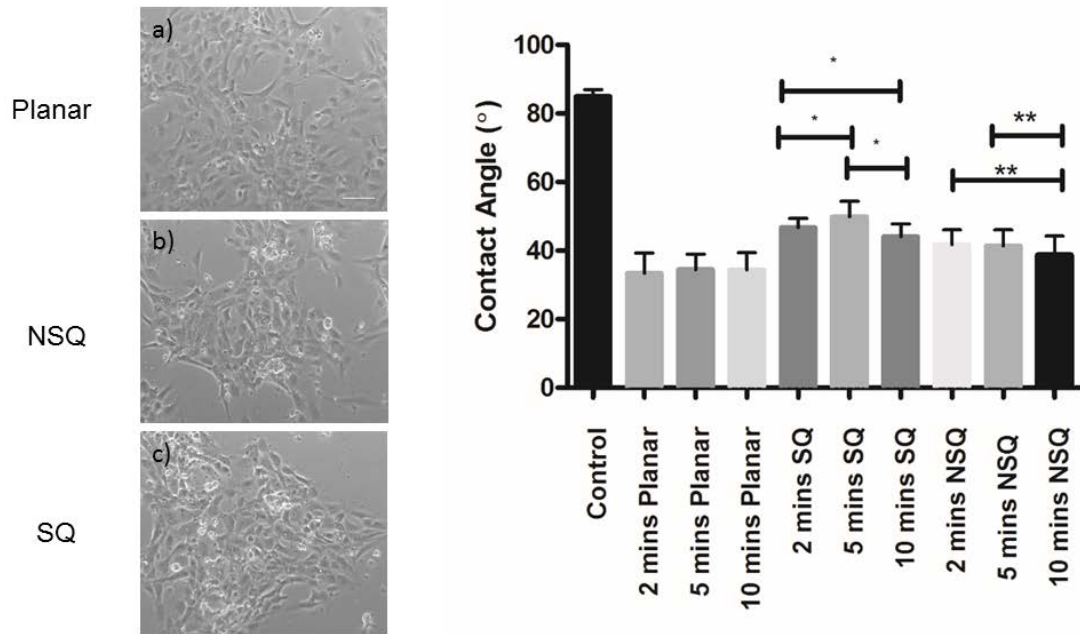


**Figure 6-2** This figure shows normal microscopy of Day 1 post-seeding of the HUVECs on the PC substrates where a) planar, b) NSQ and c) SQ surfaces where the treatment has been 10 minutes of exposure to air plasma. The cells are noted to have adhered successfully to the surfaces. The graph on the right shows the significant differences (\* in SQ and \*\* in NSQ). The control bar is used for comparison purposes. It should also be noted that there is a statistical significant difference with all the planar treatments and both SQ and NSQ topographies but there is no significance between the three planar treatments. [Scale bar is 10  $\mu$ m] (n = 4)

Increasing time in the plasma chamber was therefore used and treatment times of 2, 5 and 10 minutes were used. Interestingly, with increasing times the planar contact angles seem to have reached an equilibrium and no further treatment caused any significant difference in the contact angles. In the SQ topography, there was a significant difference between all three treatment times. In the NSQ topography, there was significant difference between 2 and 10 minutes and 5 and 10 minutes but no difference between 2 and 5 minutes.

Substrate	Mean Contact Angles (°)
Control (No treatment)	84.93
Planar (2 mins)	33.37
Planar (5 mins)	34.42
Planar (10 mins)	34.40
SQ (2 mins)	46.71
SQ (5 mins)	49.92
SQ (10 mins)	44.08
NSQ (2 mins)	41.75
NSQ (5 mins)	41.37
NSQ (10 mins)	38.82

**Figure 6-3** This figure highlights the contact angles which seem to promote endothelial cell adhesion on the polycarbonate substrates. On the left is a table which shows the mean of all the contact angles and highlighted in ‘orange’ colour are the contact angles which have consistently and successfully been able to grow HUVECs on.

It was also noted that at 10 minutes of exposure to air plasma, this is a consistent optimal duration of treatment in which the HUVECs will adhere and proliferate on the surface, and this optimal contact angle appears to be different on the three topographies. It is thought that the treatment times are crucial to getting the surfaces to a level in which endothelial cells are able to adhere. As can be seen in Figure 6.3, the means of the contact angles in which the HUVECs are able to adhere to are highlighted in yellow. It is these contact angles, not the plasma treatment time of 10 minutes, which is consistently and reliably able to produce these contact angles. The plasma treatment times are more reflective of the plasma cleaner itself and will need evaluating for every different plasma cleaner utilised (other than the one used in these set of experiments). Interestingly, there is a statistical significant difference between all the optimal contact angles, with the most hydrophobic being SQ followed by NSQ and then planar. It is thought that the slight increase in hydrophobicity in the nanotopographies is due to nanopits.

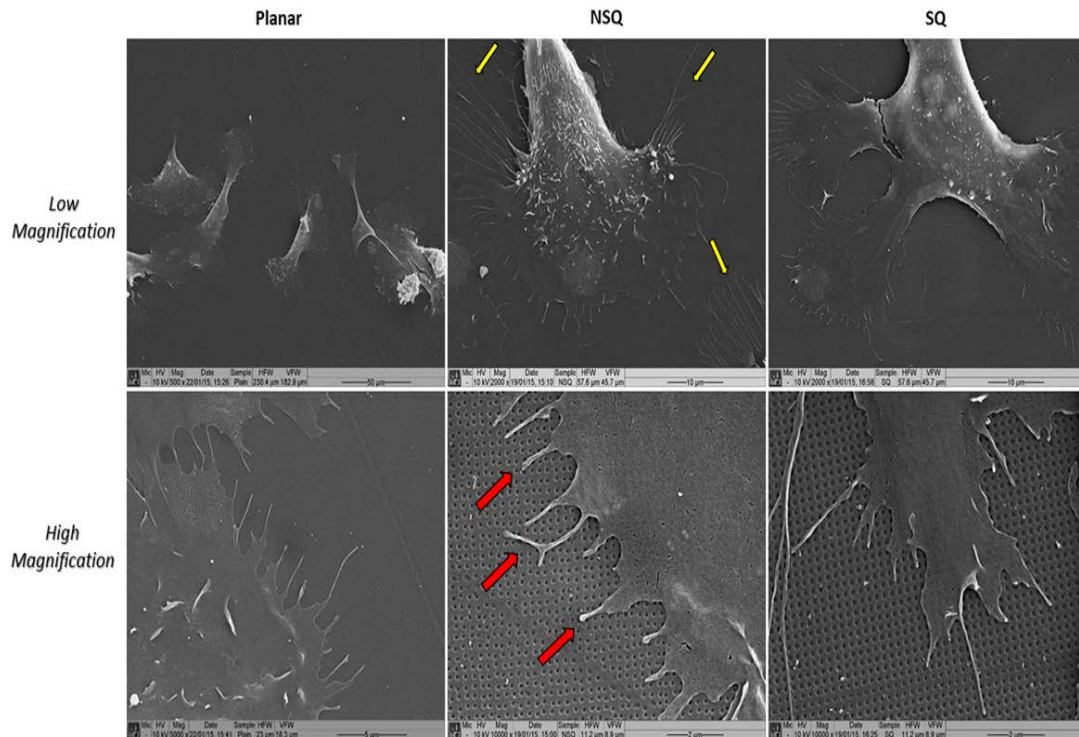


**Figure 6-4 SEM images of the endothelial cells on the surface of the three topographies, planar, NSQ and SQ in both low and high magnifications. Red arrows indicate the filopodia of the HUVECs and these tend to be found in the leading edge of the cell. Yellow arrows indicate the retraction fibers of the cell found at the tail-end of the migrating cell.**

The SEM images show the HUVECs on the three topographies at both high and low magnifications. The morphology of the HUVECs show that they are spread out on all three of the topographies. Interestingly there seems to be an increase in retraction fibres seen on the topographies, which may indicate that the cells are migrating. Retraction fibres tend to be the fibres which appear longer, almost like the ‘strings attaching pegs to a tent.’ Filopodia is more prominent and much smaller than the retraction fibres and can be seen ‘sensing’ the surface topography. On the topographies, there are more retraction fibres seen and this can be an indication that cells are more likely to be migrating on the topographies over the planar surfaces. Despite this, it is possible to ‘capture’ a migrating endothelial cell and be able to identify the leading edge of the cell.

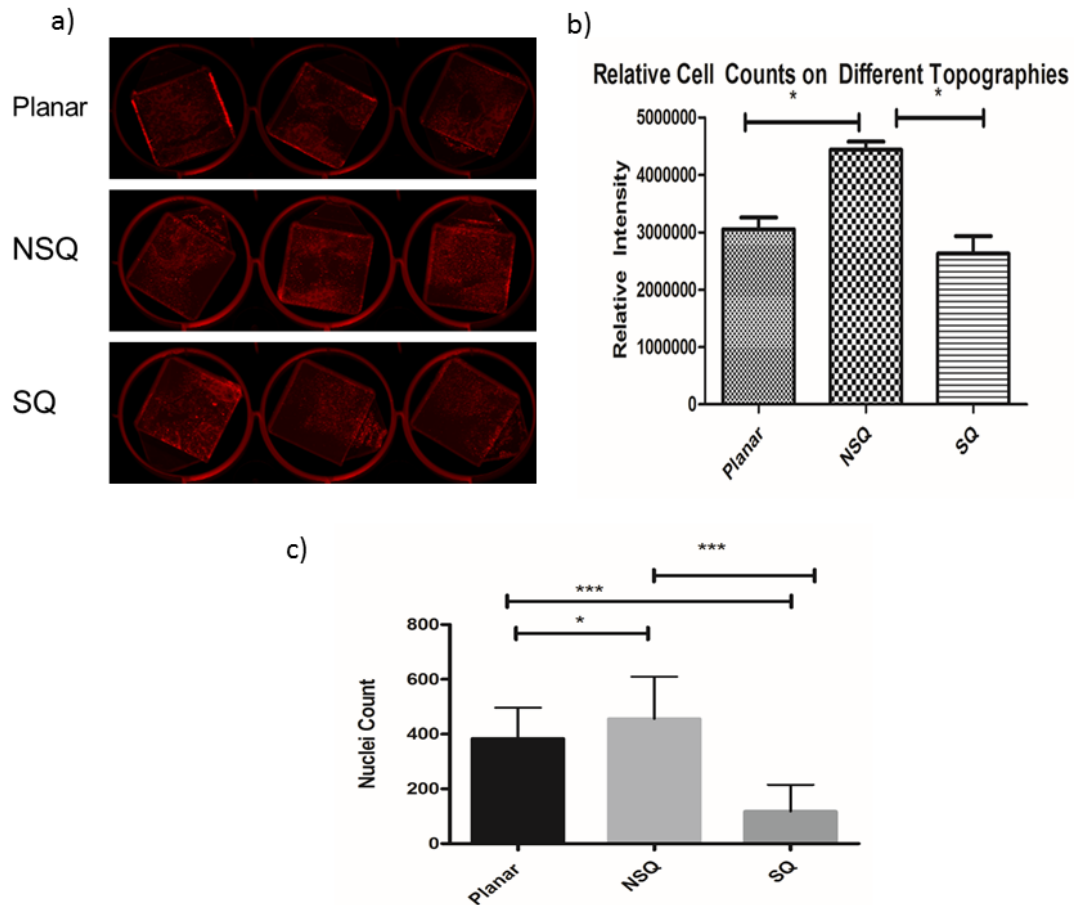


**Figure 6-5** This figure shows the cell stain on the substrates when using ICW as a detection method for conducting cell counts, where a) shows the intensity of the cell stain as visualised by the ICW plate reader and b) the quantifiable data comparisons. C) uses DAPI count to count the number of nuclei on the substrates. (\*  $p < 0.05$ , \*\*\*  $p < 0.0005$ )

Two different methodologies were used to ascertain the cell count of the HUVECs on the surface of the PC substrates. The first was ICW which has been used to give a quantitative determination of protein expression. In the traditional Western Blots, the protein expression is usually compared with a housekeeping protein (such as GAPDH) and although these housekeeping proteins can also be utilised in ICW protocols, an alternative can also be performed. This is cell stain which stains the entire cell and therefore the intensity of the cell stain can be estimated using the ICW reader. The second methodology was that using the same method used previously in an earlier chapter, using DAPI to stain the nuclei and the use of fluorescence microscopy to take images. A count of the nuclei gave a quantitative estimation of the number of cells on the substrates.

Both methodologies have shown a very similar graph, thus validating both methods as usage for cell count comparison. It is seen that there are less HUVECs growing on the SQ topography and that the highest cell count or cell stain seems to be that of NSQ. This patterns seems to be consistent across the two methodologies. The HUVECs express a preference to the NSQ topography over the SQ and planar.

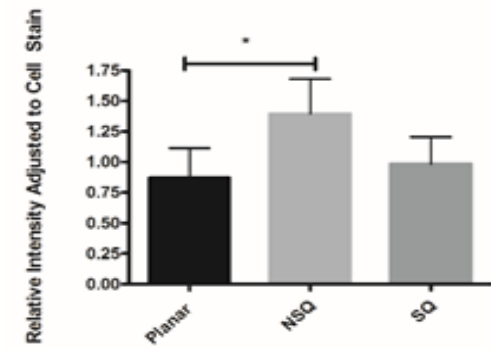
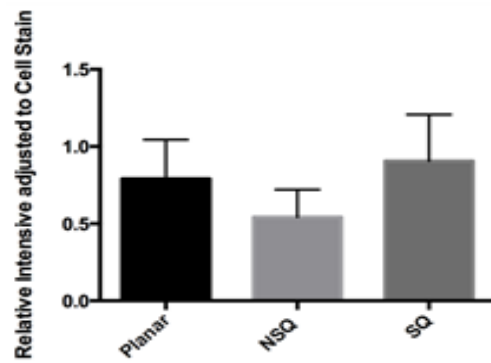
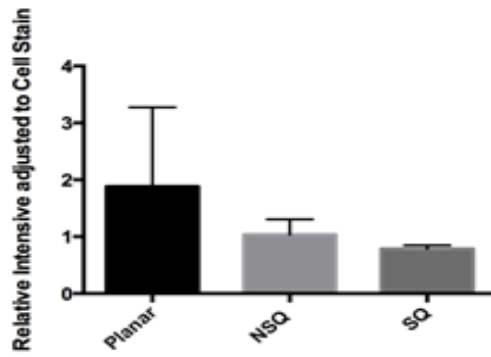
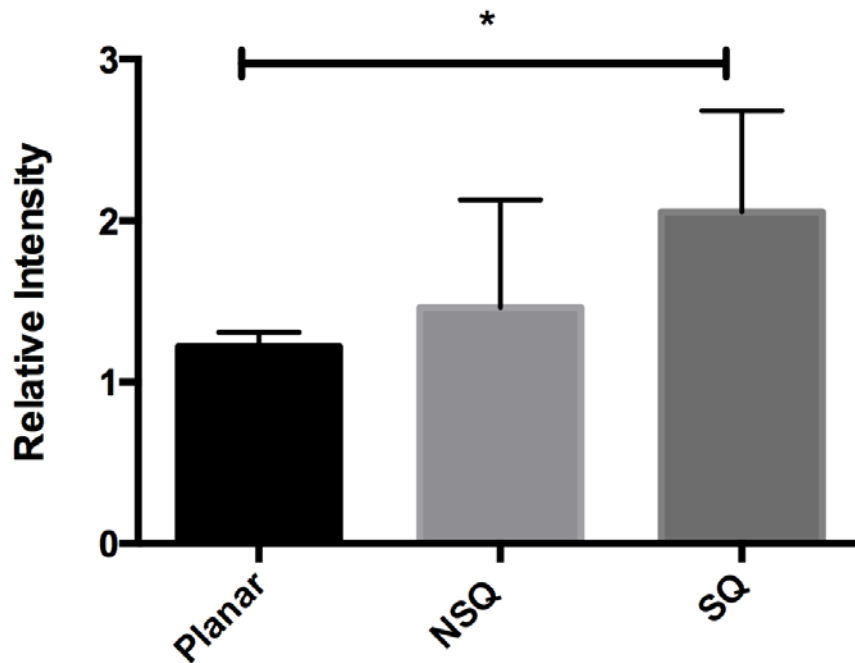


Figure 6-6 Graphs to show P-myosin expression by the HUVECs on the different topographies (Planar, NSQ and SQ on polycarbonate substrates) at different time points of Day 1 (top graph), 3 (middle graph) and Day 5 (bottom graph) using In Cell Western analysis. As can be seen on Day 5, there starts to be seen a statistical significance in the expression of P-myosin on the NSQ surface (\*  $p < 0.05$ ) (n = 4)

The expression of P-myosin was investigated in a variety of time-points as an indication of endothelial cell adhesion to the topographies. P-myosin expression is interestingly not seen to have any significant difference in Days 1 and 3. However on Day 5 there is a significant expression of P-myosin on the NSQ topography over planar. This shows that over the days there is increased of cell contractility of cells on the NSQ topography over the other topographies.



**Figure 6-7** Graph to show VE-Cadherin expression by HUVECs on the different topographies (planar, NSQ and SQ on polycarbonate substrates) after 5 days of cell culture (\*  $p < 0.05$ ) (n=3)

To further investigate HUVEC adhesion on the topographies using In-Cell Western, another protein expression was investigated. This was VE-Cadherin which is an endothelial cell-to-cell contact. After 5 days of HUVEC culture on the different topographies, there was a significant increase in VE-Cadherin expression on the SQ topography over planar. These show that for adherence on SQ topography, VE-Cadherin seems to play a more important role than P-myosin in cell adhesion.

## 6.5 Discussion

There has been a lot of work that has been conducted on the topographies SQ and NSQ, due to the influence that they have on MSCs maintenance or differentiation,

respectively. The SQ topography has been shown to have MSC maintenance properties, meaning that this can have a lot of implications on future stem cell therapies(97). NSQ topography, pushes MSCs towards an osteogenic lineage(42). These topographies are very similar except for a  $\pm 50\text{nm}$  offset in the NSQ topography and are interesting as such a small difference has such different outcomes on MSC phenotype. Biggs *et al* (104) measured the size of the focal adhesions of the MSCs formed on both NSQ and SQ topographies and found that larger focal adhesions were formed on the NSQ surfaces compared with the SQ surfaces. This seemed to be a strong indicator for differentiation into osteogenic lineage by the MSCs. It is thought that if the NSQ surface topography could have a similar effect on endothelial cells by inducing them to form large focal adhesions, there is potential to enhance endothelial cell adhesion to their substrates. There is a correlation of focal adhesion size and effectiveness of the adhesion strength and further observations have also shown that these focal adhesion size are enhanced on the application of flow(105).

This Chapter is an initial study on endothelial behaviour on the different topographies on the polycarbonate substrates and observing if there is a definitive effect the topographies have on the endothelial cells.

HUVECs are known to be difficult cells to culture. In this Chapter, one of the most important factors that was discerned was that the HUVECs were very sensitive to the surface hydrophilicity. Previous 'HUVEC-growing' protocols do not lower the contact angle enough. Therefore, a further optimisation step was required to render the surfaces to a contact angle that was conducive to HUVEC growth. By air plasma treating the surfaces of the polycarbonate surfaces for 10 minutes, a contact angle low enough for HUVECs to grow was achieved. Interestingly, at the lower contact angles, the MSCs are also able to adhere to the surfaces and grow in co-culture with the HUVECs. This shows that the appropriate contact angle has to be reached before HUVECs will grow on the substrates. It is important to reiterate at this point, that the power treatment levels of the plasma cleaner that was used to conduct these experiments will not be the same for every plasma cleaner. There will be a variation and it is attaining the correct contact levels which seem to be the important factor

here. Thus for a different plasma cleaner, it is likely that a period of optimisation is required to confirm the contact angles generated on the substrates.

On further examination of the contact angles on the different surfaces produced after 10 minutes in the air plasma chamber, there is no significant difference between the treatments on the planar samples. However, for SQ, there is a difference between all the treatments and for NSQ, there is initially no difference between 2 and 5 minutes but there is a statistical difference between 5 and 10 minutes. This would indicate when trying to lower the contact angle of surface topography, higher energy plasma is required. This is likely due to surfaces with topography such as nanopits, higher energy is required to 'bombard' the surfaces so that the surfaces within the nanopits also have the contact angles lowered.

Nanotopography provide a physical cue to the endothelial cells which will then have a knock-on effect for a canonical of biochemical reactions which are important. Of one of the cues, this would be cell adhesion features. Cell adhesion is important as it is the first event in a chain events leading up to successful integration of the vascular graft, especially endothelialisation. There are lots of cellular functions which occur as a result of successful cellular adhesion such as proliferation, differentiation and extracellular matrix deposition. This all happens as a result of an anchorage-dependent cell which has adhered to the biomaterial surface(99).

The SEM images indicate that the HUVECs are responding to the topography. As the SEM images show, there is a degree of cell movement on the different topographies as indicated by the presence of the leading edge and the retracting fibres. In the high magnification images, it is possible to see the interaction of the cell, via filopodia, with the surrounding nanotopography. Filopodia are important in a range of biological processes. It is part of the actin machinery and coexists with lamellipodia. Lamellipodia are protrusions on the leading cell edge of most motile cells and are persistent protrusions, whereas in contrast, filopodia appear to have both sensory and exploratory functions to steer cells, depending on cues from the environment(106). Therefore, filopodia are important for the feedback mechanism and determine how the cell reacts to the environment.

Previous work conducted by Tsimbouri(107) *et al* on the same nanotopographical substrates, showed that MSCs on all the materials were seen to have formed contractile stress fibres but this was notable more in cells on NSQ. Cell adhesion analysis also showed that the focal adhesions developed on SQ were significantly smaller than that on NSQ, which had critically larger adhesions. They also found that there was higher P-myosin found in the contractile MSCs on the NSQ than compared with planar and SQ. In the case of MSC, this is in line with previous observations that for MSCs progressing towards osteogenic lineage the focal adhesions required are larger(104). In the results from this Chapter, it can be seen that only on Day 5 does P-myosin expression on NSQ start to be statistically significantly over the planar. This seems to suggest that the contractility of the cells will developed slowly on the surfaces and it takes a few days before the cells develop these mature focal adhesions.

This seems to be consistent with the results from the cell count conducted after 5 days of cells culture. Cells need to securely adhere onto the material surface to proliferate and since the cells seems most securely attached to the NSQ surface, which would suggest that this topography allows for successful cell proliferation. P-myosin, as mentioned previously, is involved in the stabilisation of the myosin filaments which are responsible for cell contractility. Inter-pit distance appears crucial for the formation of focal adhesions. On the SQ topography inter-pit distance is the same in all aspects of the topography. However, on the NSQ topography, the  $\pm 50\text{nm}$  offset in the X and Y direction, means that a range of inter-pit distances is observed and some of these distances will be larger than those seen in the SQ topography. Focal adhesions have a larger area to form in these spaces and therefore allows for larger focal adhesions to develop.

VE-Cadherin belong to the family of Type II cadherins. The cadherins are cell adhesion molecules that mediate adhesion via homophilic,  $\text{Ca}^{2+}$ - dependent interactions(108). VE-cadherin is the major determinant and regulator of endothelial cell contact integrity. VE-cadherin is essential to regulation of the permeability of blood vessel wall for cells and substances. It is thought that VE-cadherin achieves optimal adhesion by association with the c-terminus of the catenins, which are

cytoplasmic proteins. Catenins are actin binding proteins and contribute towards cell adhesion. Endothelial cells have both adherens and tight junctions intermingled. Adherens junctions participate in multiple functions including establishment and maintenance of cell-cell adhesion, actin cytoskeleton remodeling, intracellular signalling and regulation of transcription(109).

VE-cadherins have recently been found to have a more crucial role in mechanotransduction of the cell cytoskeleton. Huveneers(110) *et al* described focal adherens junction between endothelial cells. They found that these junctions were attachments sites for radial F-actin bundles and also for junction remodeling. Molecules, such as thrombin, can activate these junctions, which then bind with vinculin in a way that is dependent on actomyosin contractility by exposing a specific vinculin-binding  $\alpha$ -catenin domain. Due to this force-dependent binding of vinculin, the mechanical stability of the focal adherens junctions are reinforced and the endothelial junctions are therefore prevented from opening (less permeable). The association of the VE-cadherin-catenin complex can also directly transduce the mechanical forces to couple with other junctional proteins, PECAM and VEGFR2. The transfer of intercellular signals from this complex modulates Src (family of intracellular signaling molecules) and other intracellular signals needed for optimal vascular homeostasis, to maintain the correct cell attachment to the matrix and to regulate the blood flow, *in vivo*(111, 112).

In addition, VE-cadherin has also been found to have anti-proliferative effects that mediate cell-contact driven inhibition of cell growth in cultured endothelial cells(113). VE-cadherin is significantly elevated in HUVECS cultivated on the SQ surface, the anti-proliferative effects of these findings were also seen in the cell count, with SQ surfaces having the lowest amount of cultured endothelial cells present. It is also interesting that the graphs do not have a similar pattern but in the expression of VE-cadherin, its expression on the planar and NSQ surfaces do not reach significance so it is not clear if this would be a factor. The anti-proliferative effects of VE-cadherin also seem to suggest that there is a 'switch' to the quiescent state, which is also associated with a downregulation of VEGFR2 (vascular endothelial growth factor receptor 2)(114).

From the results from this Chapter, it is unclear as to why there is a switch from a proliferative form for the endothelial cells when there is a switch of topographies from NSQ to SQ. However, it highlights the sensitivity of the cells to the surrounding topographies as there is only a  $\pm 50\text{nm}$  offset difference between the two topographies. It is also not clear as to whether the upregulation of VE-cadherin and therefore the reliance of cell-to-cell contact will also have an associated negative influence on the strength of the cell adhesion on SQ surfaces.

## **6.6 Conclusion**

This Chapter has illustrated that there is an effect of both the NSQ and SQ topography on the endothelial cells, especially with regards to their proliferative effect and their adhesion to the surfaces. Once again, there is evidence that the surfaces need to be of a suitable contact angle before the endothelial cells will adhere on them, and in comparison, this contact angle is much lower than those required by MSCs to adhere to the same surfaces and reiterates the importance of optimisation of the surface.

As can be seen, there is an increase in the upregulation of P-myosin on NSQ surfaces, which is also confirmed by other studies on MSCs, however the upregulation of VE-cadherin on the SQ surfaces is interesting. This seems to be linked to the anti-proliferative effect on the endothelial cells on the SQ surfaces and will require further investigation.

## **6.7 Further Work**

This Chapter has highlighted a number of unanswered questions as to the adhesion of the HUVECS on the three surfaces, planar, SQ and NSQ. Further work would focus on elucidating the biology of the cell adhesion on the surfaces. This would look at the immunofluorescence of the presence of vinculin and if possible, measurement of the size of the focal adhesions formed to compare with previous work(104). It is not clear of the switch to VE-cadherin on the SQ surfaces and if there is a direct link to cell senescence and therefore measurement of endothelial cell function on the surfaces would provide additional information to correlate with the findings.

The use of the NSQ and SQ surfaces have proven important in a number of works which has focused on using these surfaces on orthopaedic implants and self-renewal of stem cells, respectively(42, 97). Therefore, this also leads to the question of whether circulating MSCs would prove to be troublesome if these surfaces are exposed in luminal flow, such as in a vascular graft, and promote osteogenesis and subsequently calcification(115). Calcification can lead to a number of undesired events in a vascular graft, such as endothelial dysfunction, increased formation of intimal hyperplasia and altered flow patterns and shear stress, and these can also lead to premature graft failure(2). If this was the case, then these topographies can prove to be entirely inappropriate for the use in vascular graft development.

## **Chapter 7: The Influence of Mesenchymal Stem Cells on Endothelial Cells in the Presence of Nanotopography**

## **Chapter 7 The Influence of Mesenchymal Stem Cells on Endothelial Cells in the Presence of Nanotopography**

### **7.1 Introduction**

Mesenchymal stem cells (MSCs) has played an important part in the evolution of tissue-engineering and there are many new technologies which have been developed from their usage. MSCs can be harvested from a number of tissue sources and they can co-exist with a number of tissue and cell types, of which one is endothelial cells. However, it is not clear if they can potentially have a detrimental effect in vascular tissue engineering.

#### **7.1.1 Mesenchymal Stem Cells (MSCs)**

Mesenchymal stem cells (MSCs) are non-haemopoietic cells which can be isolated from a number of sources such as the bone marrow, umbilical cord, peripheral blood and adipose tissue. They have multipotent capacity meaning that they can differentiate into a number of cell types; including osteoblasts, chondrocytes, adipocytes, myoblasts and neurons. This means that they can be used in a regenerative capacity and are therefore a useful resource in tissue engineering. Other beneficial effects of MSCs include immunosuppressive and anti-inflammatory effects (they do not express the Major Histocompatibility Complex (MHC) II complex which are used in modulation of the immune system as seen in other cell types)(116).

It has proved difficult to apply a formal definition to mesenchymal stem cells as there are no definitive cell surface markers which distinguish them from haemopoietic stem cells. However, the International Society for Cell Therapy(117) have proposed the following criteria for Human MSCs:

1. Adherence to plastic (tissue culture plastic) under standard culture conditions

2. Expression of surface molecules CD73, CD90 and CD105 in the absence of CD34, CD45, HLA-DR, CD14 or CD11b, CD79a or CD19 surface molecules.
3. A capacity to differentiate into osteoblasts, adipocytes and chondroblasts in vitro.

The beneficial effects of MSCs have been acknowledged and a number of recent clinical trials have used these beneficial effects of MSCs. For example, in patients with end-stage liver disease, autologous mesenchymal stem cells improve clinical indices following injection(118). There were no adverse effects noted from this trial.

MSCs have also been found in peripheral blood. These are thought to be MSCs which have been mobilised from other tissues by the presence of pathologies which involve tissue injury and tumours. Despite this, the circulating concentrations of peripheral blood MSCs (PB-MSCs) are still extremely low. The concentrations of circulating MSCs are 1 in  $10^8$  cells comparable to MSCs from the bone marrow which have the frequency of 1 in  $10^4$  or 1 in  $10^5$  cells(119, 120).

MSCs have homing potential and they have been found to express chemokine receptors and integrins, to sites of injury and inflammation. The exact mechanisms of this 'homing' potential still requires further elucidation and this is still under great investigation. However, the engraftment properties of PB-MSCs are thought to be greater than bone marrow MSCs (BM-MSCs) and it is not clear what chemical factors accentuate the homing potential of the MSCs. There is also discussion as to whether there are actually 'circulating' MSCs as such or rather they are mobilised BM-MSCs rather than PB-MSCs which reside permanently in the peripheral circulation.

### **7.1.2 Mesenchymal Stem Cells, Nanotopography and Tissue Engineering**

MSCs have a lot of potential in tissue engineering applications and this has been the study of many research groups. As previous mentioned, the Dalby group have found

that the topographies, that are used in this thesis, NSQ and SQ, provoke a reaction from the BM-MSCs that are cultured on them, as mentioned previously. It has been shown that MSCs which are differentiating have high metabolism and exhibit the formation of large focal adhesions on the substrates which seem to predict their differentiation into an osteogenic lineage(82, 107).

For bone engineering these topographies have shown to be of immense use in the field of bone engineering and for orthopaedic implants due to their influence of MSCs. In addition, due to SQ being a topography which favours maintenance of MSCs, has meant that this topography could potentially be used to create a production line of high quality stem cell delivery. In contrast, MSCs which are not undergoing differentiation are not as metabolically active as those which are differentiating and the focal adhesion sizes formed have been seen to be much smaller(107).

However, it is not certain of the effect of these particular topographies on endothelial cells and in particular, in co-culture conditions. This Thesis has sought to explore the ways in which the topographies can affect endothelial cell behaviour especially adhesion and its potential on vascular grafts.

### **7.1.3 Calcification of Vascular Grafts**

Calcification of vascular grafts is known to vascular surgeons and this has been reported in the past(121). A recent study by Mehta(2) *et al* has shown that calcification in vascular grafts may be an underestimated issue. They looked at explanted PTFE grafts and found that 68% of vascular grafts showed evidence of calcification either within or adjacent to the PTFE grafts. Of the vascular arterial grafts that were examined, they found that 82% of them were exhibiting signs of calcification. This calcification is important as it contributes to graft failure by mechanisms such as reducing compliance, increasing stiffness and thus compliance mismatch, predisposing to graft fracture altering the haemodynamic flow patterns and exacerbating the endothelial dysfunction.

Calcification of vascular grafts are less well appreciated with less research directed at them but there has been a large amount of research based on the calcification of heart valves. There have been a number of hypotheses on why the calcification process occurs and Levy(122) *et al* propose a mechanism in which direct adsorption of calcium and phosphate by the polymer leads to subsequent subsurface crystallization. The degraded cellular components initiate the calcification and the collagen moieties can also act as additional nucleation sites for calcium phosphate minerals, which are independent of cellular components. The mineralization process is further exacerbated in the presence of haemodynamic stress and turbulent flow.

There is an active inflammatory process and foreign body reaction to the vascular implant occurring also at the time of implantation and in most cases, this is thought to be a low-grade reaction. Macrophages can be found on the surfaces of biomaterials and they can propagate the foreign body response, and have the ability to undergo phenotypic changes depending on their microenvironment.

This highlights the problem of calcification and the importance of its effect on a vascular graft. As it is currently an under-estimated problem, there is call for a registry in which to record vascular graft failures post explantation. Such a Registry is being set up in Strasbourg, France, to examine the cause of vascular graft failures and other medical devices so that with the results, a more focused approach can be undertaken(123). Although this is an ongoing registry and it will take some time before a comprehensive list of factors which cause vascular graft failures will be published, it is still thought that the problem calcification is an under-estimated cause.

#### **7.1.4 Mesenchymal Stem Cells and Endothelial Cells Cross-Talk and the Link with Surface Topography**

Recently, there has been a number of experiments which have been conducted looking at the co-culture of MSCs and endothelial cells. These experiments were conducted in a hope of elucidating the factors which will preclude MSC differentiation. In co-cultures with endothelial cells, MSCs have been shown to rely on both diffusible factors and juxtacrine mechanism by gap junctional activity for

intercommunication with endothelial cells. In fact, when cultured with MSCs, factors such as BMP-2 can be expressed by endothelial cells and these can induce osteogenic differentiation of the MSCs. In the absence of any topography, there have been a few studies which have confirmed these observations both *in vitro* and *in vivo*. *In vitro*, MSCs which have been co-cultured with endothelial cells have shown an increase in osteogenic differentiation(124). This is confirmed by similar observations in an *in vivo* animal model too where co-transplantation of EC with MSCs resulted in more bone formation than with MSCs alone(125).

The effect of these ‘Dalby and Gadegaard’ topographies on endothelial cells have not been evaluated. Earlier Chapters of this Thesis have shown that there is some merit in using a nanopit topography for the growth of endothelial cells. Unfortunately, the configuration of these topographies have been previously shown to have definitive effects on MSCs, especially the NSQ which has a propensity towards osteogenic lineage. Theoretically, circulating MSCs could potentially ‘home’ in on these topographies if they have been implanted as a vascular graft and settle on the luminal surface, differentiate down an osteogenic lineage and then cause premature calcification within the vascular graft.

## **7.2 Aims**

The aims of this Chapter is to investigate the:

- Possibility of mesenchymal stem cells also being incorporated with the HUVECs on the nanotopographies in a co-culture
- Adherence of the MSCs on exposed surfaces of the PC substrates
- Possibility of the attached MSCs to differentiate into osteogenic lineage in the presence of HUVECs and topography, thereby causing calcification

## **7.3 Materials and Methods**

### **7.3.1 Fabrication of Polycarbonate (PC) substrates**

This was previously outlined in Chapter 6 of this thesis. Electron beam lithography were used to fabricate these polycarbonate substrates. First master substrates have to be produced and they were fabricated to have an array of 120nm diameter pits of 100nm depth and 300nm pitch in a square (SQ) arrangement. The NSQ master substrates had a controlled disorder by changing the pits from perfectly square (SQ) by 50nm offset and still maintaining an average of 300nm pitch.

Nickel dies were made directly from the patterned resist samples, followed by sputter coating with a thin layer (50nm) of Ni-V on the samples as these will act as an electrode for the subsequent electroplating process. The nickel shims are then used in the injection moulder for the production of polycarbonate substrates which have the SQ, NSQ and planar topographies.

### **7.3.2 Mesenchymal Cell Culture**

MSCs were purchased from Promocell® and cultured in basal media (DMEM, 10% Fetal Bovine Serum (FBS), 2% antibiotic mix (containing penicillin-streptomycin, Fungizone® and L-glutamine), 1% Non-essential Amino Acids, 1% Sodium Pyruvate). They are then cultured in a humidified incubator (20% O<sub>2</sub>/ 5% CO<sub>2</sub>) until ready for use. The cells are all used for experiments at P1-P3.

### **7.3.3 MSC/ HUVEC Co-culture**

The co-culture conditions are modified from Bidarra(43) *et al.* They found the optimal conditions for MSC/ HUVEC co-culture was at a ratio of 1:1. Therefore the basal media for MSC was used. However, the HUVECs were grown in endothelial media which was M199 (Gibco), 10% FBS (Gibco), 0.1mg/mL Heparin (Sigma), 0.03 mg/mL of endothelial cell growth supplement (ECGS)(Sigma). The HUVECs are conditioned in this media for 48 hours prior to co-culture experiments which uses the combined media, as mentioned. The ratios for seeding of cells for these experiments was 1:10 (MSC: HUVEC).

### **7.3.4 Sterilising of the PC Substrates and Seeding of the Co-Culture**

Firstly, the PC substrates surfaces have to be rendered hydrophilic and this is conducted by 10 minutes in the plasma cleaner, as optimised in the last Chapter (Harrick Plasma Cleaner). This is to render the contact angles of the substrates to the appropriate levels as seen in the last Chapter. The PC substrates are then sterilised using 70% Ethanol (2 x 10 minutes) and then rinsed in HEPES-Saline. The substrates are then placed in 6-well plates. The cell seeders (under patent application by University of Glasgow) are also sterilised in the same way and placed on top of the substrates ready for seeding. The HUVECs are first seeded at a density of  $1 \times 10^4$  cm<sup>2</sup> on the substrates. These are allowed to adhere for 4 hours and then extra media (co-culture media) added and the seeders removed. The HUVECs are then allowed to be cultured on the substrates for 48 hours until there is 'patchy' distribution on the substrates. This patchy distribution is confirmed by phase contrast microscopy and then MSCs are then seeded carefully and directly on top of the substrates by using a needle and syringe, and carefully returned to the incubator to allow attachment.

### **7.3.5 Immunofluorescence**

The protocol for immunofluorescence is as before. Samples were fixed in 4% formaldehyde for 15 minutes at 37°C then washed before placing in permeabilising buffer and blocking in 1% (w/v) bovine serum albumin/PBS. Samples were then stained with mouse anti-CD31 antibody (1:200) (Abcam) in 1% (w/v) BSA/PBS, in conjunction with rhodamine/phalloidin (1:500), and incubated at 37°C for 1 hour. Samples were subsequently washed 3 times for 5 minutes (0.5% Tween-20 in PBS) and then the secondary antibody, AlexaFluor 488 Goat anti-mouse was added (Life Technologies) at 1:500 in 1%(w/v) BSA/PBS. Samples were then incubated for 1 hour at 37°C. Samples were given a final wash before mounting using Vectashield with DAPI nuclear stain (Vector Laboratories).

### **7.3.6 Coomassie Blue Staining**

As before, a Coomassie Blue Solution (0.2% Coomassie Blue, 46.5% Methanol, 7% Acetic Acid, 46.5% water) was filtered and 1-2ml are placed in each well (assuming a 6-well plate is used). This is left for 2 minutes and then washed thoroughly with

deionised water. This is then dried thoroughly before visualising with an optical microscope.

### **7.3.7 Von Kossa Staining**

The samples were fixed after 3 weeks of co-culture using 4% formaldehyde solution and incubated for 15 minutes at 37°C. The samples are then washed thoroughly with PBS. A 5% silver nitrate solution is prepared and stirred. A second 5% sodium thiosulphate solution is also prepared and stirred. Firstly, 5% silver nitrate solution were added to the samples and then the samples were exposed to 15 minutes of ultra-violet (UV) light. The samples are then rinsed in deionised water. The 5% sodium thiosulphate solution is then added to the samples for 5-10 minutes. This is then further rinsed for 5-10 minutes under tepid water. A final rinse of the samples is then conducted using 70% Ethanol solution. The samples are then viewed under normal microscopy.

### **7.3.8 In-Cell Western**

As before then steps for ICW were conducted after three weeks of co-culture. The cells were fixed in 4% formaldehyde solution for 15 minutes at 37°C. The cells were then permeabilised in perm buffer at 4°C for 4 minutes. The buffer was removed before addition of a blocking solution (1% milk powder) for 1.5 hours at room temperature. The blocking solution is then removed and primary antibody, osteocalcin (1:50 ratio) is added and incubated in a 37°C hot room for 2 hours. The samples are then washed in 0.5% Tween/PBS and then the secondary antibody (Goat anti-mouse IRDye® 800CW (Licor®)) and CellTag 700 stain (Licor, Cambridge, UK) is added at a ratio of 1:1000 and 1:500, respectively, for 1 hour, covered. This is then thoroughly washed in 0.1% Tween/PBS and with the last wash in PBS only. The results are then analysed using an automatable infrared imager with a 2-channel imaging system (Odyssey Sa, Licor, Cambridge, UK).

### 7.3.9 Statistical Analysis

The statistical analysis for the results of this Chapter has been conducted by using the computer program Prism®. Direct comparisons between the surface topographies was conducted using the statistical test, one-way ANOVA.

## 7.4 Results

The ratios of the co-cultures are much higher than that seen in the normal human body. Unfortunately, when using lower co-culture ratios, it was noted that at times it was difficult to confirm that MSCs have also adhered and this may be due to the seeding methodology, which may need further improvement.

The morphologies for HUVECs and MSCs are very different. HUVECs have been considered to have a ‘cobblestone’ morphology especially when viewed under normal microscopy. MSCs have been described as having a fibroblast-like sharp spindle shape(126). As can be seen MSCs are much larger cells then HUVECs.

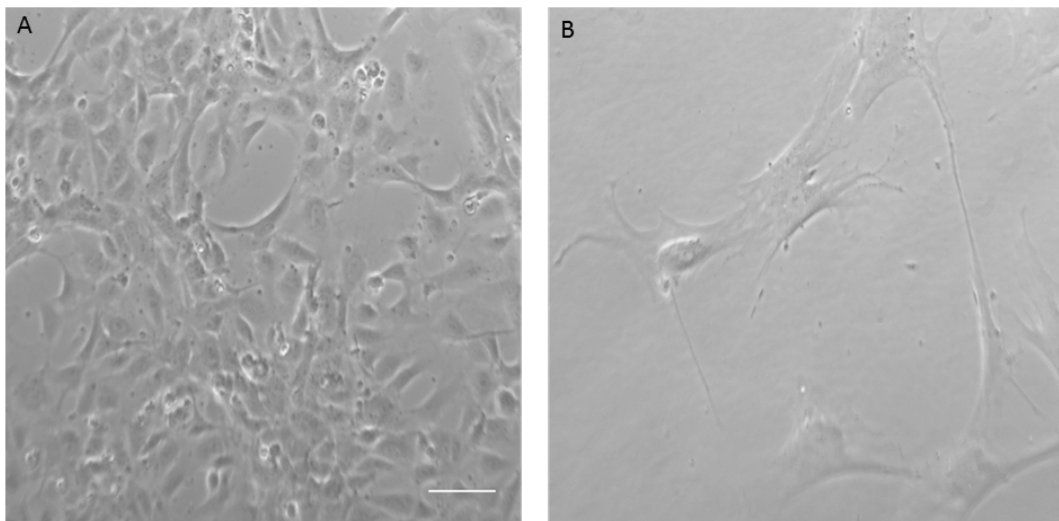


**Figure 7-1** These are phase-contrast microscopy images of a) HUVECs and b) mesenchymal stem cells (bone-marrow derived) cultured on the polycarbonate substrates (planar) [Scale Bar: 10µm]

It is important to distinguish the difference between the morphology of the two cell types in the presence of a co-culture using phase-contrast microscopy. This was also deemed important as to judge the success of the adherence of the MSCs when seeding them onto the substrates.

Again, using phase-contrast microscopy, it is possible to identify the presence of both MSCs and HUVECs on the substrates. Figure 7.2 shows an example of the image that can be seen. It shows the MSC adhering to the exposed surface of the planar substrate whilst surrounded by endothelial cells. It is also possible to notice the different morphologies of the two cell types which help distinguish them apart.

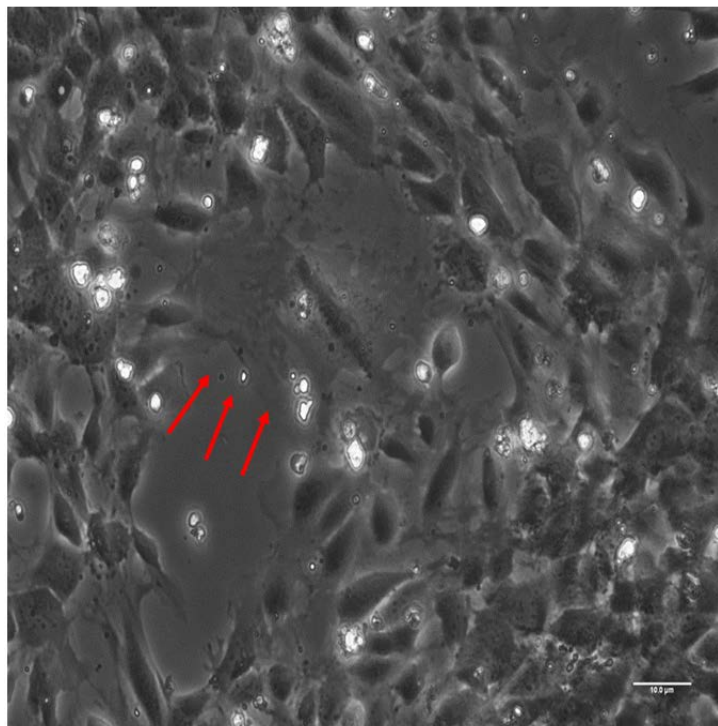


**Figure 7-2 This is a phase-contrast microscopy image of the co-culture of MSCs/ HUVECs on a planar substrate 2 days after seeding of the MSCs. The MSC (red arrows) is sitting surrounded by HUVECs and shows the effectiveness of the co-culture and hence successful 'seeding'. [Scale Bar: 10μm]**

The use of Coomassie Blue also highlights the cell morphologies as well and illustrate the presence and success of the co-culture. Although Coomassie Blue is a technique which is closely linked to the Bradford Assay, it binds to protein and therefore will bind to the proteins in the cell cultures when fixed. It gives the contrast under

microscopy to further high-light cell morphology. Again, the two cell morphologies can be delineated using this stain.

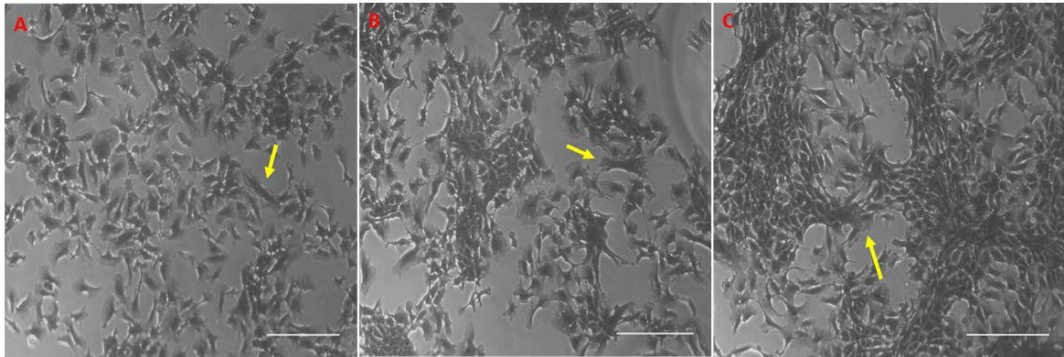


**Figure 7-3** Coomassie Blue-stained images after 5 days of co-culture of the MSCs and HUVECs at a ratio of 1:50. Yellow arrows point out the presence of the MSCs, on the different topographies planar (left), NSQ (middle) and SQ (right). As can be seen, they are adhered quite sparsely on the staining and can be quite difficult to see. [Scale bar: 20µm]

Further immunostaining was used to look at the co-cultures after 5 days of co-culture. The fluorescent microscopy images on Figure 7.4 shows that on the topographies, the MSCs are able to adhere on the exposed surfaces which have not been colonised by HUVECs yet. The uptake of the Rhodamine stain is much stronger on the MSCs compared with the HUVECs. The actin fibres are more defined and the fibroblast-like spindle shape of the MSCs can also be visualised as long, thin stress fibres which are running in parallel to the orientation of the cell. This is unlike the endothelial cells which seem to have more of the known ‘cobblestone’ morphology and appear more rounded. The actin fibres are less stained also then the MSCs. The MSCs also appear to be much larger cells comparatively to the HUVECs and this can offer an explanation as to why the actin fibres are stained strongly as they will be larger and more organised than those in endothelial cells.

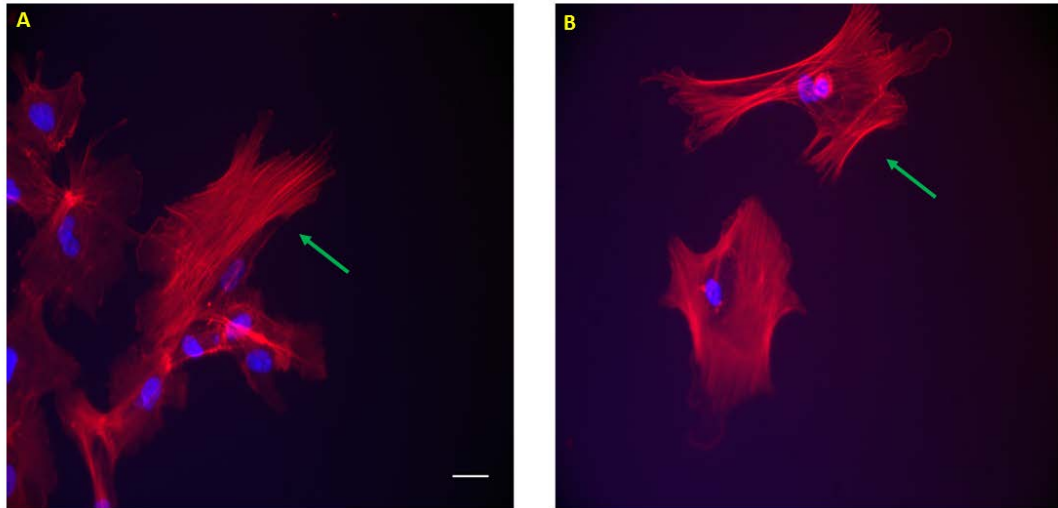


**Figure 7-4** This figure shows a fluorescence microscopy image of the immunostaining of MSCs on topographical surfaces A) NSQ and B) SQ, where red is actin (rhodamine-phalloidin) and blue is the cell nucleus (DAPI). It is interesting to find that MSCs stain with rhodamine-phalloidin more intensely and the actin fibres are more defined than endothelial cells. Note that on A) it is possible to compare with the endothelial cells on the left which are not as well stained. [Scale bar: 10 $\mu$ m]

It is also possible to see that the MSCs are able to adhere on top of the endothelial cell sheets as well as adhering to the exposed surfaces of the substrates. This is possible on all three topographies, planar, NSQ and SQ. Therefore, this shows that the MSCs can also attached to the endothelial cell sheets as well as the exposed topographies. The MSCs, despite adhering to the top of the endothelial cell sheet seems to have retained its morphology of being spindle-shape.

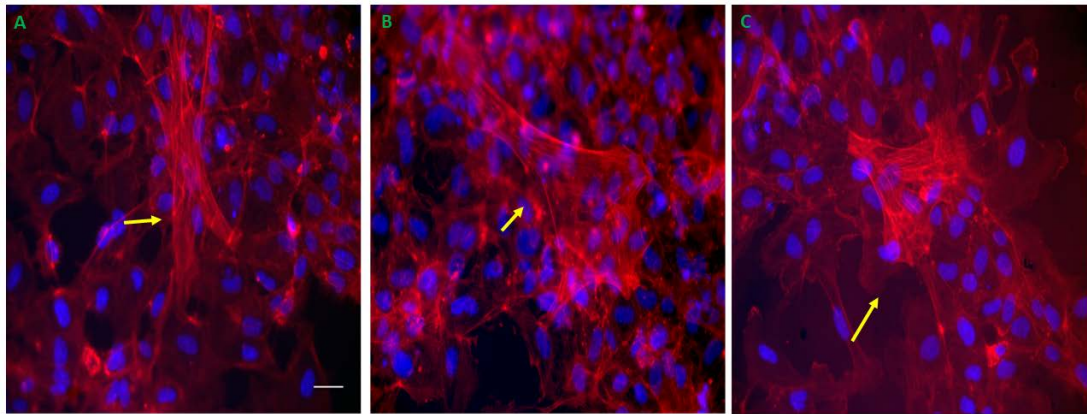


**Figure 7-5** These are fluorescent microscopy images of the MSCs also noted to be adhering on the top of the endothelial cell sheets on all three topographies, a) planar, b) NSQ and c) SQ, where red is actin (rhodamine-phalloidin) and blue is the cell nucleus (DAPI). The yellow arrows point to the MSCs on top of the endothelial cells.

To further distinguish the endothelial cells from the MSCs, the endothelial cells were immunologically tagged with anti-CD31, which is a known surface marker of endothelial cells. This is illustrated by Figure 7.6 where the endothelial cell sheets can be seen at the bottom and highlight the presence of the CD31 marker on the cell membrane (as seen as the green colour). The morphology of both cell types are maintained and this is important as it illustrates that both cell types are healthy and therefore co-culture of these two cell types is possible. Also the spindle-shape of the MSCs is maintained and therefore this is a visual confirmation that MSCs have not differentiated down a specific osteogenic lineage(126). The difference in actin fibres distribution also given an indication of the difference in cytoskeletal arrangement between the two cell types.

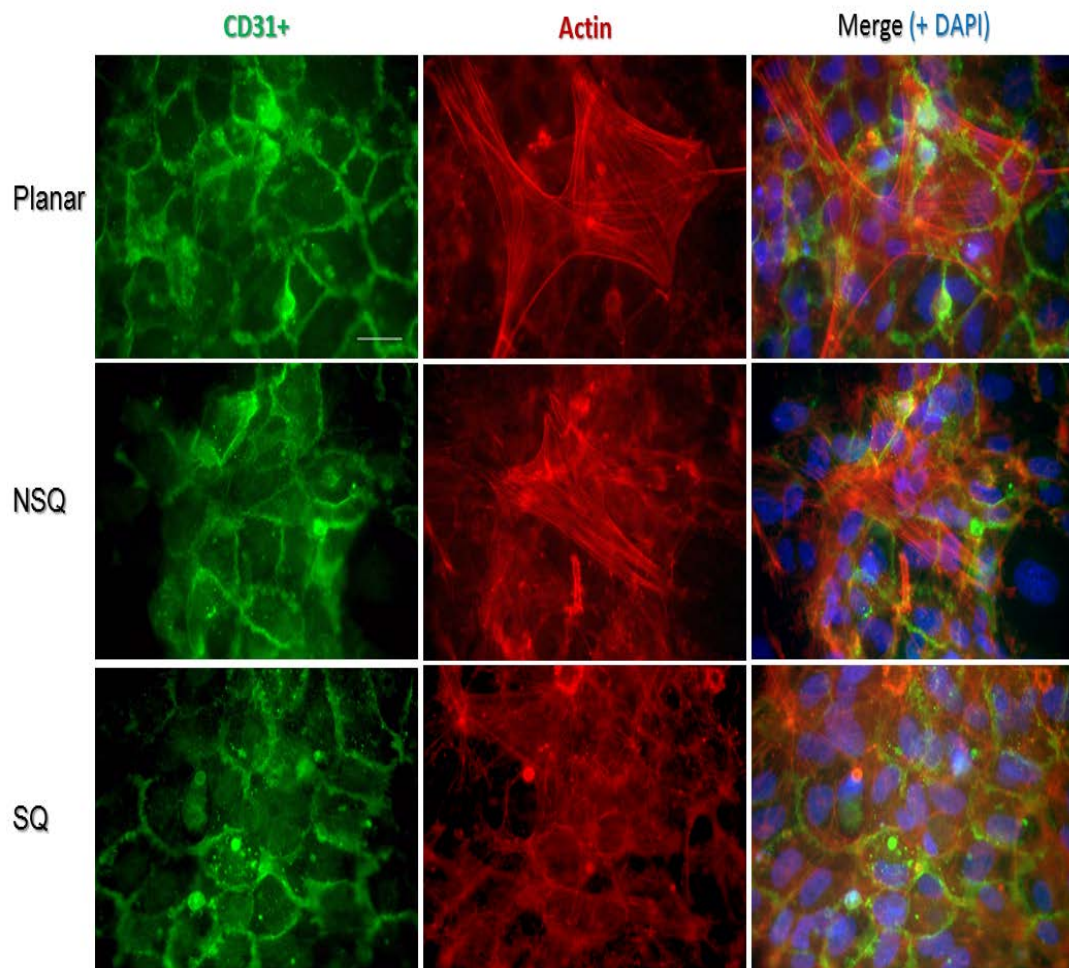


**Figure 7-6 Fluorescence microscopy images highlighting the difference between the MSCs and HUVECs. CD31+ staining (green) is a surface marker for endothelial cells and therefore it is possible to differentiate between the two types of cells. Red highlights actin (rhodamine-phalloidin) and blue is the cell nucleus (DAPI). [Scale bar: 10µm]**

Von Kossa staining is a well-known staining technique which is used to visualise mineralised nodules in cell culture. The Von Kossa method is based on the binding of silver ions to the anions (phosphates, sulfates or carbonates) of calcium salts and the reduction of silver salts to form dark brown or black metallic silver staining. The co-cultures were allowed to culture for 3 weeks and they were then fixed before visualising using Von Kossa to look for mineralised nodules under phase-contrast microscopy. On the cell cultures cultured on the 3 different topographies of the polycarbonate substrates, it was not possible to detect the presence of any mineralised nodules, indicating that there were no signs of calcification. The

presence of mineralised nodules can be seen by the positive reference sample (Figure 7.7) as black deposits within the cell culture and this was not seen in the samples.

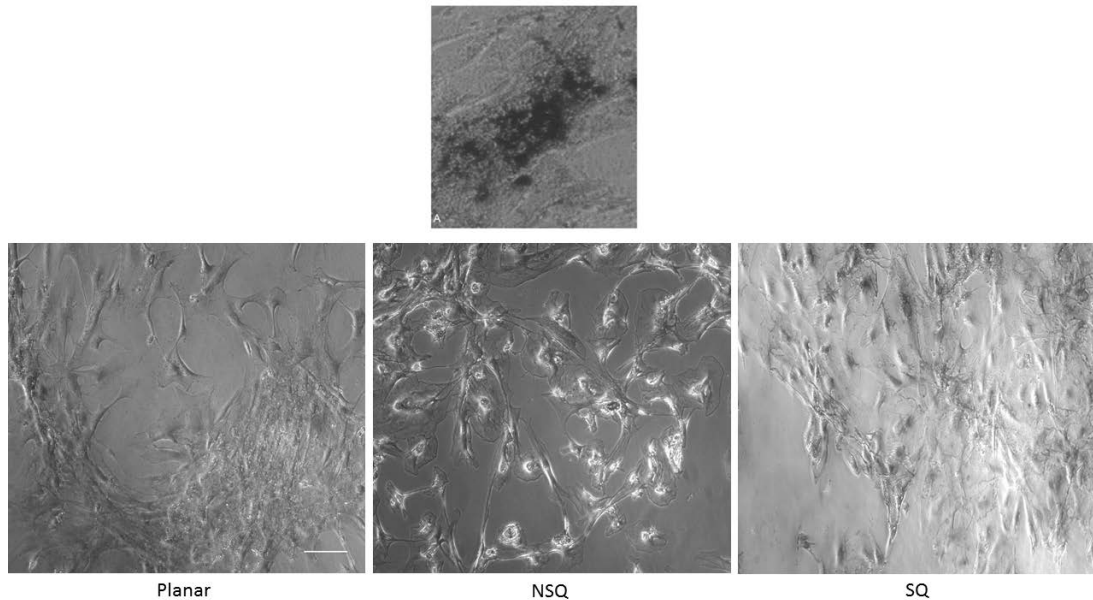


**Figure 7-7** This is phase-contrast microscopy to look at the results from Von Kossa staining on the different PC substrates and their topographies by the co-culture of MSCs/ HUVECs. A) is a positive reference sample and adapted from (127). A positive Von Kossa will show dark deposits which are not seen on our test samples on the three topographies, as highlighted. [Scale bar: 10µm]

Another study was conducted as a more sensitive detection method using ICW to look at the expression of osteocalcin. Again the co-cultures cell samples on the three PC topographies were cultured for 3 weeks before analysis. Interestingly, expression of osteocalcin can be seen on SQ topography followed by NSQ and then planar topography. Osteocalcin (OCN) is an extracellular maturation protein and is a marker of osteogenic lineage of the MSCs. This is an important indicator showing that on the SQ surface, there is a predominance towards osteocalcin expression and therefore differentiation into osteogenic lineage. This also gives an early indication that there is higher potential of calcification on this topography.

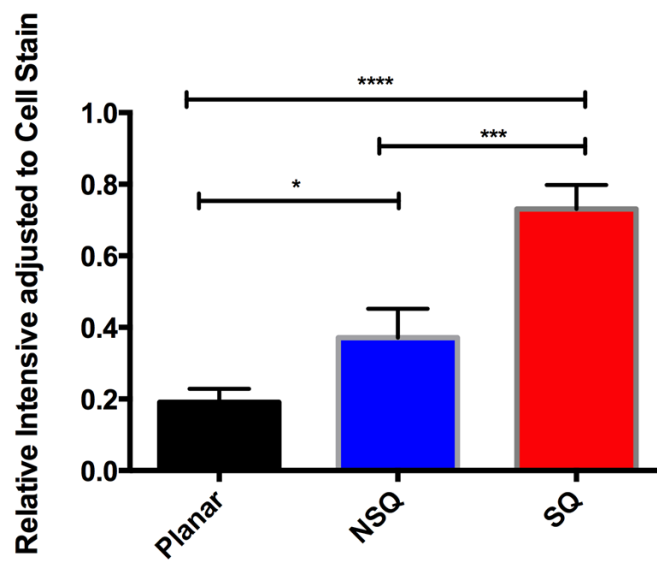


**Figure 7-8** Graph to show osteocalcin expression on the different topographies by the co-cultures of MSC/ HUVEC, using In Cell Western, after 3 weeks of cell culture. [Where \* <0.05 and \*\*\* <0.0001] (n=3)

Examination of the cell stain intensities to give us an indication of cell density on the substrates shows that there are more cells in co-culture on the planar surfaces rather than on the topographical patterns surfaces, NSQ and SQ, to statistical significance.

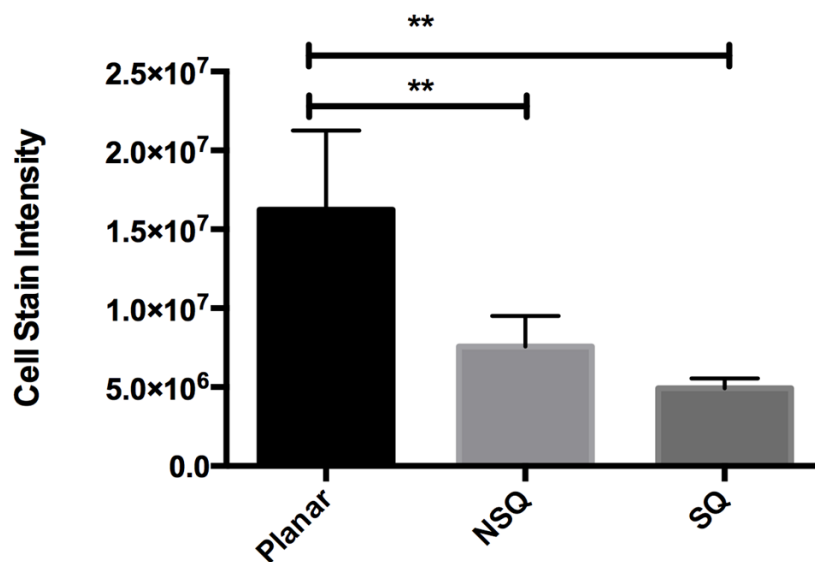


Figure 7-9 Graph to show a cell count comparison using cell stain of the ICW methodology. This shows that there are more cells on the planar surfaces with statistical significance over NSQ and SQ surfaces. [Where  $** < 0.05$ ] (n=3)

## 7.5 Discussion

This Chapter is focused on seeing if MSCs and HUVECs are able to exist in co-culture so as to test out a hypothesis on whether MSCs can potentially cause a problem by differentiating into osteogenic lineage and thereby potentially causing calcification in the vascular graft.

As mentioned, calcification within a vascular graft can cause lots of problems, not least of all, shear stress and alteration of haemodynamic flow and dysfunction of the endothelial layer. In fact, even with normal vascular graft materials in current clinical use, calcification is a highly underestimated occurrence. Mehta(2) *et al* explanted PTFE grafts and found a large number of them were calcified and may represent a previously underestimated problem. Although registries have been set up to try and further elucidate this problem, it will take time before results will follow. However, it is known that calcification can cause problems leading to premature graft failure. This data can also be extrapolated from data which have looked at heart valve calcification, in which extensive work has been conducted looking at this.

In the experiments, the HUVECs are allowed to have time to adhere to the polycarbonate surfaces first prior to seeding with MSCs for the co-culture. The reason for this is to try simulate the probability that in an in vivo model, it is likely that there will be patchy endothelial monolayers with uncovered exposed areas of nanotopography in which circulating MSCs might 'home' towards. These are the areas which would be perceived to be the areas in which MSCs would be able to settle and be influenced by HUVECs to differentiation down an osteogenic lineage.

Interestingly, although it was initially thought that these exposed surfaces would be a problem, it was quickly established that the MSCs are able to adhere to the endothelial monolayers as well as the exposed surfaces. These observations are in line with those seen by Luu *et al*(127). In the presence of flow, it has been seen that MSCs are unlikely to adhere to endothelial cells. However, in the presence of inflammation or injury, leukocyte capture molecules such as P-selectin or vascular cell adhesion molecule-1 (VCAM-1) are expressed by the endothelial cells and these are able to bind to MSCs. There appears to be a co-synergistic approach in which the MSCs which are bound to the ECs appear to upregulate IL-6 and together with IL-6 receptor. In this case, although IL-6 is commonly known as an inflammatory cytokine, it does have a dual-effect, and has been identified as the major agent which acts on the endothelial cells to reduce leukocyte recruitment(127).

In the immunostaining of the co-cultures, it was easy to distinguish between the MSCs and the HUVECs and see that MSCs adhere to both the exposed surfaces of the substrate and on to the top of the HUVECs. Although the experiments were conducted under static conditions, previous work has suggested that under low flow conditions MSCs adhere to HUVECs, illustrates the 'homing' ability of MSCs. The ability of MSCs to bind to HUVECs is due to leukocyte capture molecules. This is an interesting prospect as implantation of a synthetic vascular graft can illicit an initial inflammatory response and in some individuals, it has been shown that a persistent low-grade response can be seen for a long time post-implantation. It then leads to the postulation that under these circumstances there could be potentially increase of MSC recruitment, which can have some beneficial effect in suppressing the inflammatory response.

However, in the presence of the topography, there is an added risk of calcification. Using Von Kossa staining as an evaluation tool, there was no signs of calcified nodules after 3 weeks of co-culture. However, 3 weeks of co-culture may not be enough time for calcium and phosphate deposition for Von Kossa to be positive. Therefore, ICW was exploited to investigate the possibility of osteogenic differentiation more directly.

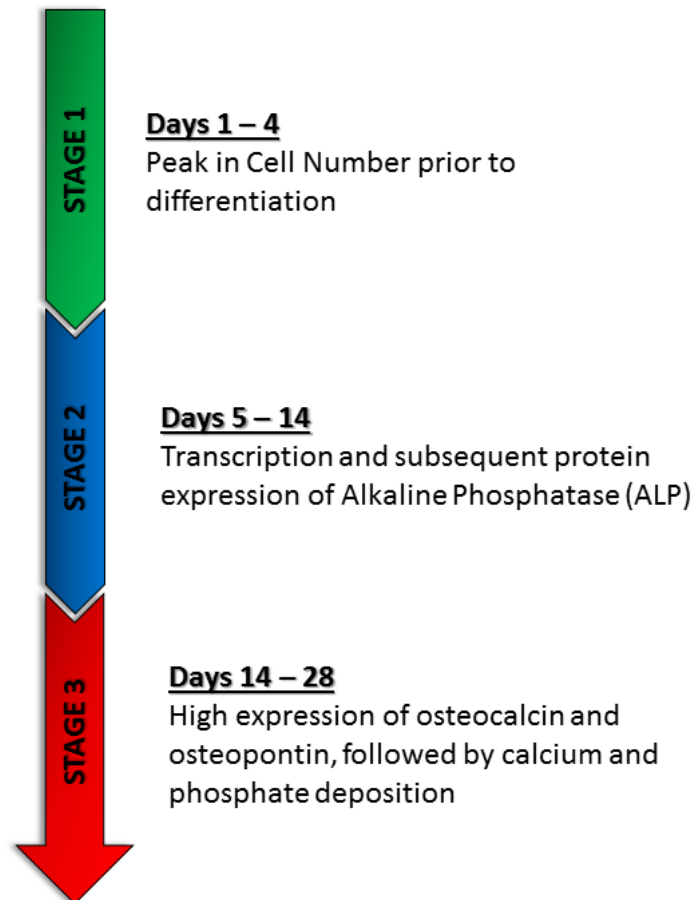


**Figure 7-10 Simplified diagram to show the three stages of MSC differentiation down towards osteogenic lineage and the timeline of the expression of different protein markers and deposition of calcium and phosphate.**

Osteocalcin was evaluated. Osteocalcin is upregulated in MSCs that differentiate down the osteogenic lineage and is present after Day 14. It is a protein which is expressed by mature osteoblasts and is a later stage osteogenic marker(124). ICW was used to evaluate the presence of this protein at Day 21. It was found to be highly

upregulated on the SQ surfaces followed by the NSQ surfaces and then planar surface.

As previously mentioned, when MSCs are grown primarily on the SQ surfaces, they can be maintained as MSCs rather differentiating into an obvious osteogenic lineage as on the NSQ surfaces(97). This maintenance can be maintained for at least 8 weeks in cell culture. However, on the addition of endothelial cells, there seems to be a 'flip' in the biology and it can be seen that on the SQ surfaces, there is a significantly higher expression of osteocalcin and therefore indicating that the MSCs are more likely to be going down the osteogenic lineage. This indicates there must be some 'cross-talk' which is happening between the co-cultures which has driven the MSCs to differentiate at a higher rate than compared with those on the NSQ surfaces.

Kaigler *et al*(124) conducted a series of astute experiments looking at the effect of endothelial cells on MSCs. They found that ECs enhance the osteogenic potential of MSCs when grown in co-cultures and this was due to close or direct cell-cell contact which is required for this to take place. They noticed that endothelial cells produce BMP-2 (bone morphogenetic protein -2), which is a potent bone morphogen, and this property seems limited to endothelial cells and no other cell type and is a primary factor which induces osteogenic differentiation of MSCs.

BMP-2 is part of the transforming growth factor superfamily and is a cytokine. It was originally detected in bone and cartilage but is known to be produced by vascular endothelial cells. It is known to host and regulate a host of cellular functions, including cardiovascular development, neovascularization in tumours and smooth muscle chemotaxis in response to vascular injury. In addition to this, it has also been shown that endothelium-derived BMPs contribute to vascular calcification especially during the development of atherosclerotic plaques and BMP-2's presence in atherosclerotic plaques has also been noticed(128).

In the experiments conducted in this Chapter, the MSCs have been cultured in basal media and not in osteogenic induction culture media. This is important as this shows that there are no external stimuli to influence the osteogenic lineage progression. In the in vitro setting, the factors which are needed to add to the culture media to induce

the differentiation of the MSCs down either chondrogenic, osteogenic or adipocytic lineage is well-known. For chondrogenic differentiation, growth factors such as TGF- $\beta$  is required whereas for adipocytic lineage, the MSCs have to be cultured with dexamethasone, insulin, isobutyl methyl xanthine and indomethacin. In contrast for osteogenic differentiation of MSCs in vitro the presence of dexamethasone, ascorbic acid and  $\beta$ -glycerol phosphate is required(129). In the co-culture culture media mix used in this set of experiments, which is a 1:1 ratio of basal media: endothelial cell culture as suggested by Bidarra *et al*(43), the above listed factors are not included in the culture recipes and therefore it is assumed that the culture conditions will not be a factor in osteogenic lineage induction.

Furthermore, other experiments conducted by other researchers have shown that ECs can participate at different levels of osteogenesis as osteoinductive cells in a variety of ways. They do this by releasing BMPs and by controlling the three main transcription factors which are required for bone cell differentiation which are runx2, osterix and dlx5(130). In return, the vascular endothelial growth factor (VEGF) which can be expressed by MSCs can promote endothelial cell survival. After a long period of co-culture with endothelial cells and MSCs, the early osteoblastic markers slowly decrease with up-regulation of the markers associated with a mineralised matrix(131).

These results indicate the synergistic relationship between HUVECs and MSCs which contributes towards osteogenesis. In the field of bone tissue engineering, these results hold promise and merits further investigation. However, in a vascular graft environment the presence of any mineralised tissue deposits leading to vascular graft calcification can be disastrous. The scenario described in this Chapter is considered as a 'worst case scenario' situation. The ratios that was used for MSC: HUVEC is very high and in reality there is a much lower ratio between the two. There is quite some discussion as to the presence of 'actual' circulating MSCs within the bloodstream and their actual definition. The majority of MSCs reside in the bone marrow and it is thought that under circumstances of injury and inflammation there would be an increased mobilisation of MSCs deployed through the bloodstream to 'home' into the sites requiring immunological damping and also tissue repair and

regeneration. In addition, they have been found to express integrins and chemokine receptors which help in their 'homing' ability. An interesting study designed to investigate the presence of circulating MSCs by Hoogduijn *et al*(132) did not detect the presence of circulating MSCs in the bloodstream. They looked at the peripheral blood of patients who have undergone heart transplants or who fulfil the criteria for end-stage liver failure and kidney disease and were not able to detect cells which fulfil the criteria for MSCs. In the cases of poly-trauma patients who were also evaluated, they were able to detect MSCs in the bloodstream but this was thought to be due to release of MSCs from the bone marrow following bone fractures. The alternative theory is that MSCs reside in small quantities in all tissues within the body with perivascular localization. Thus it is these local populations which would migrate to the tissues as and when required and therefore do not really require migrating through the bloodstream. Despite this, the MSC niche in which they reside in, besides the bone marrow, and whether they are able to use the bloodstream to migrate and 'home' to locations which require their presence, still remains a controversial area of discussion within stem cell biologists. In terms of whether it would affect an implanted vascular graft, there are implications that this can be a problem. The implantation of a vascular graft does propagate an area of injury and therefore this would attract stem cells to the site and the preliminary results seem to indicate that accelerated calcification of the vascular graft tends to be a problem in the presence of MSCs.

The results for cell density for the co-cultures on the different topographies highlights an interesting result in which there are more cells on the planar substrate preferentially over NSQ and SQ. This might be due to the ability of the planar surface and the exposed surface area for the co-cultures to spread and adhere to the surface which is a bit more difficult on the nanopit topographies. It is not certain whether in the presence of another cell type as to how this would affect endothelial cell adhesion and proliferation on the surfaces but as described earlier, MSCs does have an effect on the behaviour of endothelial cells and this merits further investigation.

## **7.6 Conclusion**

This Chapter has shown that it is possible to grow MSCs and endothelial cells in a co-culture setting on the polycarbonate substrates with nanopits generated by injection molding. The MSCs are able to adhere to the monolayer of endothelial cells and also on the exposed surfaces of the substrates.

Unfortunately, this Chapter has shown that there is potentially a problem with MSCs being directed towards an osteogenic lineage when co-cultured with endothelial surface leading to vascular graft calcification. This has recently been a topic of focus and can lead to premature vascular graft failure. It has been seen that the topography SQ seems to upregulate osteocalcin and therefore promote osteogenesis highly but this has been an unexpected ‘flip’ in results as SQ has previously been known to promote maintenance of MSC. It is evident that by co-culture of MSC and endothelial cells do promote osteogenesis and has important implications for bone tissue engineering. However, in the *in vivo* system, there are lots of different interactions between cells and chemokines and the mechanisms of how many different cells reside in tissues together synergistically and their ‘cross-talk’ to help to guide and direct each other in their environment. If the exact mechanisms were elucidated, this might help in further research in vascular calcification.

## **7.7 Further Work**

In the results of this Chapter, one of the most interesting points which have been brought up has been the increase in osteocalcin production especially on the SQ surfaces, over the NSQ surfaces. This indicates that on the SQ topography endothelial cells may be stimulated to produce factors which would promote MSC differentiation towards an osteogenic lineage. This stimulation of the endothelial cells by the SQ surfaces seems to have more of an effect than the NSQ surfaces and at present, it is not entirely clear what these changes are. Further work would concentrate on elucidating the biological mechanisms underlying this ‘switch’ and this would be best approached using a high-throughput genomics approach such as Next Generation Sequencing. This would allow the study and analysis of multiple

genes at the same time and therefore identify ones which may require further investigation at a more focused level.

Additionally, the well-known link of BMP-2 being expressed by endothelial cells in the presence, either close or direct cell-cell contact, of MSCs, is known. It is therefore wondered whether topography itself can increase the production of BMP-2 within the endothelial cells and hence increase its osteoinductive properties. Therefore, experiments would be conducted on endothelial cells by themselves and looking for the expression of BMP-2 only on the different topographies. This would further confirm whether the stimulus for BMP-2 production is solely on close or direct contact with MSCs or whether external factors such as surface topography can have an effect on BMP-2 production. This would be an interesting set of experiments as previous experiments by Yang(133) *et al* have shown that in the presence of NSQ topography, MSCs have been shown to upregulate BMP-2 production. Therefore, if it can be shown that topography has an additional effect on this with endothelial cells, there will therefore be at least double the amount of BMP-2 production present.

In addition, this co-culture experiment needs to be further evaluated under flow conditions and to compare it with these experiments which have been conducted in a static in vitro environment. Flow conditions can have a separate effect on the cells and this might change the static experimental results. Flow conditions are very important especially in vascular graft engineering.

## **Chapter 8: Conclusion and Future Work**

## Chapter 8 Conclusion and Future Work

The main aim of this research has been to find a way of modifying the surface of the POSS-PCU polymer so as to incorporate endothelialisation with the POSS-PCU vascular graft. Various techniques have been employed in this Thesis in an attempt to achieve this. A multidisciplinary approach has been undertaken over the course of this Thesis, using engineering, chemistry and biology, to try and achieve a surface in which endothelial cells are able to adhere to and also to try and understand the interaction between endothelial cell and the surface.

Vascular research has employed a more multi-disciplinary approach over the last ten years. The concept of regenerative medicine has taken a more prominent place in vascular graft research. The ability to have an approach in which the body is able to regenerate a new vessel is a technology that current research tools do not have the advances to produce. Despite this, there is a plethora of ideas in which to achieve this technology.

The path chosen in this Thesis is to try and modify an existing biomaterial to incorporate endothelialisation. As previously introduced, this biomaterial is a polyurethane-based polymer with a nanoparticle, POSS, incorporated within the polymer structure. This has allowed the polycarbonate urea urethane polymer to be mechanically reinforced as well as retaining compliant and biocompatible properties. This polymer has recently been the subject of intense investigation, least of all a 'first in man' clinical trial. However, evaluation of this polymer has highlighted a similar deficiency which has plagued many other vascular graft materials, the inability to endothelialise. This deficiency means that no matter the superiority of the performance of this vascular graft when compared with ePTFE or Dacron®, it will lack the protective and beneficial measures given by the presence of an endothelial lining within the luminal surface of the graft. It has previously been mentioned that there are a three main ways to allow for endothelialisation post-implantation of a vascular graft. These have been described as inward migration, endothelial cell 'fall-out' from the circulation and transmural tissue ingrowth(134). The concept of inward migration from neighbouring vessels was initially 'binned' as despite all sorts of

modifications used at the time, it was noted that inward migration did not extend beyond 2-3 cm and other techniques were used instead(86).

There have been major technological advances in the field of nanoengineering over the last decade. This has properly allowed the study of cells on different topographical features since Harrison's observations(72). In addition, plasma treatment is also another option for surface modification. As mentioned previously, plasma is referred to as the fourth state of matter as by Langmuir. It is partly ionized gas and is defined as a quasi-neutral particle system in either a gaseous or fluid-like mix of electrons, ions and free radicals. Within this mix, there are usually neutral particles such as atoms and molecules(135). When this high-energy mixture, is used to bombard the surface of a material, chemical bonds can be broken in which new surface chemical groups can be generated. In this Thesis, this property has been exploited to modify the surface so as to increase the surface contact angle. Both of these surface modification techniques are important to enhancing cell growth on the surface of vascular grafts, and have also been exploited by quite a few research groups.

### **8.1 POSS-Nanoparticle for Chemically Altering the Surface**

The POSS-nanoparticle is a very important nanoparticle in the research conducted in this Thesis. It is the nanoparticle which has been used to reinforce the polyurethane-based polymer gives the mechanical properties which have been so desirable in this POSS-PCU polymer.

As the polymeric solution is already developed in-house, the POSS-nanoparticle is sourced commercially via Hybrid Plastics Inc. It was thought that by being able to manufacture the POSS-nanoparticle in-house, it would also mean that we can further develop the polymer to have other different chemical and physical properties by harnessing the properties of the POSS-nanoparticle.

It is possible to fabricate the POSS-nanoparticle in-house but unfortunately currently in the laboratories used for this work, it is not purpose built for chemical synthesis and techniques such as purification needs to be further optimized. However, as the

tests which have been conducted show, the final product is very similar to that produced commercially. The POSS-Chlorohydrin is the most important nanoparticle in this case.

The POSS-PCU polymer has shown itself to have a hydrophobic surface, even more hydrophobic than ePTFE, and this means that cells, especially endothelial cells, are unable to adhere on the surface. This was especially evident in the preclinical studies for this polymer when investigating its use as a vascular graft(39). The surface can be fine-tuned to either enable cells to grow or to prohibit anything from adhering to super-hydrophobic surfaces. Super-hydrophobic surfaces were thought to be a potential avenue to explore as if the contact angle was raised  $> 150^\circ$  this will deter biological material from adhering, especially platelets, to the surface. However, it was not possible to alter the surface contact angle of the POSS-PCU polymer to an extent by mixing different POSS nanoparticles with different functional groups. Following recent disappointing clinical results for the Fluoropassiv<sup>TM</sup>(54) vascular grafts, which uses a similar rationale by increasing the availability of fluorine groups, which is hydrophobic and therefore hopes to decrease thrombogenicity, this was abandoned and focus was shifted to increasing the hydrophilicity of the surface so that cells are able to adhere and proliferate leading to endothelialisation.

## **8.2 Plasma-Treatment for Increasing the Hydrophilicity and Biological Activity of the POSS-PCU surface**

It was demonstrated in Chapter 4 that it is possible to lower the water contact level using plasma treatment. This increases the hydrophilicity of the polymer surface and allows endothelial cells to adhere to the surface of the polymer. Lowering of the contact angle of the polymer surface does not affect the biocompatibility of the polymer and allows endothelial cells to grow on the surface, these properties do not appear to affect the bulk properties of the polymer, although this would require further confirmation with mechanical and compliance testing and would form further evaluation of this plasma-modified polymer. Although cells were able to grow on the POSS-PCU polymer, it was not clear if cell adhesion was adequate on the polymer as via the immunofluorescence, focal adhesions were not visualized. As the ECM exists as a complex entity *in vivo*, it is not clear if altering the surface contact angle is

enough and it is likely that other factors will come into play. Cell adherence is extremely important in the case of endothelial cells within a vascular graft as it needs to withstand the haemodynamic stress and pressure within the vessel. Failure of this will be seen by the endothelial cell sheet delaminating, and that is only if there is a chance that cell sheets have been given the chance to form.

### **8.3 Combining Plasma Treatment with Surface Topographical Modifications on POSS-PCU**

It was then thought that a combination of surface physical and chemical factors would increase the adherence of the endothelial cells. Surface topographical cues have been shown to have an effect on cells, affecting them in processes such as migration, differentiation and adherence. This is important as it means that a combination of plasma treatment as well as surface topographical modification could enhance endothelial cell adherence.

Using the optimal plasma treatment, 80W for 60s, the surface topography was tested with microgrooves and nanopits. It was found that it was possible to replicate these features with high fidelity on POSS-PCU. In addition, despite these topographical changes there was little appreciable changes in the surface contact angle. The surface topographical features also did not seem to have a detrimental effect on the endothelial cells and cells were able to adhere on the surface. This time it was possible to see the formation of focal adhesions (when staining for vinculin) on the nanopit topography, however this was not seen on the microgroove or planar (control) surfaces. However, this was such a subtle change and the decision was taken to further investigate the role of nanotopography on endothelial cells.

### **8.4 Investigating the Effect of Nanopits on Endothelial Cells Adhesion**

Nanopits have been visualized to be part of the normal surface topographical in an arterial vessel in a rhesus macaque(75). As mentioned, it is still not possible to completely replicate the ECM in its entirety, however, the presence of these nanopits can potentially have an important effect on endothelial cells and this Chapter was designed to investigate this.

The two main topographies used was NSQ and SQ on PC substrates with planar substrates acting as the control. It was possible to note that the nanopits do have an effect on endothelial cell adhesion but it is not 100% clear what that reaction is. The results indicate that there is a gradual increase in the expression of P-myosin over the first few days after cell seeding. NSQ topography increases the expression of P-myosin whereas SQ topography increases the expression of VE-Cadherin, indicating that the 50nm offset seems to play an important role in dictating cell adhesion. The upregulation of P-myosin on the NSQ topography has also previously been seen with MSCs. However, the upregulation of VE-Cadherin on the SQ surfaces seem to be linked to the anti-proliferative effect also observed. This will require further investigation as to how SQ topography dictates this reaction in the HUVECS.

### **8.5 Will Nanopit Topography have an effect on Calcification leading to Premature Vascular Graft Failure?**

The nanopit topographies used in this Thesis have gained significant interest after they were found to have a significant effect on MSCs especially in bone tissue engineering(42, 97). This Chapter was dedicated to looking if this could potentially have an effect on vascular graft development as this can cause a host of problems which will lead to premature vascular graft failure.

The MSCs were found to be able to adhere to the patchy endothelial cell coverage on the different PC topography substrates as well as the exposed areas of the substrates and were able to co-exist in a co-culture system. Two experiments were then designed to look at whether calcification can be a problem in the co-culture system. Although on more conventional Von Kossa staining it was not possible to see signs of calcification after three weeks of cell culture, it was found that the SQ topography seem to upregulate the production of osteocalcin over NSQ and Planar. This was a surprise as SQ topography has traditionally been known to be the topography which promotes MSC maintenance but in a co-culture system, it was the topography which seem to direct MSC towards osteogenic lineage, even over the NSQ surface. It is known that in co-culture systems of MSC and HUVECs, the MSC can be directed towards osteogenic lineage. It is therefore hypothesise that it is primarily the

expression of BMP-2 by the HUVECs which causes this but it seems that the surface topography can also have an additional influence.

## **8.6 Future Work**

The results presented in this Thesis have shown that there is potential in the use of nanotopography in the luminal surface of the vascular graft. Endothelial cells have been found to react to the nanotopography but it would seem that further understanding into the adhesion factors is important so this can be improved on. It would be important to have a more in-depth analysis of the focal adhesions involved in cell adherence on the different topographies and why this is changed on the different configurations of the nanopits. This understanding would be essential in counteracting against delamination when the endothelial cells are applied to flow.

Calcification can be a problem when it occurs in vascular grafts and induces premature failure. It can be seen that this produces a lot of downstream effects such as endothelial dysfunction as well as alteration of the haemodynamic flow, all of which can contribute to the eventual failure of the graft. It can be seen that this can potentially be a problem especially topographies which have a strong effect on MSCs. Therefore, it is vital that further work is focused on the relationship between endothelial cells and MSCs to explore which is the trigger towards predisposition towards an osteogenic lineage. Especially with specific focus on replicating the *in vivo* ratios of MSCs to endothelial cells as this would dictate whether this is an effect which needs further research which would look to reducing the calcification effect.

Finally, the most important part of future work should be focused on testing the endothelial cells on topography under stress flow conditions. This will test the endothelial cells adherence in an environment in which it will experience *in vivo*. As stress flow factors can also provide an additional cue to the endothelial cells, this will also need to be further investigated. Live cell imaging would be beneficial at this point This would be the ultimate test of the stability of the endothelial cell adherence.

The overall aim of this research would be to create a self-endothelising small diameter vascular graft made from the POSS-PCU material utilizing surface plasma

treatment and topography to achieve this. These vascular grafts would benefit patients requiring peripheral bypass surgery, especially in emergency situations which would require 'off the shelf' grafts.

## **Chapter 9: References**

## Chapter 9 References

1. Hirsch AT, Duval S. The global pandemic of peripheral artery disease. *The Lancet*. 2013;382(9901):1312-4.
2. Mehta RI, Mulcherjee AK, Patterson TD, Fishbein MC. Pathology of explanted polytetrafluoroethylene vascular grafts. *Cardiovasc Pathol*. 2011;20(4):213-21.
3. Fowkes FGR, Rudan D, Rudan I, Aboyans V, Denenberg JO, McDermott MM, et al. Comparison of global estimates of prevalence and risk factors for peripheral artery disease in 2000 and 2010: a systematic review and analysis. *The Lancet*. 382(9901):1329-40.
4. Taylor LM, Jr., Edwards JM, Porter JM. Present status of reversed vein bypass grafting: five-year results of a modern series. *J Vasc Surg*. 1990;11(2):193-205; discussion -6.
5. Donaldson MC, Mannick JA, Whittemore AD. Femoral-distal bypass with in situ greater saphenous vein. Long-term results using the Mills valvulotome. *Annals of Surgery*. 1991;213(5):457-65.
6. Kapadia MR, Popowich DA, Kibbe MR. Modified prosthetic vascular conduits. *Circulation*. 2008;117(14):1873-82.
7. Post S, Kraus T, Müller-Reinartz U, Weiss C, Kortmann H, Quentmeier A, et al. Dacron vs Polytetrafluoroethylene Grafts for Femoropopliteal Bypass: a Prospective Randomised Multicentre Trial. *European Journal of Vascular and Endovascular Surgery*. 2001;22(3):226-31.
8. Twine CP, McLain AD. Graft type for femoro-popliteal bypass surgery. *The Cochrane database of systematic reviews*. 2010(5):Cd001487.
9. Soldani G, Losi P, Bernabei M, Burchielli S, Chiappino D, Kull S, et al. Long term performance of small-diameter vascular grafts made of a poly(ether)urethane-polydimethylsiloxane semi-interpenetrating polymeric network. *Biomaterials*. 2010;31(9):2592-605.
10. Wiggins MJ, MacEwan M, Anderson JM, Hiltner A. Effect of soft-segment chemistry on polyurethane biostability during in vitro fatigue loading. *Journal of Biomedical Materials Research Part A*. 2004;68A(4):668-83.

11. Ward RS, White KA. Surface-modifying endgroups for biomedical polymers. Google Patents; 1996.
12. Seifalian AM, Salacinski HJ, Tiwari A, Edwards A, Bowald S, Hamilton G. In vivo biostability of a poly(carbonate-urea)urethane graft. *Biomaterials*. 2003;24(14):2549-57.
13. Kannan RY, Salacinski HJ, Butler PE, Seifalian AM. Polyhedral oligomeric silsesquioxane nanocomposites: the next generation material for biomedical applications. *Accounts of chemical research*. 2005;38(11):879-84.
14. Dorigo W, Pulli R, Castelli P, Dorrucchi V, Ferilli F, De Blasis G, et al. A multicenter comparison between autologous saphenous vein and heparin-bonded expanded polytetrafluoroethylene (ePTFE) graft in the treatment of critical limb ischemia in diabetics. *Journal of Vascular Surgery*. 2011;54(5):1332-8.
15. Bosiers M, Deloose K, Verbist J, Schroë H, Lauwers G, Lansink W, et al. Heparin-bonded expanded polytetrafluoroethylene vascular graft for femoropopliteal and femorocrural bypass grafting: 1-year results. *Journal of Vascular Surgery*. 2006;43(2):313-8.
16. Albers M, Battistella VM, Romiti M, Rodrigues AA, Pereira CA. Meta-analysis of polytetrafluoroethylene bypass grafts to infrapopliteal arteries. *J Vasc Surg*. 2003;37(6):1263-9.
17. Lindholt JS, Gottschalksen B, Johannesen N, Dueholm D, Ravn H, Christensen ED, et al. The Scandinavian Propaten® Trial – 1-Year Patency of PTFE Vascular Prostheses with Heparin-Bonded Luminal Surfaces Compared to Ordinary Pure PTFE Vascular Prostheses – A Randomised Clinical Controlled Multi-centre Trial. *European Journal of Vascular and Endovascular Surgery*. 2011;41(5):668-73.
18. Pashneh-Tala S, MacNeil S, Claeysens F. The Tissue-Engineered Vascular Graft-Past, Present, and Future. *Tissue engineering Part B, Reviews*. 2015.
19. Berardinelli L. Grafts and graft materials as vascular substitutes for haemodialysis access construction. *Eur J Vasc Endovasc Surg*. 2006;32(2):203-11.
20. Dukkupati R, Peck M, Dhamija R, Hentschel DM, Reynolds T, Tammewar G, et al. Biological grafts for hemodialysis access: historical lessons, state-of-the-art and future directions. *Semin Dial*. 2013;26(2):233-9.

21. Chemla ES, Morsy M. Randomized clinical trial comparing decellularized bovine ureter with expanded polytetrafluoroethylene for vascular access. *The British journal of surgery*. 2009;96(1):34-9.
22. Lantz GC, Badylak SF, Hiles MC, Coffey AC, Geddes LA, Kokini K, et al. Small intestinal submucosa as a vascular graft: a review. *Journal of investigative surgery : the official journal of the Academy of Surgical Research*. 1993;6(3):297-310.
23. Seifu DG, Purnama A, Mequanint K, Mantovani D. Small-diameter vascular tissue engineering. *Nat Rev Cardiol*. 2013;10(7):410-21.
24. Mancuso L, Gualerzi A, Boschetti F, Loy F, Cao G. Decellularized ovine arteries as small-diameter vascular grafts. *Biomedical materials (Bristol, England)*. 2014;9(4):045011.
25. Gui L, Muto A, Chan SA, Breuer CK, Niklason LE. Development of decellularized human umbilical arteries as small-diameter vascular grafts. *Tissue Eng Part A*. 2009;15(9):2665-76.
26. Shin'oka T, Imai Y, Ikada Y. Transplantation of a tissue-engineered pulmonary artery. *The New England journal of medicine*. 2001;344(7):532-3.
27. Hibino N, McGillicuddy E, Matsumura G, Ichihara Y, Naito Y, Breuer C, et al. Late-term results of tissue-engineered vascular grafts in humans. *The Journal of thoracic and cardiovascular surgery*. 2010;139(2):431-6, 6.e1-2.
28. Patterson JT, Gilliland T, Maxfield MW, Church S, Naito Y, Shinoka T, et al. Tissue-engineered vascular grafts for use in the treatment of congenital heart disease: from the bench to the clinic and back again. *Regenerative medicine*. 2012;7(3):409-19.
29. Vogel G. Tissue engineering. Mending the youngest hearts. *Science*. 2011;333(6046):1088-9.
30. Wu W, Allen RA, Wang Y. Fast-degrading elastomer enables rapid remodeling of a cell-free synthetic graft into a neoartery. *Nat Med*. 2012;18(7):1148-53.
31. Dahl SLM, Kypson AP, Lawson JH, Blum JL, Strader JT, Li Y, et al. Readily Available Tissue-Engineered Vascular Grafts. *Science Translational Medicine*. 2011;3(68):68ra9-ra9.

32. Weinberg CB, Bell E. A blood vessel model constructed from collagen and cultured vascular cells. *Science*. 1986;231(4736):397-400.
33. L'Heureux N, Dusserre N, Konig G, Victor B, Keire P, Wight TN, et al. Human tissue-engineered blood vessels for adult arterial revascularization. *Nat Med*. 2006;12(3):361-5.
34. Peck M, Gebhart D, Dusserre N, McAllister TN, L'Heureux N. The Evolution of Vascular Tissue Engineering and Current State of the Art. *Cells, Tissues, Organs*. 2011;195(1-2):144-58.
35. McAllister TN, Maruszewski M, Garrido SA, Wystrychowski W, Dusserre N, Marini A, et al. Effectiveness of haemodialysis access with an autologous tissue-engineered vascular graft: a multicentre cohort study. *The Lancet*. 2009;373(9673):1440-6.
36. Wystrychowski W, McAllister TN, Zagalski K, Dusserre N, Cierpka L, L'Heureux N. First human use of an allogeneic tissue-engineered vascular graft for hemodialysis access. *Journal of Vascular Surgery*. 2014;60(5):1353-7.
37. Chong DST, Lindsey B, Dalby MJ, Gadegaard N, Seifalian AM, Hamilton G. Luminal Surface Engineering, 'Micro and Nanopatterning': Potential for Self Endothelialising Vascular Grafts? *European Journal of Vascular and Endovascular Surgery*. 2014;47(5):566-76.
38. Deutsch M, Meinhart J, Zilla P, Howanietz N, Gorlitzer M, Froeschl A, et al. Long-term experience in autologous in vitro endothelialization of infrainguinal ePTFE grafts. *J Vasc Surg*. 2009;49(2):352-62; discussion 62.
39. Ahmed M, Hamilton G, Seifalian AM. The performance of a small-calibre graft for vascular reconstructions in a senescent sheep model. *Biomaterials*. 2014;35(33):9033-40.
40. Zorlutuna P, Rong Z, Vadgama P, Hasirci V. Influence of nanopatterns on endothelial cell adhesion: Enhanced cell retention under shear stress. *Acta Biomater*. 2009;5(7):2451-9.
41. Dalby MJ, Riehle MO, Johnstone H, Affrossman S, Curtis AS. In vitro reaction of endothelial cells to polymer demixed nanotopography. *Biomaterials*. 2002;23(14):2945-54.

42. Dalby MJ, Gadegaard N, Tare R, Andar A, Riehle MO, Herzyk P, et al. The control of human mesenchymal cell differentiation using nanoscale symmetry and disorder. *Nat Mater.* 2007;6(12):997-1003.
43. Bidarra SJ, Barrias CC, Barbosa MA, Soares R, Amedee J, Granja PL. Phenotypic and proliferative modulation of human mesenchymal stem cells via crosstalk with endothelial cells. *Stem Cell Res.* 2011;7(3):186-97.
44. Kuo SW, Chang FC. POSS related polymer nanocomposites. *Prog Polym Sci.* 2011;36(12):1649-96.
45. Haddad TS, Choe E, Lichtenhan JD. Hybrid Styryl-Based Polyhedral Oligomeric Silsesquioxane (Poss) Polymers. *MRS Online Proceedings Library Archive.* 1996;435:25.
46. Cordes DB, Lickiss PD, Rataboul F. Recent Developments in the Chemistry of Cubic Polyhedral Oligosilsesquioxanes. *Chemical Reviews.* 2010;110(4):2081-173.
47. Li G, Wang L, Ni H, Pittman C, Jr. Polyhedral Oligomeric Silsesquioxane (POSS) Polymers and Copolymers: A Review. *Journal of Inorganic and Organometallic Polymers.* 2001;11(3):123-54.
48. Haddad TS, Stapleton R, Jeon HG, Mather PT, Lichtenhan JD, Phillips S. Nanostructured hybrid organic/inorganic materials. Silsesquioxane modified plastics. *Abstr Pap Am Chem Soc.* 1999;217:U608-U.
49. Feher FJ, Newman DA, Walzer JF. SILSESQUIOXANES AS MODELS FOR SILICA SURFACES. *J Am Chem Soc.* 1989;111(5):1741-8.
50. Feher FJ. Polyhedral oligosilsesquioxanes and heterosilsesquioxanes. Gelest, Inc.
51. Toes GJ, van Muiswinkel KW, van Oeveren W, Suurmeijer AJH, Timens W, Stokroos I, et al. Superhydrophobic modification fails to improve the performance of small diameter expanded polytetrafluoroethylene vascular grafts. *Biomaterials.* 2002;23(1):255-62.
52. Guidoin R, Marois Y, Zhang Z, King M, Martin L, Laroche G, et al. The benefits of fluoropassivation of polyester arterial prostheses as observed in a canine model. *ASAIO journal (American Society for Artificial Internal Organs : 1992).* 1994;40(3):M870-9.

53. Rhee RY, Gloviczki P, Cambria RA, Miller VM. Experimental evaluation of bleeding complications, thrombogenicity and neointimal characteristics of prosthetic patch materials used for carotid angioplasty. *Cardiovascular Surgery*. 1996;4(6):746-52.
54. Robinson BI, Fletcher JP. Fluoropolymer coated Dacron or polytetrafluoroethylene for femoropopliteal bypass grafting: a multicentre trial. *ANZ journal of surgery*. 2003;73(3):95-9.
55. Hill A, Li C, Tio F, Imran M. Peptide-Coated Vascular Grafts: An In Vivo Study in Sheep. *Hemodialysis International*. 2004;8(1):78-.
56. Langmuir I. Oscillations in ionized gases. *P Natl Acad Sci USA*. 1928;14:627-37.
57. Vogler EA. Structure and reactivity of water at biomaterial surfaces. *Adv Colloid Interface Sci*. 1998;74:69-117.
58. Seeger JM, Ingegno MD, Bigatan E, Klingman N, Amery D, Widenhouse C, et al. Hydrophilic surface modification of metallic endoluminal stents. *J Vasc Surg*. 1995;22(3):327-35; discussion 35-6.
59. Kannan RY, Salacinski HJ, De Groot J, Clatworthy I, Bozec L, Horton M, et al. The antithrombogenic potential of a polyhedral oligomeric silsesquioxane (POSS) nanocomposite. *Biomacromolecules*. 2006;7(1):215-23.
60. Ahmed M, Hamilton G, Seifalian AM. Viscoelastic behaviour of a small calibre vascular graft made from a POSS-nanocomposite. Conference proceedings : Annual International Conference of the IEEE Engineering in Medicine and Biology Society IEEE Engineering in Medicine and Biology Society Conference. 2010;2010:251-4.
61. Wang PF, Ding SJ, Zhang W, Wang JT, Lee WW. Effects of O-2 plasma treatment on the chemical and electric properties of low-k SiOF films. *J Mater Sci Technol*. 2001;17(6):643-5.
62. Nissan AH. Density of Hydrogen-Bonds in H-Bond Dominated Solids. *Macromolecules*. 1977;10(3):660-2.
63. Nissan AH. H-Bond Dissociation in Hydrogen-Bond Dominated Solids. *Macromolecules*. 1976;9(5):840-50.
64. Rosenman JE, Kempczinski RF, Pearce WH, Silberstein EB. Kinetics of endothelial cell seeding. *J Vasc Surg*. 1985;2(6):778-84.

65. Ramalanjaona GR, Kempczinski RF, Ogle JD, Silberstein EB. Fibronectin coating of an experimental PTFE vascular prosthesis. *J Surg Res.* 1986;41(5):479-83.
66. Matsushita H, Chang E, Glassford AJ, Cooke JP, Chiu CP, Tsao PS. eNOS activity is reduced in senescent human endothelial cells: Preservation by hTERT immortalization. *Circ Res.* 2001;89(9):793-8.
67. Aguilar HN, Zielnik B, Tracey CN, Mitchell BF. Quantification of Rapid Myosin Regulatory Light Chain Phosphorylation Using High-Throughput In-Cell Western Assays: Comparison to Western Immunoblots. *PLoS ONE.* 2010;5(4):e9965.
68. Vicente-Manzanares M, Ma X, Adelstein RS, Horwitz AR. Non-muscle myosin II takes centre stage in cell adhesion and migration. *Nat Rev Mol Cell Biol.* 2009;10(11):778-90.
69. Dettin M, Conconi MT, Gambaretto R, Bagno A, Di Bello C, Menti AM, et al. Effect of synthetic peptides on osteoblast adhesion. *Biomaterials.* 2005;26(22):4507-15.
70. Vroman L, Adams AL. Effect of heparin on reactions at aminated polymer—blood interfaces. *Journal of Colloid and Interface Science.* 1969;31(2):188-95.
71. Keselowsky BG, Collard DM, Garcia AJ. Surface chemistry modulates focal adhesion composition and signaling through changes in integrin binding. *Biomaterials.* 2004;25(28):5947-54.
72. Harrison RG. On the stereotropism of embryonic cells. *Science.* 1911;34(1):279-81.
73. Chong DS, Dalby M, Gadegaard N, Lindsey B, Seifalian A, Hamilton G. Plasma and Patterning: The New Focus for the Development of Nanocomposite Vascular Grafts. *Journal of Vascular Surgery.* 2014;59(6):85S-S.
74. Feynman RP. There's plenty of room at the bottom [data storage]. *Microelectromechanical Systems, Journal of.* 1992;1(1):60-6.
75. Liliensiek SJ, Nealey P, Murphy CJ. Characterization of endothelial basement membrane nanotopography in rhesus macaque as a guide for vessel tissue engineering. *Tissue Eng Part A.* 2009;15(9):2643-51.
76. del Campo A, Arzt E. Fabrication Approaches for Generating Complex Micro- and Nanopatterns on Polymeric Surfaces. *Chemical Reviews.* 2008;108(3):911-45.

77. Mijatovic D, Eijkel JCT, van den Berg A. Technologies for nanofluidic systems: top-down vs. bottom-up-a review. *Lab on a Chip*. 2005;5(5):492-500.
78. Urban G. Microstructuring of organic layers for microsystems. *Sensor Actuat a-Phys*. 1999;74(1-3):219-24.
79. Hasan A, Memic A, Annabi N, Hossain M, Paul A, Dokmeci MR, et al. Electrospun scaffolds for tissue engineering of vascular grafts. *Acta biomaterialia*. 2014;10(1):11-25.
80. Phillips DB, Padgett MJ, Hanna S, Ho YLD, Carberry DM, Miles MJ, et al. Shape-induced force fields in optical trapping. *Nat Photon*. 2014;8(5):400-5.
81. Biggs MJP, Richards RG, Dalby MJ. Nanotopographical modification: a regulator of cellular function through focal adhesions. *Nanomedicine: Nanotechnology, Biology and Medicine*. 2010;6(5):619-33.
82. Biggs MJ, Richards RG, Gadegaard N, Wilkinson CD, Oreffo RO, Dalby MJ. The use of nanoscale topography to modulate the dynamics of adhesion formation in primary osteoblasts and ERK/MAPK signalling in STRO-1+ enriched skeletal stem cells. *Biomaterials*. 2009;30(28):5094-103.
83. Biggs MJ, Richards RG, McFarlane S, Wilkinson CD, Oreffo RO, Dalby MJ. Adhesion formation of primary human osteoblasts and the functional response of mesenchymal stem cells to 330nm deep microgrooves. *J R Soc Interface*. 2008;5(27):1231-42.
84. Uttayarat P, Chen M, Li M, Allen FD, Composto RJ, Lelkes PI. Microtopography and flow modulate the direction of endothelial cell migration. *Am J Physiol Heart Circ Physiol*. 2008;294(2):H1027-H35.
85. Li S, Bhatia S, Hu YL, Shiu YT, Li YS, Usami S, et al. Effects of morphological patterning on endothelial cell migration. *Biorheology*. 2001;38:101-8.
86. Zilla P, Bezuidenhout D, Human P. Prosthetic vascular grafts: wrong models, wrong questions and no healing. *Biomaterials*. 2007;28(34):5009-27.
87. Gadegaard N, Thoms S, Macintyre DS, McGhee K, Gallagher J, Casey B, et al. Arrays of nano-dots for cellular engineering. *Microelectron Eng*. 2003;67-68:162-8.
88. Miller JD, Veeramasuneni S, Drelich J, Yalamanchili MR, Yamauchi G. Effect of roughness as determined by atomic force microscopy on the wetting

- properties of PTFE thin films. *Polymer Engineering & Science*. 1996;36(14):1849-55.
89. Forstermann U, Munzel T. Endothelial nitric oxide synthase in vascular disease: from marvel to menace. *Circulation*. 2006;113(13):1708-14.
90. Teixeira AI, Abrams GA, Bertics PJ, Murphy CJ, Nealey PF. Epithelial contact guidance on well-defined micro- and nanostructured substrates. *J Cell Sci*. 2003;116(Pt 10):1881-92.
91. Geiger B, Spatz JP, Bershadsky AD. Environmental sensing through focal adhesions. *Nat Rev Mol Cell Biol*. 2009;10(1):21-33.
92. Zaidel-Bar R, Itzkovitz S, Ma'ayan A, Iyengar R, Geiger B. Functional atlas of the integrin adhesome. *Nat Cell Biol*. 2007;9(8):858-67.
93. Mierke C. The Role of Vinculin in the Regulation of the Mechanical Properties of Cells. *Cell Biochem Biophys*. 2009;53(3):115-26.
94. Reynolds PM, Pedersen RH, Riehle MO, Gadegaard N. A dual gradient assay for the parametric analysis of cell-surface interactions. *Small*. 2012;8(16):2541-7.
95. Kesler KA, Herring MB, Arnold MP, Park HM, Baughman S, Glover JL. Short-term in vivo stability of endothelial-lined polyester elastomer and polytetrafluoroethylene grafts. *Annals of vascular surgery*. 1986;1(1):60-5.
96. Gourevitch D, Jones CE, Crocker J, Goldman M. Endothelial cell adhesion to vascular prosthetic surfaces. *Biomaterials*. 1988;9(1):97-100.
97. McMurray RJ, Gadegaard N, Tsimbouri PM, Burgess KV, McNamara LE, Tare R, et al. Nanoscale surfaces for the long-term maintenance of mesenchymal stem cell phenotype and multipotency. *Nature Materials*. 2011;10(8):637-44.
98. Zorlutuna P, Vadgama P, Hasirci V. Both sides nanopatterned tubular collagen scaffolds as tissue-engineered vascular grafts. *Journal of tissue engineering and regenerative medicine*. 2010;4(8):628-37.
99. Berry C, McCloy D, Affrossman S. Endothelial Cell Response to Narrow Diameter Nylon Tubes Exhibiting Internal Nanotopography. *Current Nanoscience*. 2008;4(2):219-23.
100. Dalby MJ, Riehle MO, Johnstone HJ, Affrossman S, Curtis AS. Nonadhesive nanotopography: fibroblast response to poly(n-butyl methacrylate)-poly(styrene) demixed surface features. *Journal of biomedical materials research Part A*. 2003;67(3):1025-32.

101. Seunarine K, Meredith DO, Riehle MO, Wilkinson CDW, Gadegaard N. Biodegradable polymer tubes with lithographically controlled 3D micro- and nanotopography. *Microelectron Eng.* 2008;85(5–6):1350-4.
102. Pranov H, Rasmussen HK, Larsen NB, Gadegaard N. On the injection molding of nanostructured polymer surfaces. *Polym Eng Sci.* 2006;46(2):160-71.
103. Stormonth-Darling JM, Gadegaard N. Injection Moulding Difficult Nanopatterns with Hybrid Polymer Inlays. *Macromol Mater Eng.* 2012;297(11):1075-80.
104. Biggs MJ, Richards RG, Gadegaard N, McMurray RJ, Affrossman S, Wilkinson CD, et al. Interactions with nanoscale topography: adhesion quantification and signal transduction in cells of osteogenic and multipotent lineage. *Journal of biomedical materials research Part A.* 2009;91(1):195-208.
105. Tsuruta D, Jones JC. The vimentin cytoskeleton regulates focal contact size and adhesion of endothelial cells subjected to shear stress. *J Cell Sci.* 2003;116(Pt 24):4977-84.
106. Mejillano MR, Kojima S, Applewhite DA, Gertler FB, Svitkina TM, Borisy GG. Lamellipodial versus filopodial mode of the actin nanomachinery: pivotal role of the filament barbed end. *Cell.* 2004;118(3):363-73.
107. Tsimbouri P, Gadegaard N, Burgess K, White K, Reynolds P, Herzyk P, et al. Nanotopographical Effects on Mesenchymal Stem Cell Morphology and Phenotype. *J Cell Biochem.* 2014;115(2):380-90.
108. Vestweber D. VE-cadherin: the major endothelial adhesion molecule controlling cellular junctions and blood vessel formation. *Arteriosclerosis, thrombosis, and vascular biology.* 2008;28(2):223-32.
109. Harris ES, Nelson WJ. VE-cadherin: at the front, center, and sides of endothelial cell organization and function. *Current Opinion in Cell Biology.* 2010;22(5):651-8.
110. Huveneers S, Oldenburg J, Spanjaard E, van der Krogt G, Grigoriev I, Akhmanova A, et al. Vinculin associates with endothelial VE-cadherin junctions to control force-dependent remodeling. *The Journal of cell biology.* 2012;196(5):641-52.

111. Tzima E, Irani-Tehrani M, Kiosses WB, Dejana E, Schultz DA, Engelhardt B, et al. A mechanosensory complex that mediates the endothelial cell response to fluid shear stress. *Nature*. 2005;437(7057):426-31.
112. Giannotta M, Trani M, Dejana E. VE-Cadherin and Endothelial Adherens Junctions: Active Guardians of Vascular Integrity. *Developmental Cell*. 2013;26(5):441-54.
113. Caveda L, Martin-Padura I, Navarro P, Breviario F, Corada M, Gulino D, et al. Inhibition of cultured cell growth by vascular endothelial cadherin (cadherin-5/VE-cadherin). *J Clin Invest*. 1996;98(4):886-93.
114. Hayashi M, Majumdar A, Li X, Adler J, Sun Z, Vertuani S, et al. VE-PTP regulates VEGFR2 activity in stalk cells to establish endothelial cell polarity and lumen formation. *Nat Commun*. 2013;4:1672.
115. Xu L, Li G. Circulating mesenchymal stem cells and their clinical implications. *Journal of Orthopaedic Translation*. 2014;2(1):1-7.
116. Caplan AI. Adult mesenchymal stem cells for tissue engineering versus regenerative medicine. *Journal of cellular physiology*. 2007;213(2):341-7.
117. Dominici M, Le Blanc K, Mueller I, Slaper-Cortenbach I, Marini F, Krause D, et al. Minimal criteria for defining multipotent mesenchymal stromal cells. The International Society for Cellular Therapy position statement. *Cytotherapy*. 2006;8(4):315-7.
118. Kharaziha P, Hellstrom PM, Noorinayer B, Farzaneh F, Aghajani K, Jafari F, et al. Improvement of liver function in liver cirrhosis patients after autologous mesenchymal stem cell injection: a phase I-II clinical trial. *European journal of gastroenterology & hepatology*. 2009;21(10):1199-205.
119. Castromalaspina H, Gay RE, Resnick G, Kapoor N, Meyers P, Chiarieri D, et al. Characterization of Human-Bone Marrow Fibroblast Colony-Forming Cells (Cfu-F) and Their Progeny. *Blood*. 1980;56(2):289-301.
120. Kuznetsov SA, Mankani MH, Gronthos S, Satomura K, Bianco P, Robey PG. Circulating skeletal stem cells. *Journal of Cell Biology*. 2001;153(5):1133-9.
121. Park JC, Song MJ, Hwang YS, Suh H. Calcification comparison of polymers for vascular graft. *Yonsei medical journal*. 2001;42(3):304-10.

122. Levy RJ, Schoen FJ, Anderson HC, Harasaki H, Koch TH, Brown W, et al. Cardiovascular implant calcification: a survey and update. *Biomaterials*. 1991;12(8):707-14.
123. Georg Y, Settembre N, Marchand C, Lejay A, Thaveau F, Durand B, et al. Poor long-term stability of the Corvita abdominal stentgraft. *Eur J Vasc Endovasc Surg*. 2014;47(2):160-3.
124. Kaigler D, Krebsbach PH, West ER, Horger K, Huang YC, Mooney DJ. Endothelial cell modulation of bone marrow stromal cell osteogenic potential. *FASEB journal : official publication of the Federation of American Societies for Experimental Biology*. 2005;19(6):665-7.
125. Kaigler D, Krebsbach PH, Wang Z, West ER, Horger K, Mooney DJ. Transplanted endothelial cells enhance orthotopic bone regeneration. *Journal of dental research*. 2006;85(7):633-7.
126. Matsuoka F, Takeuchi I, Agata H, Kagami H, Shiono H, Kiyota Y, et al. Morphology-based prediction of osteogenic differentiation potential of human mesenchymal stem cells. *PLoS One*. 2013;8(2):e55082.
127. Luu NT, McGettrick HM, Buckley CD, Newsome PN, Rainger GE, Frampton J, et al. Crosstalk between mesenchymal stem cells and endothelial cells leads to downregulation of cytokine-induced leukocyte recruitment. *Stem cells (Dayton, Ohio)*. 2013;31(12):2690-702.
128. Dhore CR, Cleutjens JP, Lutgens E, Cleutjens KB, Geusens PP, Kitslaar PJ, et al. Differential expression of bone matrix regulatory proteins in human atherosclerotic plaques. *Arteriosclerosis, thrombosis, and vascular biology*. 2001;21(12):1998-2003.
129. Birmingham E, Niebur GL, McHugh PE, Shaw G, Barry FP, McNamara LM. Osteogenic differentiation of mesenchymal stem cells is regulated by osteocyte and osteoblast cells in a simplified bone niche. *European cells & materials*. 2012;23:13-27.
130. Grellier M, Bordenave L, Amédée J. Cell-to-cell communication between osteogenic and endothelial lineages: implications for tissue engineering. *Trends in Biotechnology*. 2009;27(10):562-71.
131. Grellier M, Granja PL, Fricain J-C, Bidarra SJ, Renard M, Bareille R, et al. The effect of the co-immobilization of human osteoprogenitors and endothelial cells

within alginate microspheres on mineralization in a bone defect. *Biomaterials*. 2009;30(19):3271-8.

132. Hoogduijn MJ, Verstegen MM, Engela AU, Korevaar SS, Roemeling-van Rhijn M, Merino A, et al. No evidence for circulating mesenchymal stem cells in patients with organ injury. *Stem cells and development*. 2014;23(19):2328-35.

133. Yang Y, Kulangara K, Lam RTS, Dharmawan R, Leong KW. Effects of Topographical and Mechanical Property Alterations Induced by Oxygen Plasma Modification on Stem Cell Behavior. *Acs Nano*. 2012;6(10):8591-8.

134. Baguneid MS, Seifalian AM, Salacinski HJ, Murray D, Hamilton G, Walker MG. Tissue engineering of blood vessels. *The British journal of surgery*. 2006;93(3):282-90.

135. Desmet T, Morent R, De Geyter N, Leys C, Schacht E, Dubruel P. Nonthermal plasma technology as a versatile strategy for polymeric biomaterials surface modification: a review. *Biomacromolecules*. 2009;10(9):2351-78.

## Chapter 10 Awards, Prizes, Presentations and Papers

The following prizes and grants were awarded for this PhD Thesis:

- The Royal Free Charity – Awarded £10,000
- European Society of Vascular Surgery Research Grant – Awarded €30,000
- Runner-up poster prize in European Society for Vascular Surgery Spring Meeting 2016

The following presentations resulted from this PhD Thesis:

**2013**            **DST Chong**, MJ Dalby, N Gadegaard, AM Seifalian, G Hamilton. Surface Microscale Topographical Features Promote Endothelial Cell Proliferation and Migration on a Nanocomposite Vascular Graft Material. Poster Presentation at ATVB 2013, Florida, Cardiovascular Innovations 2013, London and presented as Oral Presentation at ESVS Spring Meeting 2013, Frankfurt.

**2014**            **D Chong**, B Lindsey, MJ Dalby, N Gadegaard, AM Seifalian, G Hamilton. Plasma and Patterning: The New Focus for the Development of Nanocomposite Vascular Grafts. SVS 2014 Boston – Poster Presentation

**2014**            **D Chong**, B Lindsey, MJ Dalby, N Gadegaard, AM Seifalian, G Hamilton. Plasma and Patterning: The New Focus for the Development of Nanocomposite Vascular Grafts. ESVS Spring Meeting 2014 London, UK – Oral Presentation

**2014**            **D Chong**, N Gadegaard, AM Seifalian, MJ Dalby, G Hamilton. Nanotopography and Plasma Treatment: Redesigning the Surface for Vascular Graft Endothelialisation. ESVS Annual Meeting 2014 Stockholm, Sweden – Oral Presentation

**2015**            **D Chong**, LA Turner, U Cheema, N Gadegaard, MJ Dalby, G Hamilton

The role of nanotopography in endothelial cell adhesion. ESVB Meeting 2015 Strasbourg, France – Poster Presentation

**2016**            **D Chong**, U Cheema, N Gadegaard, MJ Dalby, G Hamilton

Engineering Vascular Graft Nanopit Surface Topography: Effects on Endothelial Cell Behaviour. ESVS Spring Meeting Poster Presentation and Runner Up Prize.

**2016**            **D Chong**, U Cheema, N Gadegaard, MJ Dalby, G Hamilton

Nanotopographical graft surface modulation to promote endothelialisation may promote calcification by directing mesenchymal stem cells to an osteogenic lineage. ESVS Spring Meeting – Oral Presentation

#### **Papers Resulting from this PhD Thesis:**

Luminal Surface Engineering, ‘Micro- and Nanopatterning – Potential for Self Endothelialising Vascular Grafts?’ **DST Chong**, B Lindsey, MJ Dalby, N Gadegaard, AM Seifalian, G Hamilton. *EJVES*, *Volume 47, Issue 5, Pages 566-576, May 2014*

Nanotopography and Plasma Treatment: Redesigning the Surface for Vascular Graft Endothelialisation. **DST Chong**, LA Turner, N Gadegaard, AM Seifalian, MJ Dalby, G Hamilton. *EJVES* (2015), *49, Pages 335-343*,

## Chapter 11 Appendix

### Appendix A

The production of POSS-Trisilanol was extremely difficult to replicate successfully each time. Unfortunately, despite changing a variety of conditions, as shown in the Table below, the final result was still T-gel. This process will need to be further optimized and it is thought that this should be handled by a professional chemists or by a commercial chemical synthesis company.

<b>Experimental Conditions</b>	<b>Results</b>
<b>Never Used Glassware</b>	<b>T-Gel</b>
<b>Slow Quenching with Hydrochloric Acid</b>	<b>T-Gel</b>
<b>Immediate Quenching with Hydrochloric Acid</b>	<b>T-Gel</b>
<b>Doubling of Quantities</b>	<b>T-Gel</b>
<b>Halving of Quantities</b>	<b>T-Gel</b>
<b>Continuous 18 hours of stirring</b>	<b>T-Gel</b>
<b>Continuous 9 hours of stirring</b>	<b>T-Gel</b>
<b>36 hours of stirring</b>	<b>T-Gel</b>

<b>Mixture left to stir at 60° (boiling)</b>	<b>T-Gel</b>
<b>Stirring at reflux</b>	<b>T-Gel</b>
<b>Stirring without reflux</b>	<b>T-Gel</b>
<b>Post-quenching with HCl – stirring for 1 hour</b>	<b>T-Gel</b>
<b>Post-quenching with HCl – stirring for 3 hours</b>	<b>T-Gel</b>
<b>Post- quenching with HCl – stirring overnight</b>	<b>T-Gel</b>

Figure 11-1 Table to show ‘trial and error’ of all the different conditions which were attempted to make the POSS-Trisilanol. This table illustrates that unfortunately despite altering of these conditions, T-Gel predominantly featured as the end product. (n=2)

## Appendix B

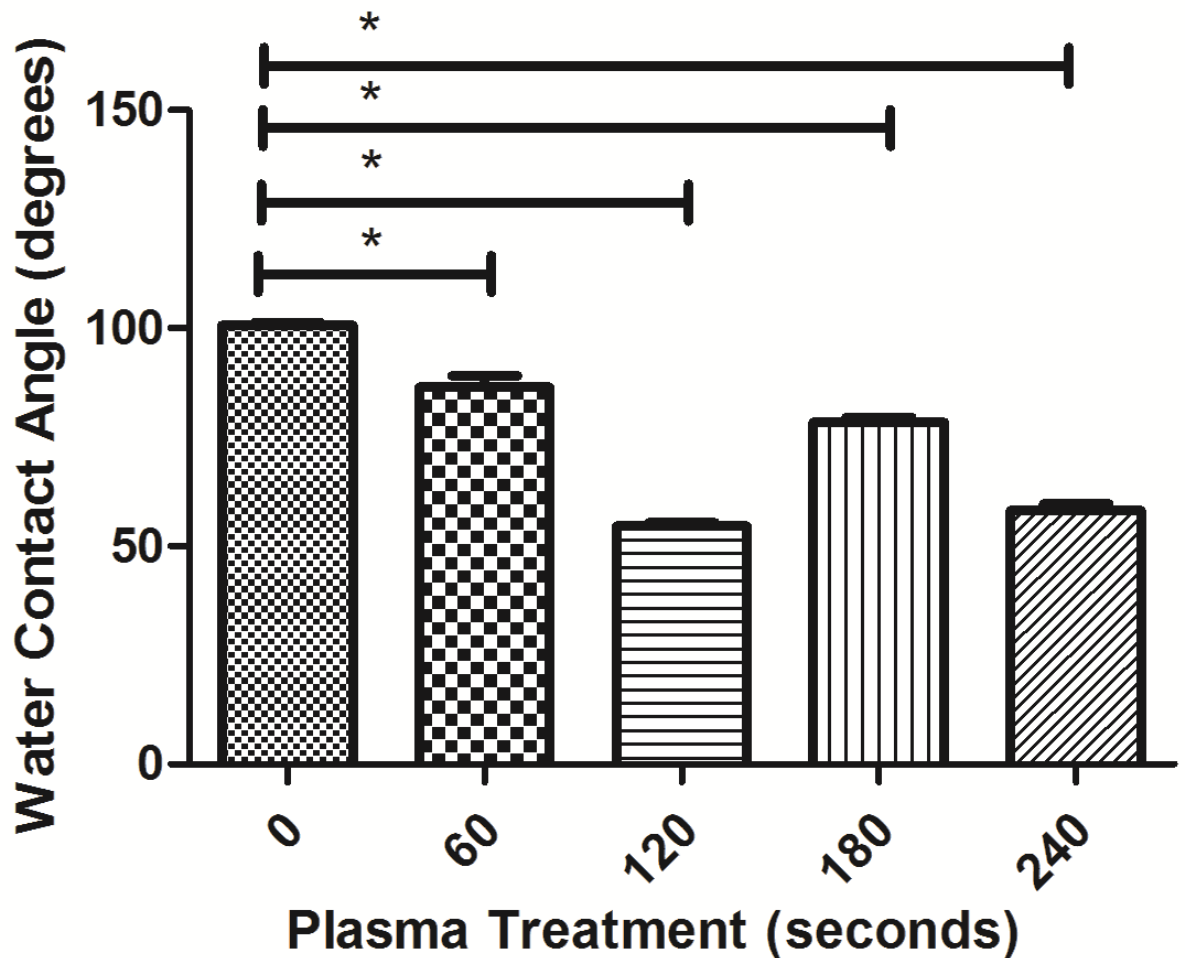


Figure 11-2 This graph shows the effect on water contact angle of POSS-PCU when the duration of plasma treatment (at 40W) is increased rather than power. (\*  $p < 0.05$ ,  $n = 6$ )

As attempts were made to lower the water contact angle of POSS-PCU, duration of plasma treatment was also tested. As the graph above shows, as the duration of plasma treatment increased, there was no difference seen between any of the treatment levels and there was no clear pattern of lowering the water contact angle. However, the graph does show that there is significant difference between the non-

treated POSS-PCU and the treated but as there was no pattern discerned with these results, this methodology of lowering water contact angle was abandoned.